VINYL CHLORIDE POLYMERIZATION

By

TUYU XIE, M. ENG.

A Thesis

Submitted to the School of Graduate Studies

in Partial Fulfillment of the Requirements

for the Degree

Doctor of Philosophy

McMaster University

Hamilton, Ontario, Canada

VINYL CHLORIDE POLYMERIZATION

DOCTOR OF PHILOSOPHY (1990) McMASTER UNIVERSITY

(Chemical Engineering) Hamilton, Ontario

TITLE : **Vinyl Chloride Polymerization**

AUTHOR : Tuyu Xie, B. Eng. (Zhejiang University, China)

M. Eng. (Zhejiang University, China)

SUPERVISORS : Professor Archie E. Hamielec

Professor Philip E. Wood

Professor Donald R. Woods

NUMBER OF PAGES : xxxviii, 355

ABSTRACT

Relevant mechanisms involved in the heterogeneous free radical polymerization of vinyl chloride have been identified including elementary chemical reactions, physical phenomena of polyvinylchloride particle formation and reactant species distributions in phases during polymerization. A comprehensive reactor model for batch and semi-batch processes has been developed on the basis of these mechanisms. The present model accounts for comprehensive elementary chemical reactions, for the effect of diffusion-controlled reactions, for the monomer and initiator distributions among phases and for radical migration between monomer and polymer phases during polymerization. Wide ranging kinetic data covering commercially significant conversion and reaction temperature ranges were measured in the present investigation to better understand the mechanisms involved and to estimate model parameters. The present model predictions are in excellent agreement with experimental data obtained in the present work and independently in other laboratories. The model allows one to predict reactor pressure development; monomer conversion histories; polymerization rates; the critical conversion at the end of two phase polymerization; the limiting conversion for polymerization at temperatures below the polyvinylchloride glassy-state transition temperature; instantaneous and accumulated molecular weight averages and distributions, and other kinetic features of vinyl chloride polymerization over temperature and conversion ranges of commercial interest.

The effect of polymerization conditions on polymer properties, especially the thermal stability of polyvinylchloride, has been elucidated. Deterioration of the thermal stability of polymer at high conversions is attributed to a decrease in monomer concentration. The secondary reactions which form the defect structures in polyvinylchloride are favoured at high conversions because of the increase in radical and polymer concentrations and the decrease in monomer concentration. The defect structures which are responsible for the low thermal stability of polyvinylchloride can be minimized significantly by using a semi-batch process at high conversions. Significant improvement in thermal stability of polyvinylchloride at high productivity by semi-batch processing at the monomer vapour pressure was demonstrated in the present investigation.

A novel method for monitoring monomer conversion online during the suspension polymerization of vinyl chloride was developed in the present study. This method provides an effective tool not only for vinyl chloride polymerization kinetic studies but also can be adapted for use with other monomer and comonomer systems.

ACKNOWLEDGEMENTS

I wish to express my sincere gratitude to various people for their support during the course of my Ph.D programme at McMaster University. I am particularly indebted to: my supervisors: Professor Archie E. Hamielec, Professor Philip E. Wood and Professor Donald R. Woods, for their enthusiasm, patience, guidance, encouragement and financial support throughout this work. My friends and Colleagues, Mr. Paul E. Gloor for his assistance in experimental preparation and data analysis; Mr. Doug Keller and Mr. Dean Anderson for their assistance in experimental preparation; Ms. Lisa Lee for her assistance in molecular weight measurements. Dr. David J. Hunkeler for his assistance in LALLS operations and helpful discussions. Professor Oscar Chiantore of University of Torino (Torino, Italy) for his assistance in PVC dehydrochlorination rate measurements and Dr. Hans Westmijze of AKZO Chemicals (Deventer, The Netherlands) for providing initiator and other additives for the experiments.

My grateful thanks also extend to: Professor Zuren Pan, Professor Kai Wang, Professor Huigen Yuan and Professor Zaizhang Yu of Zhejiang University (Zhejiang, China) for recommending and encouraging me to study abroad; Zhejiang University (China) for the first year financial support while at McMaster University and Natural Science and Engineering Research Council of Canada for subsequent financing.

TABLE OF CONTENTS

Table of Contents (continued)

Table of Contents (continued)

Table of Contents (continued)

Table of Contents (continued)

Table of Contents (continued)

LIST OF FIGURES

List of Figures (continued)

List of Figures (continued)

List of Figures (continued)

List of Figures (continued)

List of Figures (continued)

List of Figures (continued)

List of Figures (continued)

List of Figures (continued)

List of Figures (continued)

List of Figures (continued)

List of Figures (continued)

List of Figures (continued)

List of Figures (continued)

List of Figures (continued)

LIST OF TABLES

List of Tables (continued)

NOMENCLATURE

a = Mark-Houwink constant or a parameter defined in Eq.(4.22).

A = the ratio of tracer response areas at conversion X to zero conversion defined in Eq.(3.16) or the ratio of weight of monomer to polymer in the polymer phase defined in Eq.(4.11).

A_2 = second virial coefficient.

A^* = free volume factor used in K_t equation.

A_b = area of tracer response at conversion X.

A_{bo} = area of tracer response at zero conversion.

b = a parameter defined in Eq.(4.22).

B = total mass of tracer, g.

B^* = free volume factor used in K_p and K_4/K_S equations.

B_f^* = free volume factor used in $K_p f^{1/2}$ equation.

B_g = mass of tracer in the gas phase, g.

B_m = mass of tracer in the monomer, g.

B_p = mass of tracer in the polymer, g.

B_w = mass of tracer in the water phase, g.

C = concentration of polymer solution or a parameter defined in Eq.(5.51).

C^* = free volume factor used in K_d' equation.

CH^* = free volume factor used in K_1 equation.

$[Cl^\cdot]$ = chlorine radical concentration, mole/L.

Nomenclature (continued)

CM = ratio of K_{fm} to K_p.

C_p = ratio of K_{fp} to K_p.

C'_p = ratio of K'_{fp} to K'_p.

d_p = diameter of primary particle, dm.

D_b = density of n-butane, g/L.

D_{go} = density of VCM vapour under the vapour pressure, g/L.

D_m = density of monomer, g/L.

D_p = density of polymer, g/L.

D_w = density of water, g/L.

f = initiator efficiency.

f_l = fugacity of tracer in the different phases, atm.

F_l = Weight fraction of monomer in phase i.

F_I = initiator feed rate, mole/min.

F_{In} = monomer feed rate, mole/min.

$F(t)$ = normalized GPC response, fraction.

I = initiator.

$[I]$ = concentration of initiator, mole/L.

I_o = initial moles of initiator, mole.

$[I]_p$ = initiator concentration in the polymer phase, mole/L.

I_{xf} = moles of initiator at X_f, mole.

J = a parameter defined in Eqs.(4.63) and(4.64).

K = solubility constant of VCM in water.

K^* = the parameter of precipitation defined in Eq.(4.60).

Nomenclature (continued)

K_{1-5} = reaction rate constants defined in reactions (4)-(8) (see Table 4.1)

K_b = proportionality constant defined in Eq.(3.14).

K_{bm} = Henry's Law constant of tracer in monomer, atm.

K_{bp} = apparent solubility constant of tracer in PVC, atm.

K_{bw} = Henry's Law constant of tracer in water, atm.

K_C = the net rate constant for chemical reaction defined in Eq.(A.1).

K_d = decomposition rate constant of initiator, 1/sec.

K_d' = effective decomposition rate constant of initiator, 1/sec.

K_D = rate constant of primary radical diffusion out from cage.

K_{fm} = chain transfer to monomer rate constant, L/mole-sec.

K_{fp} = chain transfer to polymer rate constant, L/mole-sec.

K_{de} = radical desorption rate constant, 1/sec.

K'_{fp} = Cl˙transfer to polymer rate constant, L/mole-sec.

K_i = initiation rate constant, L/mole-sec.

K_I = initiator partition coefficient.

K_p = propagation rate constant, L/mole-sec.

K'_p = chlorine radical propagation rate constant, L/mole-sec.

K_{PVC} = Mark-Houwink constant for PVC-THF solution.

K_{PS} = Mark-Houwink constant for PS-THF solution.

K_{ki} = rate constant for inert compound formation in cage.

K_{R2} = rate constant for primary radical recombination in cage.

K_S = the net rate constant for the segmental diffusion.

Nomenclature (continued)

K_t = the total bimolecular termination rate constant, L/mole-sec.

K_T = the net rate constant for the translational diffusion.

K_{tc} = combination bimolecular termination rate constant, L/mole-sec.

K_{td} = disproportionation bimolecular termination rate constant, L/mole-sec.

$\overline{K}_{tn}$ = number-average termination rate constant, L/mole-sec.

K_x = rate constant for primary radical reacting with monomer in cage.

m = instantaneous mass fraction of polymer.

M = mass of monomer, g.

[M] = concentration of monomer, mole/L.

M_1 = mass of monomer in the monomer phase, g.

M_2 = mass of monomer in the polymer phase, g.

M_b = molecular weight of tracer, g

M_g = mass of monomer in the gas phase, g.

M_{gxf} = mass of monomer in the gas phase at X_f, g.

M_H = molecular weight of water, g.

M_L = mass of liquid monomer in the monomer phase.

M_m = molecular weight of monomer, g.

M_n = instantaneous number-average molecular weight.

$\overline{M}_n$ = number-average molecular weight of accumulated polymer.

M_o = initial monomer charged, g.

M_w = instantaneous weight-average molecular weight.

$\overline{M}_w$ = weight-average molecular weight of accumulated polymer.

Nomenclature (continued)

M_{wi} = mass of monomer in water phase, g

M_z = instantaneous Z-average molecular weight.

$\overline{M}_z$ = Z-average molecular weight of accumulated polymer.

n_o = refractive index of solvent.

N^* = number of segments in an entangled polymer molecule.

N_{av} = Avogadro's number.

N_F = total moles of monomer fed into reactor.

N_m = moles of monomer.

N_{mv} = moles of monomer in the vapour phase, mole.

N_{mp} = moles of monomer in the polymer phase, mole.

P = a parameter defined in Eq.(4.10).

P_b = the partial pressure of n-butane.

P_m = the partial pressure of monomer, atm.

P_{mo} = the vapour pressure of monomer, atm.

P_o = the initial total pressure of the system, atm.

PQ_2 = a parameter defined in Eq.(5.45).

PQ_3 = a parameter defined in Eq.(5.45).

P_r = moles of polymer with chain length r.

$[P_r]$ = concentration of polymer with chain length r, mole/L.

P_t = the total pressure, atm

q = a variable defined in Eq.(3.12).

Q = a parameter defined in Eq.(4.11).

q_f = a parameter defined in Eq.(3.20).

Nomenclature (continued)

q_1 = a parameter defined in Eq.(3.20).

q_o = a parameter defined in Eq.(3.20).

q_x = a parameter defined in Eq.(3.20).

Q_i = the i^{th} moment of polymer distribution.

r = polymer chain length.

$\bar{r}$ = average chain length of polymer.

r_c = critical chain length for precipitation of polymer radical.

R = gas constant, L-atm/mole-K or cal/mole-K.

$R^\cdot$ = polymer radical.

R_{cm} = a parameter defined in Eqs.(5.17) and (5.18).

$R_i^\cdot$ = primary radical.

R_I = initiation rate, mole/L-sec.

R_p = polymerization rate, mole/L-min.

R_p = dX/dt, conversion fraction per unit time.

R_{pi} = polymerization rate in phase i, mole/L-sec.

$[R^\cdot]$ = polymer radical concentration, mole/L.

RQ_2 = a parameter defined in Eq.(5.48).

RQ_3 = a parameter defined in Eq.(5.48).

$R_r^\cdot$ = moles of polymer radicals with chain length r.

$[R_r^\cdot]$ = concentration of polymer radicals with chain length r, mole/L.

R_t = bimolecular termination rate, mole/L-sec.

R_θ = measured excess scattering intensity of solution over that of pure solvent.

Nomenclature (continued)

S_1 = a parameter defined in Eq.(5.23).

S_2 = a parameter defined in Eq.(5.45).

t = temperature, °C or reaction time, min.

t_{xf} = polymerization time at X_f, min.

t_{xp} = polymerization time at pressure P_m, min.

T = absolute temperature, °K.

T_{gm} = glassy-state transition temperature of monomer, °K.

T_{gp} = glassy-state transition temperature of polymer, °K.

V = reaction volume, L.

V_f = free volume fraction.

V_F = hole-free volume.

V_{fp} = free volume fraction of polymer.

V_{fxf} = free volume fraction of polymer at X_f.

V_g = volume of the gas phase, L.

V_p = volume of the polymer phase, L.

V_r = reactor volume, L.

W_1 = the volume fraction of initial reactor charge.

W_p = mass of polymer.

W_w = mass of water charged, g.

W(r) = instantaneous weight chain length distribution (weight fraction of dead polymer with chain length r).

$\overline{W}(r)$ = accumulated weight chain length distribution (weight fraction of dead polymer with chain length r).

Nomenclature (continued)

X = conversion of monomer.

X_{bm} = mole fraction of tracer in monomer, tracer free basis.

X_{bp} = volume fraction of tracer in PVC, tracer free basis.

X_{bw} = mole fraction of tracer in water, tracer free basis.

X_f = the critical conversion at which the monomer phase is consumed.

X_L = limiting conversion.

X_p = conversion at time t_{xp}.

Y_b = mole fraction of tracer in the vapour phase.

Y_i = the i^{th} moment of polymer radical distribution.

Greek letters:

α = a parameter defined in Eq.(5.67).

α_1 = a parameter defined in Eq.(2.36).

α_m = thermal expansion factor for VCM.

α_p = thermal expansion factor for PVC.

β = a parameter defined in Eqs.(5.17) and (5.18).

β^* = a parameter defined in Eq.(A.3).

γ = a parameter defined in Eq.(6.17)

Γ = a parameter defined in Eq.(6.15).

δ = jump distance of a polymer chain segment.

ζ = a parameter defined in Eq.(A.19).

$[\eta]$ = intrinsic viscosity, dL/g.

Nomenclature (continued)

λ = Fraction of bimolecular termination by disproportionation (defined in Eqs.(5.73) and (5.74)).

λ_o = wavelength of light in vacuum, cm.

ξ = a parameter defined in Eq.(5.67).

τ = a parameter defined in Eqs.(5.17) and (5.18).

υ^* = a critical free volume fraction for a segment to jump.

ϕ_o = jump frequency of a polymer chain segment.

Φ_p = volume fraction of polymer in the polymer phase.

Φ_2 = volume fraction of polymer phase.

χ = VCM-PVC interaction parameter.

Ψ = a function defined in Eq.(60).

Subscripts and Superscripts:

o = initial state.

1 = monomer phase (or case 1 in chapter 6).

2 = polymer phase (or case 2 in chapter 6).

g = gas phase.

m = monomer.

p = polymer.

w = water phase.

Nomenclature (continued)

Abbreviations:

AIBN = azobis(isobutyronitrile).

ESR = electron spin resonance.

GC = gas chromatography.

GPC = gel permeation chromatography.

LALLS = low-angle laser light scattering.

MIPPT = McMaster Institute for Polymer Production Technology.

MWD = molecular weight distribution.

NMR = nuclear magnetic resonance.

P.I.D. = proportional-integral-derivative.

PS = polystyrene.

PVA = polyvinylalchohol.

PVC = polyvinylchloride.

SSH = stationary-state hypothesis.

THF = tetrahydrofuran.

VCM = vinyl chloride monomer.

CHAPTER 1

INTRODUCTION

1.1 POLYVINYLCHLORIDE PRODUCTION

Polyvinylchloride (PVC) has been manufactured commercially for about sixty (60) years and is now produced in more than forty (40) countries around the world.[1-12] As a commodity polymer, the annual production of PVC is second only to that of low density polyethylene.[11, 13-17] The total PVC resin production in 1983 was estimated to be thirty (30) billion pounds worldwide,[11] and its market demand has been increasing gradually through the 1980s.[10,15] PVC is expected to maintain its position as the second most widely used thermoplastic material in the longer term due to its unique chemical and physical properties. The reasons for its enormous versatility and range of applications derive from a combination of the basic molecular structure, with a chlorine atom situated on each alternate carbon of the polymer back bone, which gives rise to a relatively tough and rigid material, and its ability to absorb a range of plasticisers to produce various flexible products. The enormous expansion of the PVC industry, on the other hand, is also due to the fact that PVC consists of 57-wt% chlorine which makes the PVC industry an important outlet for chlorine, a by-product of sodium hydroxide production,[17] reducing its dependence on non-renewal resources, oil and natural gas liquids.

Commercially, PVC is synthesized exclusively by free radical polymerization at reaction temperatures normally in the range, 45-65°C. However, for some special applications, PVC is also synthesized at temperature as high as 80°C. Five polymerization process types are used for the commercial manufacture of PVC, namely, suspension, emulsion, bulk (or mass), microsuspension and solution polymerization.[13,17-23] Suspension, emulsion and bulk polymerization are the principal processes for PVC production. However, about 75% of PVC produced is made by the suspension polymerization technique.[21] The advantages of suspension over emulsion polymerization include much lower concentration of additives needed and much of the associated water can be removed by filtration. The main advantage over bulk polymerization process is the much more effective reaction heat removal during suspension polymerization. However, suspension and bulk polymerization PVC do compete in the same application markets. Therefore, suspension polymerization process was chosen for the present investigation.

Suspension polymerization of vinyl chloride is commercially carried out batchwise, mostly in stainless steel reactors having highly polished internal surfaces. Reactors with capacity, 30 to 200 m^3 are commonly used.[9,17,21] Better resin quality and higher productivity of PVC are achieved using larger batch reactors, but the reactor configurations and complexity increase with increase in reactor volume. Typical suspension polymerization recipes include vinyl chloride monomer (VCM), water, initiator, protective colloid (suspending agents) and an aqueous buffer to control PH. The relative amount of each component and the manner in

which the recipe components are added to the reactor as well as the time and temperature during the addition of the individual component are all closely guarded secrets for most manufacturers. This suggests that productivity and resin quality strongly depend on operational experience (know-how). In general, liquid monomer is dispersed in a continuous water phase by vigorous agitation and stabilized by a protective colloid during suspension polymerization. The dispersed monomer droplets, with mean diameters 30-150 μm,[19] contain dissolved initiator and, when the contents of the reactor are heated, the initiator decomposes, generates radicals and starts the polymerization. The polymerization reactions, therefore, occur in the dispersed monomer droplets which can be considered as small bulk reactors. The final product of suspension PVC is a powder of white porous particles with a mean particle size usually in the range, 100-150 μm.[9]

1.2 UNSOLVED PROBLEMS

Although PVC production technology is well established and PVC is the second most widely used plastic resin, polymerization mechanisms and kinetics as well as certain PVC properties, unfortunately, are not well understood, particularly the deterioration in properties which occurs at high conversions during PVC production. Most of the fundamental studies in the literature are qualitative in nature so that dynamic and kinetic models which can quantitatively describe reactor dynamics and kinetic behaviour of VCM polymerization, and be directly used for PVC reactor design did not exist prior to the present investigation.

This is largely due to the very limited kinetic data available particularly at high conversions. A comprehensive review emphasizing mechanisms, kinetics and reactor modelling for VCM polymerization was recently published by the author.[24] (Therefore, a detailed literature review is not given in this chapter and the reader is referred to the original reference.[24] However, the fundamental background of the subject is clearly illustrated in each individual chapter). The reason for the limitation of previous kinetic models, in addition to a lack of data, is that the mechanisms of VCM polymerization including elementary chemical reactions and physical phenomena were not elucidated so that most of models are oversimplified. More specifically, reactant species distributions in the polymerization system, diffusion-controlled reactions and their effect on polymer quality and the effect of reactor operating conditions on elementary reactions as well as polymer properties have not been comprehensively studied.

Reactor dynamics for VCM polymerization are only known qualitatively. The boiling point of vinyl chloride monomer is -13.8°C (at 760 mm Hg).[25,26] Therefore, the reactor is under pressure at normal polymerization temperatures 45-65°C. It is a common experience that the reactor pressure during VCM isothermal polymerization remains constant until a certain conversion then it drops gradually with increase in reaction time. Polymerization continues after the pressure drop and reactor pressure decreases with monomer conversion. Reactor pressure development and conversion history can be shown schematically as in Figure 1.1. Commercial practice usually involves terminating conversions in the range,

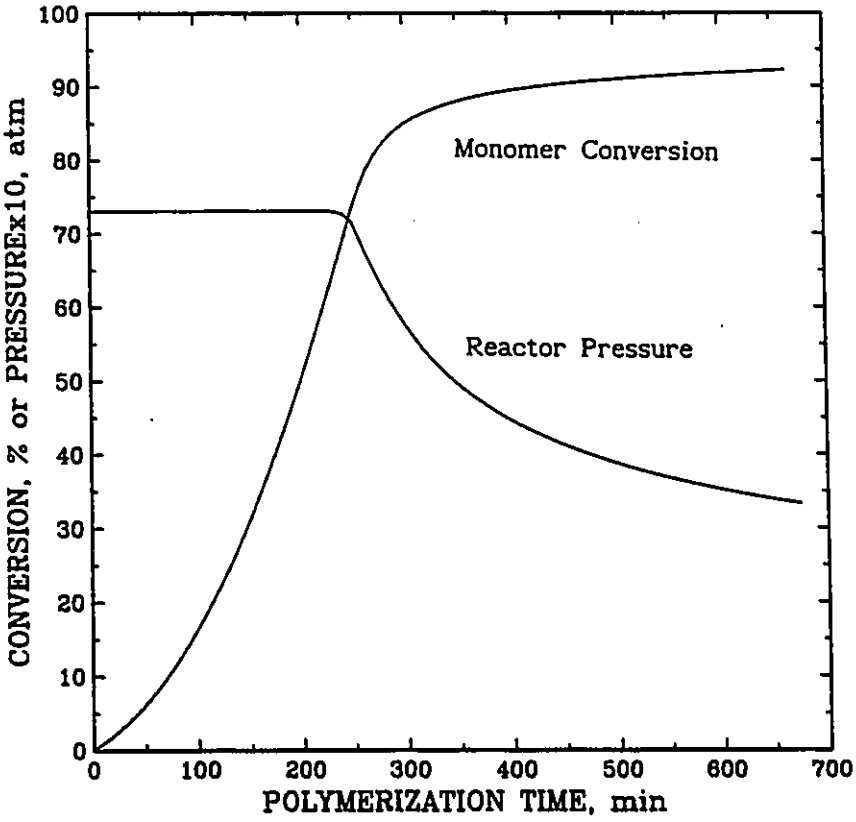

Figure 1.1. Reactor pressure development and conversion history during VCM isothermal polymerization.

85-95% that is conversions are taken beyond the pressure drop. Hence, the PVC product in the reactor experienced at least two transitional conditions, namely, isobaric and non-isobaric polymerizations in a batch process. The questions are what is the critical conversion at which the reactor pressure starts to fall and what are the relationships between conversion/pressure/temperature and other reactor operational conditions. Unfortunately, these phenomena have not been quantitatively described in the literature prior to the present investigation.

The fact that VCM polymerization rates increase with conversion almost from zero conversion up to a certain high level has been recognized for some time.[27] However, the polymerization rate decreases dramatically with conversion at higher conversions. This is shown schematically in Figure 1.2 together with the change in reactor pressure. Polymerization rate increases with conversion during the isobaric period then decreases rapidly with conversion during the non-isobaric period. Talamini et al[28,29] first proposed a two-phase polymerization (during the isobaric period) model to explain the kinetic behaviour of VCM polymerization up to the pressure drop (mechanisms and kinetics are discussed in detail in Chapter 4). Some pertinent questions are: what are the concentrations of monomer, initiator and, more importantly, radicals in the monomer and polymer phase? how do kinetic parameters differ in magnitude in the two phases (monomer and polymer phases)? and what is the contribution of each phase to the total polymerization rate? How do these variables and parameters change with conversion at conversions beyond the pressure drop? All these questions, which are relevant and answers necessary for an understanding of the polymerization process and for valid kinetic modelling, have not been quantitatively examined in the literature.

During the last fifteen years there has been considerable progress in the understanding of PVC chain microstructure due to the improvements in nuclear magnetic resonance (NMR) techniques (^{13}C-NMR in particular). The main microstructural features of PVC molecules have been well identified, and the chemical reaction mechanisms by which the

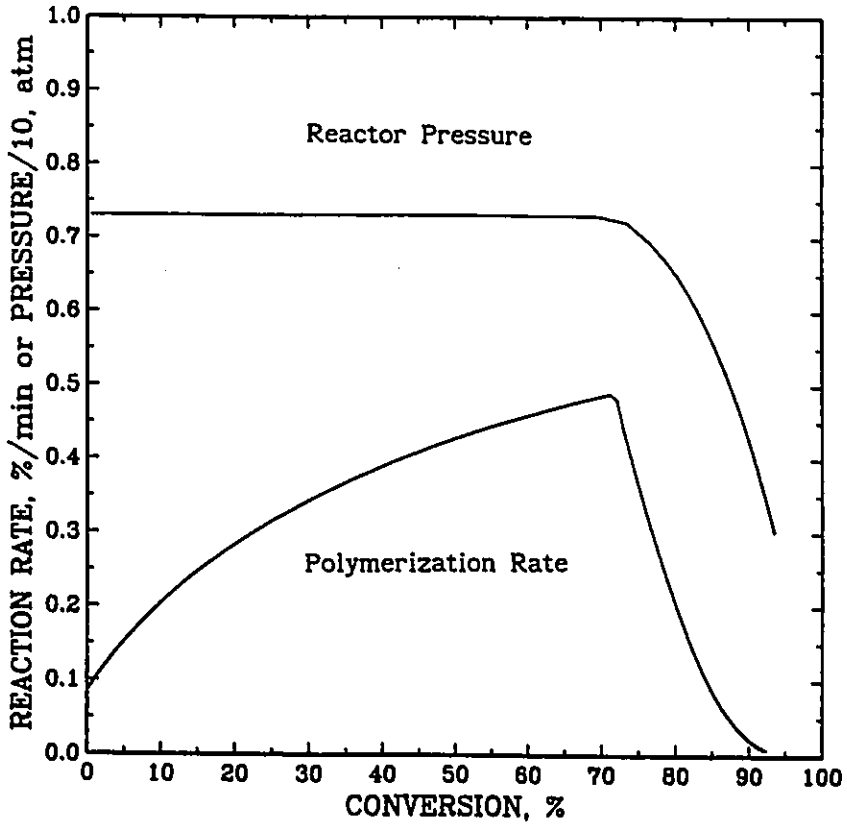

Figure 1.2. Conversion dependence of polymerization rate and reactor pressure for VCM isothermal polymerization.

different structures form have been also deduced.[30-32] One of the most important elucidations is the mechanism of chain transfer to monomer which controls PVC molecular weight development. The mechanism where a polymer radical directly transfers its radical center to a monomer molecule, in fact, does not occur during VCM polymerization. According to the now accepted mechanism (which will be discussed in detail in Chapter 4) for chain transfer to monomer, the effective rate constant for chain transfer to monomer is a function not only of temperature but

also of monomer concentration. Hence, it can vary during polymerization. It is of interest to know how this parameter varies with changes in the polymerization environment and how this change affects PVC molecular weight development. A comprehensive kinetic model based on this new mechanism has not been reported in the literature prior to this study.

A serious deficiency of PVC is its low thermal and photochemical stability. It is now well recognized that the low thermal and photochemical stability of PVC is strongly related to the amount of structural defects in the polymer chain formed due to secondary reactions during polymerization.[33,34] Hjertberg et al[35] showed that the dehydrochlorination rates (a measure of PVC thermal stability) for PVC, made by seed polymerization, increase significantly with a decrease in reactor pressure. Russo et al[36] demonstrated that the accumulated molecular weights of PVC decrease significantly and the polydispersity of the polymer distribution increases with conversion at high conversions. Therefore, at high conversions, not only do the reactor dynamics and kinetics change as shown in Figures 1.1 and 1.2 but polymer properties do also. However, the fundamental relationships between them (reactor variables versus polymer properties) have not been studied comprehensively. It is not clear what control variables cause these dramatic changes in reactor dynamics and polymer properties. As mentioned above, commercial suspension PVC is produced exclusively in a batch process. Is it possible to combine batch and semi-batch processes particularly at high conversions so that PVC is produced under isobaric pressure? In other words, how can we control VCM polymerization to minimize polymer property changes that

are undesirable.

All these unanswered questions are related to the mechanisms and kinetics of VCM polymerization. For kinetic studies, conversion histories or polymerization rates are essential information. Conventional conversion measurement methods other than those involving heat balance are not effective or valid for VCM suspension polymerization due to heterogeneity of the VCM-PVC mixture and also because of the hazards using vinyl chloride monomer.[26] This may be one of the reasons why so little kinetic information at high conversions has been accumulated. Therefore, for small reactors for which heat balance methods are ineffective, a conversion measurement method needed to be developed in order to obtain detailed kinetic information over the entire conversion range. This provided another challenge for this investigation.

Thus, many important, challenging and stimulating research problems in VCM polymerization field were defined. A fundamental understanding of VCM polymerization mechanisms and PVC microstructure and its relationship to polymerization conditions is vital to improve PVC manufacturing technology. Comprehensive dynamic reactor model development is important to provide a tool to assist in the development of new PVC products and in the design of new processes for their manufacture but also to evaluate and optimize existing manufacturing systems.

1.3 OBJECTIVES AND SCOPE OF THE STUDY

Based on the observations above, the objectives of the present investigation are to further study the mechanisms and kinetics of VCM polymerization and to develop a comprehensive and valid reactor model for VCM suspension polymerization which can quantitatively describe the phenomena mentioned in the previous section, while in batch or semi-batch operation. The present investigation should particularly emphasize the behaviour of VCM polymerization at high conversions which is of great commercial interest. The scope of the present investigation includes modelling reactor pressure, reactant species distributions among phases, conversion history, polymerization rate, molecular weight development for VCM polymerization in both batch and semi-batch reactors; developing a novel conversion measurement method; carrying out a series of experiments to obtain detailed fundamental data including the solubility of VCM in water and PVC, n-butane in VCM, conversion histories, accumulated molecular weight averages and distribution and thermal stability of PVC; and estimating a series of kinetic parameters based on the measured experimental data. The main research projects and their relationships are shown in Figure 1.3.

The main achievements of the present investigation are illustrated in the following Chapters 2 to 7. A comprehensive dynamic batch reactor model is developed in Chapter 2. It calculates reactor pressure/monomer conversion/reaction temperature relationships; the critical conversion at which the reactor pressure starts to fall and monomer distribution during VCM suspension polymerization. Chapter 3 describes

conversion measurements by the novel tracer method developed in this investigation. A comprehensive model relating conversion to tracer response was also developed. This tracer method can provide detailed conversion histories for kinetic studies. Microsopic processes, both chemical and physical, which occur during VCM polymerization are described in detail and a comprehensive kinetic model based on these mechanisms is developed in Chapter 4. The following Chapter 5 further describes PVC molecular weight development. Instantaneous and accumulated molecular weights and distribution are quantitatively illustrated in the chapter. In Chapter 6, a comprehensive semi-batch reactor model is developed, and the improvement in PVC productivity and thermal stability by a novel semi-batch process is demonstrated. The effect of polymerization conditions on polymer properties, particularly on thermal stability, is illustrated in Chapter 7. Finally, the conclusions drawn from the present investigation are summarized in Chapter 8.

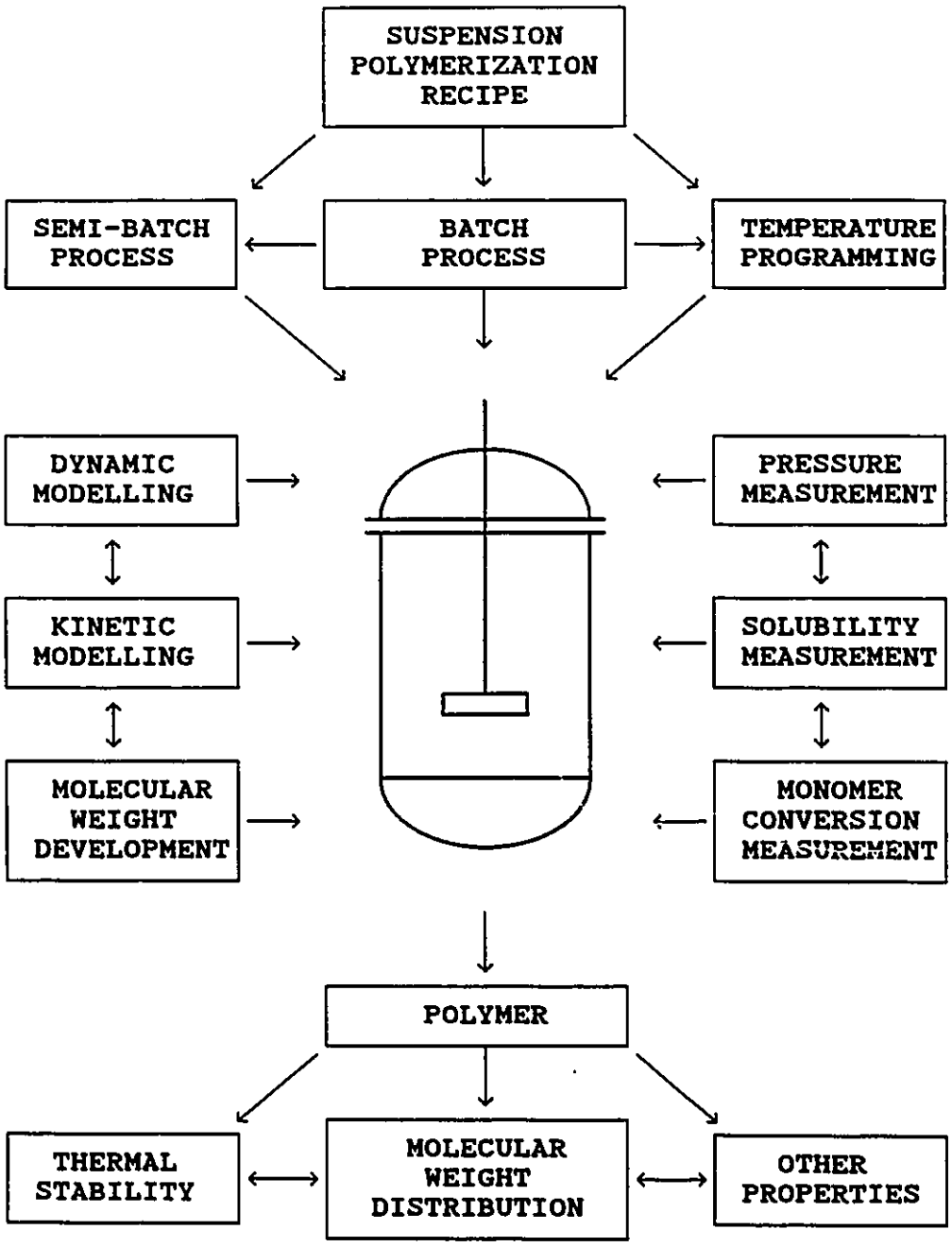

Figure 1.3. The main research projects and their relationships.

1.4 REFERENCES

1. Kaufman, M. 'The History of PVC', Maclaren and Sons Ltd., London, 1969.

2. Koleske, J. V. and Wartman, L. H. 'Poly(vinylchloride)', Gordon and Breach Sci. Publishers Inc., 1969.

3. Sarvetnick, H. A. 'Polyvinylchloride', Reinhold Book Corporation, New York, 1969.

4. Benton, J. L. and Brighton, C. A. 'Encyclopedia of Polymer science and Technology', Ed. Mark, H. F. and Gaylord, N. G., John Wiley Sons Inc., 1971, 14, 305.

5. Shelton, L. G., Hamilton, D. E. and Fisackerly, R. H. 'Vinyl and Diene Monomers', part3, Ed. Leonard, E. C., Wiley-Interscience, 1971, p1205.

6. Henson, J. H. L. and Whelan, A. 'Developments in PVC Technology', John Wiley and Sons, 1973.

7. Sitting, M. 'Vinyl Chloride and PVC Manufacture', Noyes Data Corporation, 1978.

8. Semon, W. L. and Stahl, G. A. J. Macromol. Sci.: Chem., 1982, A15, 1263.

9. Butters, G. 'Particulate Nature of PVC', Appl. Sci. Publishers Ltd., 1982.

10. Stinson, S. C. Chem. Eng. News, 1984, 64, 27.

11 Weinberg, E. L. 'Encyclopedia of PVC', 2nd Edition, Vol.1, Ed. Nass, L. I. and Heiberger, C. A., Marcel Dekker Inc., New York and Basel, 1986, p1.

12. Minsker, K. S., Kolesov, S. V. and Zaikov, G. E. 'Degradation and Stabilization of Vinyl Chloride-based Polymers',1st Edition, Pergamon Press, 1988.

13. Cameron, J. B., Lundeen, A. J., McCulley Jr.,J. M. and Schwab, P. A. J. Appl. Polym. Sci.: Appl. Polym. Symp., 1981, 36, 133.

14. Tester, D. A. 'Degradation and Stabilisation of PVC', Ed. Owen, E. D., Elsevier Appl. Sci. Publishers, London and New York, Chap.1, 1984.

15. Greek, B. F. Chem. Eng. News, 1990, 68, 11.

16 Tornell, B. Polym.-Plast. Technol. Eng., 1988, 27, 1.

17. Tornell, B. 'Handbook of Polymer Science and Technology', Ed. Cheremisinoff, N. P., Vol.1, Chap.10, Marcel Dekker, Inc., New York and Basel, 1989, p347.

18. Wheeler, Jr. R. N. Environ. Health Perspect., 1981, 41, 123.

19. Burgess, R. H. 'Manufacture and Processing of PVC', Appl. Sci. Publishers Ltd., London, 1982.

20. Corporation, R. 'Polymer Manufacturing', Noyes Data Corporation, 1986, p568.

21. Langsam, M. 'Encyclopedia of PVC', 2nd Edition, Vol.1, Ed. Nass, L. I. and Heiberger, C. A., Marcel Dekker, Inc., New York and Basel, 1986, p48.

22. Lukas, R., Paleckova, V., Mrazek, Z. and Kolinsky, M. International Polym. Sci. Technol., 1982, 9, 66.

23. Lukas, R., Paleckva, V., Mrazek, Z. and Kolinsky, M. International Polym. Sci. Technol., 1982, 9, 83.

24. Xie, T. Y., Hamielec, A. E., Wood, P. E. and Woods, R. D. **'Emulsion, Suspension and Bulk Polymerization of Vinyl Chloride — Mechanisms, Kinetics and Reactor Modelling'**, Submitted to J. Vinyl Technol., 1990.

25. Johnston, C. W. 'Encyclopedia of PVC', Ed. Nass, L. I., 1st Edition, Vol.1, Chap.3, Marcel Dekker, Inc., New York and Basel, 1976, p33.

26. Sandler, S. R. and Karo, W. 'Polymer Syntheses', Vol.2, Chap.10, Academic Press, Inc., New York, 1977, p306.

27. Bengough, W. I. and Norrish F. R. S., R. G. W. Proc. Royal Soc., (London), 1950, A200, 301.

28. Talamini, G. J. Polym. Sci., 1966, A-2, 4, 535.

29. Crosato-Arnaldi, A., Gasparini, P. and Talamini, G. Makromol. Chem., 1968, 117, 140.

30. Starnes Jr., W. H. 'Developments in Polymer Degradation-3', Ed. Grassie, N., Appl. Sci. Publishers, London, 1981, p135.

31. Hjertberg, T. and Sorvik, E. M. 'Degradation and Stabilisation of PVC', Ed.Owen, E. D., Elserviery, Appl. Sci. Publishers, London and New York, 1984, p21.

32. Starnes Jr., W. H., Schilling, F. C., Plitz, I. M., Cais, R. E., Freed, D. J., Hartless, R. L. and Bvey, F. A. Macromol., 1983, 16,790.

33. Llauro-Darricades, M. F., Bensemra, N., Guyot, A. and Petiaud, R. Makromol. Chem., Macromol. Symp., 1989, 29, 171.

34. Bensemra, N., Hoang, T. V. and Guyot, A. Polym. Degrad. Stab., 1990, 28, 173.

35. Hjertberg, T. and Sorvik, E. M. J. Polym. Sci.: Part A: Polym. Chem., 1986, 24, 1313.

36. Russo, S. and Stannett, V. Makromol. Chem., 1971, 143, 47.

CHAPTER 2

REACTOR DYNAMICS

2.1 INTRODUCTION

In the previous chapter, batch reactor pressure development is shown schematically. In this chapter, reactor pressure as a function of conversion and batch reactor operational conditions will be described quantitatively.

An important feature of VCM polymerization (which includes bulk, suspension, emulsion and microsuspension polymerization) is the low solubility of PVC in its monomer. Therefore, during polymerization, two phases (monomer and polymer phase) form at very low conversions (two phases occur in the dispersed droplets for suspension polymerization). The monomer phase is considered to be essentially pure monomer, while the PVC phase is swollen with monomer (at about 30% weight monomer).[1-9] As the polymerization proceeds, the volume of the monomer phase decreases while that of the polymer phase grows, but the composition of each phase is considered constant (the diffusion of monomer into the PVC phase is considered to be sufficiently rapid to achieve equilibrium swelling). As long as vinyl chloride monomer exists as a separate phase, it will exert its full vapour pressure and the pressure in the reactor will be a constant value during isothermal polymerization. The pressure

in the reactor begins to drop when monomer conversion approaches a critical value, X_f, at which point the monomer as a separate phase no longer exists. This critical conversion is commonly considered to occur at about 70-80%.[3-7,9-12] For many commercial suspension polymerization recipes, the conversion is taken past the critical value and the terminal conversion is estimated from the pressure drop in the range, 85-95%.[10,11] Although it is a common experience that the reactor pressure decreases with conversion after X_f for isothermal polymerization, few data on pressure drop versus conversion have accumulated in the literature.[4,13,14] Most of the kinetic studies focus on relatively low conversions and the pressure is not considered as a kinetic variable. A comprehensive model which relates conversion to reactor temperature and pressure and which should be useful to determine end points for commercial polymerizations as well as the full conversion/time history has not been published. The critical conversion X_f which is a very important kinetic parameter has never been theoretically calculated prior to the present investigation.

Furthermore, the monomer concentration in the water and vapour phases were neglected in previous kinetics calculations. Hence, these published kinetic models may overestimate the polymerization rate at high conversions. Therefore, the objectives of this chapter are to develop a comprehensive model relating conversion to reactor temperature, pressure and reactor operational conditions and one which can predict the critical conversion and monomer distribution for VCM suspension or bulk polymerization for use both in commercial production of PVC and in

further studies of kinetics of VCM polymerization.

2.2 MODEL DEVELOPMENT

The model is to relate conversion of vinyl chloride monomer to polymer as a function of temperature, reactor pressure and reactor operational conditions. Its development is based on the following assumptions:

(1). The distributions of species among phases are in instantaneous equilibrium over the entire conversion range.

(2). The solubility of PVC in its monomer is neglected (0.03% at ambient temperature,[8] <0.1% at polymerization temperature 50°C[3]).

(3). The PVT properties of the vapour phase obey the Ideal Gas Law.

(4). The solubility of VCM in water obeys Henry's Law.

(5). The solubility of VCM in PVC obeys the Flory-Huggins equation.

2.2.1 Temperature, Pressure and Conversion Relationship

For suspension or emulsion polymerization of vinyl chloride, at given conditions, the initial fillage of the reactor W_1 is given by

$$W_1 = [W_w/D_w+(M_o-M_{go})/D_m]/V_r \qquad (2.1)$$

where mass of monomer initially in the gas phase, M_{go}, can be expressed as:

$$M_{go} = (1.0-W_l)V_r P_{mo} M_{mo}/(RT) \qquad (2.2)$$

Substituting Eq.(2.2) into Eq.(2.1), one obtains:

$$W_l = (W_w/D_w + M_o/D_m - D_{go} V_r/D_m)/[V_r(1.0-D_{go}/D_m)] \qquad (2.3)$$

where

$$D_{go} = P_{mo} M_m/(RT)$$

When the monomer is converted into polymer, the total volume of liquid phases (monomer and polymer phases) shrinks because of the lower density of the monomer relative to the polymer. Therefore, the total volume of the VCM-PVC mixture in the reactor decreases and the vapour volume increases with conversion. When the vapour volume increases, liquid monomer vapourizes to maintain the the reactor pressure constant when free liquid monomer is available. Thus, the total change of the vapour phase volume is the sum of the volume shrinkage and the volume of liquid monomer vapourized to maintain constant pressure. It can be expressed as:

$$\Delta V_g = XM_o(1/D_m - 1/D_p)/(1.0-D_{go}/D_m) \qquad (X \le X_f) \qquad (2.4)$$

The monomer conversion X is defined by

$$X = (M_o - M)/M_o = W_p/M_o \qquad (2.5)$$

Therefore, the volume of vapour phase is given by

$$V_{gx} = (1.0-W_l)V_r + XM_o(1/D_m - 1/D_p)/(1.0-D_{go}/D_m) \qquad (2.6)$$

When conversion is at the critical conversion ($X=X_f$), Eq.(2.6) becomes:

$$V_{gxf} = (1.0-W_l)V_r + X_f M_o (1/D_m - 1/D_p)/(1.0-D_{go}/D_m) \qquad (2.7)$$

Eqs. (2.6) and (2.7) relate volume of the vapour phase to reactor operational conditions before and at the critical conversion X_f, respectively. When conversion is greater than the critical conversion X_f, the monomer phase no longer exists, a monomer mass balance gives:

$$M_o = M_g + M_w + M_p + W_p \qquad (X > X_f) \qquad (2.8)$$

M_g, M_w and M_p are a function of conversion and reactor pressure at high conversions. Therefore, a temperature, conversion and pressure relationship can be obtained if M_g, M_w and M_p can be expressed as a function of conversion and pressure at given reactor conditions.

Based on the assumptions above, monomer in the vapour phase for $X > X_f$ can be expressed as:

$$M_g = M_m P_m V_g/(RT) \qquad (X > X_f) \qquad (2.9)$$

where

$$V_g = V_{gxf} + \Delta V'_g \qquad (X > X_f) \qquad (2.10)$$

In the absence of the monomer phase, the shrinkage in the volume of the VCM-PVC mixture causes the pressure to drop. Hence, the pressure drop is the result of the vapour volume increase and is due to monomer from vapour diffusing into the polymer phase as polymerization proceeds.

The increment of vapour volume can be expressed as:

$$\Delta V'_g = (X - X_f)M_o(1/D_m - 1/D_p) \qquad (X > X_f) \qquad (2.11)$$

Substituting Eqs. (2.7), (2.10) and (2.11) into Eq.(2.9), one obtains an expression for the mass of monomer in the gas phase as:

$$M_g = \frac{M_m P_m}{RT}\left[(1.0-W_l)V_l + \frac{X_f M_o (1/D_m - 1/D_p)}{1.0 - D_{go}/D_m} + (X-X_f)M_o(1/D_m - 1/D_p)\right] \qquad (2.12)$$

The amount of monomer in the water phase can be expressed using Henry's Law:

$$P_m = HM_w/W_w \qquad (2.13)$$

where

$$P_m = P_t - P_w.$$

For convenience, Eq.(2.13) is rewritten as:

$$M_w = KW_w P_m/P_{mo} \qquad (X > X_f) \qquad (2.14)$$

where K is a dimensionless solubility constant defined by

$$K = P_{mo}/H.$$

The amount of monomer in the polymer phase can be expressed as a function of polymer volume fraction in the polymer phase.

$$M_p = M_o X D_m (1.0-\Phi_p)/(\Phi_p D_p) \qquad (2.15)$$

The weight of polymer in the system can be calculated from the definition given in Eq.(2.5):

$$W_p = M_o X \tag{2.16}$$

Substituting Eqs.(2.12)-(2.16) into Eq.(2.8), one obtains:

$$X = \frac{M_o - \frac{P_m M_m}{RT}\left[(1.0-W_1)V_r + X_f M_o \frac{(1/D_m - 1/D_p)D_{go}}{D_m - D_p}\right] - KW_w P_m/P_{mo}}{M_o[(1.0+D_m(1.0-\Phi_p)/(\Phi_p D_p) + P_m M_m(1/D_m - 1/D_p)/(RT)]}$$

$$(X > X_f) \tag{2.17}$$

Eq.(2.17) correlates conversion, temperature and the VCM partial pressure relationship at given operating conditions for $X > X_f$. The Polymer volume fraction in Eq.(2.17) can be found using the Flory-Huggins equation[15]:

$$\ln(P_m/P_{mo}) = \ln(1.0-\Phi_p) + (1.0-1/\bar{r})\Phi_p + \chi\Phi_p^2 \tag{2.18}$$

When the conversion is at the critical conversion X_f, the partial pressure of VCM is its saturated vapour pressure, that is

$$P_m = P_{mo} \qquad (X = X_f) \tag{2.19}$$

Thus, conversion X_f, at which the VCM partial pressure starts to drop, can be derived from Eq.(2.17) by replacing X, P_m with X_f, P_{mo}, respectively. That is

$$X_f = \frac{M_o - [D_{go}(1.0-W_l)V_r + KW_w]}{M_o[(1.0+D_{go}(1/D_m - 1/D_p)/(1.0-D_{go}/D_m) + D_m(1.0-\Phi_p)/(\Phi_p D_p)]} \qquad (2.20)$$

and Eq.(2.18) then becomes at the critical conversion:

$$\ln(1.0-\Phi_p)+(1.0-1/\bar{r})\Phi_p+\chi\Phi_p^2 = 0 \qquad (2.21)$$

From Eqs.(2.17) and (2.20), it is seen that the relationship between conversion and partial pressure of VCM depends on the initial reactor operating conditions and physical properties of VCM and PVC, but it is independent of the polymerization mechanism. Therefore, Eqs.(2.17) and (2.20) may be used in suspension, microsuspension and bulk (W_w=0) polymerization systems.

Furthermore, Eq.(2.20) may be used to estimate the saturation solubility of VCM in PVC, while Eq.(2.17) is used for condition of subsaturation pressures. Eq.(2.20) is also of important kinetic significance because it relates the kinetic parameter X_f with the VCM-PVC interaction parameter χ and reactor operational conditions.

2.2.2 Monomer Distribution Among phases During VCM Polymerization

For the suspension polymerization of vinyl chloride, with the above assumptions, the monomer mass balance is given by:

$$M_o = M_g + M_w + M_L + M_p + W_p \qquad (X \le X_f) \qquad (2.22)$$

The monomer mass balance for $X > X_f$ is given in Eq.(2.8).

The monomer weight fraction in the different phases is defined as:

$$F_i = M_i/M_o \qquad (i=g,\ w,\ m,\ p) \qquad (2.23)$$

Therefore, the task is to find F_i by calculating the amount of the monomer M_i in the different phases: vapour, water, polymer and monomer phase.

Monomer fraction in the vapour phase:

For $X \le X_f$, using Eq.(2.6), one has:

$$M_g = \frac{P_{mo} M_m}{RT}\left[(1.0-W_i)V_r + \frac{XM_o(1/D_m - 1/D_p)}{1.0-D_{go}/D_m}\right] \qquad (2.24)$$

Therefore, monomer weight fraction in the vapour phase is given by

$$F_g = \frac{P_{mo} M_m}{M_o RT}\left[(1.0-W_i)V_i + \frac{XM_o(1/D_m - 1/D_p)}{1.0-D_{go}/D_m}\right] \qquad (X \le X_f) \qquad (2.25)$$

For $X > X_f$, substituting Eq.(2.12) into Eq.(2.23), one obtains:

$$F_g = \frac{P_m M_m}{M_o RT}\left[(1.0-W_i)V_r + \frac{X_f M_o(1/D_m - 1/D_p)}{1.0-D_{go}/D_m} + (X-X_f)M_o(1/D_m - 1/D_p)\right]$$

$$(X > X_f) \qquad (2.26)$$

Monomer fraction in the water phase:

Substituting Eq.(2.14) into Eq.(2.23), one finds:

$$F_w = M_w/M_o = KW_w/M_o \qquad (X \le X_f) \qquad (2.27)$$

$$F_w = KW_w P_m/(P_{mo} M_o) \qquad (X > X_f) \qquad (2.28)$$

Monomer fraction in the polymer phase:

Because the composition of the polymer phase remains constant up to conversion X_f, the ratio of monomer to polymer weight in the polymer phase can be written as:

$$\frac{M_o - M_{gxf} - M_{wxf} - M_o X_f}{M_o X_f} = \frac{M_p}{M_o X} \qquad (X \le X_f) \qquad (2.29)$$

Hence,

$$F_p = X[M_o(1.0-X_f) - M_{gxf} - M_{wxf}]/(X_f M_o) \qquad (X \le X_f) \qquad (2.30)$$

where

$$M_{gxf} = \frac{M_m P_{mo}}{RT}\left[(1.0-W_i)V_r + \frac{X_f M_o (1/D_m - 1/D_p)}{1.0 - D_{go}/D_m}\right]$$

and

$$M_{wxf} = KW_w$$

When the conversion is greater than X_f, the monomer fraction in the polymer phase is given by:

$$F_p = [M_o(1.0-X)-M_g-M_w]/M_o \qquad (X > X_f) \qquad (2.31)$$

where M_g and M_w are given in Eqs.(2.12) and (2.14).

Monomer fraction in the liquid monomer phase:

$$F_m = [M_o(1.0-X)-M_g-M_w-M_p]/M_o \qquad (X \leq X_f) \qquad (2.32)$$

where M_g, M_w and M_p are given by Eqs.(2.24), (2.14) and (2.29), respectively.

Monomer fraction converted to polymer:

$$F_{PVC} = X \qquad (0 \leq X \leq X_L) \qquad (2.33)$$

Using Eqs.(2.17), (2.18), (2.20), (2.21) and (2.25)-(2.33), one can calculate the monomer distribution in phases as a function of conversion at given reaction conditions. This relationship is useful for the calculation of the monomer concentration in the kinetic model which will be developed in Chapters 4 and 5.

2.3 EXPERIMENTAL

The solubility of VCM in water and in PVC and the pressure/ conversion data in the temperature range 40-70°C were measured in order to find the parameters K and χ necessary to evaluate the present model.

The equipment used in these experiments consisted of an agitated

5-liter stainless steel reactor with a calibrated vacuum-pressure gauge. Temperature was maintained by a steam-and-water mixture that circulated in the jacket, which was controlled by a P. I. D. controller.

PVC used for the present measurements was made by the Rhone Poulenc Bulk Process (Diamond Shamrock/Alberta Gas Company, Fort Saskatchewan, Alberta, Canada and now B. F. Goodrich).

VCM was provided by the B. F. Goodrich Company (Niagara Falls, Ontario, Canada).

To the reactor was added a weighed amount of distilled, deionized water and a weighed amount of PVC powder. A weighed amount of monomer was injected into the reactor after the reactor was evacuated. Then the reactor temperature was raised progressively to each of the four temperature levels (40, 50, 60 and 70°C) used. The pressure reached a steady level after about 90 minutes for each temperature level.

Conversion was calculated using the relationship

$$X = PVC/(PVC + VCM) \tag{2.34}$$

Thus, conversion and partial pressure data were obtained by repeating this procedure.

The solubility of VCM in water was similarly determined in the same temperature range. Suspension polymerization experiments are described in Chapters 3 and 4.

2.4 RESULTS AND DISCUSSION

2.4.1 Solubility of VCM in Water

The solubility of vinyl chloride in water has been measured by a few authors,[16-21] but few data in the normal commercial polymerization temperature range are reported. Heretofore, a correlation between solubility and temperature has not been published.

The present results are shown in Figures 2.1 and 2.2 where the solubility is plotted against the relative pressure of VCM, (P_m/P_{mo}), at the temperature of measurements. P_{mo} is the vapour pressure of vinyl chloride monomer. It can be seen that the data follow Henry's Law over the entire pressure range. Therefore, the solubility constant K in Eq.(2.14) can be found using a least squares fit. The results are shown in Table 2.1 together with other reported data.[16,17,19-21] The present resuits are in agreement with the reported data at 50° and 60°C. However, at 40°C and at 70°C, present data are in less agreement with data reported in the literature.[17,20,21] The reasons for the deviations are not known.

The solubility constant calculated based on the present experimental data seems to be a weak function of temperature as shown in Figure 2.3. The following correlation was obtained using the least squares method:

$$K = 0.0472 - 11.6/T(^{\circ}K) \qquad (2.35)$$

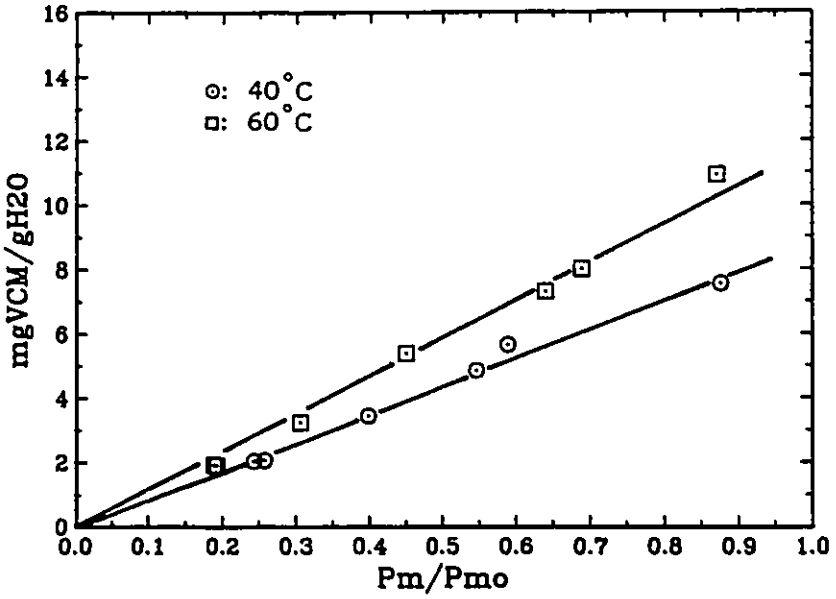

Figure 2.1. Solubility of VCM in water at temperatures 40°and 60°C.

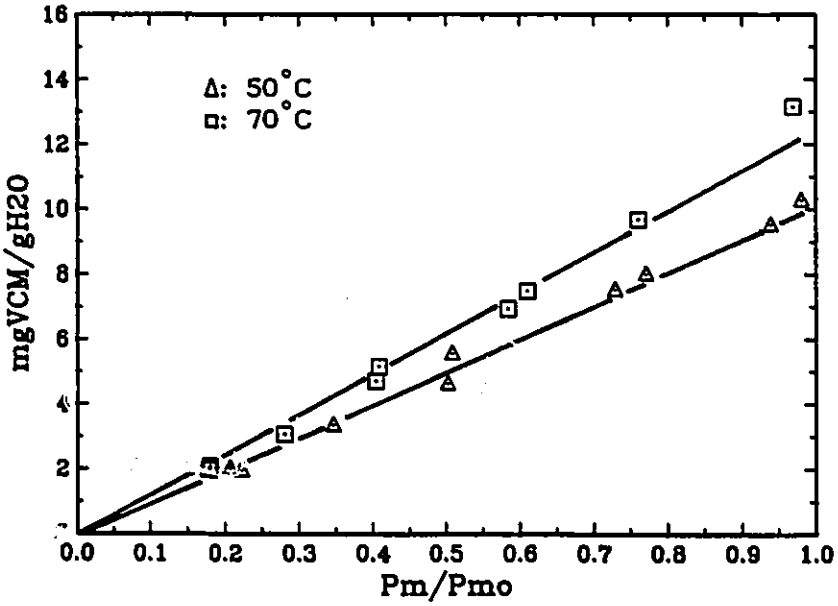

Figure 2.2. Solubility of VCM in water at temperature 50°and 70°C.

Table 2.1. Solubility constant of VCM in water at different temperatures.

Temperature °C	$Kx10^3$ Present	Literature	References
25		7.94, 9.05	[21], [20]
30		8.42, 9.56	[16], [17]
40	10.6	8.10	[17]
50	11.4	11.95, 11.28, 9.75	[16], [20], [21]
55		11.43	[21]
60	12.9	12.88	[17]
65		10.68	[21]
70	13.5	17.07	[17]
75		10.85, 10.86	[20], [21]
80		9.89	[21]

For suspension polymerization, the water phase is a surfactant solution. Hayduk et al[20] reported the effect of soap concentration on the solubility of VCM in water. When the soap concentration is more than 0.5-wt%, the solubility of VCM in soap solution increases, but when the soap concentration is less than 0.1-wt%, the soap concentration appears to have no effect on the solubility of VCM. Therefore, for the usual aqueous medium VCM polymerization systems where the soap concentration is less than 0.1-wt%, Eq.(2.35) can be used to estimate solubility of VCM in the water phase. Thus, within the usual polymerization temperature range, saturation solubility of VCM in water phase is around 1.0-1.5-wt%.

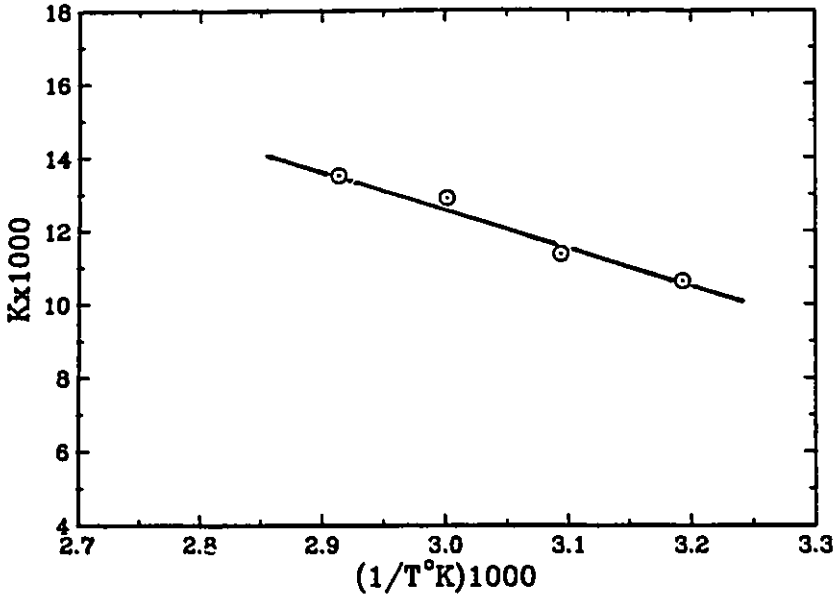

Figure 2.3. Temperature dependence of solubility constant of VCM in water.

2.4.2 VCM-PVC Interaction Parameter

Eq.(2.18) can be rewritten as follows:

$$\ln[\alpha_1/(1.0-\Phi_p)]-\Phi_p = \chi\Phi_p^2 \qquad (2.36)$$

where $\alpha_1=P_m/P_{mo}$, and the polymer molecular weight effect is neglected because the average degree of VCM polymerization is over 800 in the normal polymerization temperature range. Hence, if the left hand side of Eq.(2.36) is plotted against Φ_p^2, a straight line passing through the origin should result. The slope of the line is the interaction parameter χ. The present experimental results are shown in Figures 2.4 and 2.5. The interaction parameter was found by means of the least squares method.

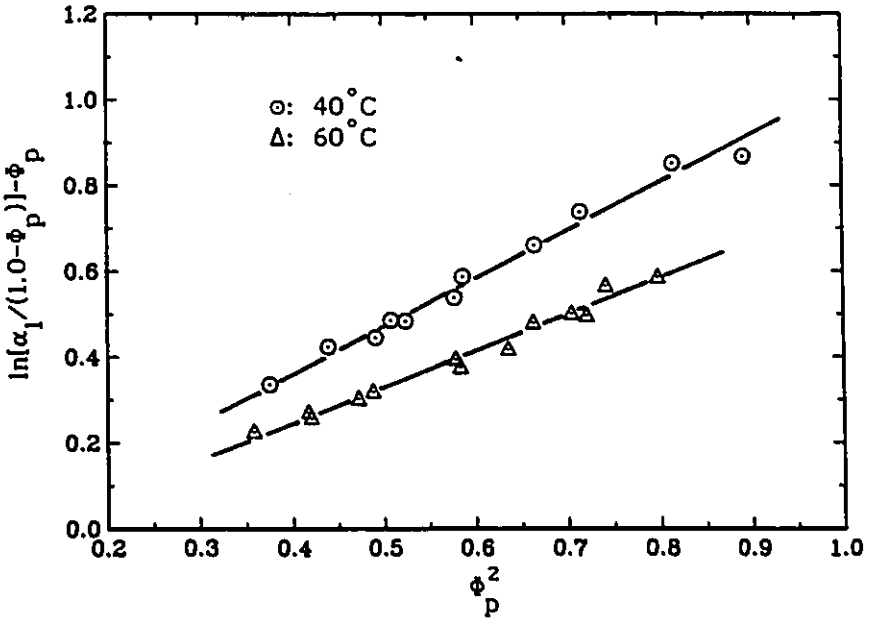

Figure 2.4. Solubility of VCM in PVC at temperature 40°and 60°C.

Gerrens et al[2] first used the Flory-Huggins equation in the emulsion polymerization of VCM and found χ=0.88 at 50°C. Berens[16,22,23] estimated χ=0.98 in VCM-PVC powder system from 30°to 60°C. Abdel-Alim[11] obtained χ=0.985 from plant data at 57°and 65°C. The present results are shown in Figure 2.6. It can be seen from Figure 2.6 that the present result (at 50°C) is in agreement with that of Gerrens et al.[2] The data show that the interaction parameter is a function of temperature. This is in disagreement with that of Berens.[16,22,23] On the basis of the present results, a correlation between the VCM-PVC interaction parameter and temperature is as follows:

$$\chi = 1286.4/T(^{\circ}K) - 3.02 \qquad (2.37)$$

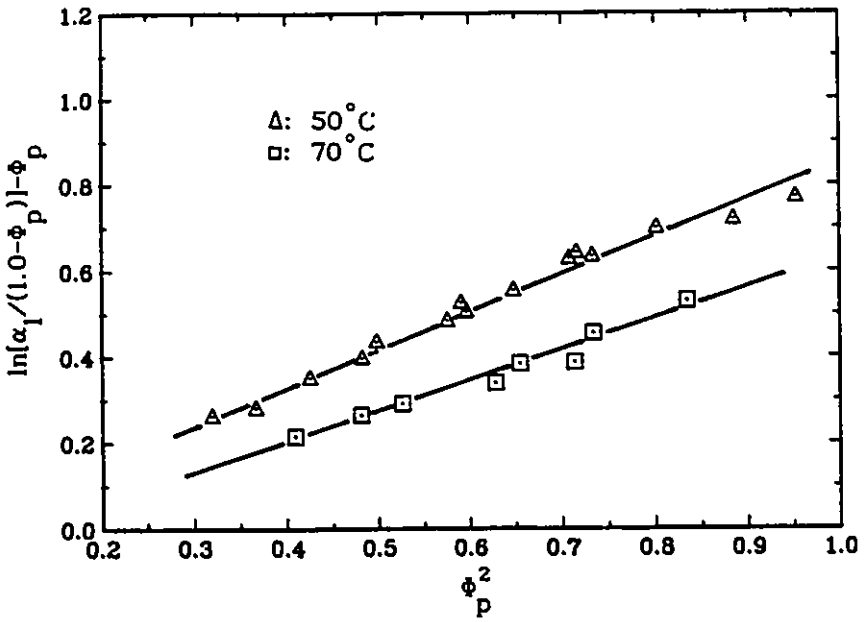

Figure 2.5. Solubility of VCM in PVC at temperature 50°and 70°C.

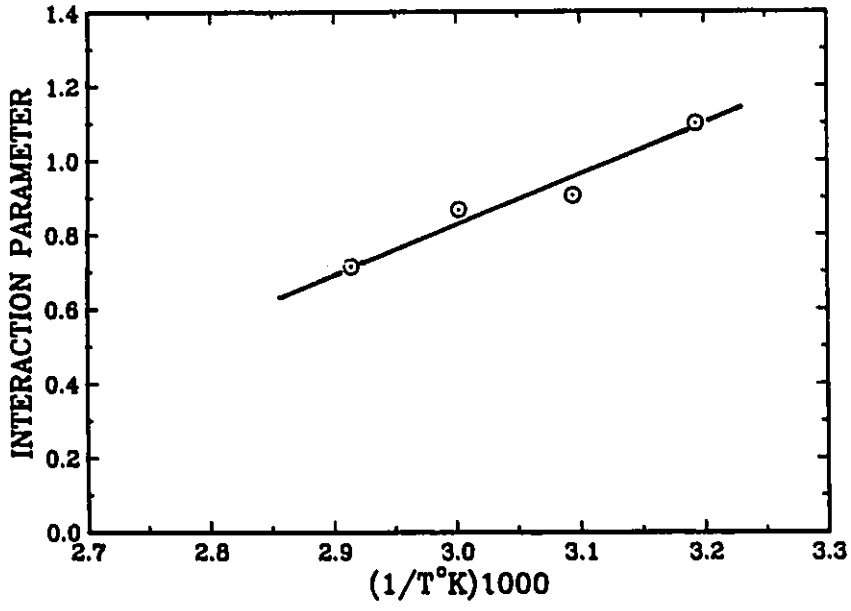

Figure 2.6. Temperature dependence of VCM-PVC interaction parameter χ.

Eq.(2.37) shows that χ decreases with increase in temperature. This suggests that PVC can increase swelling VCM with increase in temperature. This is in agreement with experimental observations.

Scamehorn et al[24] found that the VCM-PVC interaction parameter was a function of VCM volume fraction and their results are much lower than those shown above. These authors believed that the solubility of VCM in PVC may be a function of resin type.

2.4.3 Model Evaluation

From Eqs.(2.35) and (2.37), the solubility constant and VCM-PVC interaction parameter can be found at a given temperature. Some physical properties used in the present model are given as follows:

$$D_m = 947.1-1.746t-3.24\times10^{-3}t^2(^\circ C) \qquad (g/L)^{25,26} \qquad (2.38)$$

$$D_p = [\exp(0.4296-3.274\times10^{-4}T(^\circ K))]10^3 \qquad (g/L)^{27-29} \qquad (2.39)$$

$$P_{mo} = 1.27\times10^4\exp(-2.41\times10^3/T(^\circ K)) \qquad (atm)^{30} \qquad (2.40)$$

Combining the thermal expansion factor for PVC which can be found from Hellwege et al's data[27] with Pezzin et al[28] and Nakajima et al's[29] PVC density data leads to yield Eq.(2.39). Eq.(2.40) was obtained from Johnston's data.[30] In the present study, measurements of the vapour pressure data are in excellent agreement with Eq.(2.40). The water density can also be given as a function of temperature. Thus, all the

equations in the model can be solved by inputting initial conditions — temperature, monomer and water charged and the reactor volume.

The present experimental conditions are as follows:

reactor volume : 5.0 L

Temperature : 40°, 50°, 60°, 70°C

Initial monomer : 1200 g (PVC + VCM in this work)

Water : 2[illegible] g

Relationship between conversion and vapour pressure

The comparison of the experimental data with the model predictions is shown in Figures 2.7-2.10. Figure 2.7 shows that the model predictions are in excellent agreement with the equilibrium experimental data at different temperatures. In Figures 2.8 and 2.9, the data were obtained from experiments during VCM suspension polymerization. The conversions were measured by an on-line tracer method which will be described in Chapter 3. One can see that the present model predictions are in excellent agreement with the experimental data for suspension polymerization over the entire monomer conversion range (from zero to limiting conversion). In Figure 2.10, the data were taken from continuous experimental curves reported by Meeks.[4] Hence it is also shown that the present model predictions are consistent with experimental results for different polymerization systems (different suspending agent and initiator types). All these results suggest that the equilibrium assumption is valid for suspension polymerization under the present

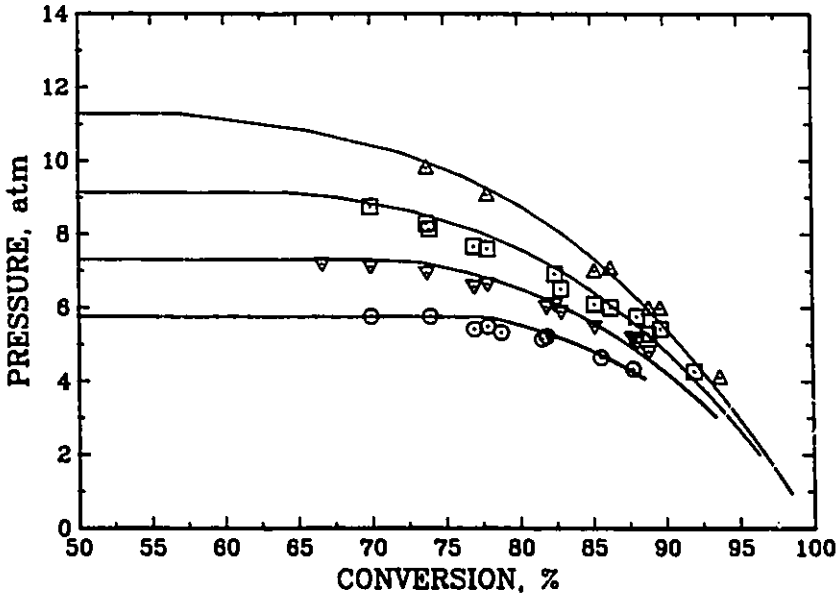

Figure 2.7. Conversion and temperature dependence of reactor pressure for equilibrium experiments.
⊙:40°C; ∇:50°C; □:60°C; Δ:70°C; ——— :model

experimental conditions. From Figures 2.7–2.10, it is clear that the model satisfactorily describes the relationship between conversion and partial pressure of VCM after monomer as a separate phase is depleted. Both the present model and experimental data clearly show batch reactor dynamics during suspension polymerization. This is the first successful attempt to quantitatively model batch reactor pressure development during suspension polymerization. The present model is not only useful for PVC quality control and PVC reactor safety calculations but is also useful for advanced kinetic studies.

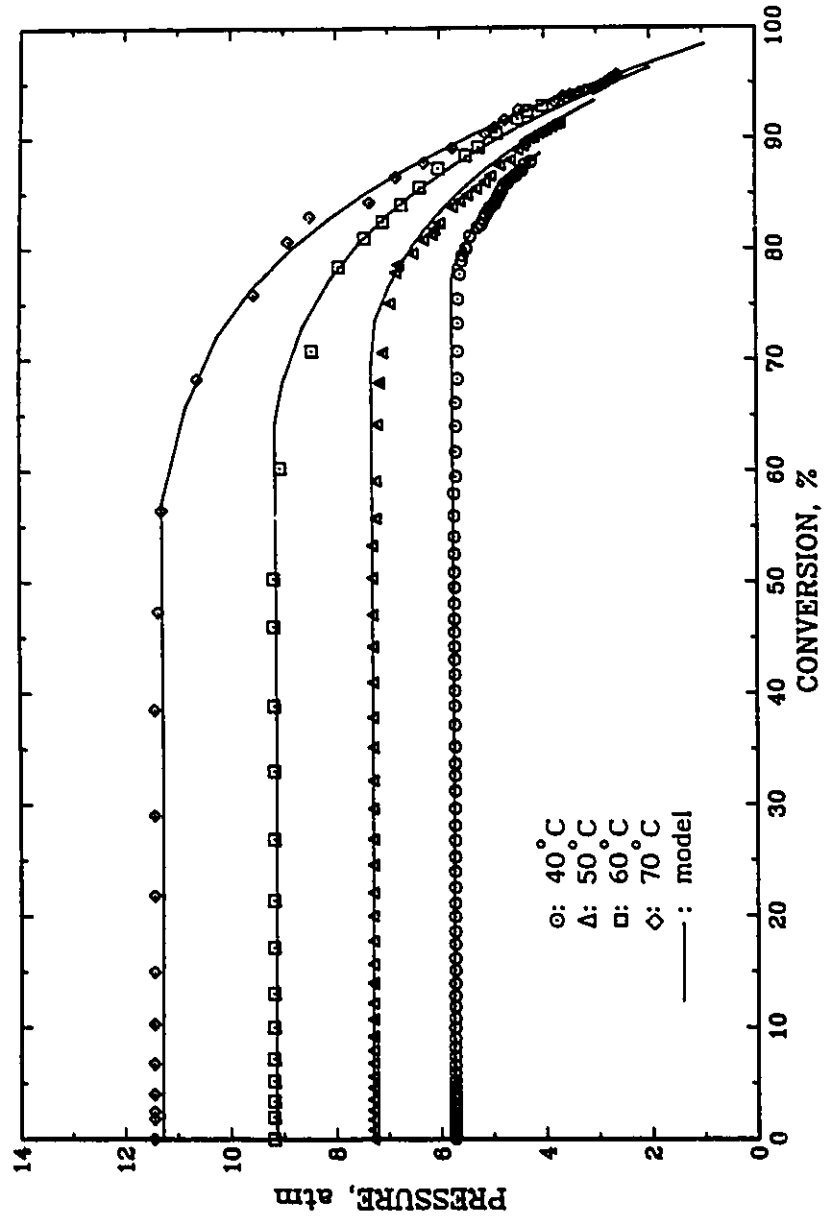

Figure 2.8. Conversion and temperature dependence of reactor pressure for suspension polymerization of VCM.

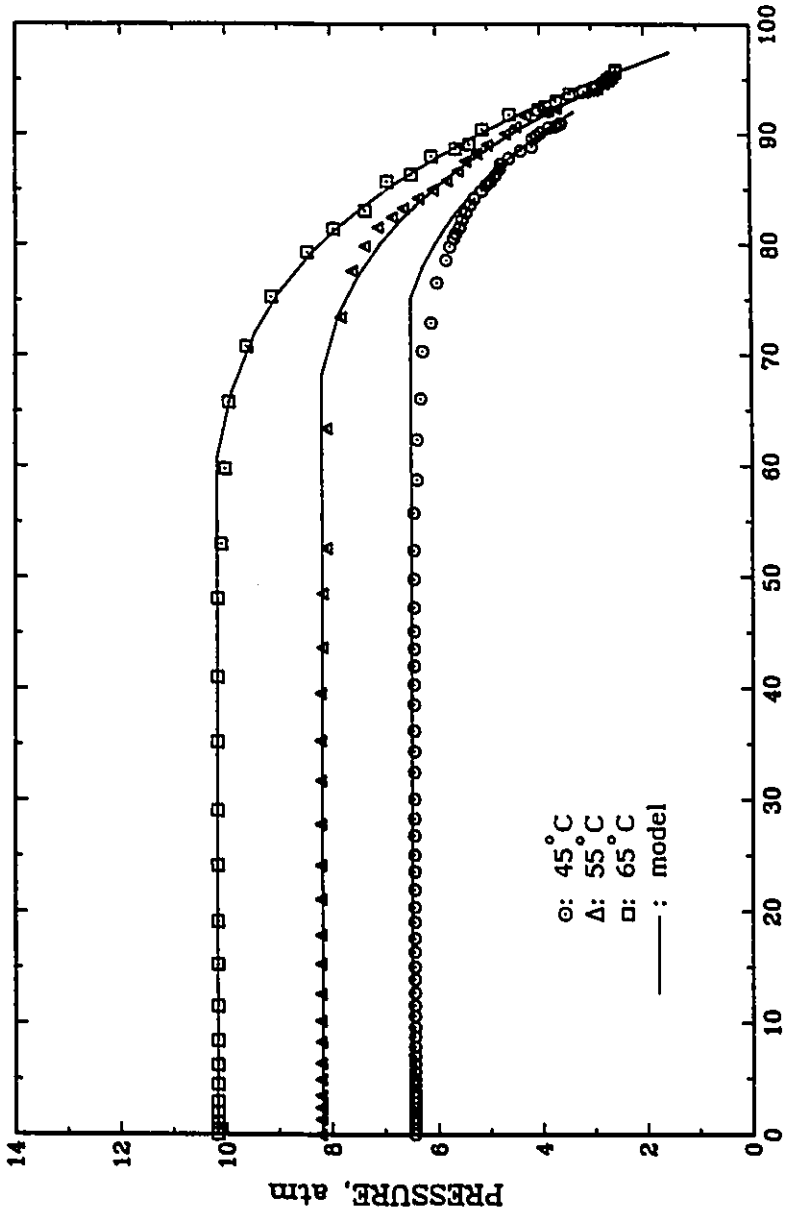

Figure 2.9. Conversion and temperature dependence of reactor pressure for suspension polymerization of VCM.

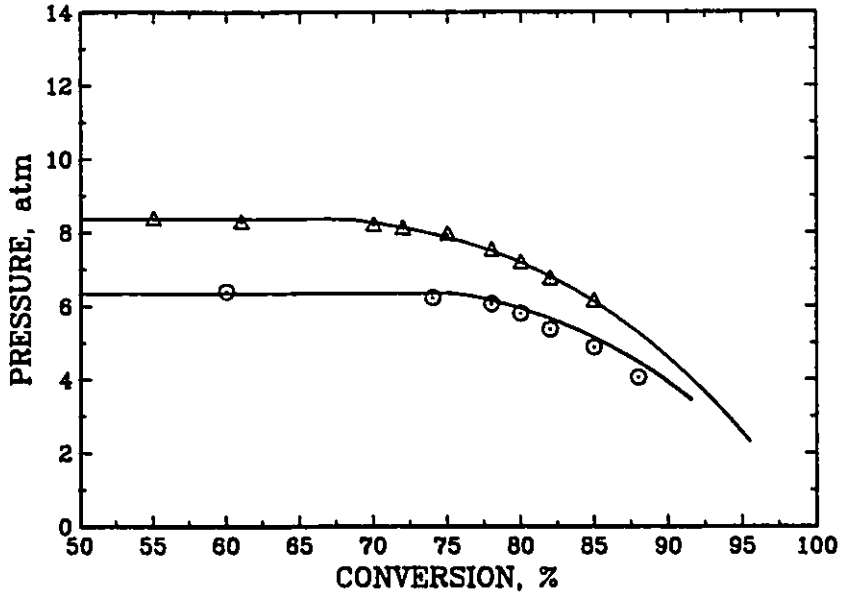

Figure 2.10. Conversion and temperature dependence of reactor pressure for suspension polymerization of VCM.
Meeks' data[4]: ⊙:44°C; Δ:56°C; ——— : model

Critical conversion X_f

Since Talamini[1] proposed a two-phase kinetic model on the basis of Gerrens' solubility data for VCM in PVC[2], a lot of data, on conversion at which reactor pressure begins to fall, have been reported, as shown in Table 2.2. However, a correlation between X_f and reactor operational conditions has not been reported prior to the present investigation.

Eq.(2.20) indicates that X_f is a function not only of temperature but also of other reactor operating variables. According to the initial conditions in this work, X_f was obtained at a given temperature, as shown in Table 2.3. X_f for bulk polymerization conditions was also

predicted using the present model with W_w=0. These results show the effect of VCM partition in the water phase on the conversion history for VCM polymerization. Plotting temperature versus X_f, one obtains a curve similar to the equilibrium solubility curve, as shown in Figure 2.11, however, it is not a true solubility curve because it depends on non-equilibrium parameters such as reactor charge. Solid and dotted lines are for suspension and bulk conditions, respectively. At the same fillage of the reactor, X_f in bulk polymerization is 2-2.5% greater than that in suspension polymerization. The circular points and the square points which are literature values shown in Table 2.2 were estimated from the solubility of VCM in PVC and from kinetic curves, respectively. Figure 2.11 shows that the modelling results are in satisfactory agreement with the literature values. Some data from the kinetic curves

Table 2.2. A relationship between critical conversion and temperature.

Temperature, °C	X_f	Methods	Reference
50	0.71	solubility (emulsion)	[2]
55	0.70	kinetics (suspension)	[3]
44-56	0.70-0.75	solubility (suspension)	[4]
65	0.687	solubility (suspension)	[5]
30	0.80	kinetics (bulk)	[6]
50	0.77	kinetics (bulk)	[6]
70	0.72	kinetics (bulk)	[6]
50	0.677	solubility (bulk)	[7]
60	0.63-0.64	kinetics (suspension)	[8]
50-60	0.70-0.75	kinetics (suspension)	[9]
-	0.70	kinetics (suspension)	[10]
57-65	0.776	solubility (suspension)	[11]
-	0.77	kinetics (bulk)	[12]
30-60	0.77	solubility (bulk)	[13]

Table 2.3. A relationship between critical conversion and temperature —— model predictions.

Temperature, °C	X_f suspension	bulk
0	0.909	0.922
10	0.886	0.902
20	0.858	0.877
30	0.823	0.845
35	0.803	0.827
40	0.781	0.805
45	0.756	0.781
50	0.726	0.752
55	0.693	0.719
60	0.653	0.680
65	0.606	0.632
70	0.550	0.575
75	0.479	0.502
80	0.390	0.409

are somewhat higher than those predicted from the present model because the conversion at which polymerization rate begins to decrease may not be the same as the conversion at which the vapour pressure starts to drop. In fact, the conversion at which polymerization rate begins to decrease strongly depends on the initiator systems used.[9] The polymerization rate begins to decrease either before, at or after the pressure starts to fall according to the activity of the initiator. Figure 2.11 can be used as a phase diagram for VCM polymerization. The left side of the curve indicates two-phase polymerization, and the right side of the curve represents single phase polymerization. Therefore, the present model is essential for advanced kinetic modelling. Figure 2.12 shows a comparison between model predictions and the present experimental data obtained using suspension polymerization. One may notice that the

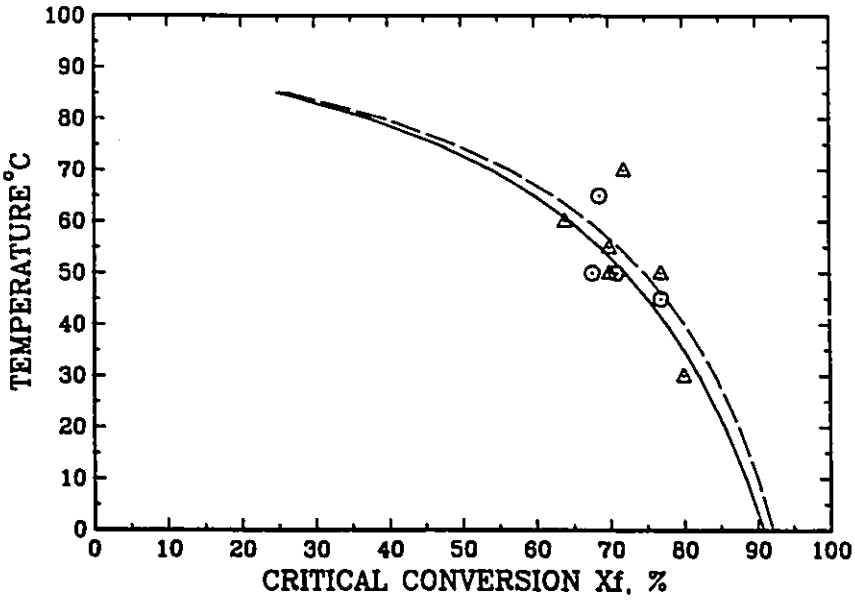

Figure 2.11. Temperature dependence of the critical conversion.
⊙:solubility data; Δ:kinetic data;
——— :suspension; – – – :bulk.

conversions at which the reactor pressure begins to fall are about 5-7% lower than the model predictions. However, conversions at 98-99% saturation pressure of VCM are in excellent agreement with the model predictions. This phenomenon suggests that the reactor pressure starts to fall before the liquid monomer is completely consumed for suspension polymerization. This can also be seen in Figures 2.8 and 2.9. The same phenomenon was noticed by Meeks[4] and Nilsson et al.[13] However, a similar phenomenon was not observed in emulsion polymerization, where the reactor pressure remains constant as long as VCM droplets are present.[13] Nilsson et al[13] explained the pressure starting to fall before liquid monomer is consumed during suspension polymerization as capillary condensation of

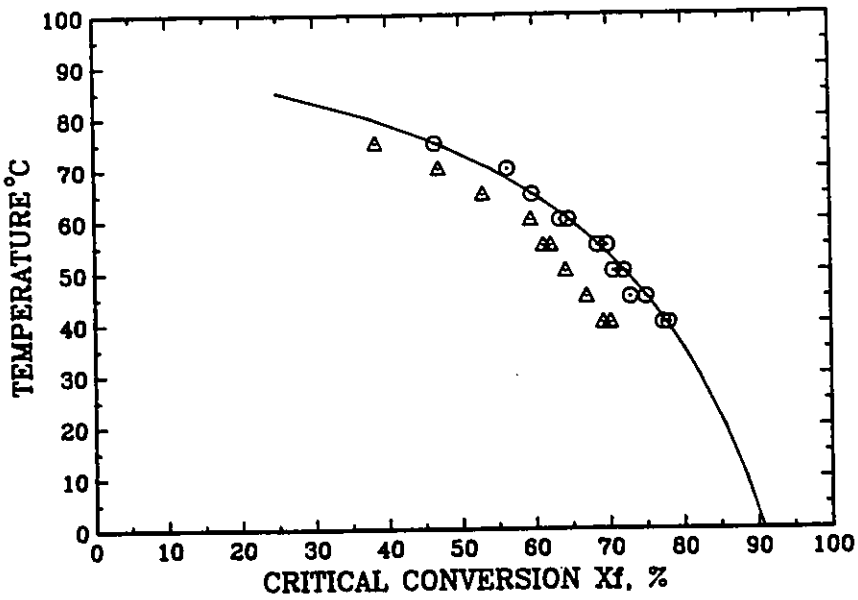

Figure 2.12. Temperature dependence of the critical conversion for suspension polymerization of VCM.
Δ:at pressure starting to drop; ⊙:at 98-99% P_{mo}
——— :model prediction.

monomer in the fine pores of the particles. Therefore, the pressure drop for suspension polymerization may depend on morphology of PVC particles. Reactor pressure drop could result from an increase in volume of the vapour phase, a decrease in the number of moles of VCM in the vapour phase or both. However, before the monomer phase is consumed, VCM will not diffuse from the vapour phase into the polymer phase. Thus, the only possibility to cause a pressure drop is due to an increase in volume of the vapour phase as a result of monomer being converted to polymer while the monomer in the pores of particles cannot exert its vapour pressure due to the rigid PVC structure at this conversion stage. Thus, the

pressure drop for suspension polymerization can be divided into two stages. The first stage is due to the increase in volume of the vapour phase and to the decrease in rate of monomer transfer from the monomer phase to the vapour phase because of the resistance from the fixed PVC particle structure. As a consequence the pressure drops slowly. The second stage is due to both the increase in the volume of the vapour phase and to the fact that VCM in the vapour phase diffuses into the polymer phase since the liquid monomer phase no longer exists. Pressure drops dramatically in this stage. The second stage starts at about when the pressure equals 98-99% of the vapour pressure of VCM based on the present experimental data. Therefore, strictly speaking, the monomer phase is consumed at a pressure which equals about 98-99% of the vapour pressure of VCM for suspension polymerization. For emulsion polymerization, the monomer phase (no initiator or radicals in the monomer phase) is not in the interstices of the polymer particles. Particles in emulsion polymerization system are similar to the primary particles in suspension PVC. The monomer phase can exert its vapour pressure to maintain the reactor pressure constant up to the very point where the monomer phase is consumed. Therefore, the reactor pressure starts to drop at X_f. This is the reason why the reactor pressure drops at a higher conversion compared with suspension polymerization as demonstrated by Nilsson et al[13] experimentally.

The effect of reactor fillage on X_f is shown in Figure 2.13. At a given temperature, the critical conversion X_f increases slightly with reactor fillage. For example, X_f will increase about 2% at 50-60°C when

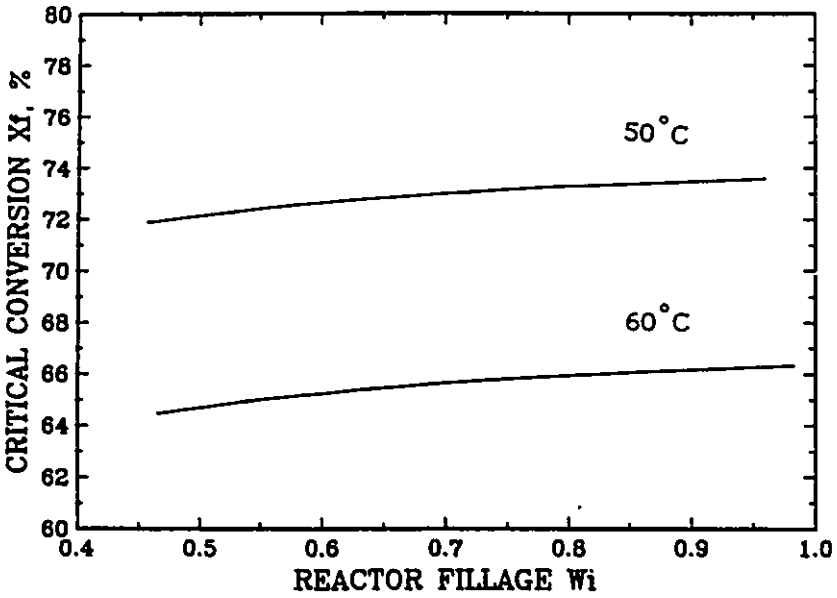

Figure 2.13. Effect of reactor fillage on the critical conversion.

the reactor fillage increases from 50% to 95%. This indicates that the reactor pressure will start to drop earlier if the reactor fillage is smaller at the same polymerization temperature.

Monomer Distribution

Generally, the monomer in the water and vapour phases has been neglected in previous kinetic studies. Chan et al[14] calculated the monomer distribution in vapour, water and polymer phases, respectively, using partition coefficients. It was found that monomer in the water and vapour phases is significant at the peak exotherm.

Once the relationship between the conversion and the reactor pressure is established, then the monomer distribution among phases can be found. From Eqs.(2.25)-(2.32), the monomer weight fraction in the different phases as a function of conversion can be obtained at given reactor operating conditions. The typical theoretical results are shown in Figure 2.14 together with the present experimental data. Under conditions shown in Figure 2.14, monomer in the water, vapour, and monomer phases is about 2.4%, 2.0% and 95.6%, respectively, at zero conversion. When conversion increases to X_f, monomer in the water, vapour and polymer phase is 2.4%, 2.5% and 23%, respectively. Monomer in the vapour and polymer phase reach maximum at X_f. The monomer in the water and vapour phase is about 20% of that in the polymer phase at the critical conversion X_f. This is in agreement with that estimated by Chan et al.[14] Therefore, neglecting the monomer dissolved in water and that in the head space of the reactor would cause a serious overestimation of the polymerization rate and result in an overdesign of the cooling system for the reactor. On the basis of the present results monomer distribution should be considered in the calculation of the monomer concentration for a valid kinetic modelling.

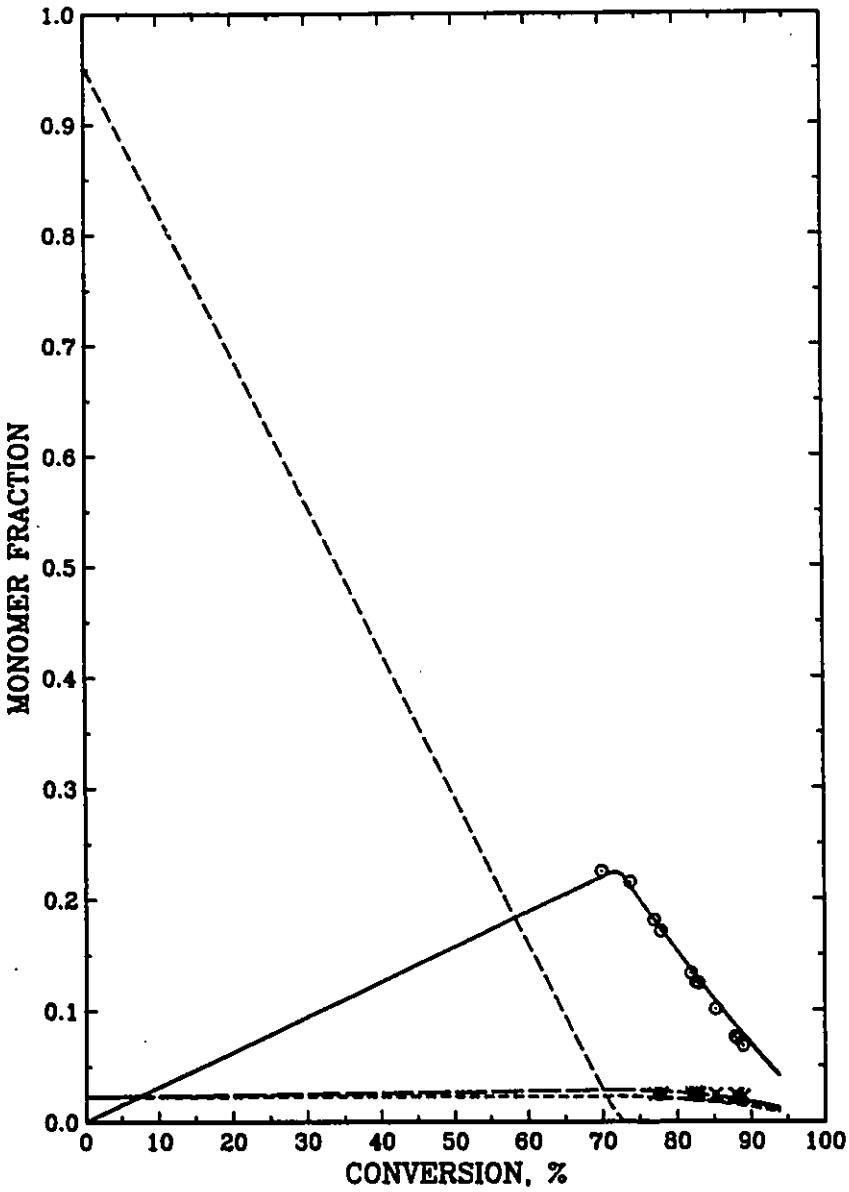

Figure 2.14. Monomer distribution during suspension polymerization of VCM at 50°C.
Δ:monomer fraction in the water phase;
x:monomer fraction in the vapour phase;
⊙:monomer fraction in the polymer phase.
– – – :monomer phase; ———:polymer phase;
— — :vapour phase; .....:water phase.

2.5 SUMMARY

In this chapter, a comprehensive model which predicts the reactor pressure/temperature/conversion relationship and monomer distribution during VCM suspension polymerization has been developed. A comparison of model predictions with the present and published experimental data confirms that the assumptions made in the model derivation are reasonable. Both the solubility constant of VCM in water and the VCM-PVC interaction parameter depend on temperature. The present model can satisfactorily describe the relationship between conversion and reactor pressure development over the entire conversion range and can be used to estimate terminal conversion with a pressure measurement and the pressure of the reactor under runaway conditions. The model also permits one to calculate the critical conversion at the point the monomer phase is consumed and to estimate the monomer distribution among phases. This kind of information should make polymerization kinetic models more reliable when used for PVC reactor calculations at high conversions.

2.6 REFERENCES

1. Talamini, G. J. Polym. Sci., A-2, 1966, 4, 535.

2. Gerrens, H., Fink, W. and Kohnlein, E. J. Polym. Sci., 1967, C16, 2781.

3. Crosato-Arnaldi, A., Gasparini, P. and Talamini, G. Makromol. Chem., 1968, 117, 140.

4. Meeks, M. R. Polym. Eng. Sci., 1969, 9(2), 141.

5. Hause, A. F. J. Polym. Sci., 1971, C33, 1.

6. Abdel-Alim, A. H. and Hamielec, A. E. J. Appl. Polym. Sci., 1972, 16, 703.

7. Ugelstad, J., Flogstad, H., Hertzberg, T. and Sund, E. Makromol. Chem., 1973, 164, 171.

8. Ravey, M., Waterman, J. A., Shorr, L. M. and Kramer, M. J. Polym. Sci., Polym. Chem. Ed., 1974, 12, 2821.

9. Xie, T. Y., Yu, Z. Z. Cai, Q. Z. and Pan, Z. R. J. Chem. Ind. and Eng. (China), 1984, No.2, 93.

10. Albright, L. F. Chem. Eng., 1967, 74, (June 5), 145.

11. Abdel-Alim, A. H. J. Appl. Polym. Sci., 1978, 22, 3697.

12. Kesall, D. G. and G. C. Maitland, 'Polymer Reaction Engineering' Ed. Reichert, K. H. and Geiseler, W., Munich, Vienna, New York, 1983, p131.

13. Nilsson, H., Silvegren, C. and Tornell, B. Angew. Makromol. Chem., 1983, 112, 125.

14. Chan, R. K. S., Langsam, M. and Hamielec, A. E. J. Macromol. Sci. Chem., 1982, A17, 969.

15. Flory, P. J. 'Principles of Polymer Chemistry', Cornell University Press, Ithaca, New York, 1953.

16. Berens, A. R. Angew. Makromol. Chem., 1975, 47, 97.

17. Benton, J. L. and Brighton, C. A. 'Encyclopedia of Polymer Science and Technology', Ed. Mark, H. F. and Gaylord, N. G., Vol. 14, John Wiley and Sons, Inc. 1971, p305.

18. Hayduk, W. and Laudie, H. AIChE Journal, 1973, 19(3), 1233.

19. Berens, A. R. Polym. Prepr., 1974, 15(2), 197.

20. Hayduk, W. and Laudie, H. J. Chem. Eng. Data, 1974, 19(3), 253.

21. Patel, C. B., Grandin, R. E., Gupta, R., Philips, E., M., Reynolds, C. E. and Chan, R. K. S., Polym. J., 1979, 11, 43.

22. Berens, A. R. Makromol. Chem. Macromol. Symp., 1989, 29, 95.

23. Berens, A. R. J. Appl. Polym. Sci., 1989, 37, 901.

24. Scamehorn, J. F. and Yang, K. Polym. Eng. Sci., 1978, 18, 841.

25. Dana, L. I., Burdick, J. N. and Jenkins, A. C. J. Amer. Chem. Soc., 1927, 49, 2801.

26. Arita, K. and Stannett, V. J. Polym. Sci.: Polym. Chem. Ed., 1973, 11, 1565.

27. Hellwege, K. H., Knappe, W. and Lehmann, P. Kolloid Z., 1962, 183, 110.

28. Pezzin, G. and Gligo, N. J. Appl. Polym. Sci., 1966, 10, 1.

29. Nakajima, A., Hamada, H. and Hayashi, S. Makromol. Chem., 1966, 95, 40.

30. Johnston, C. W. 'Encyclopedia of PVC, Ed. L. I. Nass, Vol. 1, Marcel Dekker, Inc., New York, 1976, p98.

CHAPTER 3

CONVERSION/TRACER RELATIONSHIP

3.1 INTRODUCTION

In Chapter 2, the reactor dynamics for VCM polymerization were described in detail. In the present chapter, a novel method for online conversion measurements is illustrated. This technique permitted extensive kinetic measurements.

Conversion measurements for polymerization can be classified as direct and indirect methods. The former analyzes the mass of monomer or polymer directly and the latter measures a property change of the polymerization system which relates to the mass of monomer or polymer formed. Typical experimental techniques for the measurement of monomer conversion include gravimetry, dilatometry, densitometry, viscometry, calorimetry, refractometry, spectrometry, chromatographic and thermoanalytical methods and other physico-chemical methods. A detailed review of these experimental techniques used to investigate free radical polymerization kinetics is given by Stickler[1] in a recent publication. However, most conversion monitoring techniques are difficult to apply to the suspension polymerization of VCM due to the mechanical difficulties in handling the heterogeneous mixture of water, monomer and polymer particles of various size at high pressure. The most common method for

conversion measurements of VCM suspension and bulk polymerization on a small scale is gravimetric analysis[2-6] which is performed by the time-consuming operations of loading reactors (glass ampoules, glass bottles, or stainless steel cells), polymerizing for a given time, venting the unreacted monomer, washing, filtering, drying and weighing the polymer formed. With gravimetric analysis, the difficulties and inaccuracies of polymerization times and initiator and monomer uniformity are obvious. Besides, it is very difficult with these experimental operations to avoid exposing the researcher to VCM, a health hazard.[7] Calorimetry, which is not burdened with the above problems, has been used to measure the polymerization rate,[8-11] and is particularly effective with large commercial reactors. The main limitation of this experimental technique is the effectiveness of the insulation of the reactor in preventing heat losses to the surroundings. Besides, this is an integral technique, errors in heat generation accumulate, and this yields errors in estimating conversions. Therefore, the potential for serious error in conversion estimates is great with small reactors.

More recently, a stirred batch reactor with a device sampling the VCM-PVC mixture was used for VCM kinetic studies.[12-15] This method is based on the periodic sampling of small volumes of representative samples of reaction mixtures and on the analysis of the monomer or polymer contained therein. A complicated sampling system is involved in handling the heterogeneous reactant mixture. Uncertainty is caused due to sampling error and the treatment of each sample under pressure.

A novel method which should avoid the above problems is the tracer analysis method developed in this research. This method involves the use of an internal calibration reference or tracer which is a chemically inert compound. The tracer should have high solubility in monomer and low solubility in water and polymer, and yet have an appropriate vapour pressure at the polymerization temperature. The tracer is added to the VCM polymerization system at the beginning of polymerization. With an increase in VCM conversion, the concentration of the tracer in the gas phase increases, giving a correlation between conversion and tracer concentration in the gas phase (it can readily be determined online by gas chromatography). Therefore, this method only analyzes the gas phase and avoids the treatment of VCM-PVC mixtures. Only one paper[16] reported the application of this method to a VCM polymerization system. However, the relationships between the vapour properties and conversion were not reported. A comprehensive model which relates conversion to tracer response has not been published prior to the present investigation. The development of a valid model which correlates conversion with tracer response, therefore, is vital for the application of the tracer method to monitor conversion during VCM polymerization. Hence, the objective of this chapter is to develop such a valid model which can be used to estimate VCM conversions online during suspension polymerization using tracer responses measured by gas chromatography; to estimate all the parameters involved; and to apply this method to conversion online measurements during VCM suspension polymerization.

3.2 MODEL DEVELOPMENT

The monomer distribution among phases during VCM suspension polymerization has been described in detail in Chapter 2. The present model relates conversion of monomer to polymer as a function of polymerization conditions and the tracer response by gas chromatography. During the course of suspension polymerization of VCM, the tracer exists in the vapour, monomer, water, and polymer phases, respectively. However, the partition of the tracer between these phases is quite different because the tracer selected should have a high solubility in VCM but low solubilities in water and PVC. During polymerization, the mass of VCM in the monomer phase decreases gradually with conversion; thus the concentrations of tracer in the monomer and gas phases increase. Therefore, one should be able to find a relationship between conversion and the tracer concentration in the vapour phase assuming equilibrium partitioning.

The model development is based on the following assumptions:

(1). The distributions of species among phases are in instantaneous equilibrium over the entire conversion range.

(2). The PVT properties of the vapour phase obey the Ideal Gas Law.

(3). The solubility of tracer in water, monomer and polymer phase follows Henry's Law.

(4). The solubility of PVC in the monomer phase is negligible.

(5). The solubility of tracer in the monomer is independent of PVC, ie. both the free monomer and the monomer swollen in PVC are treated as equivalent when calculating the tracer concentration.

According to these assumptions, both the tracer and monomer distributions in the phases of the polymerization system were considered and the following equations were theoretically derived.

At equilibrium, the fugacities of the tracer in the different phases are equal, ie.:

$$f_g = f_m = f_w = f_p \tag{3.1}$$

For an ideal gas,

$$f_g = Y_b P_t \tag{3.2}$$

According to Henry's Law, the fugacities of tracer in monomer, water and polymer can be written as:

$$f_l = K_{bl} X_{bl} \qquad (l = m, w, p) \tag{3.3}$$

Substituting Eqs.(3.2) and (3.3) into Eq.(3.1), one obtains:

$$Y_b P_t = K_{bw} X_{bw} = K_{bm} X_{bm} = K_{bp} X_{bp} \tag{3.4}$$

where X_{bw} and X_{bm} are mole fractions of tracer in the water and monomer, respectively. X_{bp} is the volume fraction of tracer in the polymer.

The total mass balance for the tracer is as follows :

$$B_m + B_p + B_g + B_w = B \tag{3.5}$$

The mass of tracer in the vapour phase is given by

$$B_g = \frac{P_t V_g}{RT} Y_b M_b \tag{3.6}$$

The mass of tracer in the water phase can be expressed as:

$$B_w = \frac{W_w P_t}{M_H K_{bw}} Y_b M_b \tag{3.7}$$

From Eq.(3.4), one can find B_p as:

$$B_p = \frac{K_{bm} B_m M_m M_o D_b X}{(M_o - M_o X - M_g - M_w) M_b K_{bp} D_p} \tag{3.8}$$

Substituting Eqs.(3.6)-(3.8) into Eq.(3.5), one obtains

$$B_m = \frac{(B - Y_b q)(M_o - M_o X - M_g - M_w) M_b K_{bp} D_p}{(M_o - M_o X - M_g - M_w) M_b K_{bp} D_p + K_{bm} M_m M_o D_b X} \tag{3.9}$$

From Eq.(3.4), Y_b is given by

$$Y_b = \frac{K_{bm} B_m M_m}{P_t (M_o - M_o X - M_g - M_w) M_b} \tag{3.10}$$

Combining Eqs.(3.9) and (3.10), one can obtain:

$$Y_b = \frac{K_{bm} M_m K_{bp} D_p B}{P_t [(M_o - M_o X - M_g - M_w) M_b K_{bp} D_p + K_{bm} M_m M_o X D_b] + q K_{bm} M_m K_{bp} D_p} \tag{3.11}$$

where

$$q = \frac{P_t V_g M_b}{R T} + \frac{M_w P_t M_b}{M_H K_{bw}} \qquad (3.12)$$

Eq.(3.11) relates the mole fraction of tracer in the gas phase to polymerization conditions over the entire conversion range. Initial value of Y_b can be obtained by setting the conversion to zero in Eq.(3.11), ie.:

$$Y_{bo} = \frac{K_{bm} M_m K_{bp} D_p B}{P_o (M_o - M_{go} - M_{wo}) M_b K_{bp} D_p + q_o K_{bm} M_m K_{bp} D_p} \qquad (3.13)$$

The mole fractions of tracer in the gas phase, Y_b and Y_{bo}, can be measured by gas chromatography since it is proportional to the area of the GC response, ie.:

$$Y_b = K_b A_b \qquad (3.14)$$

$$Y_{bo} = K_b A_{bo} \qquad (3.15)$$

Hence, the ratio of the mole fractions is equal to the ratio of tracer response areas determined by GC, that is

$$Y_b / Y_{bo} = A_b / A_{bo} = A \qquad (3.16)$$

Substituting Eqs.(3.11) and (3.13) into Eq.(3.16), one can get the following relation between tracer response and conversion:

$$A = \frac{P_o(M_o - M_{go} - M_{wo})M_b K_{bp} D_p + q_o K_{bm} M_m K_{bp} D_p}{P_t[(M_o - M_o X - M_g - M_w)M_b K_{bp} D_p + K_{bm} M_m M_o X D_b] + q K_{bm} M_m K_{bp} D_p} \quad (3.17)$$

The advantage in the use of the ratio of tracer response areas instead of the absolute tracer response area is that the constant of instrument, K_b, and the total mass of tracer charged are not required. Hence errors in the instrument constant and the tracer charge are avoided. Eq.(3.17) is the relation between tracer response and conversion. However, it is only an implicit form because M_g and q in the Eq.(3.17) are also a function of conversion. Expressions for M_g and V_g as a function of conversion have been derived in Chapter 2. Hence, M_g and q in Eq.(3.17) can be given by

$$M_g = M_{g1} + X M_{gx} \quad (3.18)$$

$$q = q_1 + X q_x \quad (3.19)$$

Substituting Eqs.(3.18) and (3.19) into Eq.(3.17), one can get the following explicit relation between conversion and tracer response:

$$X = \frac{A(P_t M_{l1} M_b + q_1 K_{bm} M_m) - (P_o M_{lo} M_b + q_o K_{bm} M_m)}{A[P_t(M_o + M_{gx})M_b - K_{bm} M_m M_o D_b / (K_{bp} D_p) - q_x K_{bm} M_m]} \quad (3.20)$$

where

$$M_{li} = M_o - M_{gi} - M_{wi}$$

$$M_{lo} = M_o - M_{go} - M_{wo}$$

$$q_o = \frac{P_o M_b}{R\ T}(1.0-W_l)V_r + \frac{W_w M_b P_o}{M_H K_{bw}}$$

$$M_{go} = \frac{M_m P_{mo}}{R\ T}(1.0-W_r)V_r$$

$$M_{wo} = K\ W_w$$

When $X < X_f$:

$$M_{wl} = M_{wo}$$

$$q_l = q_o$$

$$M_{gl} = M_{go}$$

$$q_x = \frac{M_b P_t M_o (1/D_m - 1/D_p)}{R\ T\ (1.0 - D_{go}/D_m)}$$

$$M_{gx} = \frac{M_m P_{mo} M_o (1/D_m - 1/D_p)}{R\ T\ (1.0 - D_{go}/D_m)}$$

When $X \geq X_f$:

$$q_f = (1.0 - W_l)V_r + X_f M_o (1/D_m - 1/D_p)[1/(1.0 - D_{go}/D_m) - 1.0]$$

$$q_l = \frac{P_t M_b Q_f}{R\ T} + \frac{W_w M_b P_t}{M_H\ K_{bw}}$$

$$M_{gl} = \frac{M_m P_m q_f}{R\ T}$$

$$q_x = \frac{P_t M_o M_b (1/D_m - 1/D_p)}{R\ T}$$

$$M_{gx} = \frac{P_m M_o M_m (1/D_m - 1/D_p)}{R\ T}$$

$$M_{wl} = K\ W_w P_m / P_{mo}$$

Eq.(3.20) shows that the conversion is an explicit function of tracer response and polymerization conditions over the entire conversion range. This is a general model for the tracer method. If Henry's Law

constants K_{bm}, K_{bw} and K_{bp} are given, Eq.(3.20) is ready to be used to calculate the conversion given tracer response and polymerization conditions.

3.3 EXPERIMENTAL

To evaluate the model, tracer responses and conversions must be measured and Henry's Law constants in the model calculated.

The equipment used for the experiments included a Hewlett Packard (5880 A) Gas Chromatograph (GC) with an automatic gas sampler controlled by a microcomputer, and an agitated 5-L stainless steel reactor using the same conditions as those described in Chapter 2. The gas sample flows through the top valve of the reactor and into the GC via a pressure regulator, a rotameter and a gas sampler. The flowrate of the gas mixture was controlled to within 5-7 mL/min at atmospheric pressure. The volume of the gas sampler is about 0.35 mL.

n-Butane was selected as the tracer for the present work, because it is a chemically inert compound (its chain transfer activity is negligible —— measurements of molecular weight of PVC with and without n-butane were done), and has an appropriate vapour pressure. It also displays a suitable retention time and has a reasonable distribution among the phases. For a non-reacting mixture system, the reactor was filled with a weighed amount of distilled, deionized water, and a

weighed amount of PVC powder. A weighed amount of n-butane (~1% based on VCM) and monomer were injected into the reactor respectively after the reactor was evacuated. The reactor temperature was then raised progressively to each of the temperature levels used. The concentration of n-butane in the vapour phase was determined by GC online. Similarly, for the suspension polymerization of VCM, the stabilizer and initiator were charged into the reactor instead of PVC powder. The resulting PVC product was weighed to get the conversions. Thus, tracer response and conversion data at different temperatures can be obtained by repeating this procedure. The solubility of n-butane in VCM was similarly determined.

The VCM and PVC used in the experiments were the same as those described in Chapter 2.

Stabilizer: polyvinylalchohol (KP-08) (degree of hydrolysis was 71-75 mole%) and initiator: Bis(4-tert-butylcyclohexyl) peroxydicarbonate (Perkadox 16-W40) (40% aqueous suspension) were provided by AKZO Chemicals. Azobis(isobutyronitrile) (AIBN) recrystallized was used as an initiator for polymerization at higher temperatures.

n-Butane (CP. grade) was purchased from Canadian Liquid Air Company.

The experimental conditions are as follows:

Preparation of H_2O/VCM/PVC inert mixtures (ie.: non-reacting mixtures):

Reactor volume	:	5.0 L
Temperature	:	40°, 50°, 60°, 70°C
Initial monomer	:	445–1841 g (PVC+VCM in this case)
Water	:	2500 g
n-Butane	:	~1-wt% (based on monomer)

Suspension polymerization:

Temperature range	:	40–80°C
Initial monomer	:	1116 g
Water	:	2232 g
Stabilizer	:	0.08-wt% (based on water)
Initiator	:	various amounts
n-Butane	:	~1-wt% (based on initial monomer)

The gas chromatograph had a Poropak QS column (80/100 mesh, diameter 3.2 mm, length 3.66 m). The analysis conditions were as follows: carrier gas helium, 37.5 mL/min; oven and injection temperature, 150°C; thermal conductivity detector temperature, 200°C.

3.4 RESULTS AND DISCUSSION

To calculate the conversions of VCM with Eq.(3.20), one needs the area of the tracer response using the vapour mixture sample. Therefore, appropriate operating conditions of the GC should be set to clearly separate the peaks for n-butane and VCM. Under the present

experimental conditions (mentioned above), the GC responses were obtained as shown in Figure 3.1. One can see that there is very good separation between VCM and n-butane under the present GC conditions. According to the retention time of n-butane shown in the Figure, the run time of the GC can be set for six minutes with an additional output time of one or two minutes. Therefore, the online gas sampler controlled by a microcomputer can automatically sample every seven or eight minutes. This sampling period is adequate for kinetic studies.

There are three Henry's Law constants in the model which, unfortunately, cannot be estimated independently using measured conversions and tracer responses. Independent experiments, therefore, must be carried out to obtain these parameters. If two of them are known the remaining one can be estimated using nonlinear estimation techniques.

3.4.1 Solubility of n-Butane in Water and VCM

Extensive data have been published on the solubility of n-butane in water.[17] The Henry's Law constant for n-butane in water has been calculated from twelve sources over the temperature range, 15–76.1°C, as shown in Figure 3.2. There is an excellent linear relationship between K_{bw} and inverse absolute temperature. The following correlation was obtained using the least squares estimation.

$$K_{bw} = (5.78-1580/T^{\circ}K)10^{5} \quad \text{(atm)} \qquad (3.21)$$

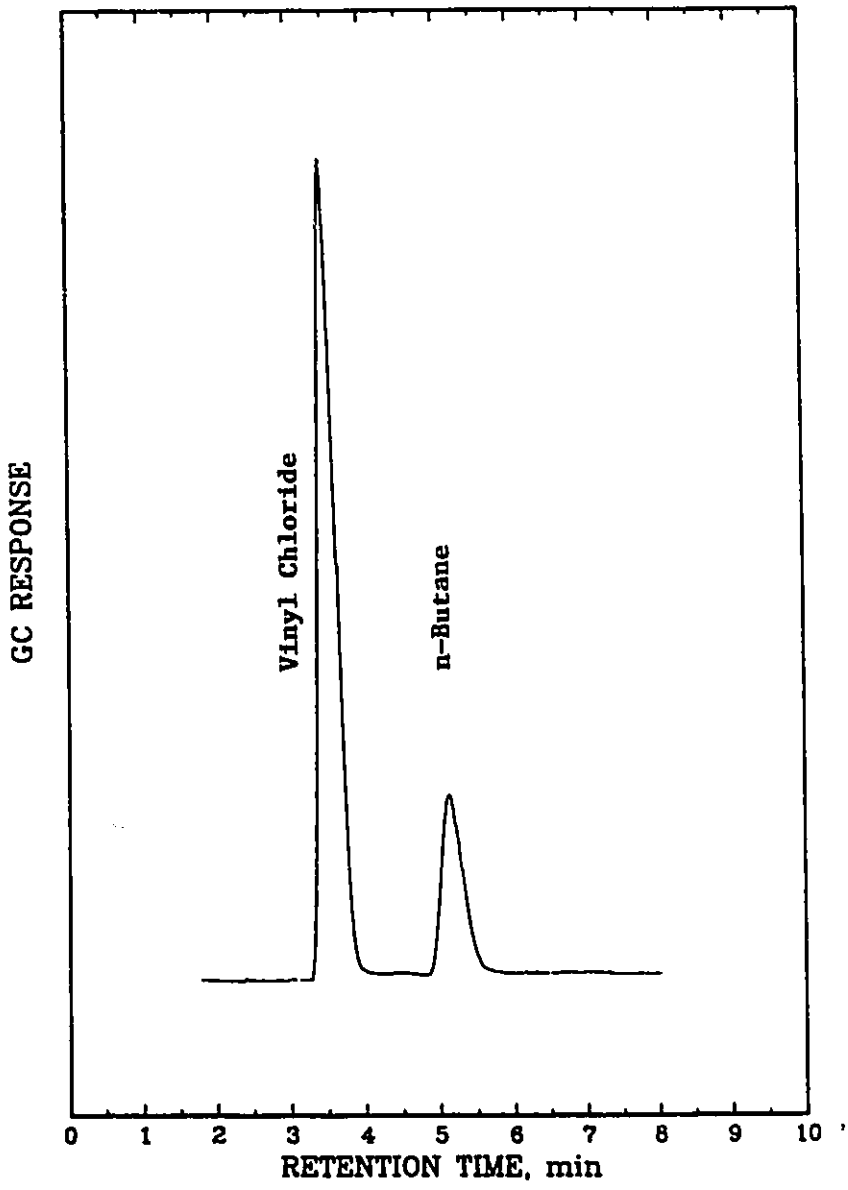

Figure 3.1. GC detector responses for vinyl chloride and n-butane under the present GC conditions.

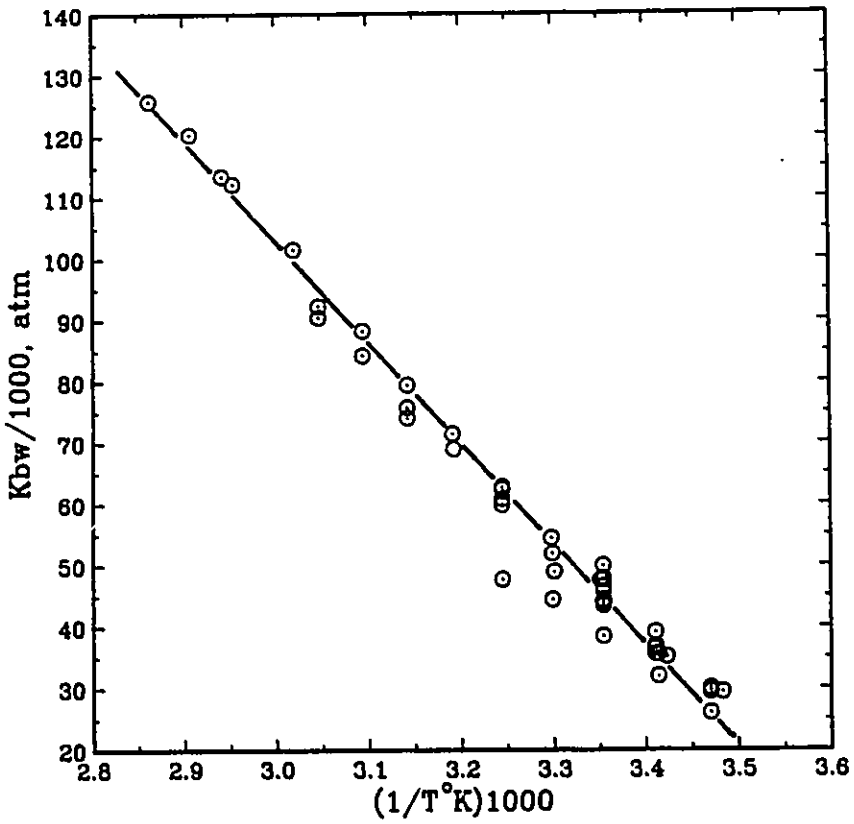

Figure 3.2. Temperature dependence of Henry's Law constant for n-butane in water.

The solubilities of n-butane in VCM and PVC have not been previously reported. The solubility of n-butane in VCM measured in the present work is shown in Figures 3.3 and 3.4. The partial pressure of n-butane was obtained by determining the mole fraction of n-butane in the gas phase with a GC and the total pressure. The mole fraction of n-butane in liquid VCM was obtained by gravimetry. From Figures 3.3 and 3.4, one can see that the solubility of n-butane in VCM obeys Henry's

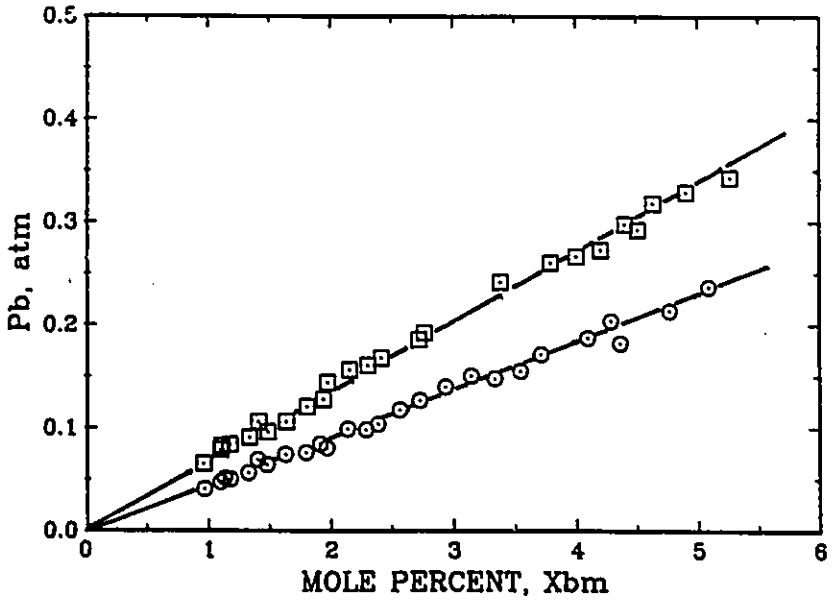

Figure 3.3. Solubility of n-butane in vinyl chloride monomer. ⊙:40°C; □:60°C.

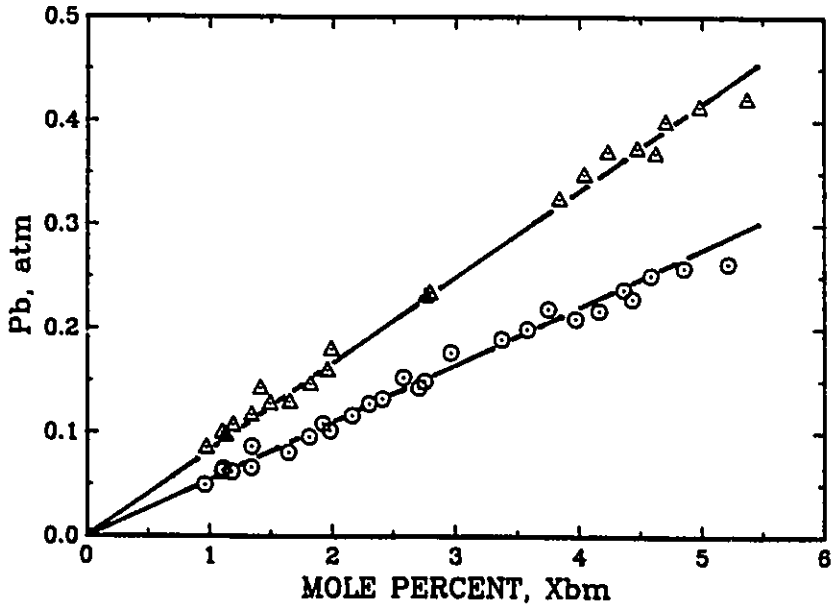

Figure 3.4. Solubility of n-butane in vinyl chloride monomer. ⊙:50°C; Δ:70°C.

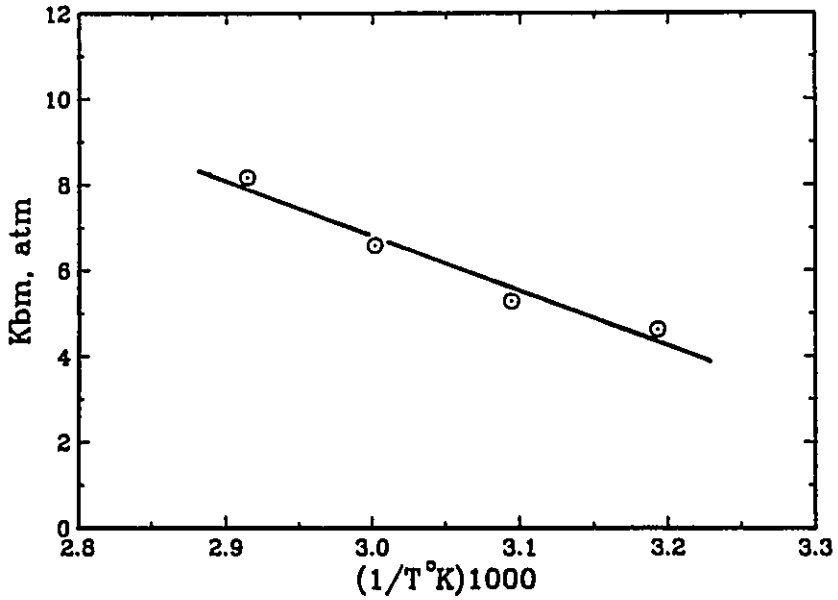

Figure 3.5. Temperature dependence of Henry's Law constant for n-butane in vinyl chloride monomer.

Law within the range of experimental concentrations of interest. The Henry's Law constant of n-butane in VCM can be obtained using least squares analysis with the data shown in these figures. The results are shown in Figure 3.5. The correlation of K_{bm} with temperature obtained, again, using the least squares method is the following:

$$K_{bm} = 45.3 - 12800/T\ ^{\circ}K \qquad \text{(atm)} \qquad (3.22)$$

Both K_{bw} and K_{bm} increase with increasing temperature, hence the solubility of n-butane in water and VCM decreases with increasing temperature at the same partial pressure.

3.4.2 Model Evaluation

Once K_{bw} and K_{bm} are known, K_{bp} can be estimated from Eq.(3.20) by nonlinear regression methods. The physical properties of VCM and PVC and critical conversion X_f used in the model are given in Chapter 2. The density of n-butane is given by

$$D_b = 601.7 - 1.14\ t\ (^\circ C) \qquad (g/L) \qquad (3.23)$$

Eq.(3.23) was obtained from the literature data[18-20] in the temperature range, 0-80°C.

(1). Inert Mixture System

With inert mixtures of H_2O/VCM/PVC, the solubility constant of n-butane in PVC, K_{bp}, was estimated using Eq.(3.20) and a nonlinear regression method. The results are shown in Figure 3.6. With K_{bp} values, one can notice that the solubility of n-butane in PVC changes dramatically with temperature. Unlike the solubility of n-butane in water and VCM, the solubility in PVC increases with increasing temperature. The correlation between K_{bp} and temperature is given by

$$K_{bp} = 2.28\times10^{-17}\exp(15000/T\ ^\circ K) \qquad (atm) \qquad (3.24)$$

Using K_{bw} K_{bm}, K_{bp} values, one can estimate the concentration of n-butane in the different phases. For example, the solubility of n-butane in the monomer is about 5 orders of magnitude higher than that in water, and about 2 orders of magnitude higher than that in PVC at 50°C. Therefore, as expected, n-butane dissolves mainly in monomer,

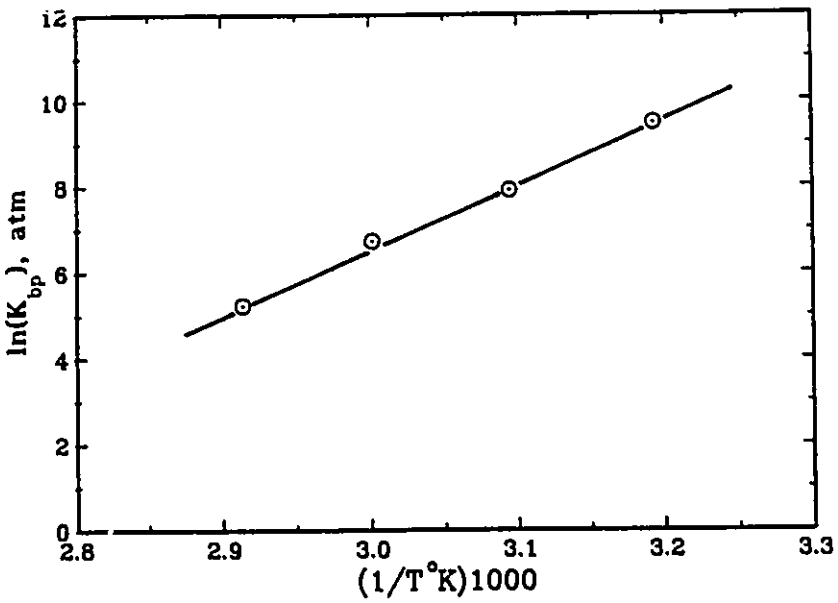

Figure 3.6. Temperature dependence of apparent solubility constant for n-butane in PVC.

dissolves slightly in polymer, and hardly dissolves in water.

Using the parameters developed above and knowing the area of the n-butane peak measured by GC and the experimental conditions, one can calculate conversions using Eq.(3.20). Typical results are shown in Figure 3.7. The points are the present experimental data; the solid line is the model prediction. This figure shows that the model agrees well with the experimental data. The standard deviation between experimental data and model predictions for the conversion is within 2-3%. One can also see that the ratio of n-butane areas is very sensitive to the conversion, particularly at higher conversions. Hence n-butane is a good tracer for the conversion measurements during VCM suspension polymerization.

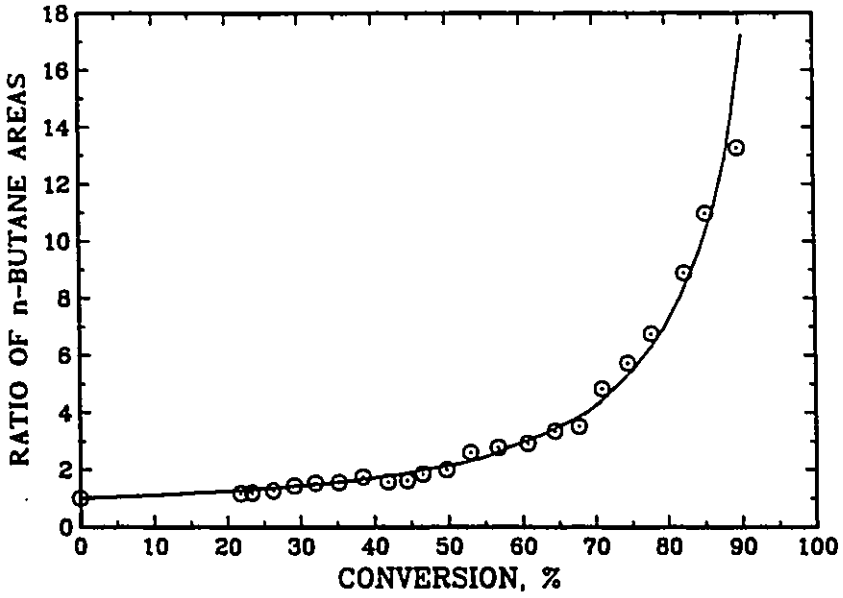

Figure 3.7. Ratio of GC detector response areas for n-butane versus conversion of VCM at 60°C.
⊙:experimental data; ——— : model prediction.

(2). Suspension Polymerization System

Figure 3.7 shows that the model is in good agreement with the equilibrium data measured using non-reacting mixtures; however, one can not besure how close to equilibrium one is for conversion measurements during suspension polymerization of VCM. Therefore, it is necessary to carry out VCM suspension polymerizations to reexamine the validity of the parameter K_{bp} estimated using equilibrium data under polymerization conditions. Surprisingly, the conversions calculated by the model with equilibrium constant K_{bp} are much lower than those measured by gravimetry except in the high conversion range where agreement is reasonable as shown in Figure 3.8. Therefore, the parameter K_{bp} estimated using inert

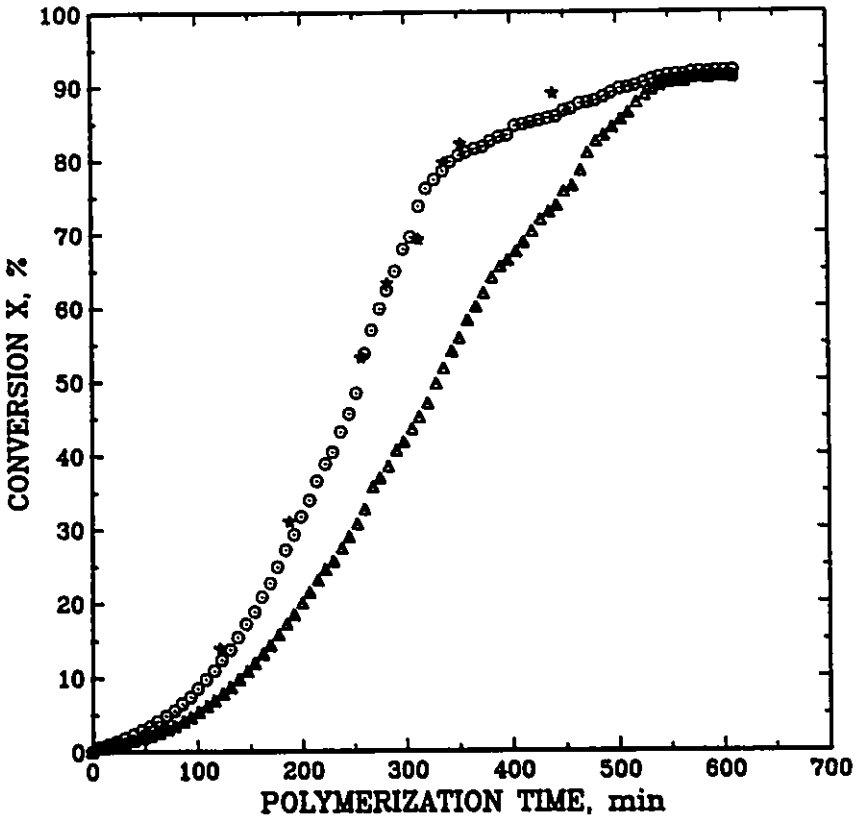

Figure 3.8. Comparison between the calibrations based on gravimetry measurements and the equilibrium model for suspension polymerization of VCM at 50°C.
Perkadox 16-W40, [I] = 0.15-wt% (based on pure peroxide).
⊙: n-butane tracer measurements using parameters obtained via gravimetry measurements.
Δ: n-butane tracer measurements using equilibrium parameters.
*: gravimetry measurements.

equilibrium mixtures is not valid for this suspension polymerization system. In other words, for the purpose of conversion measurements during polymerization, the system must be recalibrated based on gravimetry. The assumption of instantaneous equilibrium for the tracer is not

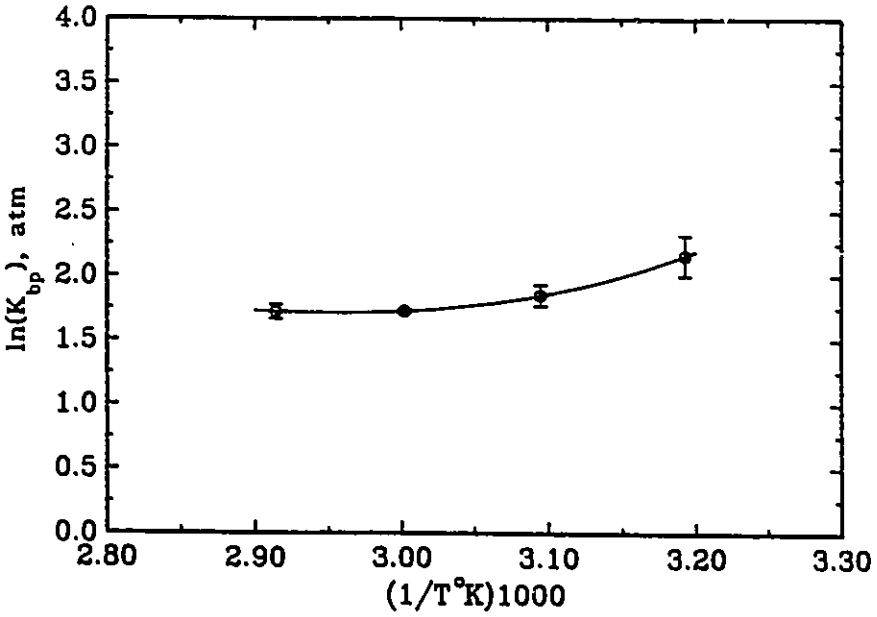

Figure 3.9. K_{bp} versus temperature for suspension polymerization of vinyl chloride (nonequilibrium values measured by gravimetry).

valid under these experimental conditions.

The parameter K_{bp} estimated using suspension polymerization data is much smaller than that found using inert mixtures (see Figure 3.6) as shown in Figure 3.9. Unlike the inert mixture system, the temperature dependence of K_{bp} for suspension polymerization is nonlinear. The data are best fitted by the following empirical equation:

$$\ln(K_{bp}) = a + \frac{b}{T} + \frac{c}{T^2} + \frac{d}{T^3} \qquad (3.25)$$

where

$$a = -1.73\times10^{2}$$

$$b = 1.95\times10^{5}$$

$$c = -7.18\times10^{7}$$

$$d = 8.77\times10^{9}$$

The model is in agreement with equilibrium data of the inert system over the entire conversion range as shown in Figure 3.7. However, the model with modified K_{bp} (according to Eq.(3.25) can only fit the data for suspension polymerization up to about 80% conversion as shown in Figures 3.10 and 3.11. The standard deviations between experimental data and model prediction shown in Figures 3.10 and 3.11 are within 1-3%.

At higher conversions, the GC responses of n-Butane increase dramatically and fall on a single curve for the present experimental temperature range (40-80°C) as shown in Figure 3.12. The relationship between conversion and ratio of n-Butane areas can be expressed by the empirical equation as follows:

$$X = 79.5 + 1.25A - 4.24\times10^{-2}A^{2} + 5.76\times10^{-4}A^{3} \qquad (3.26)$$

where the constants were estimated by a nonlinear regression.

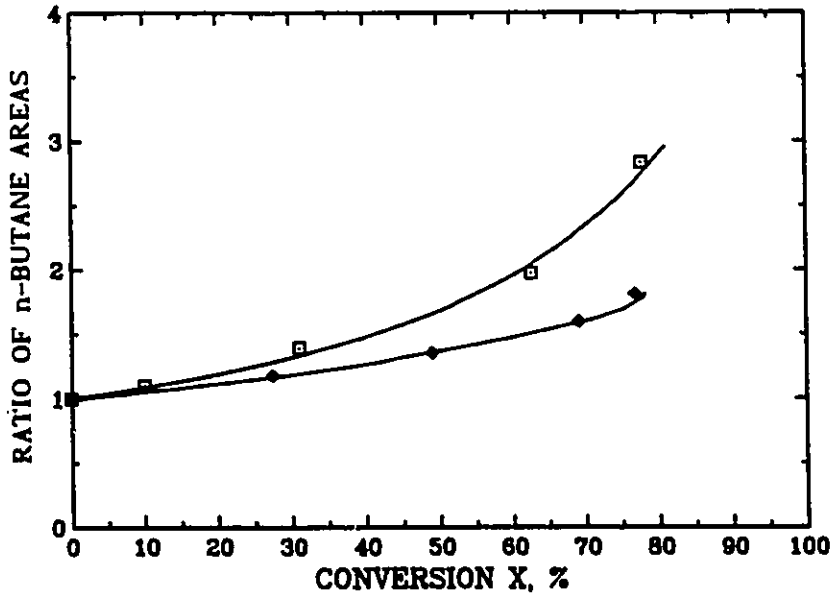

Figure 3.10. Ratio of n-butane areas versus conversion for suspension polymerization of VCM.
□: at 40°C, ◇: at 60°C, —— :model.

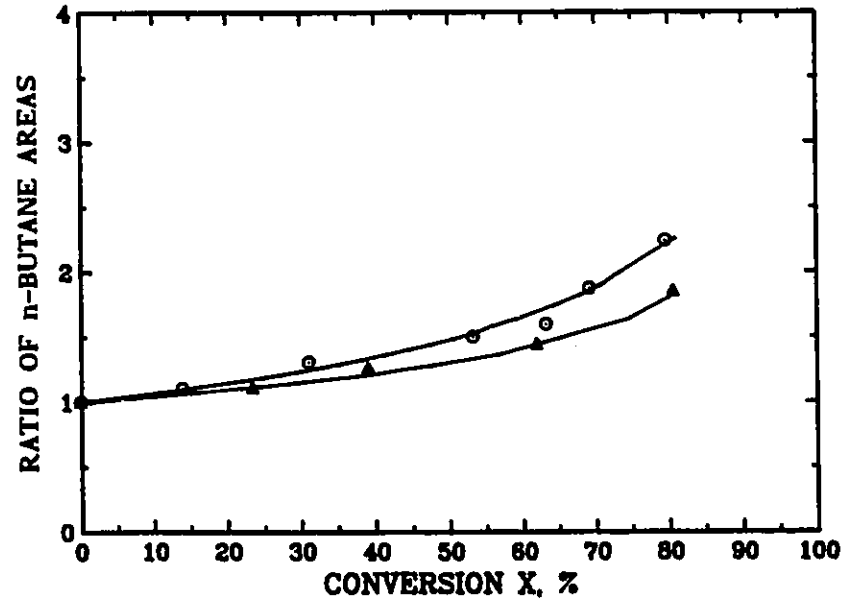

Figure 3.11. Ratio of n-butane areas versus conversion for suspension polymerization of VCM.
⊙: at 50°C, Δ: at 70°C, —— :model.

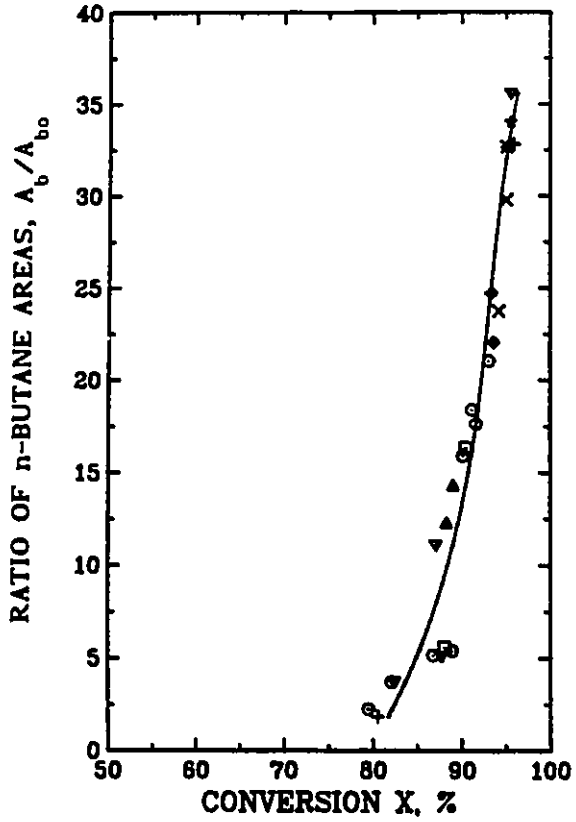

Figure 3.12. Ratio of n-butane areas versus conversion for suspension polymerization of vinyl chloride at higher conversion stage.
Δ : 40°C, □ : 45°C, ⊙ : 50°C, ◇: 55°C, x : 60°C,
∇ : 65°C, + : 70°C, * : 75°C, ✳: 80°C.
—— : empirical calibration curve (Eq.(3.26)).

With the model using parameter estimated using gravimetry and the empirical equation (3.26), one can recalculate the conversion histories of suspension polymerization of VCM over the entire conversion range for the same run as shown in Figure 3.8. One can see in Figure 3.8, that the model with parameters based on gravimetry measurements is in excellent agreement with conversions measured by gravimetry.

From Figures 3.7-3.12, one can see that the suspension polymerization system of vinyl chloride is quite different from the inert mixture system in terms of the GC responses of n-Butane. This disagreement is likely due to nonequilibrium effects. The tracer distribution in the reaction system may not reach equilibrium and therefore the GC response for n-butane is much lower in the reaction system than in the inert system. The morphology of PVC may play an important role in changing the resistance to mass transfer of VCM and n-butane in this regard. With increasing conversion, the particles of PVC experience several structural transition stages.[21,22] The solubility, as well as the diffusion coefficient, may depend on the morphology of PVC. At high conversions, the liquid monomer phase has been consumed and monomer in the vapour phase diffuses into the polymer phase and n-butane diffuses from the polymer phase into the vapour phase so that the concentration of n-butane in the vapour phase increases dramatically. In the meantime, the monomer concentration in the polymer phase decreases dramatically due to polymerization so that the solubility of n-butane in the polymer phase decreases. As a result, the GC response of n-butane increases dramatically at high conversions.

If the polymerization rate were slow enough, it is possible for the n-butane distribution in the polymerization system to approach equilibrium closely. To further evaluate the equilibrium model, a series of experiments with higher water/VCM ratios and lower initiator concentrations was done by AKZO Chemicals.[23] The experimental procedure used by AKZO is similar to that used in the present work except that a lower

heating rate to achieve polymerization temperature was employed. The heating time was about 60 minutes at AKZO and about 5 minutes in the present work. Slower heating rates and lower initiator concentrations permit the polymerization system to approach equilibrium with respect to n-butane diffusion. The results are shown in Figure 3.13. The solid curve is the model prediction with equilibrium-based parameters. The experimental points were obtained by stopping the polymerization at different conversion levels and weighing the dried PVC. It should be pointed out that the model predictions for the different temperatures overlap. One can see that the experimental data also give essentially one graph under these experimental conditions. The model is in excellent agreement with the experimental data up to 60% conversion. At higher conversions, the model predictions are lower than the experimental measurements obtained by gravimetry. These results suggest that the equilibrium model can be used to estimate conversions when polymerizations are relatively slow.

(3). Precision of the Tracer method

As mentioned above, the ratio of n-butane areas is used in the model instead of the absolute area. It is essential, therefore, to obtain an accurate initial area for n-butane for later conversion calculations. Unfortunately, it is very difficult to obtain an accurate A_{bo} experimentally because of system noise at the beginning of the polymerization. In fact, the n-butane area often decreases with time at the beginning of the polymerization. This phenomenon was observed at both McMaster and AKZO laboratories.[23] To obtain A_{bo} accurately, the

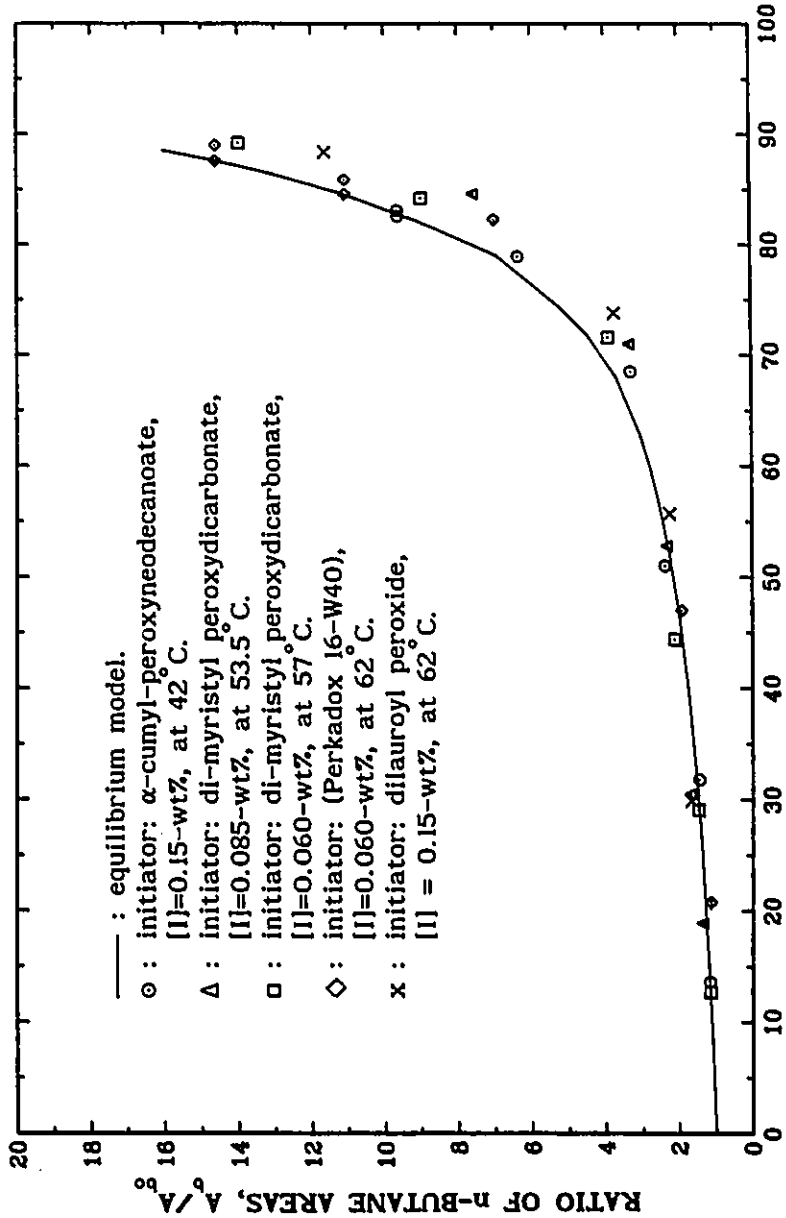

Figure 3.13. Comparison of equilibrium model predictions with gravimetry measurements done by AKZO Chemicals (ref.23).
Reactor: 5.0 liter, water: 2700 grams, VCM: 675 grams.

following empirical equation was used to smooth the experimental data:

$$A_b = A_{bo} + A_1 t + A_2 t^2 + A_3 t^3 \qquad (3.29)$$

where t is polymerization time, A_1, A_2, and A_3 are parameters. A typical GC response of n-butane for VCM suspension polymerization is shown in Figure 3.14. With this technique, one can not only estimate A_{bo} satisfactorily for each run but also smooth the original data. The scatter due to experimental noise, therefore, is avoided.

Figures 3.15 and 3.16 show replicate experiments for conversion measurements by the tracer technique. One can see that the reproducibility of the conversion histories of VCM polymerization are satisfactory. The maximum deviations appear in the conversion range 50-80%. The average variances and standard deviations corresponding to data in Figures 3.15 and 3.16 are shown in Table 3.1. One can see, from Table 3.1, that the standard deviation is within 2% conversion which indicates the good precision for the present tracer method.

Table 3.1. Reproducibility of conversion measurements by the tracer method.

Temperature °C	Average variance %	Average standard deviation %	degrees of freedom
50	1.7	1.3	68
60	2.3	1.5	60
70	3.0	1.7	45

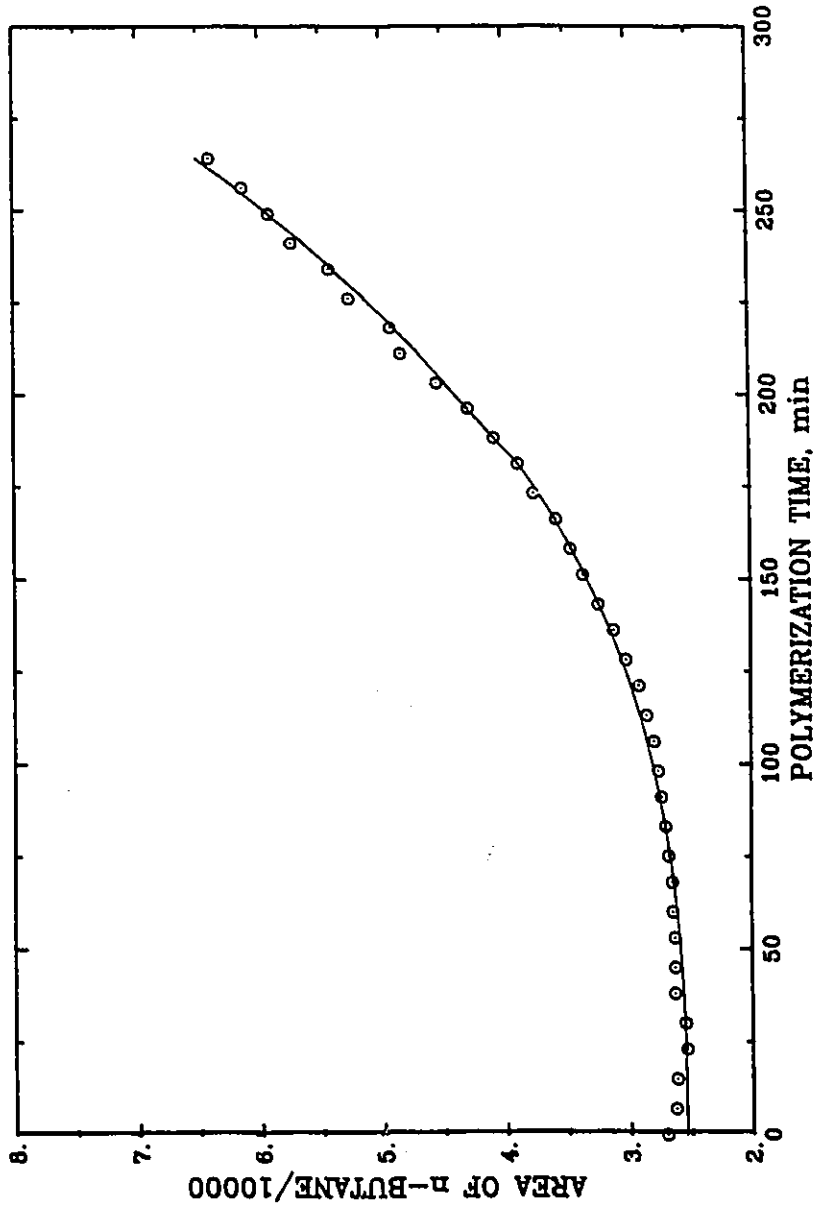

Figure 3.14. GC response area of n-butane versus reaction time for suspension polymerization of VCM at 60°C.
⊙: experimental data, ——— : best fit curve.

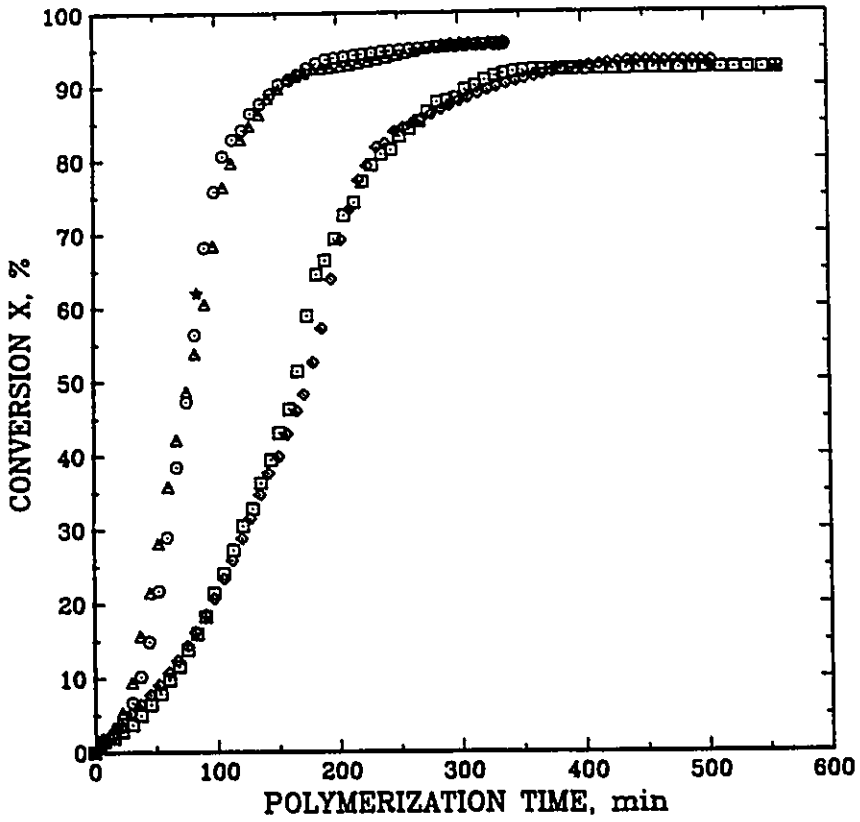

Figure 3.15. Reproducibility of conversion histories for suspension polymerization of VCM measured by the online n-butane tracer method.
⊙ and Δ : at 70°C, AIBN, [I] = 0.25-wt%.
□ and ◇ : at 50°C, Perkadox 16-W40,
[I] = 0.20-wt% (based on pure peroxide).
*: measured offline by gravimetry.

Figure 3.17 shows conversion-time histories for the suspension polymerization of vinyl chloride as measured by the n-butane-tracer method with calioration based on gravimetry. The final points (stars) were obtained by point gravimetry measurements as a check. The errors for final conversions measured by the tracer method and gravimetry are

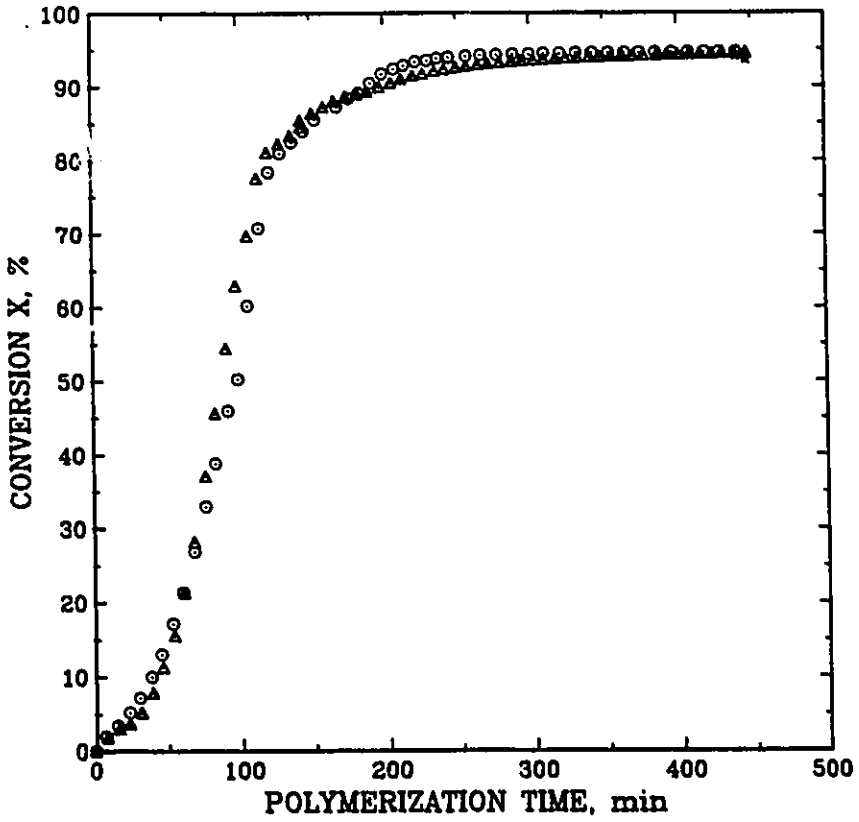

Figure 3.16. Reproducibility of conversion histories for the suspension polymerization of VCM at 60°C measured by the online n-butane tracer method.
Perkadox 16-W40, [I]= 0.175-wt% (based on pure peroxide).

less than 1%. The conversion data using the tracer method are very smooth over the entire conversion range. With the tracer method, one can get very detailed kinetic information. One can easily estimate the instantaneous polymerization rate every 7-8 minutes. Therefore, the tracer method can be used to obtain extensive rate data for comprehensive studies of kinetics.

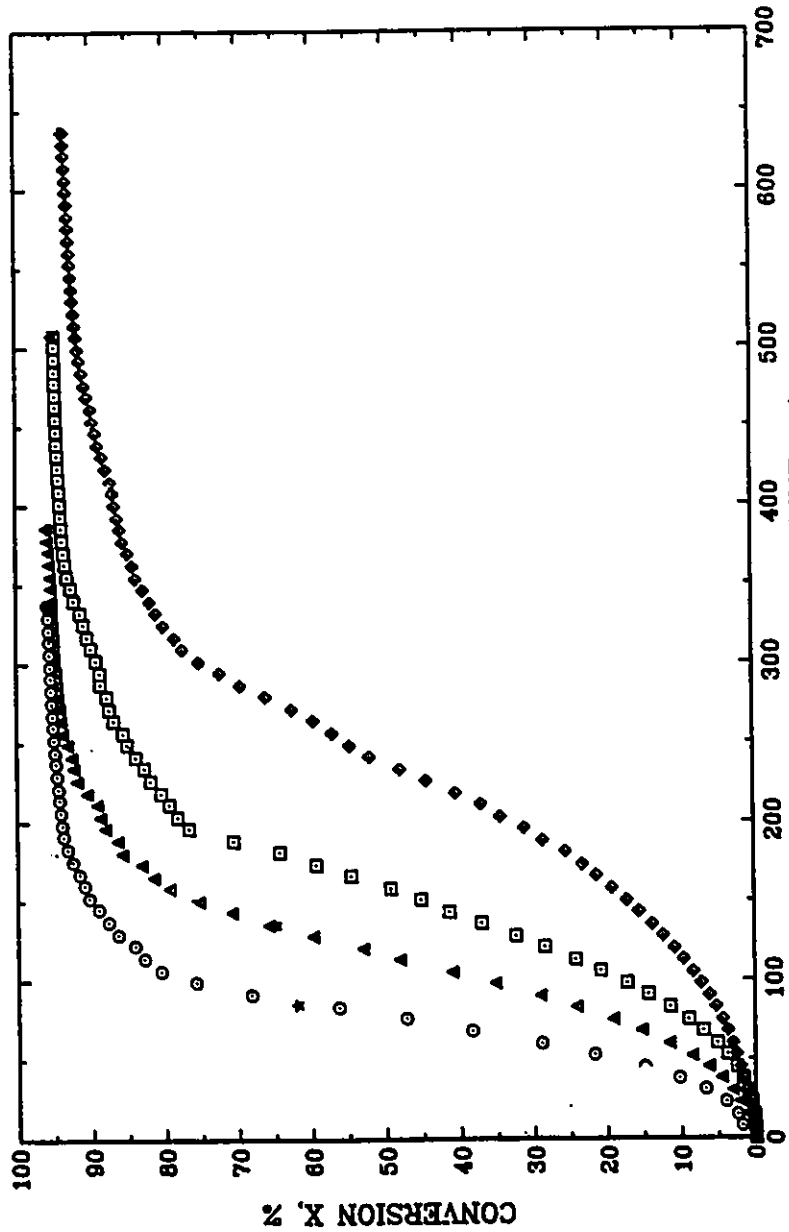

Figure 3.17. Typical conversion histories for the suspension polymerization of VCM measured by the online n-butane tracer method.
Initiator: AIBN, [I] = 0.25-wt%. ⊙: 70°C; Δ: 65°C; □: 60°C; ◇: 55°C.

As mentioned above, the sample flowrate of headspace vapour was controlled to within 5-7 mL/min at atmospheric pressure. Therefore, for a long run, say, 10 hours, the loss of material due to sampling is less than 10 grams. For the present reactor charge (1116 grams of VCM), the relative error due to sampling is less than 1%. Therefore, under the present operating conditions, the error due to sampling can be neglected.

Because all of the parameters are available as a function of temperature and the other variables in Eq.(3.20) are a function of polymerization conditions, this model can be used not only for isothermal batch polymerization but also for nonisothermal and semi-batch polymerizations.

Compared with gravimetry, the present method has the following advantages: It has higher efficiency, is safer, is more flexible for different reactor processes, and more detailed kinetic information can be obtained. The calculation procedure is, however, more complicated than that for gravimetry. However, with the use of a computer, only a few seconds are required to calculate a hundred pairs of conversion data points using the present model.

3.5 SUMMARY

The present model for the n-butane tracer method relates monomer conversion to tracer response measured by gas chromatography. The tracer n-butane has an appropriate retention time with good separation from VCM under the present experimental conditions. The partition of n-butane between the different phases meets the requirements for the tracer method. The detector response of n-butane is very sensitive to the conversion of VCM, particularly at high conversions. The model is in reasonable agreement with the experimental results over the entire conversion range when equilibrium is closely followed, and it is in agreement with the experimental results up to the limiting conversion (glassy-state transition) for fast suspension polymerization when non-equilibrium calibration parameters are used. The model can be used not only for isothermal batch but also for nonisothermal batch, and semi-batch polymerizations. The sampling period under the present experimental conditions is adequate for kinetic studies of VCM polymerization. This method permits one not only to study kinetics of VCM polymerization but also to evaluate new VCM polymerization recipes, with new initiation systems of unknown decomposition rate constants and initiator efficiencies.

3.6 REFERENCES

1. Stickler, M. Makromol. Chem., Macromol. Symp., 1987, 10/11, 17.

2. Bengough, W.I. and Norrish, R.G.W. Proc. Royal Soc. (London), 1950, A200, 301.

3. Farber E. and Koral, M. Polym. Eng. Sci., 1968, 8, 11.

4. Crosato-Arnaldi, A., Gasparini, P. and Talamini, G. Makromol. Chem., 1968, 117, 140.

5. Abdel-Alim, A. H. and Hamielec, A. E. J. Appl. Polym. Sci., 1972, 16, 783.

6. Xie,T. Y., Yu, Z. Z., Cai, Q. Z. and Pan, Z. R. J. Chem. Ind. Eng. (China), 1984, 2, 93.

7. Malhotra, V. P.and Saroop, U. K. Pop. Plast., 1984, 29, 17.

8. Meeks, M. R. Polym. Eng. Sci., 1969, 9, 141.

9. Nilsson, H., Silvegren, C. and Törnell. B. Br. Polym. J., 1981, 13, 164.

10. Nilsson, H., Silvegren, C. and Törnell, B. Chem. Scripta, 1982, 19, 164.

11. Nilsson, H., Silvegren, C. and Törnell, B. Angew, Makromol. Chem., 1983, 112, 125.

12. Mrazek, Z., Jungwirt, A. and Kolinsky, M. J. Appl. Polym. Sci., 1982, 27, 1513.

13. Mrazek, Z., Jungwirt, A. and Kolinsky, M. J. Appl. Polym. Sci., 1982, 27, 2079.

14. Mrazek, Z. and Lukas, R. Makromol. Chem. Macromol. Symp., 1989, 29, 155.

15. Cebollada, A. F., Schmidt, M. J., Farber, J. N., Capiati, N. J. and Valles, E. M., J. Appl. Sci., 1989, 37, 145.

16. Langsam, M. J. Polym. Sci., Polym. Letter Ed., 1984, 22, 549.

17. Hayduk, W. IUPAC, Solubility Data Series, 1986, 24, 16.

18. Weast, R. C., Astle, M.J. and Beyer, W. H. 'CRC Handbook of Chemistry and Physics', CRC Press Inc., Boca Raton, Florida 64th edition, 1983- 1984.

19. Selected Values of Properties of Hydrocarbons and Related Compounds, American Petroleum Institute Research Project 44, (API 44), Vol.1 and 2, 1969.

20. Gallant, R. W. Hydrocarbon Processing and Petroleum Refiner, 1965, 44, 95.

21. Xie, T. Y., Hamielec, A. E., Wood, P. E. and Woods, D. R. **"Suspension, Bulk and Emulsion Polymerization of Vinyl Chloride — Mechanism, Kinetics and Reactor Modelling"**, AKZO PVC Symposium, 1988, The Netherlands.

22. Xie, T. Y., Hamielec, A. E., Wood, P. E. and Woods, D. R. **"Suspension, Bulk and Emulsion Polymerization of Vinyl Chloride — Mechanism, Kinetics and Reactor Modelling"**, Submitted to J. Vinyl Technol., 1990.

23. Westmijze, H., Personal Communications, 1988.

CHAPTER 4

MECHANISMS, KINETICS AND BATCH REACTOR MODELLING

4.1 INTRODUCTION

Previous chapters describe preliminary work required for the later studies of kinetics of VCM polymerization. Detailed VCM polymerization mechanisms, kinetics and batch reactor modelling are now illustrated in the present chapter.

Mechanisms and kinetics of free radical bulk or suspension polymerization of vinyl chloride have been extensively studied experimentally. VCM polymerization mechanisms proposed are based mainly on polymerization kinetics, chain microstructure and particle morphology studies. The extent and variety of research work dealing with the same problem reflect not only the great interest in, and extensive practical use of PVC, but also the complexity of VCM polymerization. The considerable experimental data in the literature more or less reflect the pattern of VCM polymerization kinetics, although a comprehensive kinetic model which can predict with adequate accuracy physical and chemical property changes during VCM polymerization has not been published prior to the present study.

In the present chapter, the main contributions to the mechanisms

and kinetics of VCM polymerization in terms of elementary chemical reactions, physical phenomena and kinetic modelling are discussed and summarized. A comprehensive kinetic model which accounts for these elementary reactions, physical phenomena and reactor operational conditions for VCM polymerization over the entire conversion range is then clearly derived and evaluated. Extensive kinetic experiments were carried out to estimate kinetic and thermodynamic parameters in the present model. The main features of heterogeneous free radical polymerization of VCM with diffusion-controlled reactions are accounted for quantitatively.

4.2 MECHANISMS OF VCM POLYMERIZATION

4.2.1 Chemical Reaction Types

A typical free radical polymerization mechanism includes initiation, propagation, chain transfer to small molecules and bimolecular termination steps. However, recent research has revealed that some reactions, such as chain transfer to monomer, involve a more complicated mechanism for VCM polymerization.[1-9]

Initiation reactions for VCM polymerization have not been studied in detail. In kinetic modelling, it is assumed that initiation reactions occur in both monomer and polymer phases.[10-17] Lewis et al[18] studied the sites of initiation and concluded that the main site of initiation at low conversions during VCM bulk polymerization is the continuous monomer phase. Marinin et al[19] measured the decomposition

rate constants of some peroxide initiators in the polymer phase under subsaturated pressure and found that the decomposition rate constants of these initiators in the polymer phase can be significantly lower than those in the monomer phase. Sielfeld et al[20] found that the decomposition rate of dicyclohexyl peroxydicarbonate is much smaller in the VCM-PVC mixture than that in a dilute solution. These phenomena have not been considered in previous kinetic modelling. Important parameters for kinetic modelling, such as initiation efficiency, initiator partition coefficient and decomposition rate constant for VCM polymerization, have not been extensively studied in the literature.

The propagation reaction is considered to be mainly a head-to-tail addition of the monomer double bond to the radical center.[3,21] However, the existence of a small number of head-to-head structures in PVC has been suggested in the literature.[22] Rigo et al[1] first proposed that the head-to-head propagation reaction causes the formation of chloromethyl branches in PVC. Bovey et al[3] gave evidence for the presence of this structure by ^{13}C-NMR measurements on reduced PVC. Starnes et al[4,5] provided further evidence for the proposed mechanism. This mechanism can more reasonably explain how chain transfer to monomer occurs during free radical polymerization of VCM. Hence, propagation reactions can involve several types of radicals in addition to the most common radical types as shown in Figure 4.1.

Chain transfer to monomer plays a very important role in controlling the molecular weight development in VCM polymerization. In

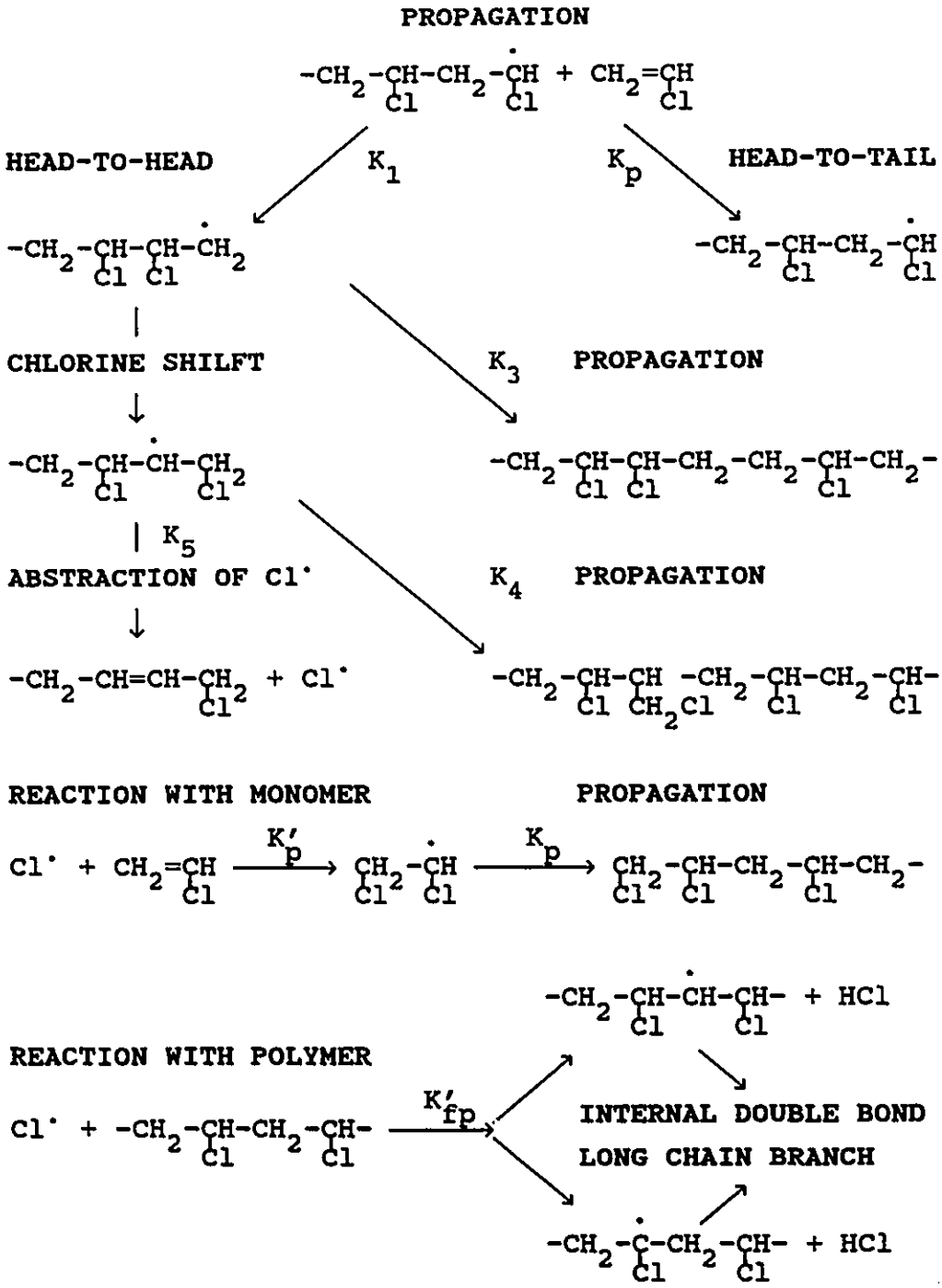

Figure 4.1. Mechanism of radical transfer to monomer and formation of some defect structures in PVC.

classical kinetic studies of VCM polymerization, chain transfer to monomer was considered to involve a polymer chain transferring its radical center to monomer directly[23-29] by the abstraction of a chlorine or hydrogen from the VCM.[25,28] However, the unsaturated end groups formed by this chain transfer mechanism can not be found by NMR measurements.[30,31] Therefore, Caraculacu et al[30,31] suggested that transfer to monomer would be realizable only by abstracting an atom from a high energy structure such as from head-to-head addition polymer radicals, the monomer being the acceptor. Detailed NMR measurements showed that chain transfer to monomer involves a more detailed mechanism as shown in Figure 4.1. As mentioned above, the head-to-head addition was proposed by Rigo et al.[1] The chlorine abstraction step was suggested by Bezdaea et al[2], while Caraculacu et al[30,31] and Starnes et al[4,5] suggested the subsequent chlorine addition to the monomer double bond. Hjertberg et al[9] suggested that the chlorine atoms which result from head-to-head addition also abstract hydrogen atoms from the polymer backbone and this results in the formation of internal double bonds or long chain branches. This mechanism of chain transfer to monomer is supported by the following findings:

(1). the major part of the unsaturated chain ends has 1-chloro-2-alkene structure.[7,32,33]

(2). the major part of the saturated chain ends consists of the 1,2-dichloro-alkane structure.[4,7,8,32,33]

(3). the presence of chloromethyl branches in PVC chain.[3-6,34-36]

(4). the absence of unsaturated end groups formed by the classical chain transfer to monomer mechanism.[30,31]

Thus, the classical mechanism involving macroradical direct chain transfer to monomer is not valid for VCM polymerization.

Whether the bimolecular termination reaction between polymer radicals is combination or disproportionation is difficult to determine because of the significance of chain transfer to monomer in this system. Razuvayev et al[37] were the first to investigate the mechanism of bimolecular termination in the free radical polymerization of VCM by ^{14}C-labelled initiators. It was found that, in the bulk and suspension polymerization of VCM, the average number of initiator end groups per polymer molecule is 0.19-0.40, i.e.: a maximum of 19-40% of the polymer molecules are produced by bimolecular termination reactions. Park et al[38] studied solution polymerization of VCM using ^{14}C-labelled initiator azobis(isobutyronitrile) (AIBN) and found that 25% of bimolecular termination occurs by combination and 75% by disproportionation. Hence, a maximum of 5-10% of the polymer molecules are produced by combination termination. More recently, Starnes et al[39,40] examined the PVC structural segments derived from AIBN by NMR and found the copolymer structure of VCM and methacrylonitrile in PVC chains. Therefore, Park et al's experimental results are open to question. It should be mentioned that the resulting structure from combination termination is similar to that by head-to-head addition. But the content of head-to-head structure in PVC chain is so low that it can not be detected by ^{13}C-NMR[4]. Hjertberg et al[41] estimated the head-to-head structure to be less than 0.2 per 1000 monomeric units using a chemical method. Assuming the degree of polymerization to be 1000, one may estimate that there is a maximum of

20% of the polymer molecules with one head-to-head structure. Therefore, 10-15% of the polymer molecules experience one head-to-head followed by tail-to-tail propagation addition on the basis of Park et al[38] and Hjertberg's[41] results.

In addition to bimolecular termination and propagation, macro-radicals experience some other reactions, including chain transfer to polymer, intramolecular chain transfer or back-biting etc. reactions.[6, 33,40,42] All these reactions result in short or long chain branches. Primary radical termination may also occur in VCM polymerization.[43-45] However, the significance of this reaction for the calculation of total radical concentration is uncertain.

All of the chemical reactions which have been identified by kinetic and microstructural studies and that are important for kinetic and reactor modelling are summarized in Table 4.1.

All the reactions shown in Tabnle 4.1 may occur in both monomer and polymer phases simultaneously. A kinetic model involving all these chemical reactions has not been reported prior to the present investigation. In the present model development, these elementary reactions will be considered, and their effects on polymerization rate discussed in some detail.

Table 4.1. Summary of elementary reactions for VCM polymerization.

	Reaction	Description
Initiation:		
(1).	$I \xrightarrow{K_d} R_1^{\cdot}$	decomposition of initiator
(2).	$R_1^{\cdot} + M \xrightarrow{K_i} R_1^{\cdot}$	generation of polymer radicals
Propagation and chain transfer reactions:		
(3).	$R_r^{\cdot} + M \xrightarrow{K_p} R_{r+1}^{\cdot}$	head-to-tail propagation
(4).	$R_r^{\cdot} + M \xrightarrow{K_1} R_{r+1}^{\cdot *}$	head-to-head propagation
(5).	$R_r^{\cdot *} \xrightarrow{K_2} (R_r^{\cdot *})'$	chlorine shift reaction
(6).	$R_r^{\cdot *} + M \xrightarrow{K_3} R_{r+1}^{\cdot}$	tail-to-tail propagation
(7).	$(R_r^{\cdot *})' + M \xrightarrow{K_4} R_{r+1}^{\cdot}$	formation of chloromethyl branches
(8).	$(R_r^{\cdot *})' \xrightarrow{K_5} P_r + Cl^{\cdot}$	splitting off $Cl^{\cdot}$
(9).	$Cl^{\cdot} + M \xrightarrow{K_p'} R_1^{\cdot}$	initiation of polymer radicals by $Cl^{\cdot}$
(10).	$Cl^{\cdot} + P_r \xrightarrow{K_{fp}'} R_r^{\cdot\prime} + HCl$	$Cl^{\cdot}$ transfer to polymer
(11).	$R_r^{\cdot\prime} + M \xrightarrow{K_p} R_{r+1}^{\cdot}$	propagation towards formation of a long chain branch

Table 4.1. (continued)

	Reaction	Description
Propagation and chain transfer reactions:		
(12).	$R_r^{\bullet\bullet} \xrightarrow{K_e} P_r + Cl^{\bullet}$	formation of an internal double bond
(13).	$R_r^{\bullet} + P_s \xrightarrow{K_{fp}} R_s^{\bullet\bullet} + P_r$	chain transfer to polymer
(14).	$R_s^{\bullet\bullet} + M \xrightarrow{K_p} R_{s+1}^{\bullet}$	formation of a long chain branch
Termination:		
(15).	$R_r^{\bullet} + R_s^{\bullet} \xrightarrow{K_{tc}} P_{r+s}$	combination
(16).	$R_r^{\bullet} + R_s^{\bullet} \xrightarrow{K_{td}} P_r + P_s$	disproportionation
(17).	$R_r^{\bullet} + R_l^{\bullet} \xrightarrow{K_{tl}} P_r$	primary radical termination
(18).	$R_r^{\bullet} + Cl^{\bullet} \xrightarrow{K_{tCl}} P_r$	termination with $Cl^{\bullet}$
Other reactions:		
(19).	$R_r^{\bullet} \xrightarrow{K_b} R_{r,b}^{\bullet}$	back biting reaction
(20).	$R_{r,b}^{\bullet} + M \xrightarrow{K_p} R_{r+1,b}^{\bullet}$	propagation towards formation of a short chain branch

4.2.2 Physical Phenomena

From the previous section, it is clear that VCM polymerization involves rather complex chemical reactions. Because PVC is effectively insoluble in its own monomer, VCM polymerization is a heterogeneous process which involves several physical transitions throughout the course of polymerization. The final PVC product of bulk or suspension polymerization is made up of primary particles and their agglomerates. Therefore, all the complex chemical reactions mentioned above occur in this complicated environment. For valid kinetic modelling it is necessary to understand the mechanisms for formation, growth and aggregation of primary particles. PVC morphological terminology and units have been summarized in a recent publication[46] as shown in Table 4.2. This terminology is used in the following discussion.

The formation of primary particles has been studied by many investigators.[47-63] Based on turbidimetric measurements, Boissel et al[52] found that polymer precipitates from the monomer phase at conversions as low as 0.001%. This value is much lower than that (0.03% solubility of PVC in monomer at ambient temperature) measured by Ravey et al.[64] Cotman et al[47] estimated that macroradicals become insoluble in the monomer at a degree of polymerization of 25-32. Rance et al[58] recently suggested that the solubility of polymer in the monomer is limited to polymer chains containing 10 monomer units or fewer based on the Flory interaction parameter. Although the range of these values is large, they do indicate that phase separation during VCM polymerization occurs at a very low conversion level. The first particles which appear at these low

Table 4.2. PVC morphology development.[46]

Particle unit	Approximate diameter Range (μm)	Average (μm)	Origin or Description
Grain	50-250	100-130	Visible constituents of free flowing powders, made up of more than one monomer droplet.
Sub-Grain	10-150	40-60	Polymerized monomer droplet.
Agglomerate	3-10	~5.0	Formed by coalescence of primary particles (1μm), grows with conversion.
Primary particle	0.6-1.5	~1.0	Growth from domain. Formed at low conversions by coalescence of microdomain.
Domain	0.1-0.3	~0.2	Primary particle nucleus. Contains about 10^3 microdomains. Only observed at low conversions.
Microdomain	0.01-0.02	~0.02	Smallest species so far identified. Aggregate of polymer chains.

conversions are so called microdomains, which are 0.01-0.02 μm in diameter. They are believed to result from precipitation and coagulation of dead polymer/polymer radicals. Their life times are less than thirty seconds and therefore cannot be measured by photon correlation spectroscopy methods.[58] The aggregation of microdomains produces domains (primary particle nuclei, 0.1-0.3 μm in diameter), the first observable entities of the new monomer swollen polymer phase.[51-58,65-67] Willmouth et al[59] and, more recently, Törnell et al[68] studied the conversion

dependence of particle size and number density at earlier stages of polymerization. From information in the literature, one can conclude that a domain is formed and grows by the following processes:

(1). aggregation of microdomains;

(2). precipitation of macroradicals and macromolecules (chain length $r > r_c$) on the formed microdomain or domain;

(3). polymerization inside the microdomain or domain.

These three processes occur simultaneously during the early stages of VCM polymerization.

Further aggregation or growth of domains results in the formation of primary particles. The primary particles grow with conversion at almost the same rate.[47-50,53,69] The average diameter of primary particles is about 0.8-1.0 μm. Much of the existing work on grain formation has involved studying the very early stages of the process or over a narrow conversion range. Recently, Smallwood[70,71] studied the later stages of the polymerization process at commercial polymerization temperatures (51-71°C). PVC samples were taken at 5-90% conversion. A series of scanning electron micrographs shows that the primary particles increase in size until 50-70% conversion, depending on reaction temperature. Then the primary particles fuse together at higher conversions (aggregation of primary particles has occurred since low conversion). By examining those results,[70,71] one may find that the primary particles increase in size with conversion until the critical conversion X_f at

which point the free monomer phase disappears as described in Chapter 2. Hence, one can conclude that the primary particles grow by:

(a). accretion of microdomains or domains onto their surface;

(b). polymerization inside the primary particles.

The limiting size of primary particle is about 1.4 μm and the final number of primary particles is approximately $2.0 \times 10^{11} cm^{-3}$ for all reaction temperatures (51-71°C).[70]

Wilson et al[54] and Davidson et al[57] demonstrated that the primary particles carry negative charges which may result from the presence of HCl formed during polymerization (see reaction (10) in Table 4.1). According to Törnell et al's competitive growth mechanism,[62] a single charge on a microdomain is far too little to prevent it from coagulating with a domain or a primary particle, but a charged microdomain would certainly interact with larger, highly charged domain or primary particles. Thus, the growth by coagulation of the smaller particles is favoured so that, finally, all the primary particles will have about the same size and surface charge density. This mechanism is in agreement with the experimental results of the same authors.[68] In addition, the stability of primary particles is affected by polymerization temperature,[50,66,70,71] reactor agitation strength[51,52,57,68,72-74] and additives type and level.[53,60,61,75-77]

As the primary particles increase in size and the volume fraction of the polymer phase increases, aggregation will involve multiparticle contacts. Thus, aggregation will result in a decrease in primary particle number and in the formation of a continuous network of primary particles throughout the polymer particle/monomer droplet. The continuous network is likely to form between 10-30% conversion.[70] According to Smallwood's results,[70,71] after the monomer phase disappears, further polymerization leads to the fusion of primary particles and the formation of agglomerates. Hence, at high conversions, only agglomerates of primary particles can be seen, and their size strongly depends on polymerization temperature.

In view of the preceding observations, one can summarize the mechanism of formation of PVC grains as follows:

Stage one: macroradicals or macromolecules with chain length more than a critical value r_c begin to precipitate from the monomer phase (at about 0.001% conversion).

Stage two: aggregation of macroradicals and macromolecules after precipitation produces microdomains (0.01-0.02 μm, at < 0.01% conversion). The microdomain is not well defined.

Stage three: aggregation of microdomains produces domains (0.1-0.3 μm, < 1% conversion) stabilized by negative charge. This stage is completed at 5-10% conversion.

Stage four: aggregation and growth of domains cause the formation of primary particles until continuous networks form in the droplets (about 15-30% conversion).

Stage five: growth and aggregation of primary particles until the free monomer phase disappears, the diameter of final primary particles is about 1.2-1.5 μm (50-70% conversion).

Stage six: primary particles fuse together as agglomerates (5-10 μm) until the limiting conversion is reached.

There is no clear boundary line between stages, two neighbouring stages may occur simultaneously during polymerization. Allsopp[78,79] proposed a schematic representation of the mechanism of morphology development in VCM polymerization. With the recent findings considered, a modified scheme of the mechanism for PVC particle formation during VCM polymerization is suggested as shown in Figure 4.2.

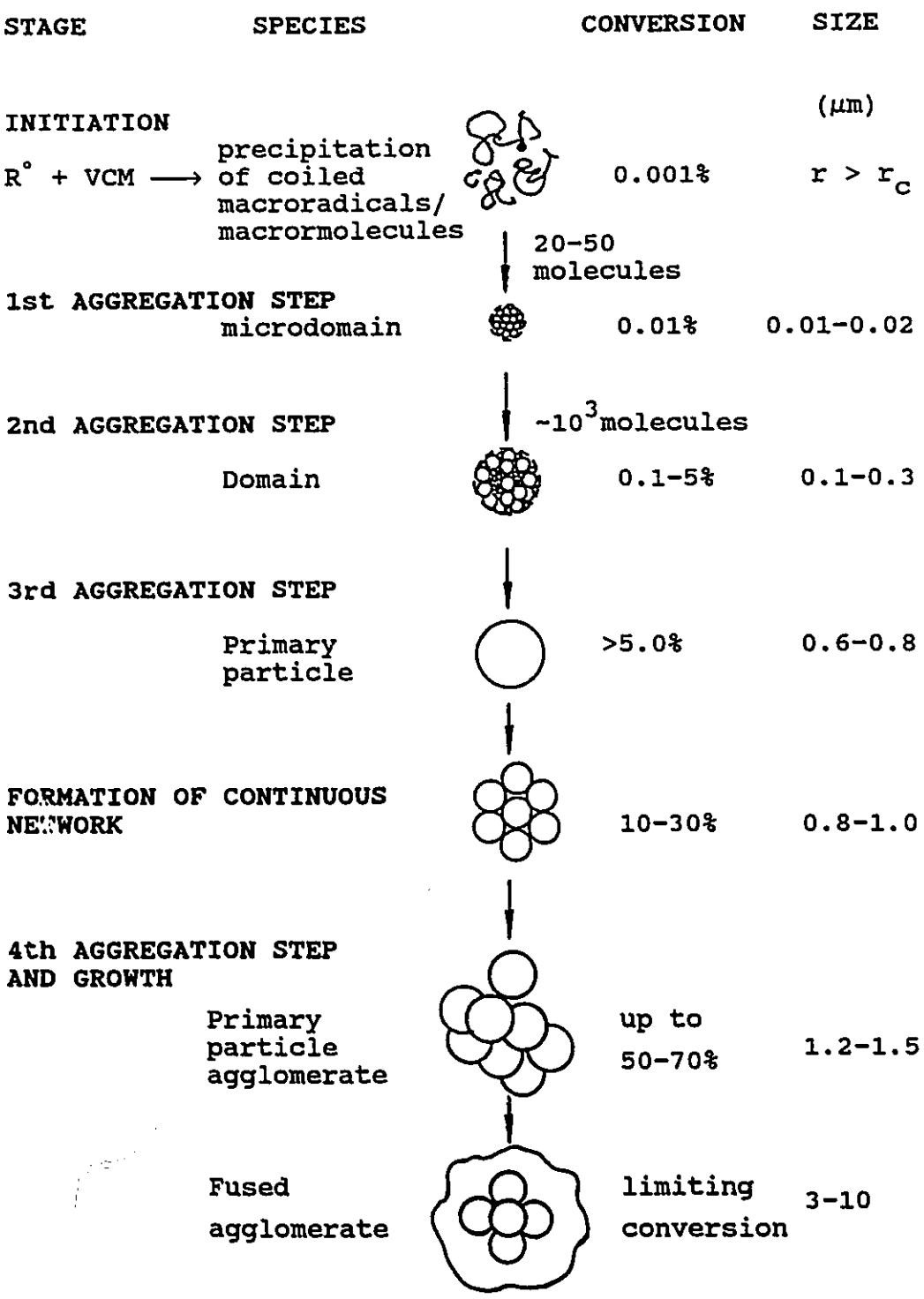

Figure 4.2. Scheme of PVC grain formation

4.2.3 Dynamics and Modelling of VCM polymerization

The dynamics of VCM polymerization process should include:

(1). Conversion development with time, from which the polymerization rate and heat generation profile etc. can be obtained.

(2). Molecular weight and molecular structure development with conversion, from which the polymer chemical and physical properties can be found.

(3). PVC particle size and porosity development with conversion and reaction conditions, from which the processing properties of PVC can be obtained.

(4). Reactor pressure development with conversion, from which the polymer quality control and reactor operation optimization policy can be achieved.

The dynamics of VCM polymerization processes, as a whole, have not been studied comprehensively. Meeks[80] first measured conversion, polymerization heat and rate, reactor pressure, cooling water temperature and flow rate simultaneously as a function of polymerization time. Nilsson et al[81] measured polymerization rate, reactor pressure and the amount of liquid monomer as a function of conversion in suspension and emulsion polymerization systems. More recently, Cebollada et al[82] determined conversion, polymerization rate and reactor pressure as a function of time experimentally. This suggests that studies of the dynamics of VCM polymerization have been emphasized recently. However, in most of the kinetic studies in the literature, only conversion as a function of time was measured.

Based on previous work in the literature, one can summarize the main dynamic features of VCM polymerization as follows:

(1). The polymerization rate increases with conversion at a low critical conversion, i.e.: the so-called auto-acceleration.[12-15,23,26,29,47,64,80,83-96] In general, the maximum rate of polymerization occurs just after the reactor pressure starts to drop.[80-82] Then the polymerization rate decreases dramatically with conversion.[13,64,80,81,96] The polymerization rate effectively decreases to zero before 100% conversion of monomer at commercial polymerization temperatures.

(2). The reactor pressure, for isothermal polymerization, remains constant until a certain high conversion, then the pressure decreases gradually with conversion.[80,81] The pressure may start to drop slowly before the monomer phase disappears.[81] This phenomenon has been described in detail in Chapter 2.

(3). The reaction order with respect to initiator concentration is between 0.5-0.8.[13,15,23,43,47,83,91,92,96-98] These results were based on relatively low conversion rate measurements.

(4). The molecular weight of PVC does not strongly depend on monomer conversion or initiator concentration,[11,13,23,83,99] but it increases with decreasing polymerization temperature.[13] At very high conversions, the molecular weight decreases with conversion.[86,100]

(5). Chain transfer to monomer plays a dominant role in controlling molecular weight development of PVC.[13] The ratio of the chain transfer to monomer rate constant to the propagation rate constant is as large as $1.0\text{-}5.0\times10^{-3}$ at commercial polymerization temperatures.[13,15,28,47,83,91] According to the new mechanism of chain transfer to monomer, this value is for a group of kinetic rate constants and a function of monomer concentration. This will be discussed later and further described quantitatively in Chapter 5.

A comprehensive kinetic/reactor model which can describe these dynamic features of VCM polymerization has not been reported prior to the present study. Most of kinetic studies to date emphasized polymerization rate modelling only.

Based on the pertinent phenomena of VCM polymerization discussed above, one knows that phase separation occurs at very low monomer conversions. From a kinetic modelling point of view, therefore, it is reasonable to assume that polymerization occurs in the monomer and polymer phases simultaneously from the very beginning of the polymerization. The solubility of PVC in monomer is so low (about 0.001%) that the monomer phase is considered to be essentially pure monomer, while the polymer phase is swollen with about 30-wt% monomer. As the reaction proceeds, the mass of the monomer phase decreases while that of the polymer phase grows, but the composition of each phase is essentially constant,[10,83] because the rate of monomer diffusion into polymer particles is sufficiently high to ensure equilibrium during polymerization with a constant

equilibrium concentration of monomer in the particles[14] before the monomer phase is consumed. As long as VCM exists as a separate phase, it will exert its own vapour pressure, and the pressure in the reactor will be essentially constant during isothermal polymerization. When conversion reaches a value X_f the pressure in the reactor begins to drop, and then polymerization proceeds in the polymer phase until a limiting conversion is reached (the slight drop of pressure due to effect of particle morphology described in Chapter 2 is negligible for kinetic modelling). Therefore, a model valid for the entire conversion range must describe two-phase polymerization before the critical conversion X_f and single phase polymerization after the critical conversion X_f.

When the conversion is less than X_f, the following equations apply for a batch reactor:

$$-\frac{dN_m}{dt} = K_{p1}[M]_1[R^\cdot]_1V_1 + K_{p2}[M]_2[R^\cdot]_2V_2 \qquad (4.1)$$

If $K_{p1} = K_{p2} = K_p$, then Eq.(4.1) becomes

$$-\frac{dN_m}{dt} = K_p[M]_1[R^\cdot]_1V\left[1 + \left(\frac{[M]_2[R^\cdot]_2}{[M]_1[R^\cdot]_1} - 1\right)\Phi_2\right] \qquad (4.2)$$

where K_p depends only on temperature; $[M]_1$ and $[M]_2$ are also constant and $[M]_1 > [M]_2$ when conversion is less than X_f; $[R^\cdot]_1$ will decrease gradually due to a decrease in initiator concentration; the total volume V will decrease due to the larger polymer density; the polymer phase volume fraction Φ_2 is a positive value ($\Phi_2 < 1.0$) and will increase

gradually with conversion. Considering typical polymerization rate profiles, one may conclude that only one of three cases is possible for the VCM heterogeneous polymerization, that is

$$\text{If} \quad \frac{[M]_2[R^\cdot]_2}{[M]_1[R^\cdot]_1} - 1 < 0, \quad \text{then}$$

$$-\frac{dN_m}{dt} < K_p[M]_1[R^\cdot]_1 V \tag{4.3}$$

The polymerization rate would decrease with conversion, which is not the case for VCM polymerization.

$$\text{If} \quad \frac{[M]_2[R^\cdot]_2}{[M]_1[R^\cdot]_1} - 1 = 0, \quad \text{then}$$

$$-\frac{dN_m}{dt} = K_p[M]_1[R^\cdot]_1 V \tag{4.4}$$

This is the same as the rate expression for homogeneous (solution) free radical polymerization. The reaction rate must decrease gradually with conversion. This is not the case for VCM polymerization, either.

Therefore, only the following condition can be true, that is

$$\frac{[M]_2\,[R^\cdot]_2}{[M]_1\,[R^\cdot]_1} - 1 > 0 \tag{4.5}$$

In this case, polymerization rate will increase with conversion or reaction time according to the mechanism described above. From Eq.(4.5), one can obtain:

$$([R^{\cdot}]_2/[R^{\cdot}]_1) > ([M]_1/[M]_2) \tag{4.6}$$

Both $[M]_1$ and $[M]_2$ are constant for $X < X_f$ because the composition of both phases does not change in the conversion range, $X < X_f$. At 50°C, the density of monomer is 856 g/L and the density of saturated PVC/VCM mixture is 1208 g/L.[59] Assuming PVC is swollen with 30-wt% monomer, one can easily get:

$$[M]_1/[M]_2 = 2.4 \tag{4.7}$$

Thus, at least,

$$[R^{\cdot}]_2/[R^{\cdot}]_1 > 2.4 \qquad \text{(at } 50^{\circ}\text{C)} \tag{4.8}$$

Therefore, the following inequality is always true for VCM polymerization:

$$[R^{\cdot}]_2 > [R^{\cdot}]_1 \qquad (X < X_f) \tag{4.9}$$

It is clear that to develop a valid model for the rate of polymerization the most important task is to properly express $[R^{\cdot}]_2/[R^{\cdot}]_1$ as a function of the variables which are known or that can be measured experimentally. This is the main reason why most kinetic models differ, the relations used for radical concentrations in the two phases vary.

Although polymerization in the polymer phase was suggested in the literature[48] (and refs. therein), Talamini[10,83] first proposed a two-phase polymerization scheme and modelling approach to describe the kinetic behaviour of VCM polymerization. The major assumption in Talamini's model was setting $[R^{\cdot}]_2/[R^{\cdot}]_1$ constant, that is

$$[R^{\cdot}]_2/[R^{\cdot}]_1 = (K_{t1}/K_{t2})^{1/2} = P \qquad (4.10)$$

An oversimplified model with adjustable parameter P was thus derived as:

$$\frac{dX}{dt} = K(1+QX)[I]_o^{1/2} \qquad (4.11)$$

where

$$Q = AP - A + 1$$

and A is the ratio of weights of monomer/polymer in the polymer phase, K is an overall kinetic constant. This was the first model to fit experimental rate data reasonably well over a range of conversions less than X_f. However, besides the adjustable parameter P, the following important factors were neglected in Talamini's model: unequal initiator partition between the two phases; consumption of initiator; volume shrinkage due to the density difference between VCM and PVC; and radical migration between the two phases.

Abdel-Alim et al[13] modified Talamini's model by considering the reaction volume change and initiator consumption and first extended the model to conversions above X_f. The following rate expressions were

derived:

$$\frac{dX}{dt} = \frac{1+QX}{(1-BX)^{1/2}} K [I]_o^{1/2} \exp(-K_d t/2) \qquad (X < X_f) \qquad (4.12)$$

$$\frac{dX}{dt} = \frac{PK}{1-X_f} [I]_o^{1/2} \frac{(1-X)}{(1-BX)^{1/2}} \exp(-K_d t/2) \qquad (X \geq X_f) \qquad (4.13)$$

where B is a volume shrinkage coefficient, and K_d is the decomposition rate constant of initiator. Again, unequal initiator partition and radical migration between phases were neglected in the model.[13]

To modify Talamini's model, Ugelstad et al[12,94,95] proposed radical exchange between the two phases, with the population balance equations for radicals as follows:

$$\frac{d(R^\cdot)_1}{dt} = 2K_d[I]_1V_1 - K_a[R^\cdot]_1 + K_{de}[R^\cdot]_2 - 2K_{t1}[R^\cdot]_1^2V_1 = 0 \qquad (4.14)$$

$$\frac{d(R^\cdot)_2}{dt} = 2K_d[I]_2V_2 + K_a[R^\cdot]_1 - K_{de}[R^\cdot]_2 - 2K_{t2}[R^\cdot]_2^2V_2 = 0 \qquad (4.15)$$

where K_a and K_{de} are absorption and desorption constants of radicals, respectively. Ugelstad et al assumed very rapid absorption and desorption of radicals obtaining again a constant value for $[R^\cdot]_2/[R^\cdot]_1$. The rate equation is given by

$$\frac{dX}{dt} = K_p(K_dI/K_tV)^{1/2}(1 - X - AX + APX) \qquad (4.16)$$

Therefore, the kinetic model remains the same in form as that after

Talamini but is based on different assumptions.

Kuchanov et al[14] considered that the desorption of radicals from the polymer phase can be ignored because only a small fraction of the radicals with short chain lengths can desorb from the polymer phase. These authors further assumed that the ratio of the mole fractions of initiator in both phases remains constant. They proposed the following population balance equations for radicals:

$$\frac{d(R^{\cdot})_1}{dt} = 2K_d[I]_1V_1 - K_a[R^{\cdot}]_1 - 2K_{t1}[R^{\cdot}]_1^2V_1 = 0 \qquad (4.17)$$

$$\frac{d(R^{\cdot})_2}{dt} = 2K_d[I]_2V_2 + K_a[R^{\cdot}]_1 - 2K_{t2}[R^{\cdot}]_2^2V_2 = 0 \qquad (4.18)$$

A relatively complicated rate expression was derived. Unfortunately, they only compared the model predictions with low conversion data. However, when the authors extended the model to high conversions (X > 77%), they still considered the monomer as a separate phase. This seems in contradiction to the observed physical phenomena discussed earlier.

Olaj[15] further assumed that all of the radicals formed in the monomer phase transfer to the polymer phase, i.e.: there is no termination reaction in the monomer phase. Therefore, the population balance equations for radicals become:

$$\frac{d(R^{\cdot})_1}{dt} = 2K_d[I]_1V_1 - K_a[R^{\cdot}]_1 = 0 \qquad (4.19)$$

$$\frac{d(R^{\cdot})_2}{dt} = 2K_d[I]_2V_2 + K_a[R^{\cdot}]_1 - 2K_{t2}[R^{\cdot}]_2^2V_2 = 0 \qquad (4.20)$$

and the associated rate expression is given by

$$\frac{dX}{dt} = K_p\left(\frac{2\,K_d[I]}{K_a}\right)\left(\Phi_m^* - \frac{\Phi_m D_m X}{\Phi_p D_p}\right) + K_p\left[\frac{2\,K_d[I]D_m\Phi_m^2}{K_{t2}D_p\Phi_p}X\right]^{1/2} \qquad (4.21)$$

where Φ_m and Φ_p are the volume fraction of monomer and polymer, respectively, in the polymer phase. Φ_m^* is the volume fraction of monomer at the site of reaction of the radical chain in the monomer phase. In Olaj's model the reaction order with respect to initiator concentration is 1.0 which is higher than that observed experimentally. Olaj[15] concluded that even at low conversions, the last term in Eq.(4.21) will be the dominant one. Therefore, Eq.(4.21) can be simplified as:

$$\frac{dX}{dt} = a + bX^{1/2} \qquad (4.22)$$

More recently, Suresh et al[16] proposed the concept of "kinetic solubility" which assumes that rapidly growing polymer chains have considerably greater solubility than the thermodynamic solubility of preformed polymer molecules of the same size and so can remain in solution even under thermodynamically unfavourable conditions. In the model development, radical precipitation and transfer to monomer were considered, but radical termination in the monomer phase was also neglected. Hence, their rate equation has features which are similar to Olaj's model.

Based on the two phase model and classical reaction mechanisms, Kelsall et al[17] considered the unequal partition of initiator between the two phases and derived a set of model equations. During their simulation of VCM polymerization, radical migration between phases was treated as a mass transfer process. The validity of their model has not been examined experimentally.

In view of these observations, one can conclude that polymerization in two phases is commonly accepted. The significance of radical migration between the two phases still remains unclear. All the modelling arguments focus on the relation of radical concentrations in both phases and some assumptions are in conflict. However, radical concentrations in the different phases have never been quantitatively described. Russo et al[98] examined the occluded and long-lived macroradicals in the radiation-induced polymerization of vinyl chloride in bulk by using electron spin resonance (ESR) with the postpolymerization reaction. The results show only minor contributions to the polymerization rate from these species. Hence, the steady-state approach in model development seems justified. Radical exchange processes between the two phases have not been clearly defined in previous kinetic modelling. As discussed above, $[R^{\cdot}]_2$ is much larger than $[R^{\cdot}]_1$, so there is no mass transfer of polymer radicals from the monomer phase to the polymer phase if chain length r is less than r_c chain length at which macroradicals start to precipitate from the monomer phase. Only polymer radicals with $r > r_c$ can migrate from monomer to polymer phase by precipitation. The opposite is true for desorption of radicals from polymer phase. Therefore, the

only radical species which can desorb from the polymer phase are the chlorine radical, $Cl^{\cdot}$, and possibly small polymer radicals. Therefore radical exchange between phases involves a more complicated process than that described in previous modelling. Based on Eq.(4.7) and the discussion above, the processes of radical exchange between two phases can be expressed as:

$$(R^{\cdot})_m \underset{\text{mass transfer}}{\overset{\text{precipitation}}{\rightleftharpoons}} (R^{\cdot})_p$$

It is now clear that radical transfer from the monomer phase to the polymer phase depends on the nature of VCM-PVC system and is thermodynamically and kinetically controlled. On the other hand, the driving force for the reverse process is the concentration difference and depends on the radical size and primary particle diameter. Based on above discussion, the main ideas for a two-phase model are summarized in Figure 4.3.

Very little study of the kinetics of polymerization at high conversions ($X > X_f$) has been done. Abdel-Alim et al[13] first extended the two-phase model to single phase polymerization at high conversions as shown in Eq.(4.13). Kelsall et al[17], more recently, simulated the VCM polymerization to high conversion levels. Hamielec et al[101] first accounted for diffusion-controlled bimolecular termination and propagation at high conversions. In fact, sufficient experimental kinetic data for high conversions ($X > X_f$) have not accumulated in the literature to

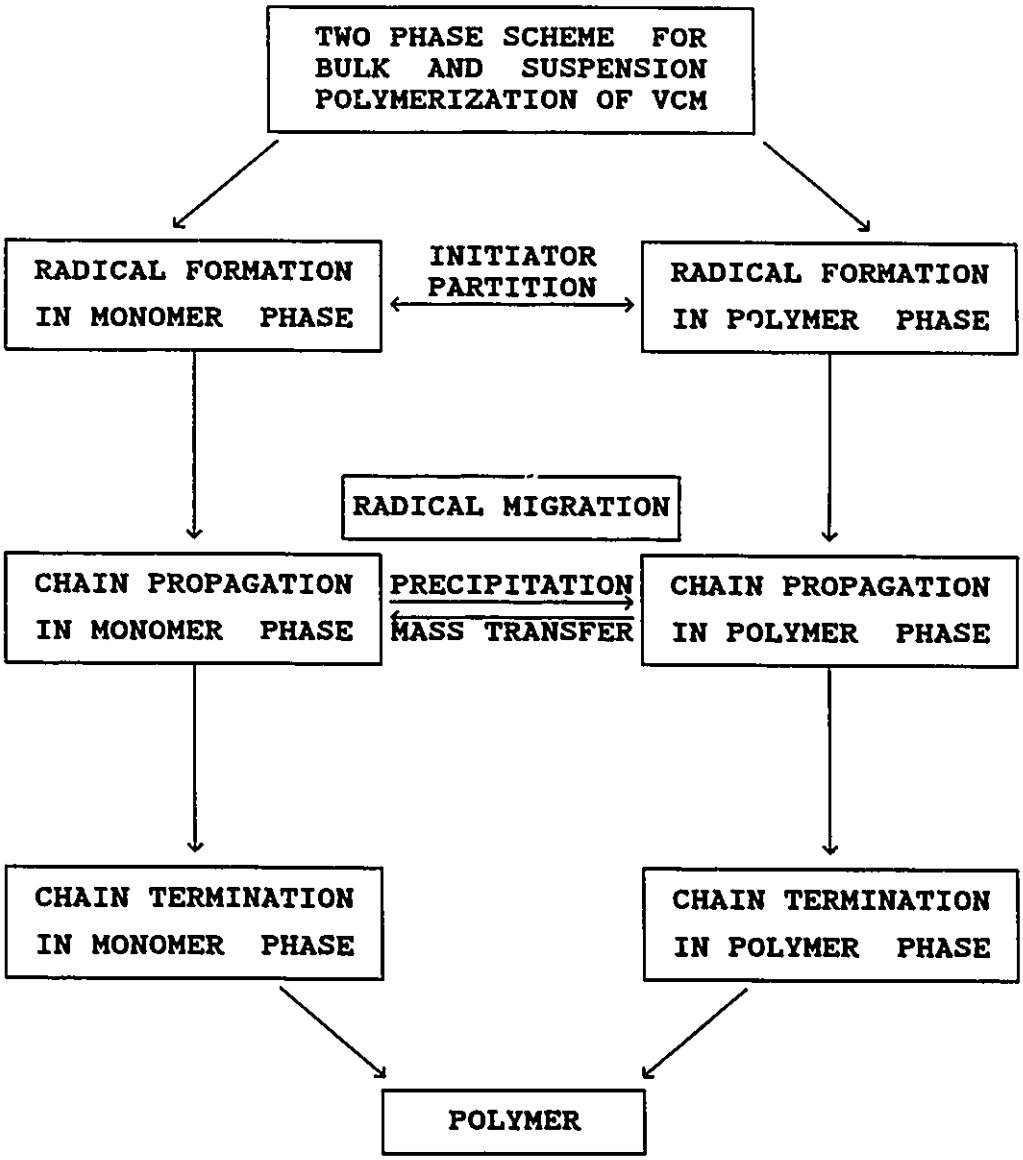

Figure 4.3. Radical history for VCM polymerization.

test the validity of existing kinetic models in a comprehensive manner.

Although there has been a steady improvement in the quality of kinetic modelling, none of the existing models are directly applicable to commercial processes. The main reasons are:

(1). The mechanisms of VCM polymerization including elementary chemical reactions and physical phenomena are not comprehensively understood during previous kinetic modelling.

(2). Species distributions and reactor operation conditions have not been considered in the kinetic modelling.

(3). Diffusion-controlled bimolecular termination and propagation and initiation efficiency and decomposition rate of initiator in the polymer phase have not been studied in detail, particularly, at higher monomer conversion levels which are commercially important.

(4). Valid kinetic parameters have not been estimated for VCM polymerization over the entire conversion range due to the lack of sufficient kinetic data.

For the kinetic/reactor model development, the present work considers the entire conversion range and with particular emphasis on the high conversion levels. Extensive kinetic experiments, covering commercial reaction temperature range, were carried out to estimate the kinetic parameters and evaluate the present model.

4.3 MODEL DEVELOPMENT

The kinetic mechanisms of VCM polymerization discussed above will be accounted for in the present model. The following assumptions are made in the model development:

(1). All droplets in the polymerization system are assumed to have the same chemical composition and the same physical conditions.

(2). Polymerization of VCM in the water and vapour phases is negligible.

(3). Polymerization of VCM proceeds in two phases —— monomer and polymer phases —— when the conversion is less than X_f. When the conversion is greater than X_f, polymerization proceeds in the polymer phase only.

(4). Polymer radicals can transfer from the monomer phase into the polymer phase by precipitation and capture. Transfer of polymer radicals in the reverse direction is limited to small radicals with chain length less than the critical chain length ($r < r_c$). Instantaneous equilibrium with respect to the transfer of mobile radicals between monomer and polymer phases is assumed.

(5). Monomer and initiators diffuse into and out of the polymer phase rapidly so that equilibrium partition of these species is assumed at all time.

(6). Bimolecular termination of polymer radicals in the monomer phase is chemically-controlled, but bimolecular termination in the polymer phase is diffusion-controlled over the entire conversion range. Propagation reactions are also diffusion-controlled at $X > X_f$ and

initiator efficiency falls rapidly at high monomer conversions due to a large increase in radical recombination in the cage (the so called "cage effect").

Thus, if the long chain approximation is considered valid for both monomer and polymer phases, with the assumptions above, the polymerization rate in terms of conversion per unit time can be expressed as:

$$\frac{dX}{dt} = \frac{K_p}{N_o M_m} ([R^\cdot]_1 M_1 + [R^\cdot]_2 M_2) \qquad (4.23)$$

where N_o is the initial number of moles of VCM, M_m is molecular weight of VCM, M_1 and M_2 are weights of monomer in the monomer and polymer phases respectively (they can be expressed as a function of conversion and reactor operation conditions as described in Chapter 2).

Strictly speaking, all of the radicals consuming monomer should be included in $[R^\cdot]_1$ and $[R^\cdot]_2$. However, according to the microstructure of ordinary PVC,[102] the structure due to initiation reactions (2) and (9) in Table 4.1 is about one unit per polymer molecule. Hence monomer consumption due to these reactions is negligible. This is equivalent to the long chain approximation. Similarly, monomer consumption due to head-to-head and tail-to-tail propagation is less than 0.02%. Therefore, the long chain approximation is valid for VCM polymerization. It is assumed that the radical centers forming short and long chain branches have the same reactivity as radical centers on chain ends. Hence, $[R^\cdot]_1$ and $[R^\cdot]_2$

include radicals on chain ends and polymer backbone radicals. From the polymerization rate point of view, this treatment is valid. However, these radical types have to be considered individually for PVC molecular weight development and microstructure modelling.

Radical and monomer concentrations, initiation rate and kinetic parameters are essential factors in any polymerization rate expression. These factors for VCM polymerization are now discussed separately.

4.3.1. Radical Concentrations

From discussions in the previous section, one knows that the radical concentration in the polymer phase is much greater than that in the monomer phase. It is assumed that there is no mass transfer of radicals from the monomer phase to the polymer phase when the chain length r is less than r_c (chain length at which macroradicals start to precipitate from the monomer phase). Radicals with $r \geq r_c$ can transfer from the monomer to the polymer phase by precipitation and capture. On the other hand, desorption of radicals from the polymer phase is limited to the radicals with chain length less than r_c. Thus, on the basis of the elementary reactions the total radical balance for the two phases can be expressed as follows:

$$\frac{d(R^{\cdot})_1}{V_1 dt} = R_{I1} + K'_{p1}[Cl^{\cdot}]_1[M]_1 - K_{p1}[M]_1[R^{\cdot}_{rc-1}]_1 - K'_{t1}[R^{\cdot}]_1([R^{\cdot}_1] +$$

$$+[Cl^{\cdot}]_1) - K_S[R^{*\cdot}]_1 - K_{t1}[R^{\cdot}]_1^2 + K_{de}\sum_{r=1}^{n}[R^{\cdot}_r]_2 V_2/V_1 = 0 \qquad (4.24)$$

$$\frac{d(R^{\cdot})_2}{V_2 dt} = R_{I2} + K_{p1}[M]_1[R^{\cdot}_{rc-1}]_1 V_1/V_2 + K'_{p2}[Cl^{\cdot}]_2[M]_2 + K'_{fp}[Cl^{\cdot}]_2(Q_1)_2 -$$

$$- K'_{t2}[R^{\cdot}]_2([R^{\cdot}_1]_2 + [Cl^{\cdot}]_2) - K_S[R^{*\cdot}]_2 - K_{de}\sum_{r=1}^{n}[R^{\cdot}_r]_2 -$$

$$- K_{t2}[R^{\cdot}]_2^2 = 0 \qquad (4.25)$$

where

$$(R^{\cdot})_1 = \sum_{r=1}^{\infty}(R^{\cdot}_r)_1 + \text{backbone radicals} \qquad (i = 1, 2)$$

and $n < r_c$.

Based on the reaction mechanisms shown in the previous section, the radical concentrations $[R^{\cdot}_1]_2$, $[Cl^{\cdot}]$, $[R^{\cdot\cdot}]$, $[R^{*\cdot}]$, $[R^{*\cdot}]$, $[R^{\cdot}_1]$ and $[R^{\cdot}_r]_2$ can be expressed by the following population balance equations:

$$\frac{dR^{\cdot}_1}{V_2 dt} = R_{I2} + K'_p\ [Cl^{\cdot}]_2[M]_2 - K_p[M]_2[R^{\cdot}_1]_2 - K_{t2}[R^{\cdot}]_2[R^{\cdot}_1]_2 -$$

$$- K_{de}\ [R^{\cdot}_1]_2 = 0 \qquad (4.26)$$

$$\frac{d(Cl^{\cdot})_1}{V_1 dt} = K_S\ [R^{*\cdot}]_1 + K_{e1}[R^{\cdot\cdot}]_1 + K_{de}[Cl^{\cdot}]_2 - K'_{p1}[Cl^{\cdot}]_1[M]_1 -$$

$$- K'_{fp}\ [Cl^{\cdot}]_1(Q_1)_1 = 0 \qquad (4.27)$$

$$\frac{d(Cl^{\cdot})_2}{V_2 dt} = K_5 [R^{\cdot *}]_2 + K_{e2}[R^{\cdot\cdot}]_2 - K_{de}[Cl^{\cdot}]_2 - K'_{p2}[M]_2[Cl^{\cdot}]_2 -$$

$$- K'_{fp}[Cl^{\cdot}]_2(Q_1)_2 = 0 \qquad (4.28)$$

$$\frac{dR^{\cdot\cdot}}{V_1 dt} = K'_{fp1}[Cl^{\cdot}]_1(Q_1)_1 - K_{p1}[R^{\cdot\cdot}]_1[M]_1 - K_e[R^{\cdot\cdot}]_1 = 0 \qquad (4.29)$$

$$\frac{dR^{\cdot *}}{V_1 dt} = K_1 [M]_1[R^{\cdot}]_1 - K_2 [R^{\cdot *}]_1 - K_3 [R^{\cdot *}]_1[M]_1 = 0 \qquad (4.30)$$

$$\frac{dR^{\cdot *},}{V_1 dt} = K_2 [R^{\cdot *}]_1 - K_4 [R^{\cdot *}]_1[M]_1 - K_5 [R^{\cdot *}]_1 = 0 \qquad (4.31)$$

$$\frac{dR^{\cdot}_1}{V_1 dt} = R_{I1} - K_{t1}[M]_1[R^{\cdot}_1]_1 - K'_{t1}[R^{\cdot}]_1[R^{\cdot}_1]_1 = 0 \qquad (4.32)$$

$$\frac{dR^{\cdot}_r}{V_2 dt} = K_{p2}[M]_2[R^{\cdot}_{r-1}]_2 - K_{t2}[R^{\cdot}_r]_2[R^{\cdot}]_2 = 0 \qquad (4.33)$$

where i = 1, 2, indicating monomer and polymer phases respectively. The phase subscripts for K_1, K_2, K_3, K_4, K_5 are neglected for simplification of symbols.

From Eq.(4.29), after application of the stationary-state hypothesis (SSH) one obtains:

$$[R^{\cdot\cdot}]_i = \frac{K_{fpi}'[Cl^{\cdot}]_i (Q_1)_i}{K_{pi}[M]_i + K_{ei}} \qquad (i = 1, 2) \qquad (4.34)$$

Because the solubility of PVC in the monomer is very low, $(Q_1)_1$ is negligible, so that $[R^{\cdot\cdot}]_1$ can be neglected.

Eq.(4.30) gives:

$$[R^{\cdot}]_i = \frac{K_1 [M]_i [R^{\cdot}]_i}{K_2 + K_3 [M]_i} \qquad (i = 1, 2) \qquad (4.35)$$

Substituting Eq.(4.35) into Eq.(4.31), one obtains:

$$[R^{\cdot\cdot}]_i = \frac{K_1 K_2 [M]_i [R^{\cdot}]_i}{(K_2 + K_3[M]_i)(K_4[M]_i + K_5)} \qquad (i = 1, 2) \qquad (4.36)$$

Substituting Eq.(4.36) into Eq.(4.27), and keeping in mind $[R^{\cdot\cdot}]_1 = 0$, one can find:

$$[Cl^{\cdot}]_1 = \left[\frac{K_1 K_2 K_5 [M]_1 [R^{\cdot}]_1}{(K_2 + K_3[M]_1)(K_4[M]_1 + K_5)} + K_{de}[Cl^{\cdot}]_2\right] / K_{p1}'[M]_1 \qquad (4.37)$$

Reaction (9) (see Table 4.1) is a very fast reaction, hence, $K_{p1}'[M]_1 \gg K_{de}[Cl^{\cdot}]_2$ can be assumed. Thus, Eq.(4.37) is simplified to:

$$[Cl^{\cdot}]_1 = \frac{K_1 K_2 K_5 [R^{\cdot}]_1}{K_{p1}' (K_2 + K_3[M]_1)(K_4[M]_1 + K_5)} \qquad (4.38)$$

Similarly, substituting Eqs.(4.34) and (4.36) into Eq.(4.28),

one can express the concentration of chlorine radicals in the polymer phase as:

$$[Cl^{\cdot}]_2 = \frac{K_1 K_2 K_5 [R^{\cdot}]_2 [M]_2}{(K_2+K_3[M]_2)(K_4[M]_2+K_5)(K'_{p2}[M]_2+K_{fp}'(Q_1)_2+K_{de}-K')} \qquad (4.39)$$

where

$$K' = \frac{K_{e2} K_{fp}' (Q_1)_2}{K_{p2}[M]_2 + K_{e2}}$$

From information on the microstructure of PVC, one knows that reaction (9) is much faster than reactions (10) and (12) (see Table 4.1), hence, $K'_{p2}[M]_2 \gg K'_{fp}(Q_1)_2$ and $K'_{p2}[M]_2 \gg K_{de}$ can be assumed. K' is a very small value because $K_{p2} \gg K_e K'_{fp}$. Therefore, $K'_{p2}[M]_2 \gg (K'_{fp}(Q_1)_2+K_{de}-K')$, and hence, Eq.(4.39) can be simplified to

$$[Cl^{\cdot}]_2 = \frac{K_1 K_2 K_5 [R^{\cdot}]_2}{K'_{p2}(K_2 + K_3[M]_2)(K_4[M]_2 + K_5)} \qquad (4.40)$$

Comparing reaction (9) in Table 4.1 with the classical chain transfer to monomer reaction, one finds that the following equation should hold:

$$K'_{p1}[Cl^{\cdot}]_1[M]_1 = (K_{fm})_1[R^{\cdot}]_1[M]_1 \qquad (4.41)$$

Substituting Eq.(4.38) into Eq.(4.41), one obtains:

$$K_{fm1} = \frac{K_1 K_2 K_5}{(K_2 + K_3[M]_1)(K_4[M]_1 + K_5)} \tag{4.42}$$

Similarly,

$$K_{fm2} = \frac{K_1 K_2 K_5}{(K_2 + K_3[M]_2)(K_4[M]_2 + K_5)} \tag{4.43}$$

From Eqs.(4.42) and (4.43), one can see that the effective rate constant for chain transfer to monomer is a function of monomer concentration and reaction temperature. This has already been shown to be true by Hjertberg et al.[103]

Using Eqs.(4.42) and (4.43), one may rewrite Eqs.(4.38) and (4.39) as

$$[Cl^{\cdot}]_1 = \frac{K_{fm1}}{K'_{p1}} [R^{\cdot}]_1 \tag{4.44}$$

$$[Cl^{\cdot}]_2 = \frac{K_{fm2}}{K'_{p2}} [R^{\cdot}]_2 \tag{4.45}$$

Using chain transfer to monomer constants reported in the literature,[13] one can estimate that the concentration of chlorine radicals is at least three orders of magnitude smaller than the polymer radical concentration. Therefore, the bimolecular termination reactions with $Cl^{\cdot}$ can be neglected.

From Eq.(4.32), the concentration of primary radicals can be

expressed as:

$$[R_1^{\cdot}]_j = \frac{R_{Ij}}{K_{1j}[M]_j + K'_{tj}[R^{\cdot}]_j} \qquad (j = 1, 2) \qquad (4.46)$$

The primary radical concentration in Eq.(4.46) is also 3-4 orders of magnitude smaller than the polymer radical concentration based on magnitude of initiation rate and species concentrations in the equation, hence, bimolecular termination with $R_i^{\cdot}$ may not be significant during VCM polymerization.

Substituting Eq.(4.45) into Eq.(4.26), one can find that

$$[R_1^{\cdot}]_2 = \frac{R_{I2} + (K_{fm})_2[R^{\cdot}]_2[M]_2}{K_{p2}[M]_2 + K_{t2}[R^{\cdot}]_2 + K_{de}} \qquad (4.47)$$

From Eq.(4.33), one obtains:

$$[R_r^{\cdot}]_2 = (\frac{1}{\tau})^{r-1}[R_1^{\cdot}]_2 \qquad (4.48)$$

where

$$\tau = K_{t2}[R^{\cdot}]_2/K_{p2}[M]_2$$

Substituting Eq.(4.47) into Eq.(4.48) and considering $K_{p2}[M]_2 \gg K_{t2}[R^{\cdot}]_2+K_{de}$ and $R_{I2} \gg K_{fm2}[R^{\cdot}]_2[M]_2$, one may simplify $[R_r^{\cdot}]_2$ as:

$$[R_r^{\cdot}]_2 = (\frac{1}{\tau})^{r-1} \frac{R_{I2}}{K_{p2}[M]_2} \tag{4.49}$$

Therefore, the desorption term in Eqs.(4.24) and (4.25) can be written as:

$$K_{de} \sum_{r=1}^{n} [R_r^{\cdot}]_2 = K_{de} \sum_{r=1}^{n} (\frac{1}{\tau})^{r-1} \frac{R_{I2}}{K_{p2}[M]_2} = K'_{de} R_{I2} \tag{4.50}$$

Based on the discussion above and noticing that

$$K_{p1}' [Cl^{\cdot}]_1 [M]_1 = K_S [R^{\cdot *}]_1$$

$$K_{p2}' [Cl^{\cdot}]_2 [M]_2 + K_{fp}' [Cl^{\cdot}]_2 (Q_1)_2 = K_S [R^{\cdot *}]_2$$

one can simplify Eqs.(4.24) and (4.25) to

$$\frac{d(R^{\cdot})_1}{V_1 dt} = R_{I1} - K_{P1}[M]_1 [R^{\cdot}_{rc-1}]_1 - K_{t1}[R^{\cdot}]_1^2 + K'_{de} R_{I2} V_2 / V_1 = 0 \tag{4.51}$$

$$\frac{d(R^{\cdot})_2}{V_2 dt} = R_{I2} + K_{p1}[M]_1 [R^{\cdot}_{rc-1}]_1 V_1 / V_2 - K_{t2}[R^{\cdot}]_2^2 - K'_{de} R_{I2} = 0 \tag{4.52}$$

where $K_{p1}[M]_1[R^{\cdot}_{rc-1}]_1$ represents the formation and precipitation rate of radicals with chain length r_c in the monomer phase. $[R^{\cdot}_{rc-1}]_1$ can be obtained by the following equations.

$$\frac{dR^{\cdot}_{r-1}}{V_1 dt} = K_p [R^{\cdot}_{r-2}]_1 [M]_1 - K_p [R^{\cdot}_{r-1}]_1 [M]_1 - K_{t1} [R^{\cdot}]_1 [R^{\cdot}_{r-1}]_1 -$$

$$- K_S [R^{\cdot *}_{r-1}]_1 = 0 \tag{4.53}$$

$$\frac{dR^{\bullet *}_{r-1}}{V_1 dt} = K_2[R^{\bullet *}_{r-1}]_1 - K_4[R^{\bullet *}_{r-1}]_1[M]_1 - K_5[R^{\bullet *}_{r-1}]_1 = 0 \tag{4.54}$$

$$\frac{dR^{\bullet *}_{r-1}}{V_1 dt} = K_1[R^{\bullet}_{r-2}]_1[M]_1 - K_2[R^{\bullet *}_{r-1}]_1 - K_3[R^{\bullet *}_{r-1}]_1[M]_1 = 0 \tag{4.55}$$

$$\frac{dR^{\bullet}_1}{V_1 dt} = R_{I1} + K'_p[Cl^{\bullet}]_1[M]_1 - K_p[M]_1[R^{\bullet}_1]_1 - K_{t1}[R^{\bullet}]_1[R^{\bullet}_1]_1 = 0 \tag{4.56}$$

From Eqs.(4.53)-(4.55), one can find

$$[R^{\bullet}_{r-1}]_1 = \frac{K_p[M]_1 - K_{fm1}[M]_1}{K_p[M]_1 + K_{t1}[R^{\bullet}]_1}[R^{\bullet}_{r-2}]_1$$

$$= \left[\frac{1 - CM}{1 + K_{t1}[R^{\bullet}]_1/K_p[M]_1}\right][R^{\bullet}_{r-2}]_1$$

$$= \left[\frac{1 - CM}{1 + K_{t1}[R^{\bullet}]_1/K_p[M]_1}\right]^{r-2}[R^{\bullet}_1]_1$$

$$= (1 - CM)^{r-2}[R^{\bullet}_1]_1 \tag{4.57}$$

where $K_{t1}[R^{\bullet}]_1/K_p[M]_1 \ll 1$ is assumed.

Let $r = r_c$, Eq.(4.57) becomes

$$[R^{\bullet}_{rc-1}]_1 = (1 - CM)^{r_c-2}[R^{\bullet}_1]_1 \tag{4.58}$$

where $CM = K_{fm1}/K_p$.

Substituting Eq.(4.44) into Eq.(4.56) and considering $K_p[M]_1 \gg K_{t1}[R^\cdot]_1$, one obtains:

$$[R_1^\cdot]_1 = \frac{R_{I1} + (K_{fm})_1 [M]_1 [R^\cdot]_1}{K_{p1}[M]_1} \tag{4.59}$$

Substituting Eq.(4.59) into Eq.(4.58), one can find

$$[R_{rc-1}^\cdot]_1 = K^* \frac{R_{I1} + (K_{fm})_1 [M]_1 [R^\cdot]_1}{K_{p1}[M]_1} \tag{4.60}$$

where

$$K^* = (1 - CM)^{r_c - 2}$$

a precipitation constant for polymer radicals.

Substituting Eq.(4.60) into Eqs.(4.51) and (4.52), one finally obtains the total radical population balance for VCM polymerization as follows:

$$R_{I1} - K^*(R_{I1} + K_{fm1}[M]_1[R^\cdot]_1) - K_{t1}[R^\cdot]_1^2 + K'_{de} R_{I2} V_2 / V_1 = 0 \tag{4.61}$$

$$R_{I2} + K^*(R_{I1} + K_{fm1}[M]_1[R^\cdot]_1) V_1 / V_2 - K_{t2}[R^\cdot]_2^2 - K_{de}' R_{I2} = 0 \tag{4.62}$$

Solving Eqs.(4.61) and (4.62), one can obtain the polymer radical concentrations for both phases (loci of polymerization) as follows:

$$[R^{\cdot}]_1 = \frac{\sqrt{J_1^2 + 4\,K_{t1}\,J_2} - J_1}{2\,K_{t1}} \tag{4.63}$$

$$[R^{\cdot}]_2 = \left[\frac{R_{I2}(1-K'_{de}) + K^{*} R_{I1} V_1/V_2 + J_1 V_1/V_2 (\sqrt{J_1^2 + 4\,K_{t1}\,J_2} - J_1)/2K_{t1}}{K_{t2}}\right]^{1/2} \tag{4.64}$$

where

$$J_1 = K^{*} K_{fm1} [M]_1$$

$$J_2 = R_{I1}(1-K^{*}) + K'_{de} R_{I2} V_2/V_1$$

From Eqs.(4.63) and (4.64), one can see that the radical concentrations for VCM heterogeneous polymerization are governed by initiator partition, radical termination in each phase and other properties associated with two phases.

4.3.2 Monomer Concentrations

During suspension polymerization, monomer partitions in monomer, polymer, water and vapour phases respectively. Monomer in the water and vapour phases was ignored in kinetic modelling by previous investigators. The total amount of monomer in the water and vapour phases is about 4-wt% under commercial reactor operation conditions. Hence, it is important to consider monomer distribution for valid kinetic/reactor modelling. The monomer distribution as a function of conversion and

reactor operation conditions was developed in Chapter 2. M_1 and M_2 used in Eq.(4.23) are as follows:

$$M_1 = M_o(1 - X) - M_g - M_w - M_2 \tag{4.65}$$

$$M_g = \frac{M_m P_{mo}}{R\ T}\left[(1.0 - W_l)V_r + \frac{X\ M_o(1/D_m - 1/D_p)}{1 - D_{go}/D_m}\right] \tag{4.66}$$

$$M_w = K\ W_w \tag{4.67}$$

$$M_2 = X\ [\ M_o(1 - X_f) - M_{gxf} - M_w]/X_f \tag{4.68}$$

where

$$M_{gxf} = \frac{M_m P_{mo}}{R\ T}\left[(1.0 - W_l)V_r + \frac{X_f M_o(1/D_m - 1/D_p)D_m}{D_m - D_{go}}\right]$$

If volume additivity is assumed, the volumes of monomer and polymer phase are:

$$V_1 = M_1/D_m \tag{4.69}$$

$$V_2 = M_2/D_m + M_o X\ /\ D_p \tag{4.70}$$

Hence

$$[M]_1 = D_m/M_m \tag{4.71}$$

$$[M]_2 = M_2/M_m V_2 \tag{4.72}$$

4.3.3 Initiator Partition/Efficiency/Decomposition Rate Constant

According to the two-phase polymerization scheme, initiation reactions occur in both monomer and polymer phases. The ratio of the initiation rates per unit volume in the monomer and polymer phases can be expressed as a constant because the monomer concentrations in the two phases are constant for the conversion range $X < X_f$, i.e.:

$$K_I = \frac{R_{I2}}{R_{I1}} = \frac{2f_2K_{d2}[I]_2}{2f_1K_{d1}[I]_1} \tag{4.73}$$

If $K_{d2} = K_{d1}$ and $f_2 = f_1$ are assumed, Eq.(4.73) becomes

$$K_I = [I]_2/[I]_1 \tag{4.74}$$

where K_I is a initiator partition coefficient that depends on the solubility of the initiator in both monomer and polymer phases. Unfortunately, solubility data for initiator in monomer and polymer phases are not available, therefore, K_I has to be used as an adjustable parameter in the model. Based on a total initiator mole balance, the initiator concentrations can be written as:

$$[I]_1 = I_o \exp(-K_d t)/(V_1 + K_I V_2) \qquad \text{(mole/L)} \tag{4.75}$$

$$[I]_2 = K_I [I]_1 \qquad \text{(mole/L)} \tag{4.76}$$

Decomposition rate constants and efficiencies of initiators sepend on the initiator and solvent type as well as on the temperature.

The initiation mechanism can be expressed as follows:

(a). $I \xrightarrow{K_d} [2R_1^{\cdot}]$ radical pair in cage

(b). $[2R_1^{\cdot}] \xrightarrow{K_{R1}}$ inert recombination in cage

(c). $[2R_1^{\cdot}] \xrightarrow{K_{R2}} I$ (peroxide) recombination in cage

(d). $[2R_1^{\cdot}] \xrightarrow{K_D} 2R_1^{\cdot}$ diffusion out from cage

(e). $[2R_1^{\cdot}] + M \xrightarrow{K_x} R_1^{\cdot} + R_1^{\cdot}$ reaction of radical pair with monomer

(f). $R_1^{\cdot} + M \xrightarrow{K'_p} R_1^{\cdot}$ generation of polymer radical chain length unity

Based on the definition of initiator efficiency, f, and the use of the stationary-state hypothesis, one can find:

$$f = \frac{K_D + K_x[M]}{K_{R1} + K_D + K_x[M]} \qquad (4.77)$$

For peroxide initiators, reaction (b) may involve decarboxylation and β scission reactions. If $K_{R2} \gg K_{R1}$, reaction (b) could be neglected, then initiator efficiency for peroxide initiators can be simplified to:

$$f \cong 1 \qquad \text{(peroxide initiator)} \qquad (4.78)$$

Therefore, for the azo initiator system, f is a function of conversion. For the peroxide initiator system, the initiator efficiency is equal/close to one. However, the decomposition rate of peroxide initiator is governed by reaction (a) and (c), i.e.:

$$-\frac{d[I]}{dt} = K_d[I] - K_{R2}[2R_1^{\cdot}]$$

$$= K_d \frac{K_{R2} + K_D + K_x[M]}{K_{R1} + K_{R2} + K_D + K_x[M]} [I]$$

$$= K_d' [I] \qquad (4.79)$$

where

$$K_d' = K_d \frac{K_{R2} + K_D + K_x[M]}{K_{R1} + K_{R2} + K_D + K_x[M]}$$

an effective decomposition rate constant for a peroxide initiator.

From Eq.(4.79), one can see that the analysis of the concentration of the initiator in a solvent only gives the effective decomposition rate constant K_d' instead of the conventional decomposition rate constant K_d. This may partly explain why the decomposition rate constant of peroxide initiators always depends on solvent type. Hence, the effective decomposition rate constant of the peroxide is a function of conversion at high conversions.

Using radical and monomer concentrations and the initiator partition coefficient, one can express the polymerization rate as a function of the physical properties of the reaction system and reactor operation conditions. Substituting Eqs.(4.63) and (4.64) into Eq.(4.23), one can rewrite the polymerization rate as:

$$\frac{d\bar{X}}{dt} = \frac{i}{N_o M_m}\left\{ K_{p1}(\sqrt{J_1^2 + 4\,K_{t1}R_{I1}J_2} - J_1)\,M_1/2K_{t1} + \frac{K_{p2}}{K_{t2}^{1/2}}\left[R_{I2}(1-K'_{de}) + \right.\right.$$

$$\left.\left. + K^{*}R_{I1}V_1/V_2 + \frac{J_1 V_1}{2K_{t1}V_2}(\sqrt{J_1^2+4\,K_{t1}J_2} - J_1)\right]^{1/2} M_2\right\} \qquad (X \le X_f) \qquad (4.80)$$

where M_1 and M_2 are shown as Eqs.(4.65)-(4.68).

Eq.(4.80) describes the total polymerization rate of VCM in two phases. This model shows that the Talamini model is a special case of the present model.

If $K^{*} = 0$ and $K'_{de} = 0$, Eq.(4.80) gives:

$$\frac{dX}{dt} = \frac{i}{N_o M_m}\left(\frac{K_{p1}}{K_{t1}^{1/2}} R_{I1}^{1/2} M_1 + \frac{K_{p2}}{K_{t2}^{1/2}} R_{I2}^{1/2} M_2\right) \qquad (4.81)$$

Eq.(4.81) indicates that the polymerization occurs in two phases independently. This equation will lead to Talamini's model.

$K^* = (1 - C_m)^{r_c - 2} = 0$ means that r_c equals infinity. Hence, precipitation of radicals does not occur during polymerization, which is also the main limitation of Talamini's model.

If $K^* = 1.0$ and $K'_{de} = 0$, Eq.(4.80) becomes:

$$\frac{dX}{dt} = \frac{K_{p2}}{N_o M_m K_{t2}^{1/2}} (R_{I2} + R_{I1} V_1 / V_2)^{1/2} M_2 \qquad (4.82)$$

which means that all of the polymerization occurs in the polymer phase.

The condition that $K^* = 1.0$ is consistent with $r_c = 2$, i.e.: the critical chain length for precipitation is two monomeric units. All the radicals will precipitate and transfer to the polymer phase before further propagation and termination occur in the monomer phase.

Therefore, K^* must have a value between 0 and 1 ($0 < K^* < 1$). The value of K^* observed will show how significant the precipitation of radicals is during VCM polymerization.

When the conversion is greater than the critical conversion ($X > X_f$), the monomer phase no longer exists and the polymerization proceeds in the polymer phase. In fact, the expressions for radical and monomer concentrations in this conversion range are straight forward. However, the kinetic rates which become diffusion-controlled will have associated rate constants which depend on the polymer concentration and thus on the

monomer conversion. The modelling of diffusion-controlled reactions will be discussed later (in section 4.3.5). The polymerization rate can now be expressed in the usual form as:

$$\frac{dX}{dt} = \frac{K_{p2}}{N_o M_m} (R_{I2}/K_{t2})^{1/2} M_2 \qquad (X > X_f) \qquad (4.83)$$

where

$$M_2 = M_o (1 - X) - M_g - M_w$$

$$M_g = \frac{M_m P_m}{R T} \left[(1.0 - W_l) V_r + M_o (1/D_m - 1/D_p)(X + X_f \frac{D_{go}}{D_m - D_{go}}) \right]$$

$$M_w = K W_w P_m / P_{mo}$$

$$R_{I2} = 2 f K_d I_o \exp(-K_d t)/V_2$$

4.3.4 Limiting Conversion

The glassy-state transition temperature of commercial PVC is about 80-85°C which is higher than the normal polymerization temperatures used. The glassy-state transition temperatures of PVC-VCM mixtures (the monomer acting as a plasticizer) is lower than that of pure PVC. Therefore, for the commercial polymerization temperature range, PVC-VCM mixtures (polymer phase) will experience a glassy-state transition below 100% monomer conversion. The conversion at which the polymer phase

experiences a glassy-state transition is called the limiting conversion (if f, K_d or K_p fall to essentially zero before glassy-state transition, one could get limiting conversion before glassy-state transition of polymer-monomer mixture). Polymerization now occurs in the solid state with rates that for production purposes may be considered zero. The limiting conversion X_L may be expressed as:

$$X_L = \frac{M_o - M_2 - M_w - M_g}{M_o} \tag{4.84}$$

where

$$M_2 = \frac{M_o X_L D_m (1 - \Phi_p)}{D_p \Phi_p} \tag{4.85}$$

$$M_w = K W_w P_m / P_{mo} \tag{4.86}$$

$$M_g = \frac{M_m P_m}{R T}\left[(1-W_l)V_r + M_o(1/D_m - 1/D_p)\left(X_L + X_f \frac{D_{go}}{D_m - D_{go}}\right)\right] \tag{4.87}$$

Substituting Eqs.(4.85)-(4.87) into Eq.(4.84), one obtains:

$$X_L = \frac{M_o - K W_w P_m / P_{mo} - M'_{gxf}}{M_o\left[1 + \frac{D_m (1-\Phi_p)}{D_p \Phi_p} + M_m P_m (1/D_m - 1/D_p)/RT\right]} \tag{4.88}$$

where

$$M'_{gxf} = \frac{M_m P_m}{R T}\left[(1 - W_i)V_r + \frac{X_f M_o (1/D_m - 1/D_p)D_{go}}{D_m - D_{go}}\right]$$

According to the free volume theory,[104] the free volume fraction of the polymer-monomer mixture may be expressed as (see Appendix A for the detailed explanations):

$$V_f = [0.025+\alpha_p(T-T_{gp})]\Phi_p + [0.025+\alpha_m(T-T_{gm})](1-\Phi_p) \qquad (4.89)$$

At the glassy-state transition, the free volume fraction of PVC-VCM mixture is taken to be 0.025. Hence, polymer volume fraction at the glassy transition state can be expressed as:

$$\Phi_p = \frac{\alpha_m (T - T_{gm})}{\alpha_p (T_{gp} - T) + \alpha_m (T - T_{gm})} \qquad (T_{gm} < T < T_{gp}) \qquad (4.90)$$

Partial pressure of monomer can be calculated using the Flory-Huggins equation:[105]

$$P_m / P_{mo} = (1 - \Phi_p)\exp(\Phi_p + \chi \Phi_p^2) \qquad (4.91)$$

Substituting Eqs.(4.90) and (4.91) into Eq.(4.88), one can find the limiting conversion as a function of reactor operation conditions and the physical properties of the polymer phase.

4.3.5 Diffusion Controlled Reactions in the Polymer Phase

Several attempts have been made to model diffusion-controlled termination and propagation.[17,101] However, the fall in initiator efficiency at high conversions has been neglected. Hamielec et al[101] first applied the free-volume theory to model diffusion-controlled termination and propagation to explain the properties of PVC obtained at high monomer conversions. These modelling attempts were premature due to the inadequate amount of kinetic data at these high conversion levels.

The free radical polymerization of VCM involves four reaction types based on the size of the reactants.

1. single molecules, such as reactions (1), (5), (8), (12) and (19) (see Table 4.1).
2. two small molecules, such as reactions (2) and (9) (see Table 4.1).
3. macromolecule and a small molecule, e.g. reactions (3), (4), (6), (7), (10), (11), (14), (20) (see Table 4.1).
4. Two macromolecules, e.g. reactions (13), (15) and (16) (see Table 4.1).

These reactions occur in both monomer and polymer phases simultaneously ($X < X_f$). The monomer phase is essentially pure monomer due to the low solubility of PVC. Hence, all the reactions in the monomer phase are likely chemically controlled. However, the polymer phase contains about 70-wt% polymer over the conversion range, 0 to X_f. Therefore, the

bimolecular termination reactions involving macroradicals should be diffusion controlled in the polymer phase over the entire monomer conversion range. At some conversions, $X > X_f$, it is expected that the propagation reactions become diffusion-controlled and that the initiator efficiency or decomposition rate constant falls significantly with conversion. In the present modelling, onset of diffusion control for these reactions is assumed to be at X_f.

At or near the glassy-state transition, the propagation reaction rate should fall effectively to zero. The effect of the environment on the initiation rate depends on the chemistry of the initiator as mentioned above. For azo-initiators, the efficiency will decrease significantly with conversion because K_D would fall appreciably with increase in viscosity of the medium. For peroxide-initiators, the effective decomposition rate constant will decrease significantly with conversion, which has been demonstrated experimentally by Marinin et al[19] and Sielfeld et al.[20]

Kinetic parameters for diffusion-controlled reactions for VCM polymerization are not available in the literature. In the present model, all of the rate constants for diffusion-controlled reactions are modelled using the free volume theory (see Appendix A for detailed explanations) as follows:

$$K_{t2} = K_{t1}\exp\left[-A^*\left(\frac{1}{V_{fp}} - \frac{1}{V_{fcrl}}\right)\right] \qquad (0 \le X \le X_L) \qquad (4.92)$$

where K_{t1} and K_{t2} are number-average termination rate constants (this accounts for chain length dependent bimolecular termination).

$$K_p = K_{pxf}\exp\left[-B^*\left(\frac{1}{V_{fp}} - \frac{1}{V_{fxf}}\right)\right] \qquad (X > X_f) \qquad (4.93)$$

$$K_p f^{1/2} = (K_p f^{1/2})_{xf}\exp\left[-B_f^*\left(\frac{1}{V_{fp}} - \frac{1}{V_{fxf}}\right)\right] \qquad (X > X_f) \qquad (4.94)$$

$$K_d' = K_{dxf}'\exp\left[-C^*\left(\frac{1}{V_{fp}} - \frac{1}{V_{fxf}}\right)\right] \qquad (X > X_f) \qquad (4.95)$$

where A^*, B^*, B_f^*, and C^* can be estimated by fitting model predictions with experimental rate data. K_p and f can not be separated for an azo-initiator in the present model.

4.4 EXPERIMENTAL

To estimate the parameters for the present model, a series of kinetic experiments was carried out over a wide temperature range.

The equipment and chemicals used for the experiments are the same as those described in Chapters 2 and 3.

The reactor was filled with a weighed amount of distilled, deionized water with dissolved stabilizer and a weighed amount of initiator at a temperature around 5-10°C. A weighed amount of n-butane and

VCM was injected into the reactor after the reactor was evacuated. The reactant mixture was stirred at low temperature for about 30 minutes to allow the initiator to dissolve in the monomer. The reactor temperature was then raised to the polymerization temperature in about 5 minutes. Conversions were determined by the online n-butane tracer method which has been discussed in detail in Chapter 3.

The suspension polymerization conditions and the basic recipe are as follows:

Reactor volume	:	5.0 L
Temperature	:	40°, 45°, 50°, 55°, 60°, 65°, 70°, 80°C
Monomer	:	1116 g
Water	:	2232 g
Stabilizer (PVA)	:	0.08-wt% (based on water)
Initiator	:	various amounts

4.5 RESULTS AND DISCUSSION

The present experimental results are shown in Figures 4.4-4.7. The accuracy of the experimental results was discussed in Chapter 3.

4.5.1 Physical Properties Used in the Model

The parameters of physical properties of VCM and PVC, D_m, D_p, K, P_{mo} and χ are shown in Eqs.(2.38), (2.39), (2.35), (2.40) and (2.37), respectively.

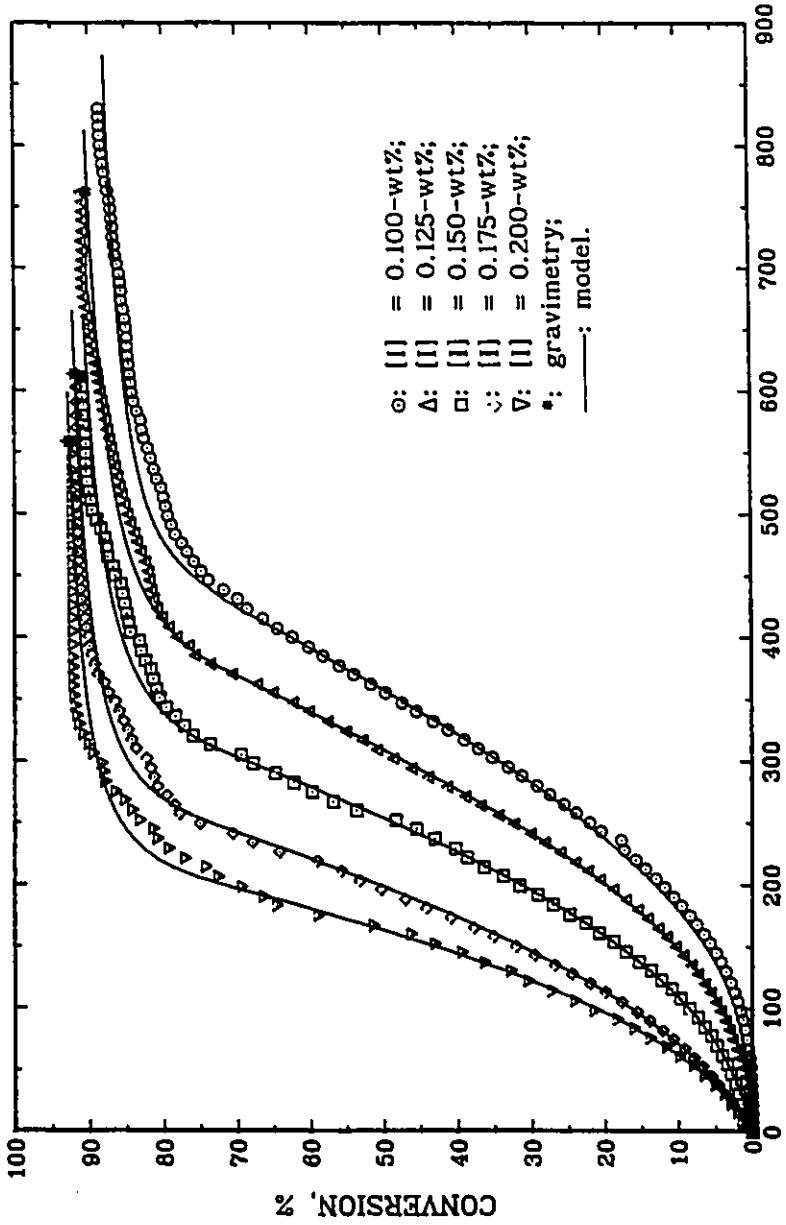

Figure 4.4. Conversions versus reaction time for suspension polymerization of VCM at 50°C. Initiator: Perkadox 16-W40.

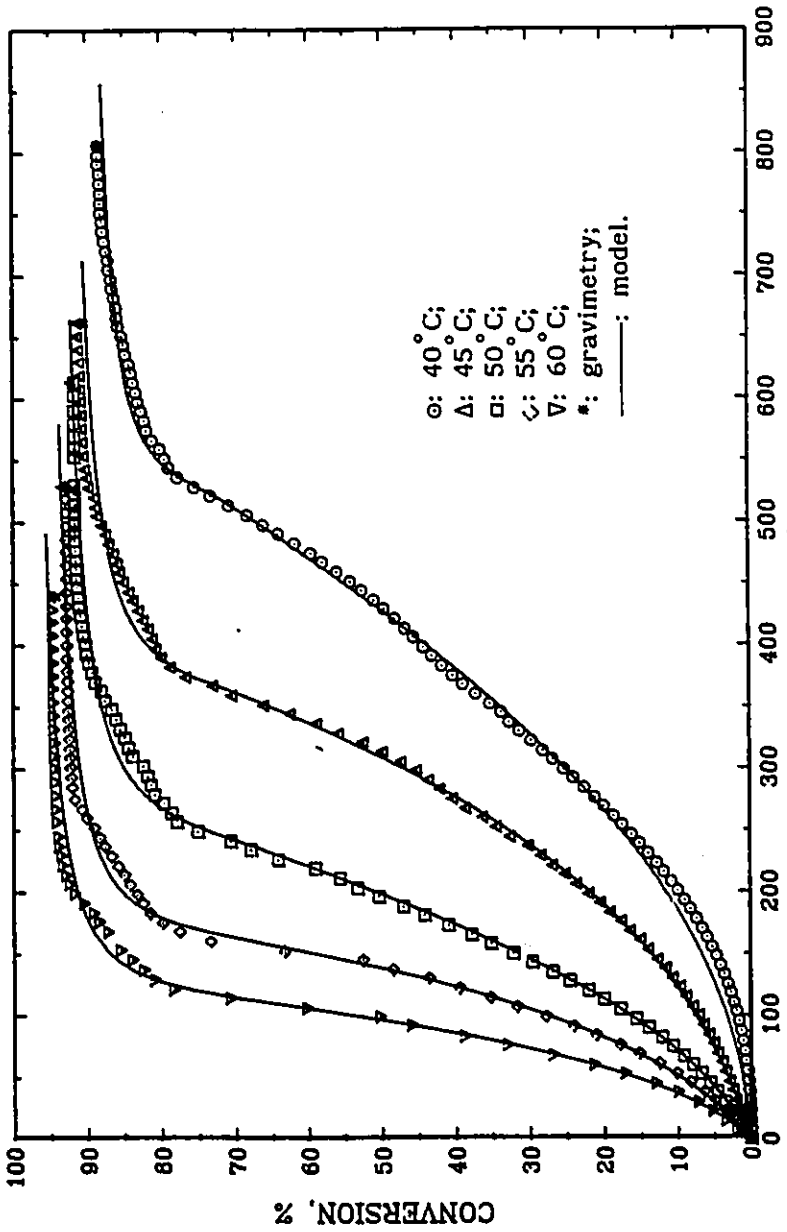

Figure 4.5. Suspension polymerization of VCM at different Temperatures with Perkadox 16-W40 as an initiator, [I]=0.175-wt%.

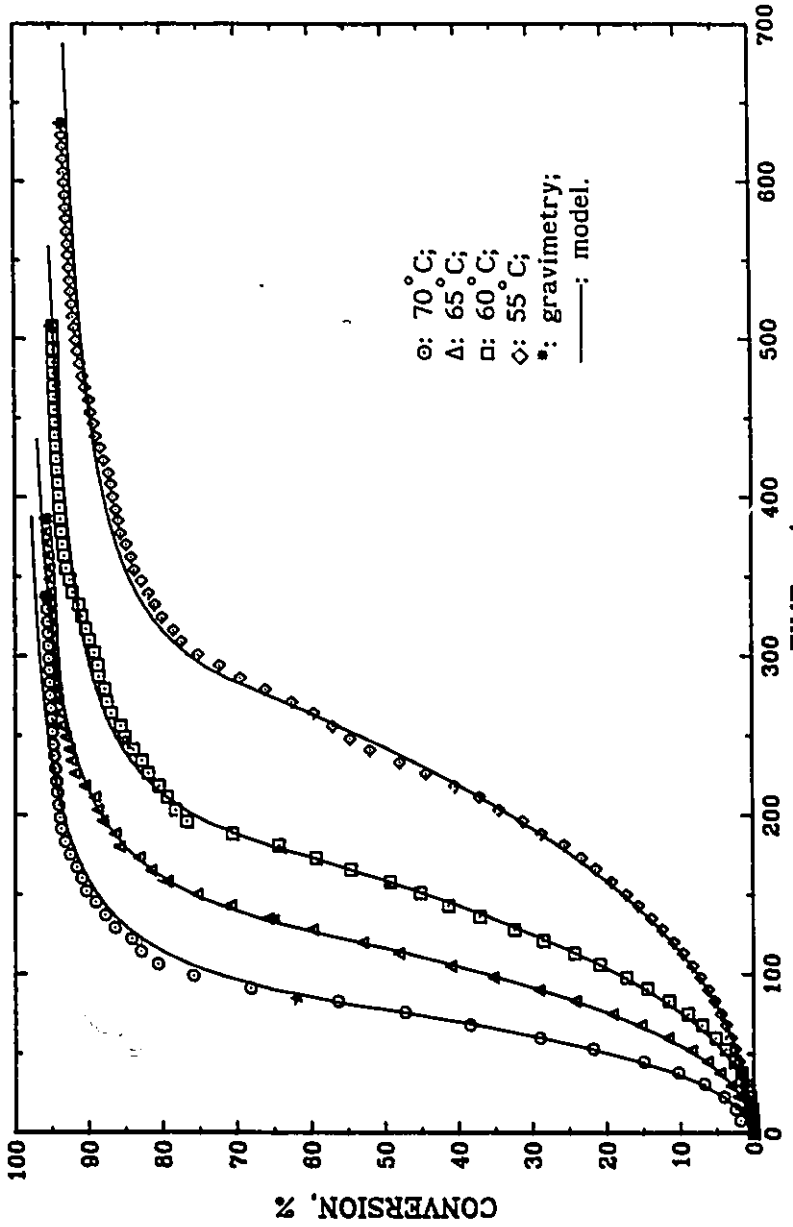

Figure 4.6. Suspension polymerization of VCM at different temperatures with AIBN as an initiator, [I] = 0.25-wt%.

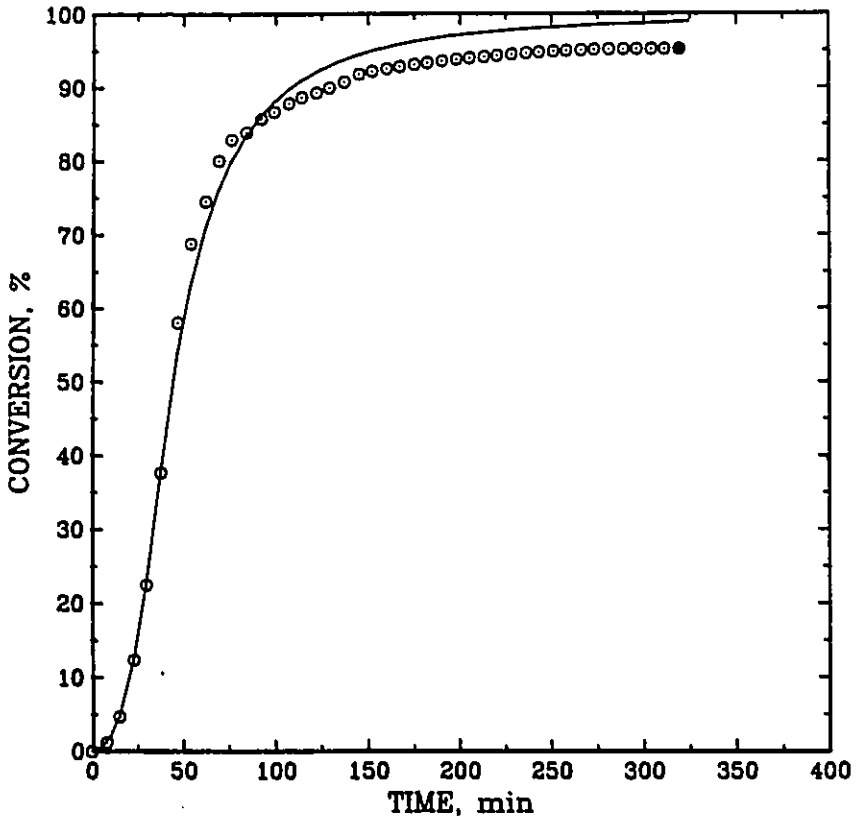

Figure 4.7. Suspension polymerization of VCM at 80°C with AIBN as an initiator, [I] = 0.15-wt%.
⊙: experimental data, ———: model.

The water density within temperatures used can be expressed as:

$$D_w = 1011.0 - 0.4484\ t\ (^{\circ}C) \qquad (g/L)^{106} \qquad (4.96)$$

The glassy-state transition temperature of VCM, T_{gm}, was estimated using Fedors's universal correlation[107] to be:

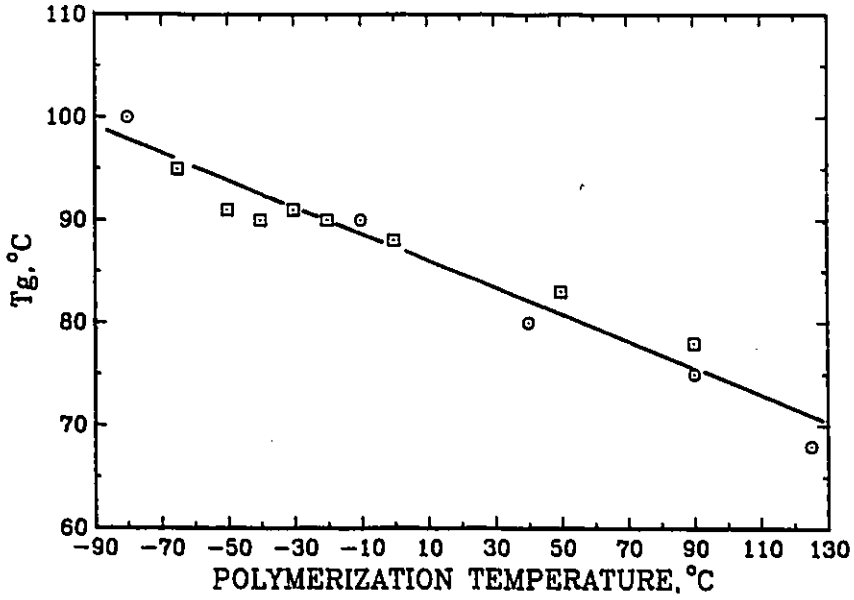

Figure 4.8. Polymerization temperature dependence of glassy-state transition temperature of PVC.
⊙: Reding et al's data (ref.108).
□: Ceccorulli et al's data (ref.109).

$$T_{gm} = 70.0\ (^{\circ}K\ ) \tag{4.97}$$

The glassy-state transition temperature of PVC, T_{gp}, depends on the synthesis temperature according to Reding et al[108] and Ceccorulli et al's[109] results as shown in Figure 4.8. The correlation between T_{gp} and polymerization temperature can be obtained using a least squares fit:

$$T_{gp} = 87.1 - 0.132\ t\ (^{\circ}C\ ) \tag{4.98}$$

The glassy-state transition temperature of PVC-VCM mixtures as reported in the literatures[110-112] are shown in Figure 4.9 together with

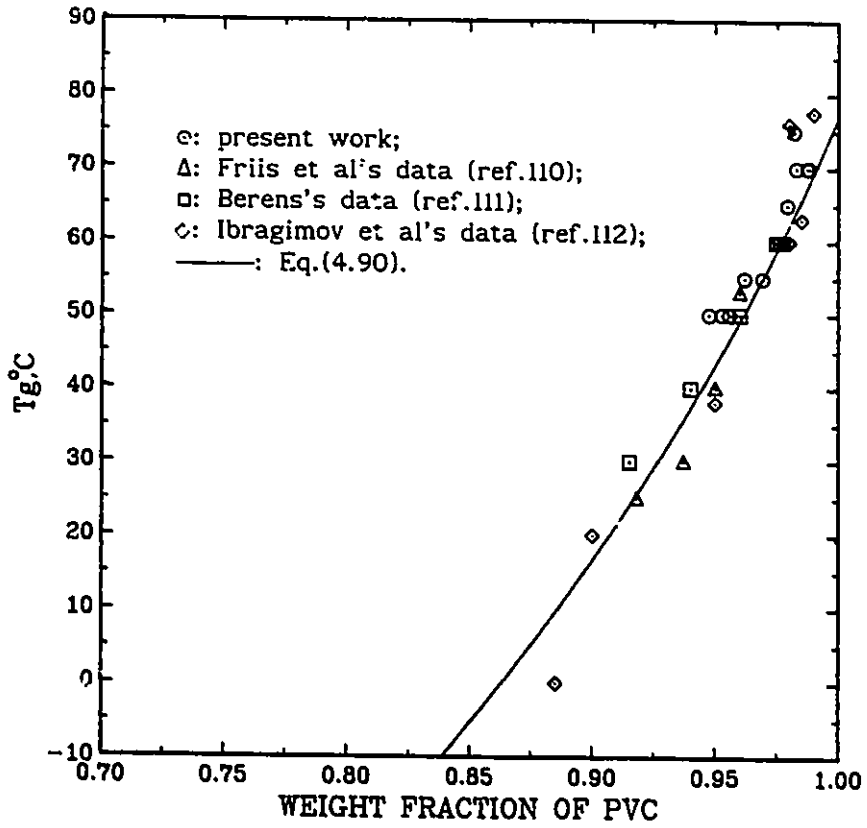

Figure 4.9. Glassy-state transition temperature of PVC-VCM mixture versus weight fraction of PVC.

the present limiting conversion data. Fitting Eq.(4.90) to these data, one can estimate the thermal expansion factors for VCM and PVC as follows:

$$\alpha_m = 9.98 \times 10^{-4} \tag{4.99}$$

$$\alpha_p = 5.47 \times 10^{-4} \tag{4.100}$$

These values are used in the present model.

4.5.2 Kinetic Parameters

The decomposition rate constant of AIBN has been estimated by many investigators[113-118] for different solvents over a wide range of temperature. These data are shown in Figure 4.10. One can see that K_d for AIBN is independent of solvent type and level. The temperature dependence of K_d can be estimated using a least squares fit as:

$$K_d = 2.88\times10^{15}\exp(-31.2\ \text{Kcal/RT}) \quad (\text{sec}^{-1}) \tag{4.101}$$

The decomposition rate of Perkadox 16-W40 has not been studied in detail although it is a common initiator in commercial processes. Very limited data have been reported by AKZO chemicals[119] as shown in Figure 4.10. The temperature dependence of K_d' for Perkadox 16-W40 can be estimated roughly as:

$$K_d' = 2.31\times10^{15}\exp(-29.1\ \text{Kcal/RT}) \quad (\text{sec}^{-1}) \tag{4.102}$$

Eq.(4.102) can only be used for $X < X_f$. When $X > X_f$, K_d' will be calculated using Eq.(4.95).

The initiator efficiency of AIBN in VCM bulk or suspension polymerization has not been determined. A value 0.77 was determined by Arnett et al[120] in solution polymerization of VCM and it will be used in the present model for $X < X_f$. For $X > X_f$, it will be estimated based on Eq.(4.94) together with K_p.

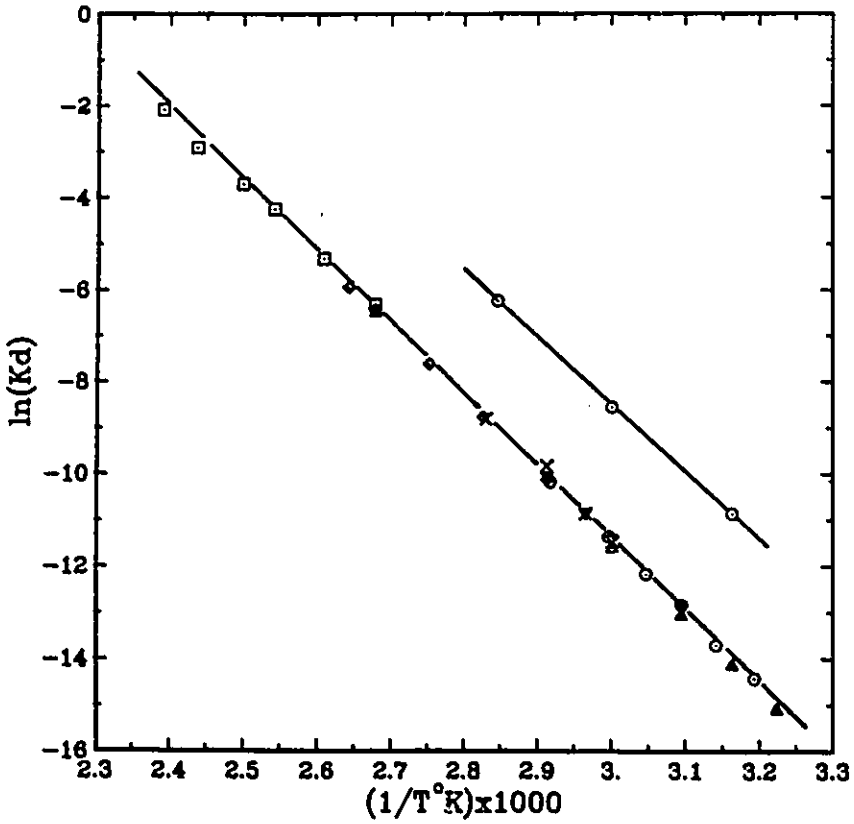

Figure 4.10. Decomposition rate constants of AIBN and Perkadox 16-W40. ⊙: AIBN in benzene (ref.113); Δ: AIBN in benzene or Toluene (ref.114); □: AIBN in di-n-butylphthalate (ref.115); ◇: AIBN in toluene (ref.116); x: AIBN in toluene (ref.117); ∇: AIBN in vinyl chloride monomer (ref.118); ⊙: Perkadox 16-W40 in chlorobenzene (ref.119).

Individual kinetic constants such as K_p, K_t for bulk or suspension polymerization of VCM are not available in the literature. Normally, the ratio $K_p/K_t^{1/2}$ is estimated based on conversion-time data.[13,14,121,122] However, the results strongly depend on model applied and conversion range used. In the present work, $K_p/K_t^{1/2}$ was estimated by using very low conversion data. At very low conversion, $K^* = 0$, $K'_{de} = 0$,

M_2 = 0 may be assumed, then Eq.(4.80) can be simplified for homogeneous polymerization, which can be integrated as:

$$-\ln(1 - X) = K_p\left(\frac{2fK_d}{K_t}\right)^{1/2}[I]_o^{1/2}t \qquad (4.103)$$

Therefore, the initial slope can be found by plotting -ln(1-X) against t as shown in Figure 4.11. $K_p/K_t^{1/2}$ can be obtained from these initial slopes as shown in Figure 4.12. The relationship between $K_p/K_t^{1/2}$ and temperature were estimated by the least squares method as:

$$K_p/K_t^{1/2} = 10.4\exp(-3.78\ \text{Kcal/RT}) \qquad (\text{L/mole-sec})^{1/2} \qquad (4.104)$$

These results are in agreement with data estimated by Kuchanov et al.[14] The rate constant ratio given by Eq.(4.104) was used for polymerization in the monomer phase.

During model evaluation, a group of kinetic constants K_{fm1}/K_{t1} was involved, which strongly correlates with other parameters in nonlinear regression calculations. The literature values determined in solution polymerization[123] were used in the present model:

$$K_{fm1} = 1.9\times10^5\exp(-7800/RT) \qquad (\text{L/mole-sec}) \qquad (4.105)$$

$$K_{t1} = 1.3\times10^{12}\exp(-4200/RT) \qquad (\text{L/mole-sec}) \qquad (4.106)$$

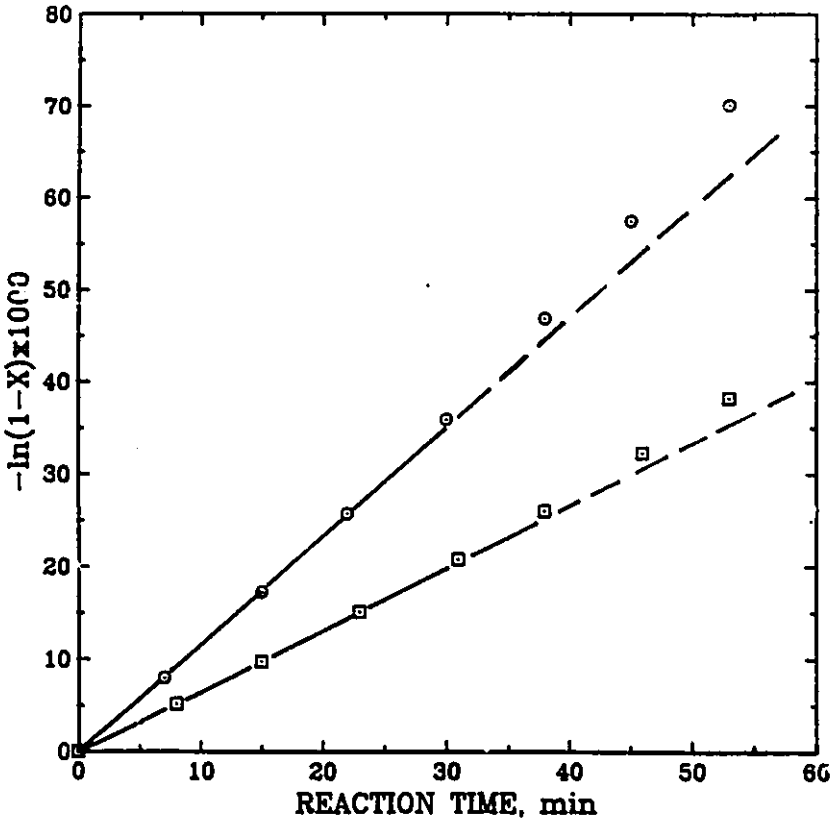

Figure 4.11. -ln(1-X) versus reaction time for VCM suspension polymerization at 50 °C.
⊙: Perkadox 16-W40, □: AIBN.

The calculation of the critical conversion X_f at which the monomer phase is consumed by the model was illustrated in Chapter 2. The critical free volume fraction V_{fxf} can be calculated for using X_f. The critical free volume fraction V_{fcrl} at which the bimolecular termination reaction of polymer phase becomes diffusion-controlled is difficult to estimate. However, the following inequality should be true:

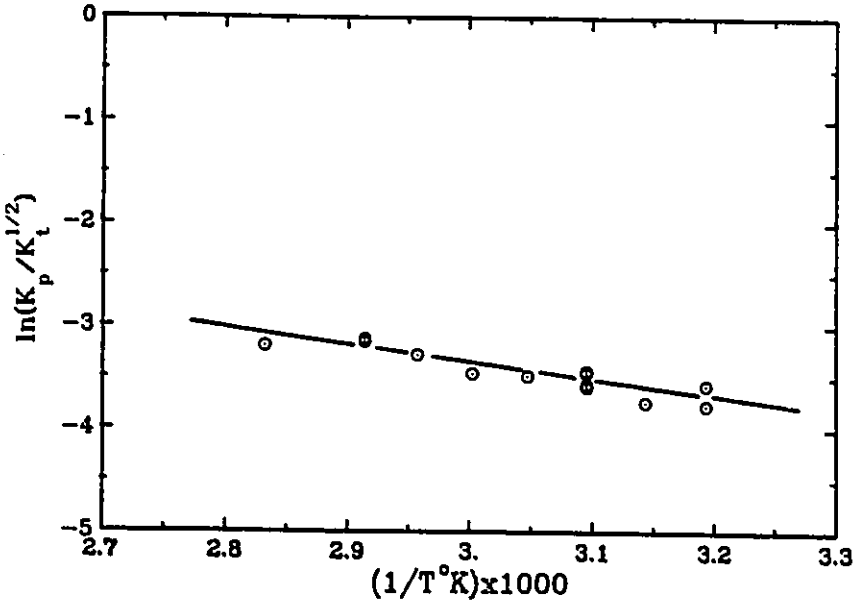

Figure 4.12. $K_p/K_t^{1/2}$ versus reaction temperature for vinyl chloride polymerization at low conversions.

$$V_{fp} < V_{fcrl} < V_{fm} \tag{4.107}$$

Both V_{fp} and V_{fm} are constant for $X < X_f$. Considering a hypothetical homogeneous PVC-VCM solution, one may assume that the bimolecular termination reaction of polymer radicals becomes diffusion-controlled at around 30% conversion. At this conversion for the hypothetical system, the V_{fcrl} is equivalent to 80% of V_{fm}. A value of 80% V_{fm} was used for V_{fcrl} in the present model.

Desorption of polymer radicals from the polymer phase into the monomer phase involves their molecular diffusion out of primary parti-

cles. The desorption rate constant, therefore, is a function of molecular diffusion coefficients and diameter of the primary particle. Applying Nomura's equation,[124] one may write the modified desorption rate constant as

$$K'_{de} = K^{*}_{de}/d_p^2 \qquad (4.108)$$

where K^{*}_{de} is a function of temperature, d_p is diameter of the primary particle which is a function of conversion and temperature.

Information about diameter of the primary particle as a function of conversion and temperature is very limited in the literature. Smallwood[70] determined the diameter of primary particles as a function of conversion over a temperature range, 51–71°C. Based on Smallwood's data, the diameter of primary particles can be expressed as the following correlation:

$$d_p=[(0.045t(^{\circ}C)-0.76)X^{1/2}-0.21]10^{-5} \quad (dm) \qquad (0.02 < X < X_f) \qquad (4.109)$$

The remaining parameters in the present model were estimated with a nonlinear regression method —— fitting the experimental data with solutions of the differential equation. The results of the model fitting are shown in Figures 4.4–4.6. One can see that the present model can satisfactorily fit the experimental data over the entire conversion range (from zero to limiting conversion).

The parameters K^{*}, A^{*}, K^{*}_{de} and K_1 were estimated by using

conversion-time data for $X < X_f$. The parameters B^*, B_f^*, and C^* were estimated by using conversion-time data for $X > X_f$. The results are shown in Figures 4.13–4.16.

In Figure 4.13, one can see that K^* increases with polymerization temperature. The temperature dependence of K^* can be expressed using the following correlation:

$$K^* = [0.25\ t\ (^\circ C) - 7.89]10^{-4} \qquad (4.110)$$

With K^* values, one can estimate significance of the precipitation of radicals from the monomer phase. At 50°C, for example, K^* is

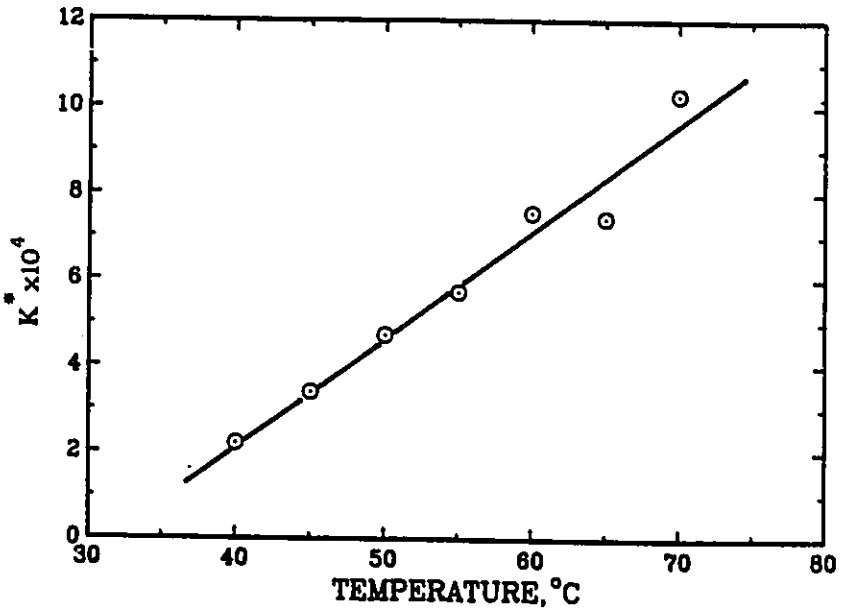

Figure 4.13. Temperature dependence of K^*.

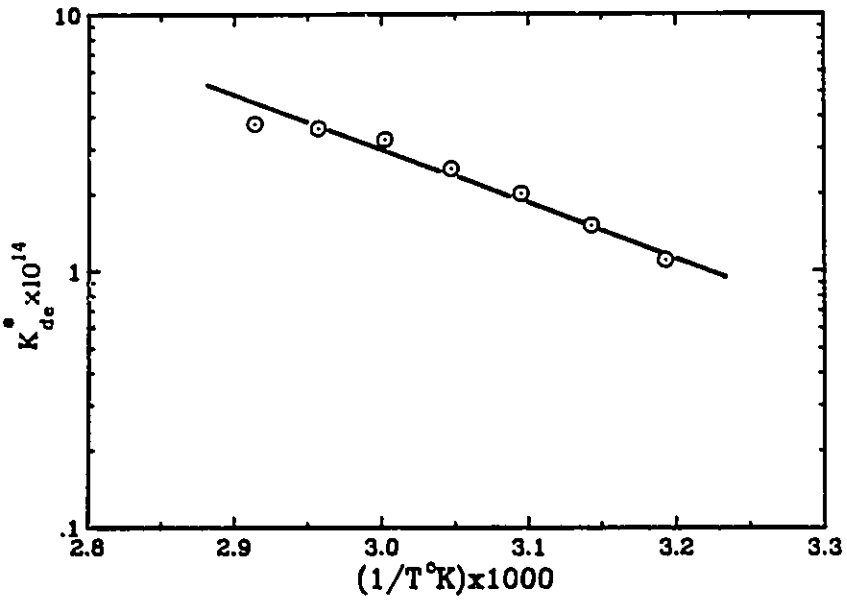

Figure 4.14. Temperature dependence of K^*_{de}.

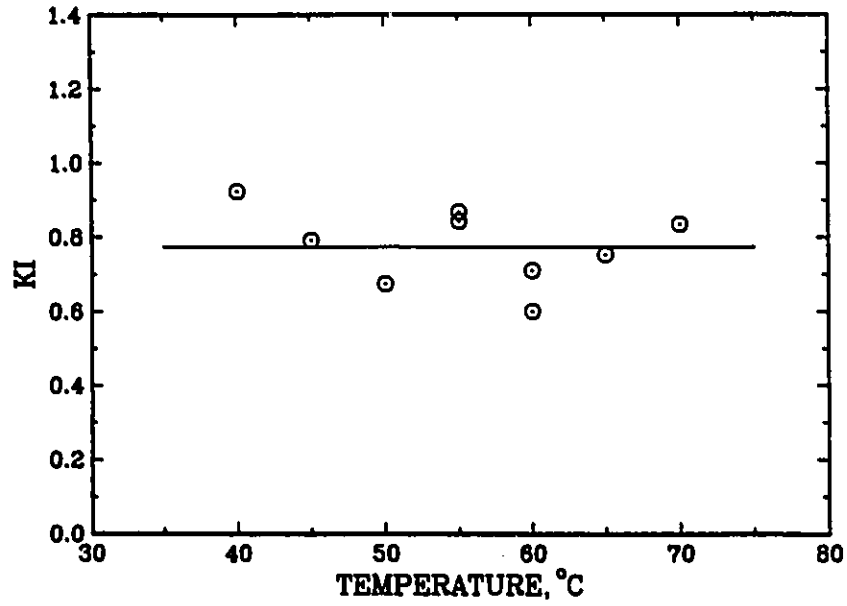

Figure 4.15. Initiator partition coefficient in vinyl chloride polymerization system.

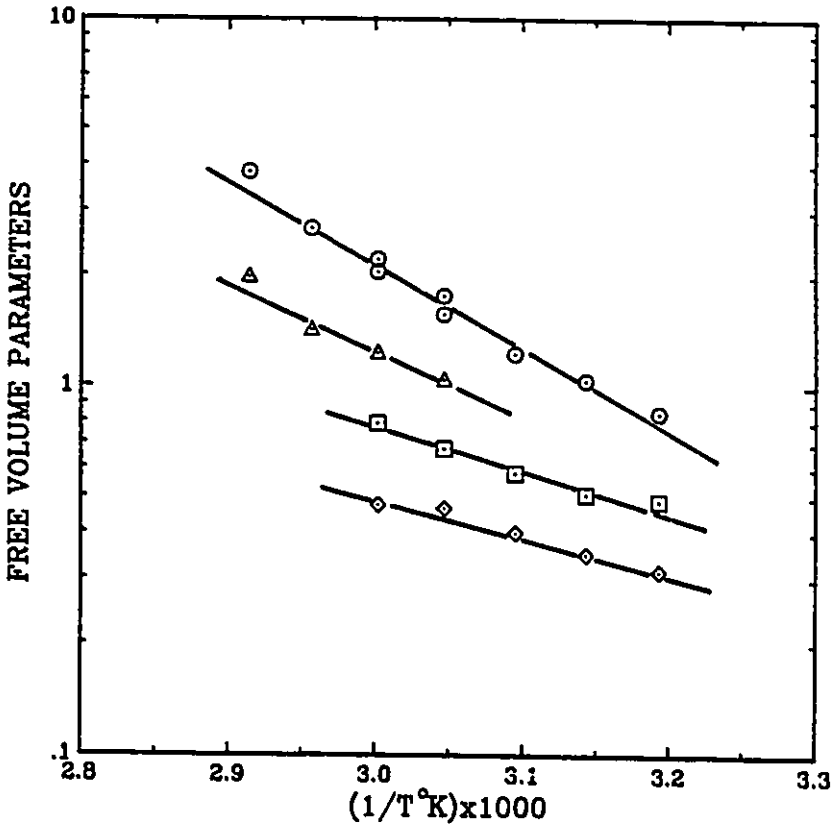

Figure 4.16. Temperature dependence of free volume parameters. ⊙: A^*; Δ: B_f^*; □: B^*; ◇: C^*.

about 4.6×10^{-4}, which indicates that about 4.6×10^{-2} percent radicals produced from initiation and transfer to monomer will precipitate out from the monomer phase before termination based on the present model Eqs.(4.61) and (4.62). This magnitude of K^* indicates that the precipitation may not affect the radical concentration in the monomer phase significantly. However, the precipitation of these radicals will increase the radical concentration in the polymer phase significantly at

relatively low conversion levels, because the ratio of reaction volume between monomer and polymer phase is very high at low conversions as shown in Figure 4.17. This effect decays dramatically with conversion. K^*, estimated in the kinetic model, is based on the radical population balance in the different phases. It may not represent the thermodynamic solubility chain length (see Appendix B for detailed explanations).

The temperature dependence of K^*_{de} is shown in Figure 4.14. It can be expressed as the following correlation:

$$K^*_{de} = 5.08 \times 10^{-8} \exp(-4790/T) \qquad (dm^2) \qquad (4.111)$$

Substituting Eqs.(4.109) and (4.111) into Eq.(4.108), one can find K'_{de}. At 50° C, for example, K'_{de} is about 0.5 when the diameter of PVC particles is about 0.02 μm at about 2% conversion. The desorption of radicals from the polymer phase is very significant at this stage. However, when the diameter of primary particle is about 0.5 μm at around 20% conversion, K'_{de} is as small as 0.0008. Therefore, the desorption of radicals is negligible when the diameter of primary particle is larger than 0.5 μm. Although the desorption of radicals is very significant at low conversions, it will not affect radical concentration in the monomer phase because the volume of polymer phase is very small compared with that in the monomer phase. With K^* and K'_{de} values, one can conclude that the absorption and desorption of radicals are significant only at very low conversions (<10% conversion). Radical exchange between phases only

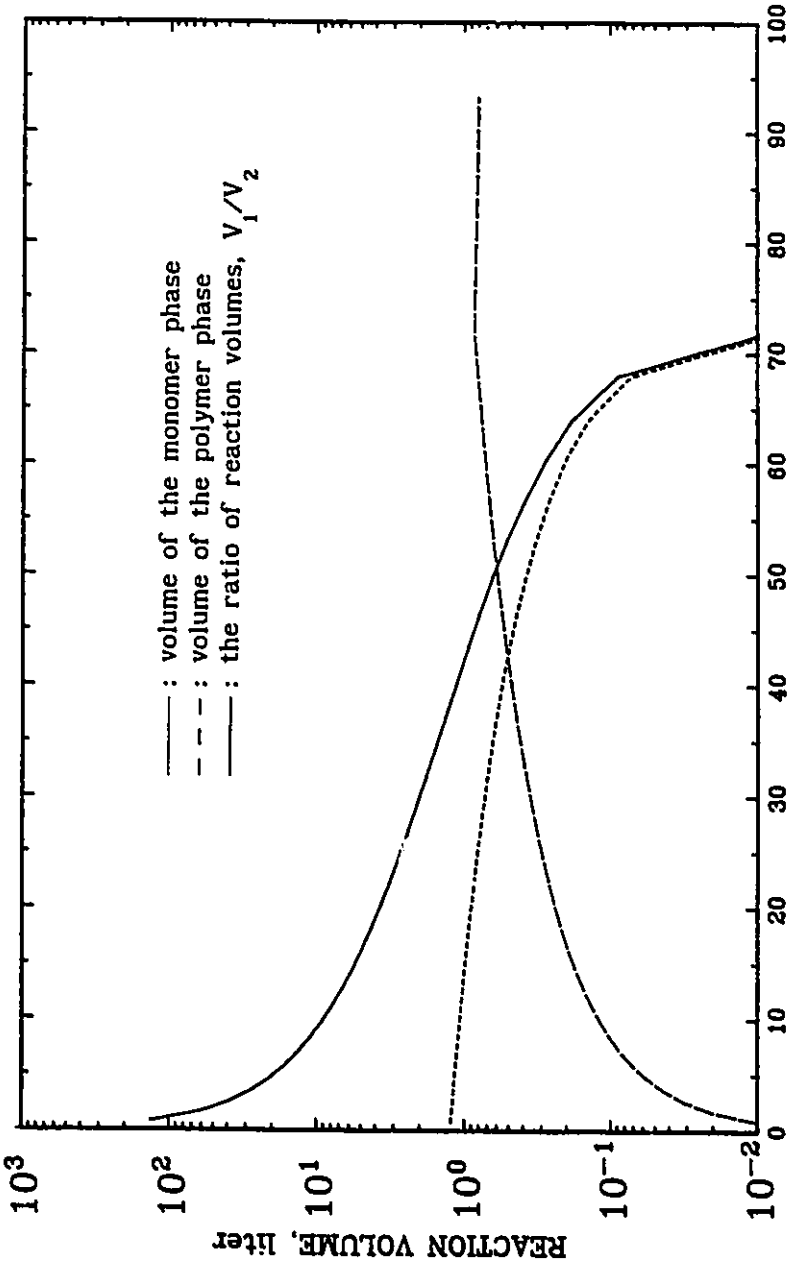

Figure 4.17. Reaction volume and the ratio of reaction volume variation with conversion at 50°C.

affects radical concentration in the polymer phase. This effect cannot dominate the radical concentrations in both phases even at very low conversions.

Initiator partition coefficients have neither been independently measured experimentally nor estimated by modelling. It was often assumed that K_I is less than or equal to unity in the literature.[16,17] It is the first time that K_I has been estimated by fitting a model with conversion-time data as done in the present study. One can see that, from Figure 4.15, K_I values are very scattered, and seems to be independent of the polymerization temperature and the initiator type. Average K_I value is 0.77 based on the present data. It should be mentioned that K^* and K_I are highly correlated in the present estimation. Therefore, it is difficult to estimate these values precisely. However, it appears that K_I is less than unity.

Figure 4.16 shows the temperature dependence of the free volume parameters. The correlations obtained by a least squares fitting follow:

$$A^* = 6.64\times10^{6}\exp(-4986/T) \quad (4.112)$$

$$B^* = 1.85\times10^{3}\exp(-2595/T) \quad (4.113)$$

$$B_f^* = 4.01\times10^{4}\exp(-3464/T) \quad (4.114)$$

$$C^* = 477.0\exp(-2291/T) \quad (4.115)$$

From Eqs.(4.112)-(4.115), one can see that $A^* > B^* > C^*$ at a given temperature. These values imply that the sensitivity of bimolecular termination, propagation and initiation to change in free volume at high conversions also follows this order.

All the parameters involved in the present model have been estimated as discussed above. This is the first attempt to comprehensively establish correlations of kinetic parameters for VCM polymerization. From Figures 4.11-4.16, one can see that the values of the parameters estimated are reasonable. This suggests that the present experimental data give consistent parameters for the present model for VCM suspension polymerization over the large conversion range studied. With these parameters, one can further predict other features of VCM polymerization quantitatively using the present model.

4.5.3 Simulations Using the Present Model

With the physical and kinetic parameters estimated above, one can quantitatively describe the features of the two-phase polymerization of VCM.

Figure 4.18 shows the partition of initiator between the two phases. Initiator concentrations in both monomer and polymer phases increase significantly, therefore, the total concentration of AIBN increases with conversion for $X < X_f$. This is because the decomposition rate of AIBN is very small and the reaction volume shrinks, the

consequence being an increase in the total concentration of AIBN. At very high conversions, the reaction rate is very slow, hence, reaction volume shrinkage rate is also very slow, but the decomposition of AIBN still proceeds. Hence, the total concentration of AIBN decreases as a result. It should be mentioned that the initiator concentration for a slow initiator system during VCM polymerization is higher than the initial concentration for a wide range of conversions. For Perkadox 16-W40, the total concentration of initiator decreases gradually because the decomposition rate of Perkadox 16-W40 is much higher than that for AIBN and thus volume shrinking rate is less important when $X < X_f$. At high conversions ($X > X_f$), the concentration of initiator increases slightly because of a decrease in K_d' and reaction volume.

Eq.(4.9) shows that, in general, the radical concentration in the polymer phase is higher than that in the monomer phase. Based on the present model predictions, as shown in Figure 4.19, radical concentration in the polymer phase is about 30 times higher than that in the monomer phase at 50°C. This is a consequence of the lower bimolecular termination rate in the polymer phase. This also explains the autoacceleration in polymerization rate observed for VCM polymerization. At high conversions, the radical concentration increases dramatically. The model prediction of radical concentration should be tested by radical concentration measurements (such as ESR analysis).

The total polymerization rate is in excellent agreement with the experimental rate data calculated by differentiating conversion-time

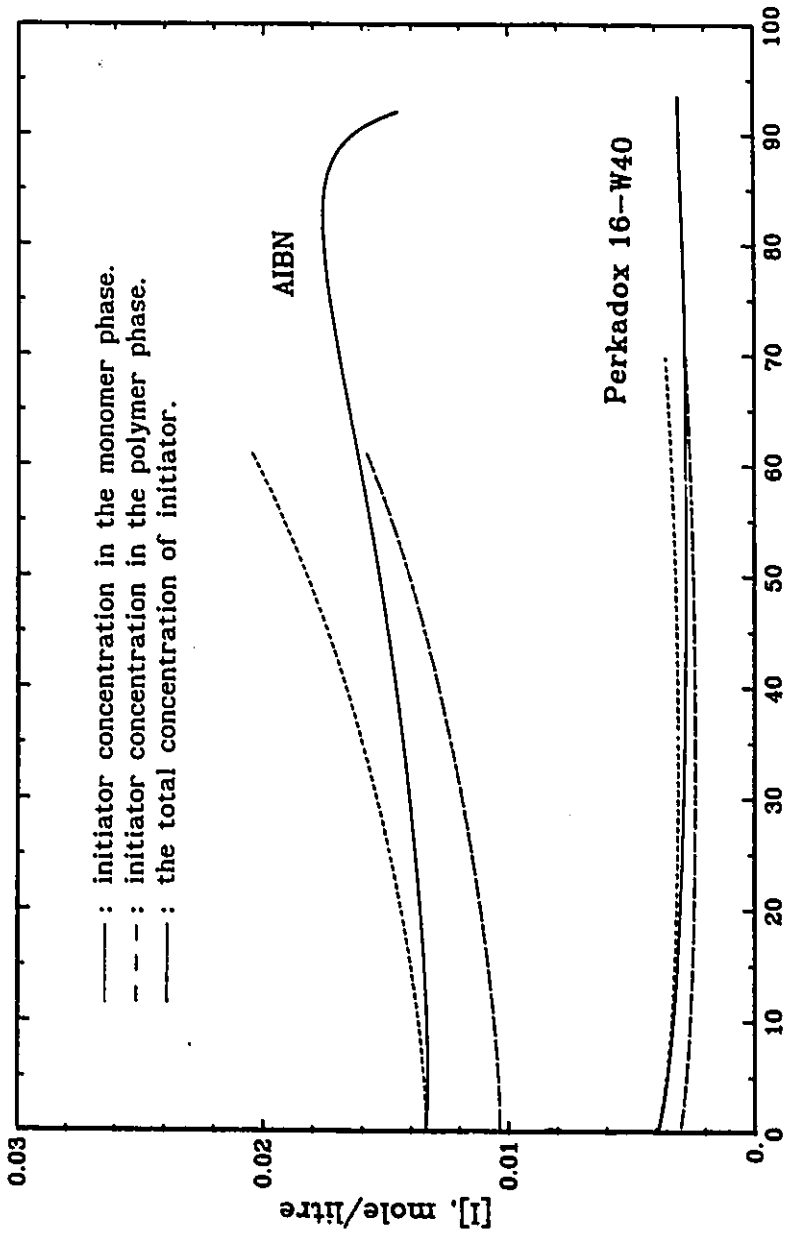

Figure 4.18. Initiator concentration variation with conversion for suspension polymerization of VCM at 50 °C.

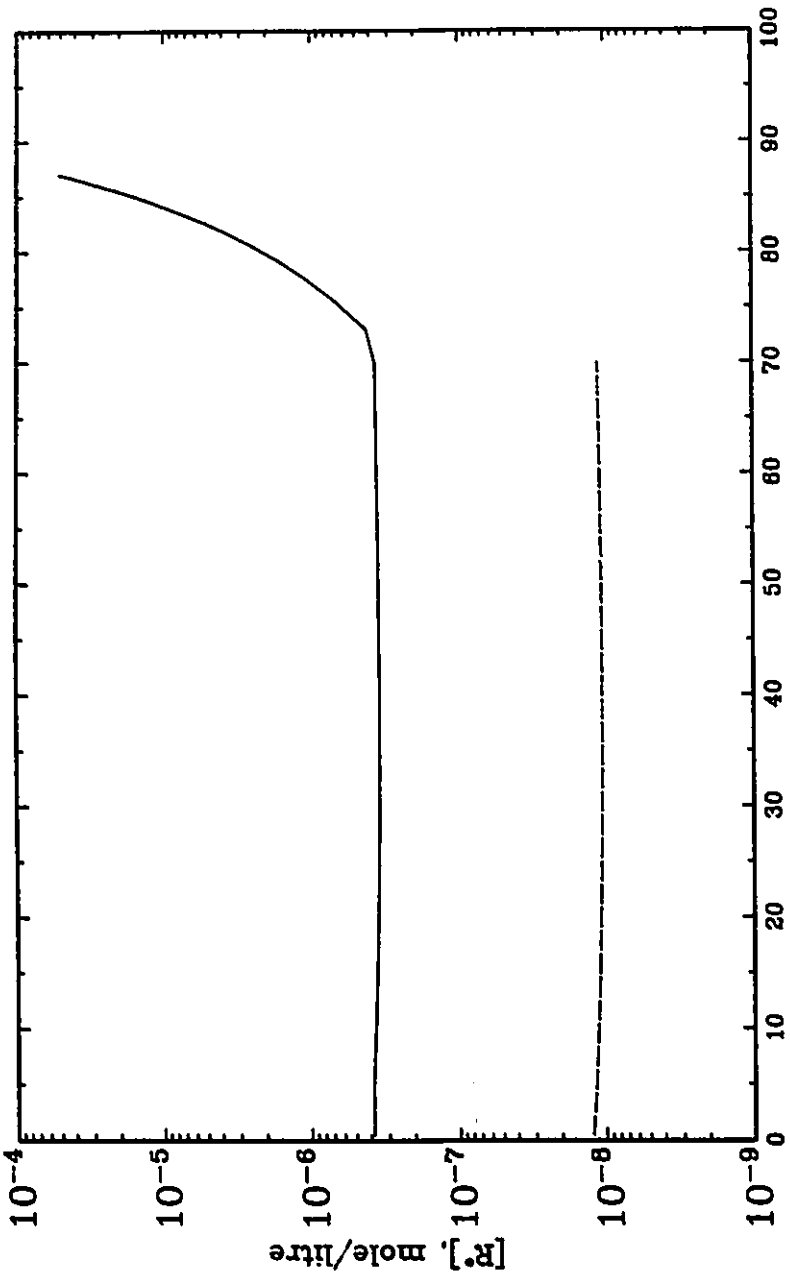

Figure 4.19. Radical concentrations in two phases at 50°C.
Perkadox 16-W40 with [I] = 0.175-wt%.
——: polymer phase; – – –: monomer phase.

data, as shown in Figure 4.20. The highest reaction rate occurs at a conversion near X_f. If K_{t1} in Eq.(4.106) is used for the monomer phase, the polymerization rates in the monomer and polymer phases can be calculated separately as shown in Figure 4.21 together with the total polymerization rate. In Figure 4.21, one can see that the reaction rate in the monomer phase decreases with conversion gradually and the reaction rate in the polymer phase increases dramatically with conversion until X_f, then decreases sharply to the limiting conversion X_L. The monomer phase dominates the polymerization rate only below about 7% conversion at 50°C. At higher conversions, polymerization in the polymer phase dominates. This is consistent with the assumptions made by several former investigators.[12,15,94]

All Figures 4.4-4.7, 20 and 21 show that the polymerization rate falls dramatically beyond conversion X_f. Figures 4.22-4.25 further show the change of model parameters. Beyond X_f, the monomer phase does not exist and polymerization continues in the primary particles and their agglomerates. Hence, the free volume fraction decreases gradually with conversion until the glassy-state transition as shown in Figure 4.22. With decreasing free volume, the termination and propagation rate constants, and initiator efficiency for AIBN and decomposition rate constant for peroxide decrease dramatically. The rate of change depends on the nature of the reactions as shown in Figures 4.23-4.25 respectively.

The limiting conversion varies with polymerization temperature as shown in Figure 4.26. The experimental data are the final conversions

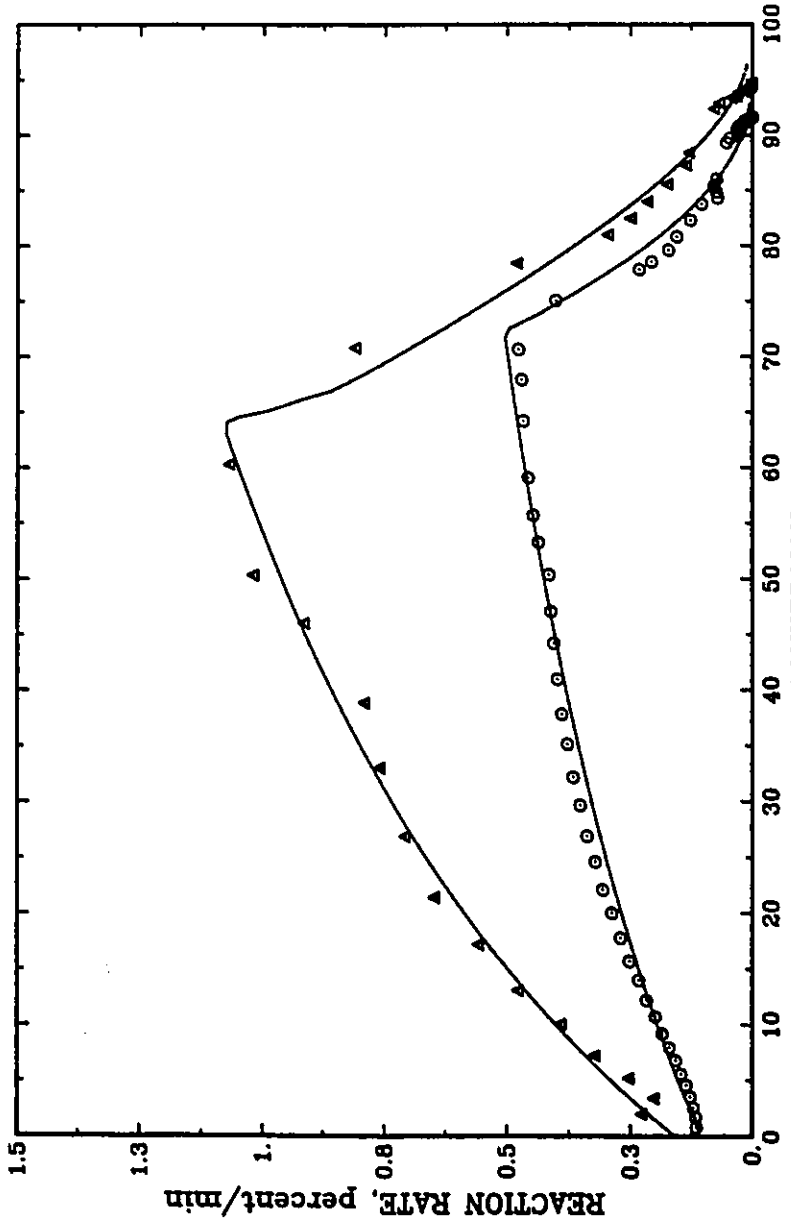

Figure 4.20. The total polymerization rate variation with conversion and temperature, Perkadox 16-W40 with [I] = 0.175-wt%. Δ : 60°C; o : 50°C; ———: model.

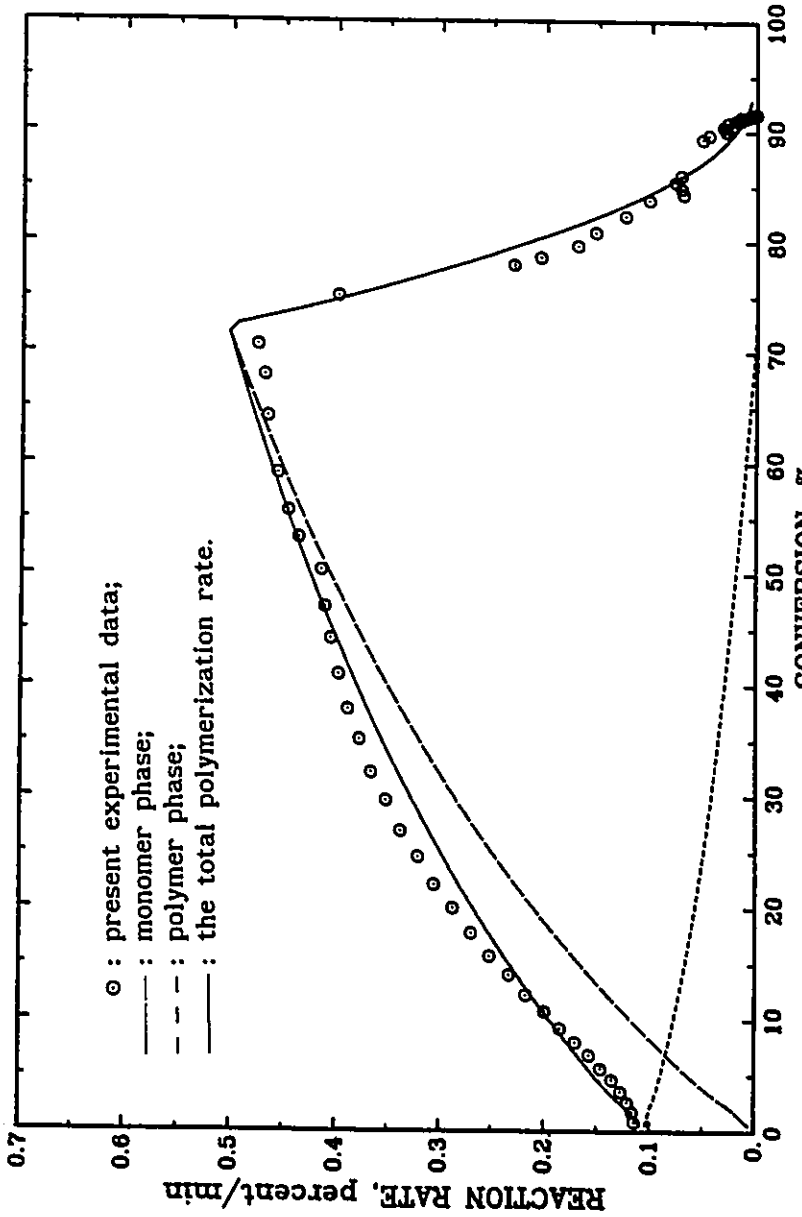

Figure 4.21. Polymerization rate variation with conversion in different phases, Perkadox 16-W40 with [I] = 0.175-wt% at 50°C.

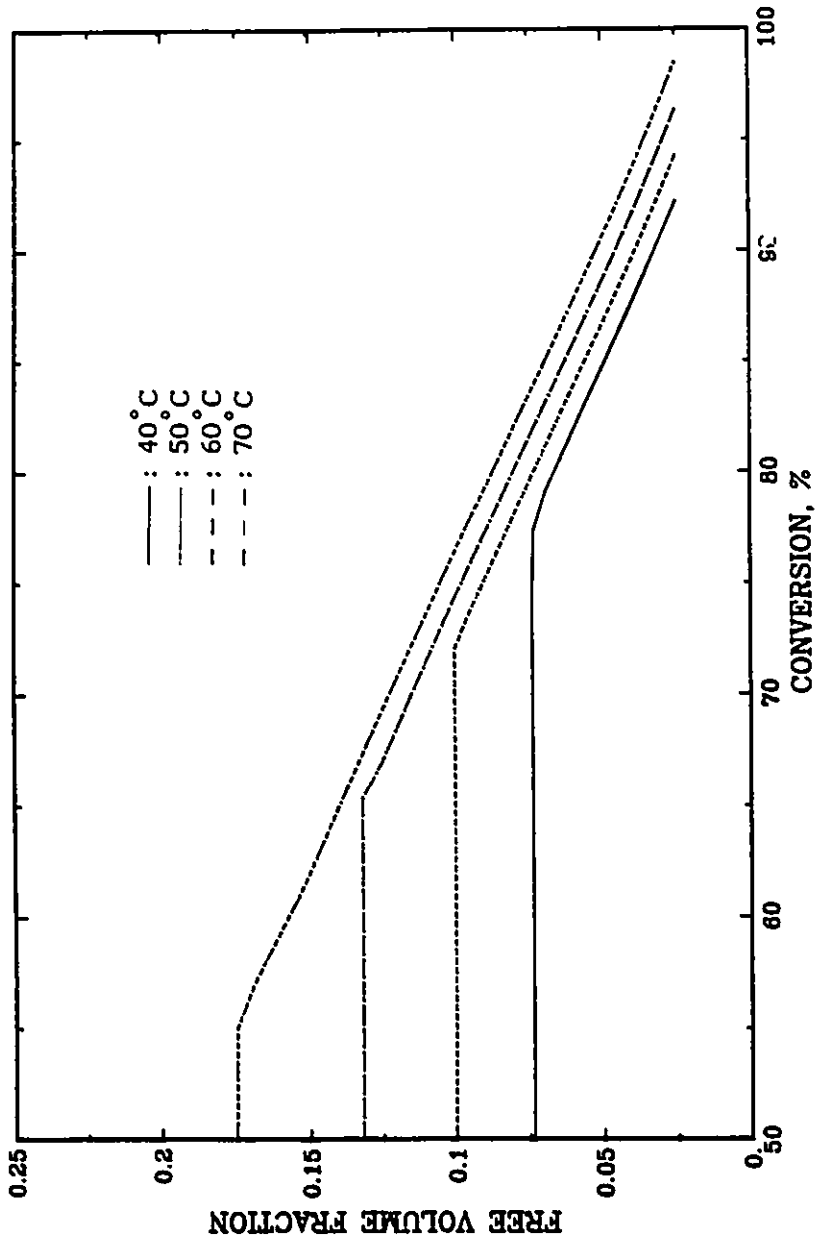

Figure 4.22. Free volume fraction of polymer phase variation with conversion at different temperatures.

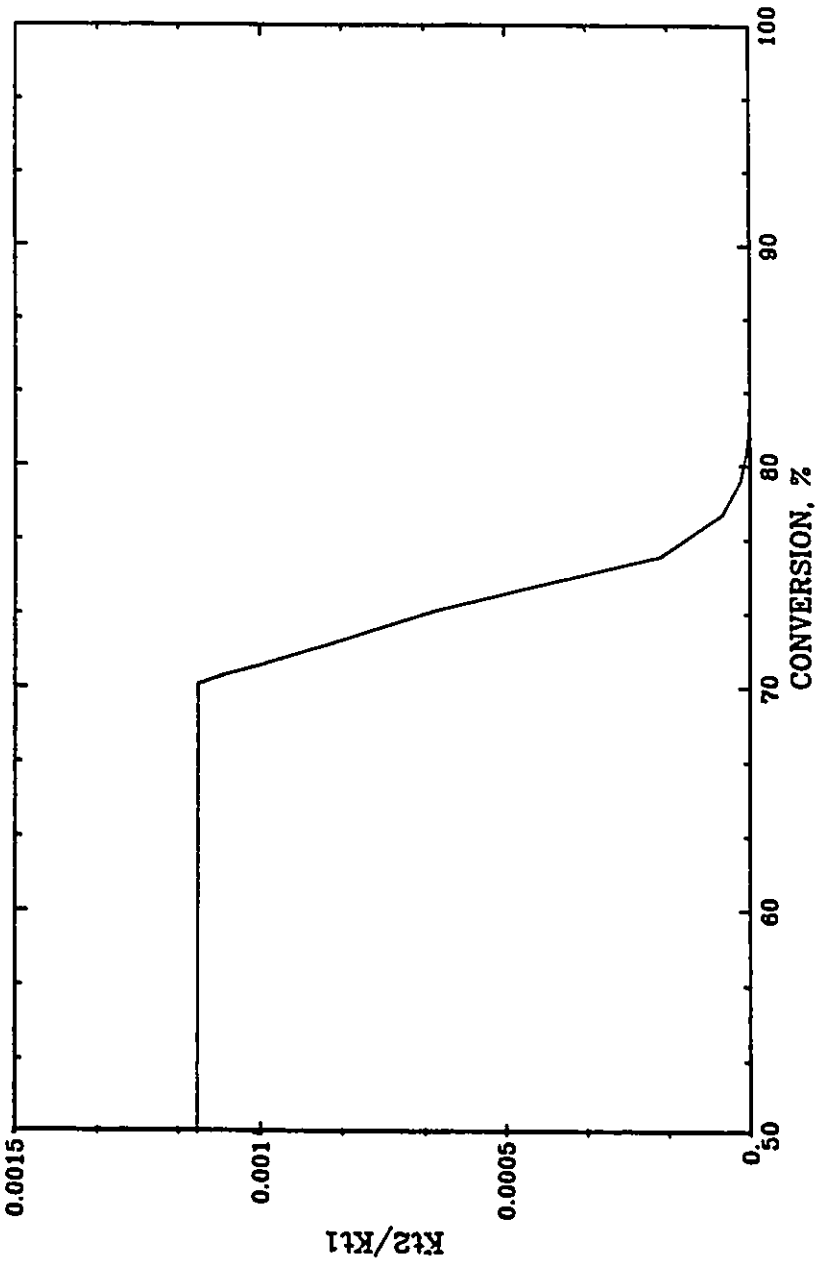

Figure 4.23. Bimolecular termination rate constant variation with conversion at 50 °C.

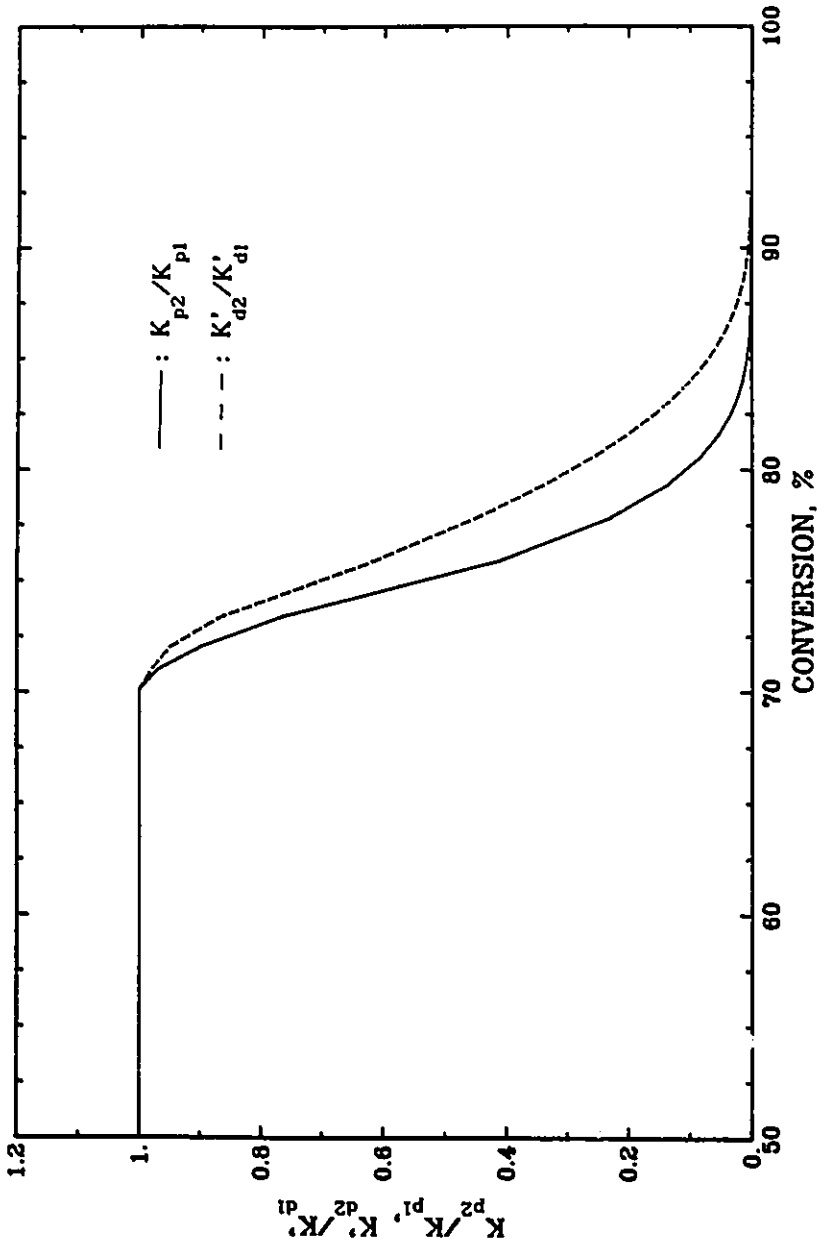

Figure 4.24. K_p and K'_d variation with conversion at 50°C.

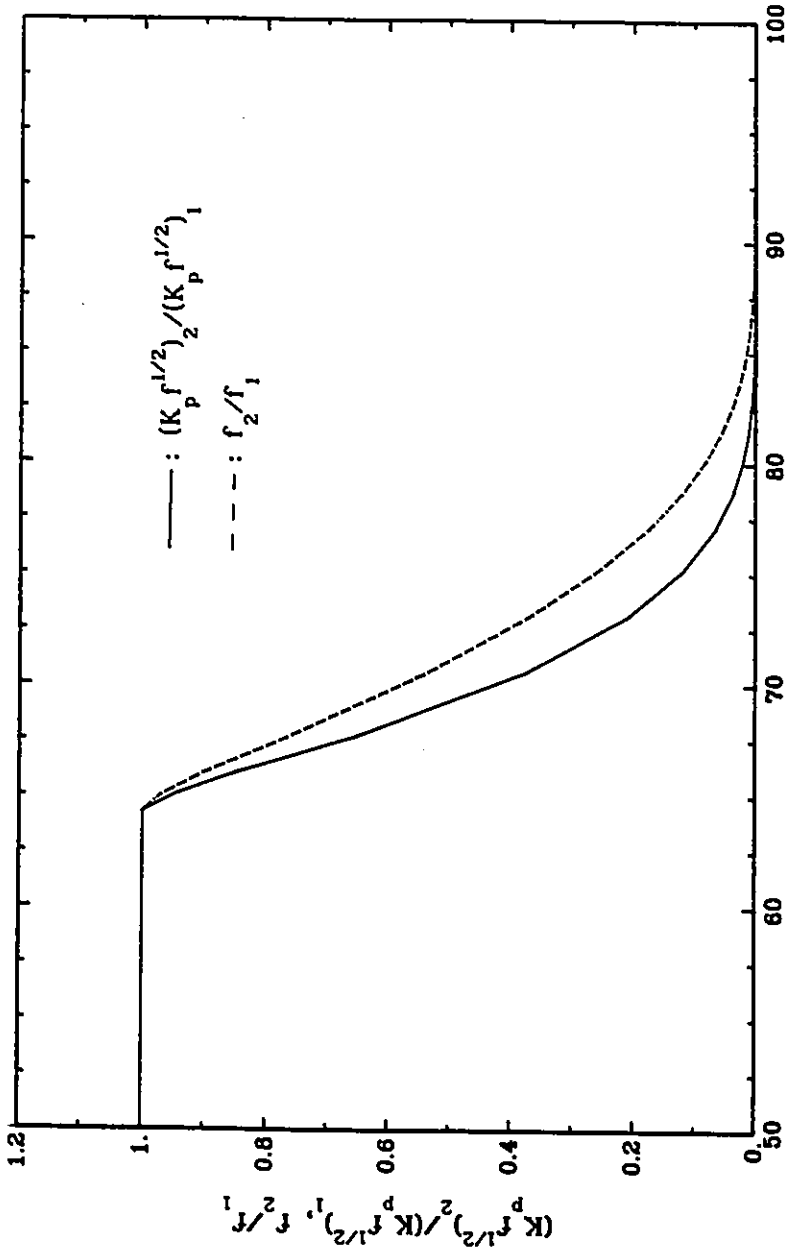

Figure 4.25. K_p and f variation with conversion at 60°C.

obtained by the present experiments. The difference between predicted limiting conversion and the experimental data is less than 1%. The polymerization times in our experiments are much longer than typical commercial polymerization times. Hence, Figure 4.26 also suggests that the limiting conversion can not be reached using commercial polymerization times. Theoretically, 100% conversion can be reached if the polymerization temperature is higher than the glassy-state transition temperature of PVC. Practically, the 100% conversion can not be obtained even for temperatures greater than T_{gp} of PVC. Figure 4.7 shows a typical run at 80°C, a temperature which is higher than the T_{gp} of PVC produced at this temperature. One can see from Figure 4.7 that the model does not fit the experimental data at high conversions. The final conversion measured by gravimetry is lower than that expected. In fact, the PVC produced at this temperature is pink rather than the normal white. This implies that dehydrochlorination occurs significantly during polymerization at high temperature. Dehydrochlorination rate of this PVC is much higher than that of ordinary PVC produced at lower polymerization temperatures. Therefore, at high temperatures and at high conversions, the VCM polymerization mechanism may be more complicated than that accounted for in the current model. Dehydrochlorination produces polyene sequences in polymer chains. Polymer radicals may react with polyene double bonds and form non-reactive radicals.

The parameter estimation and kinetic behaviour of VCM polymerization have been discussed above. Figures 4.3-4.6 show that the present model can fit the experimental data satisfactorily over the entire

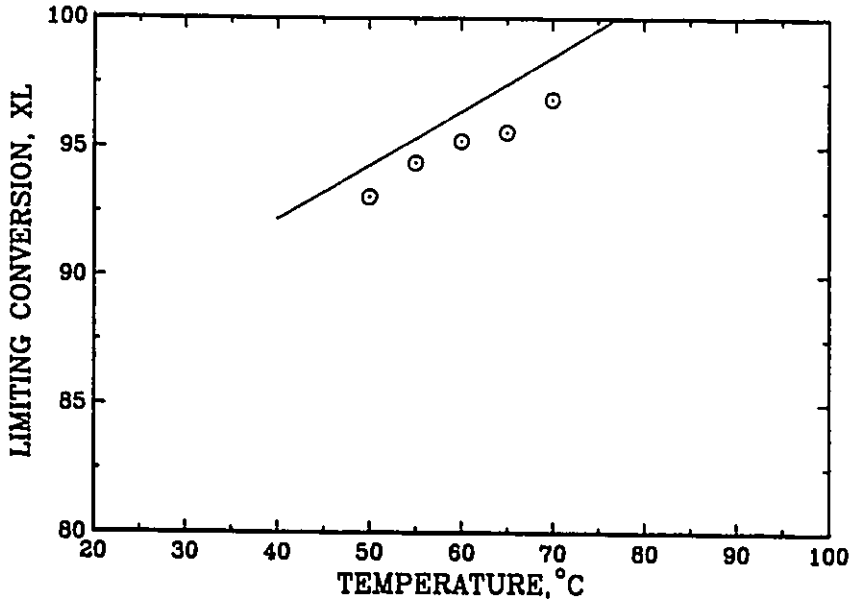

Figure 4.26. Limiting conversion variation with polymerization temperature.
⊙: present experimental data. ———: model.

conversion range but this does not mean that the parameters are valid. To further evaluate the reliability of the present model, model predictions using the estimated parameters found by fitting data measured in this investigation were compared with experimental data measured by gravimetry elsewhere, as shown in Figures 4.27-4.29. These experimental data were obtained in three laboratories (MIPPT, AKZO[125] and Zhejiang University[96]) independently with different sized reactors, different polymerization recipes and conversion measurement techniques. In Figure 4.27, one set of data were obtained by stopping the polymerization at different times and using gravimetry in the present laboratory. Another

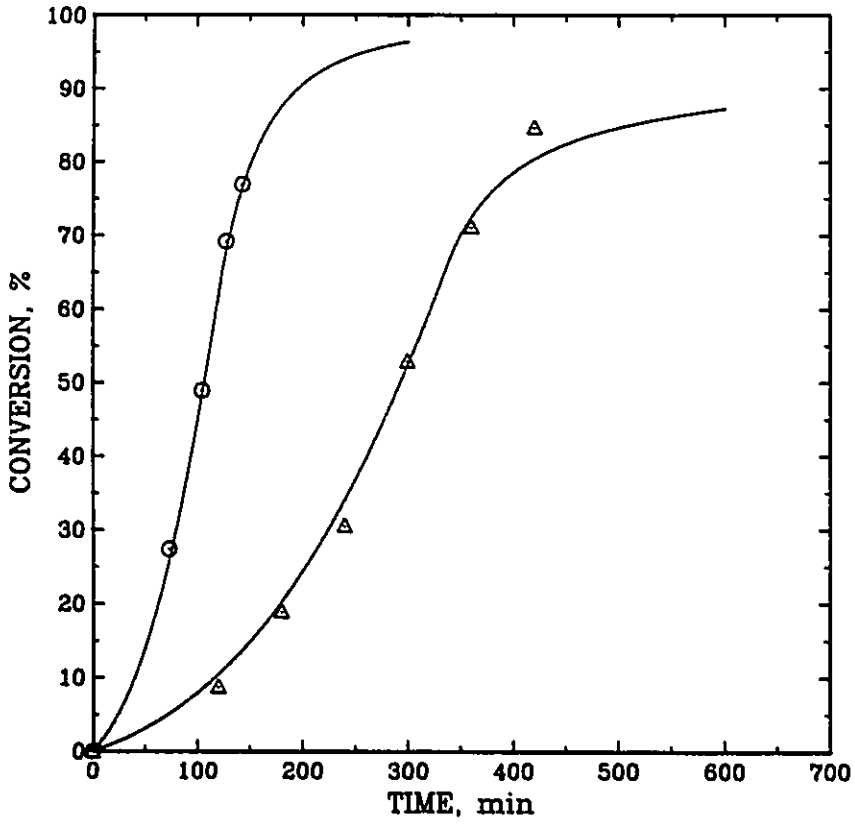

Figure 4.27. Model prediction for suspension polymerization of vinyl chloride at different conditions.
⊙: present work, Perkadox 16-W40, [I]= 0.125-wt% at 60°C.
Δ: AKZO data, reactor: 5-L, VCM: 675 g; water: 2700 g; Perkadox-26, [I] = 0.0853-wt% at 53.5°C (ref.125).
————: model prediction.

set of data were measured by AKZO with a different recipe. The data in Figures 4.28 and 4.29 were obtained by gravimetry in a smaller reactor with different operation conditions and reaction recipes.[96] Considering the accuracy of each batch by gravimetry, one can see that the model predictions are in excellent agreement with these experimental results.

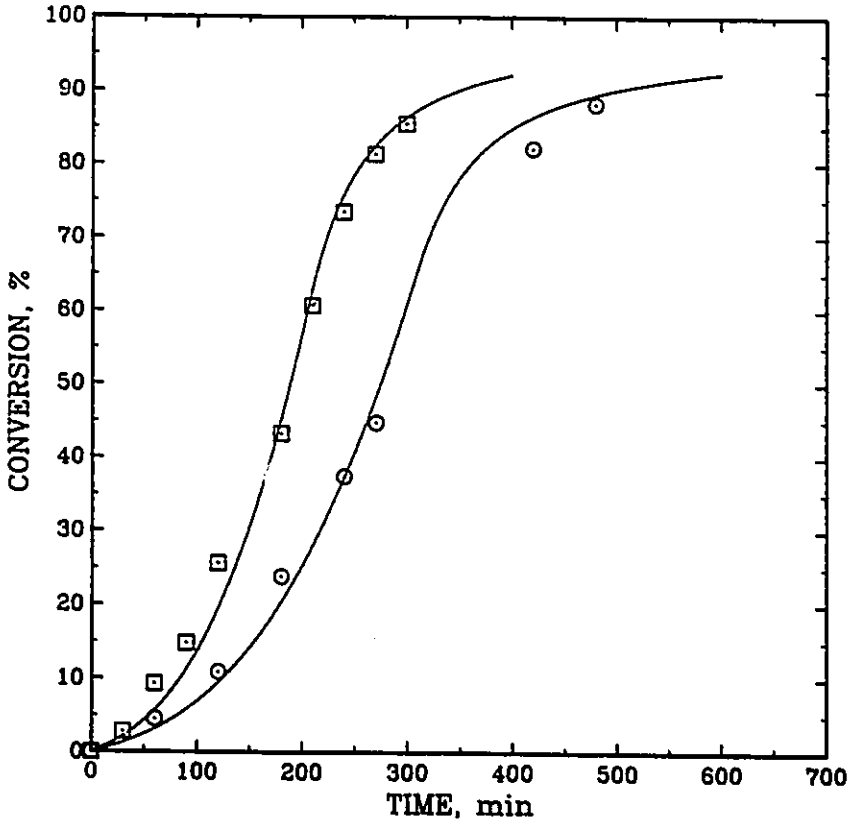

Figure 4.28. Model prediction for suspension polymerization of vinyl chloride at different temperatures.
Reactor: 0.20-L; VCM: 40 g; water: 80 g; AIBN, [I]=0.16-wt%. □: 62 °C; ⊙: 57 °C; ——: model prediction. Data by Xie et al.[96]

This not only shows the reliability of the model parameters estimated but also suggests that the type of suspending agent and conditions of mixing may not affect the kinetic behaviour significantly. It is believed that the present model should find use in the design, optimization and control of PVC reactors.

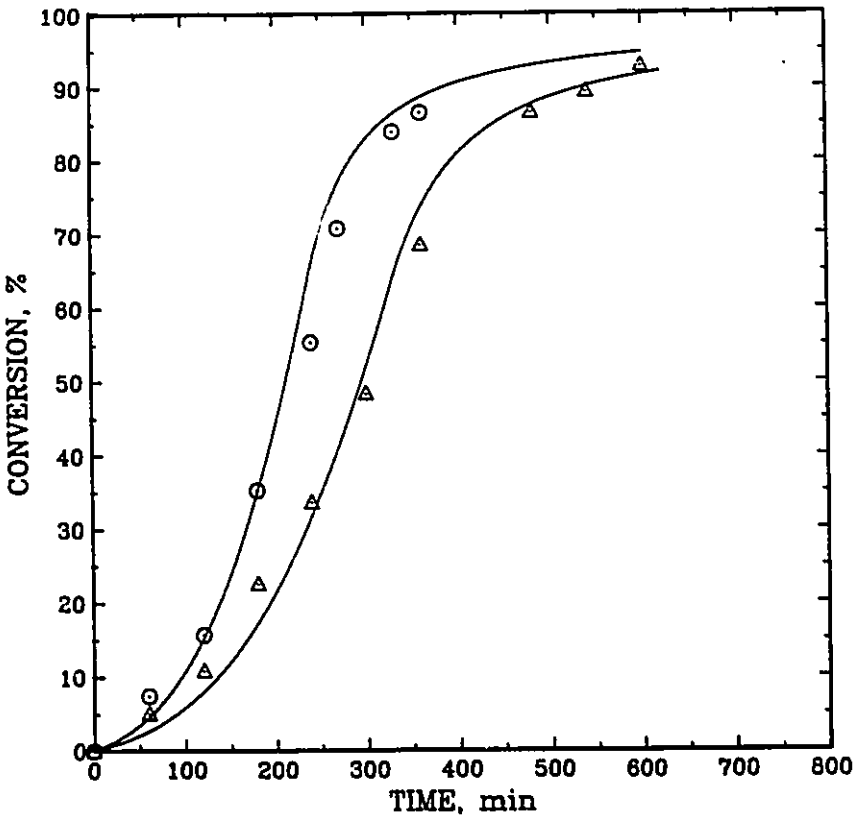

Figure 4.29. Model prediction for suspension polymerization of vinyl chloride at 60°C. Reactor: 0.20-L; VCM: 40 g; water: 80 g, initiator: AIBN, ⊙: 0.16-wt%; Δ: 0.09-wt%, ———: model prediction.
Data by Xie et al.[96]

Combining the present model with the reactor dynamic model described in Chapter 2, one can further predict the dynamic and kinetic behaviour of VCM polymerization under the present experimental conditions. Figure 4.30 shows the monomer distribution and pressure development during suspension polymerization at 50°C. The total amount of monomer decreases in the monomer phase but increases gradually in the polymer phase with conversion until X_f. For $X > X_f$, the monomer fraction

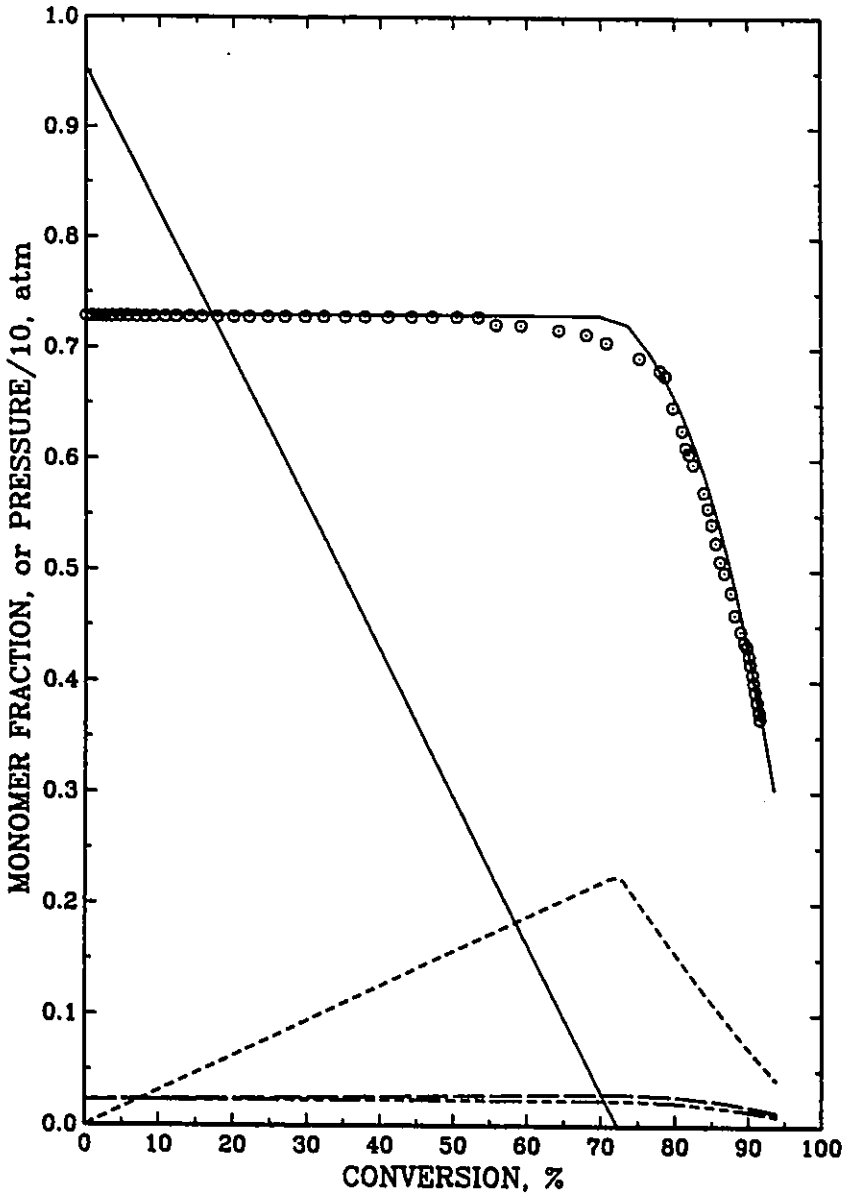

Figure 4.30. monomer distribution and pressure development at different conversions for VCM suspension polymerization at 50°C.
——— : monomer phase; ——— : polymer phase;
– – – : gas phase; – – – : water phase.
⊙: reactor pressure; ——— : model prediction.

in the polymer phase decreases gradually with conversion until the limiting conversion is reached. A total of about 4% monomer remains in the water and gas phases at the end of polymerization. The reactor pressure drops dramatically after X_f. However, the pressure starts to drop slowly when the monomer phase still exists, as described in Chapter 2.

Figure 4.31 shows the conversion and reactor pressure development during VCM polymerization. The figure clearly shows isobaric and nonisobaric polymerization from low to high conversions. Again, the model predictions are in excellent agreement with the experimental data. Figure 4.32 further shows reactor pressure and polymerization rate relationships at different conversions. During the isobaric polymerization period, the reaction rate increases with conversion; however, the polymerization rate decreases dramatically during the nonisobaric period. This figure suggests that the potential for the optimization of batch reactors: to linearize polymerization rate when $X < X_f$ and to increase polymerization rate for $X > X_f$. With the present model, together with the dynamic model in Chapter 2, one can answer quantitatively the questions raised in Chapter 1.

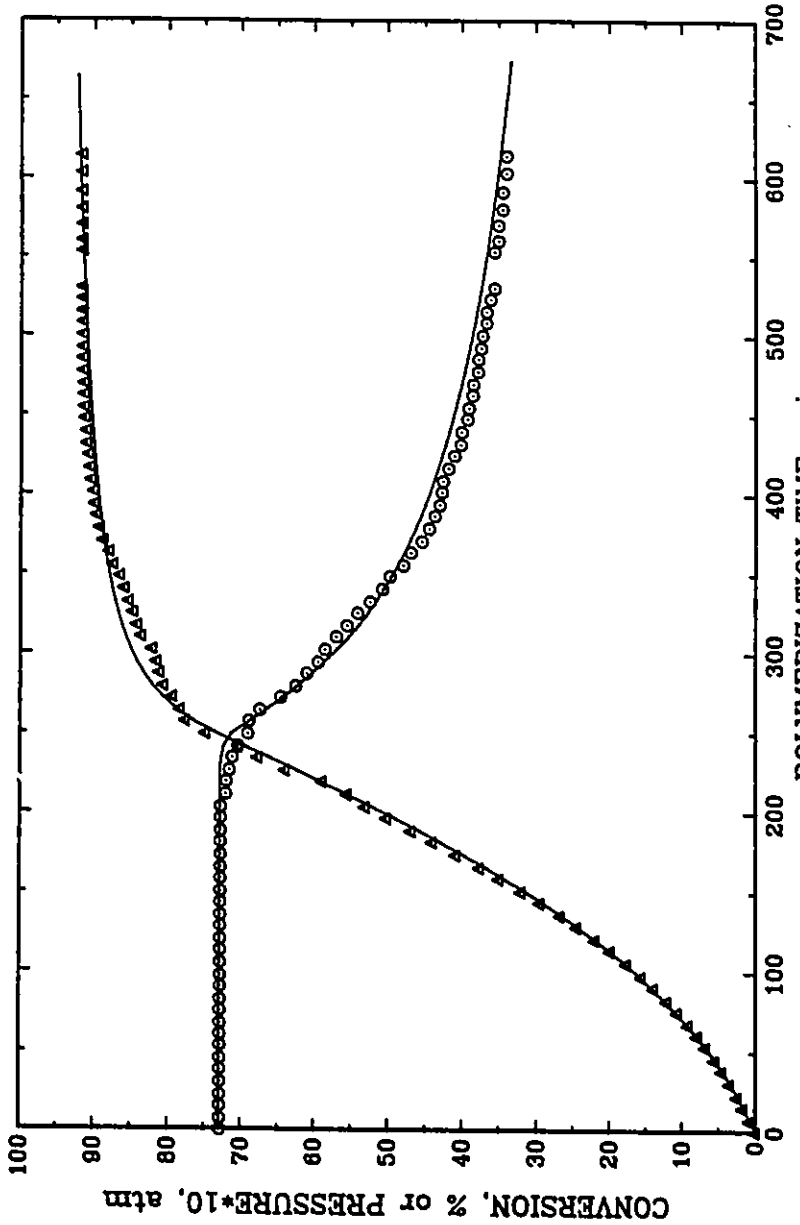

Figure 4.31. Reaction time dependence of conversion and reactor pressure development for VCM suspension polymerization at 50 °C.
Initiator: Perkadox 16-W40, [I]=0.175-wt%.
o: pressure; Δ: conversion; ——: model prediction.

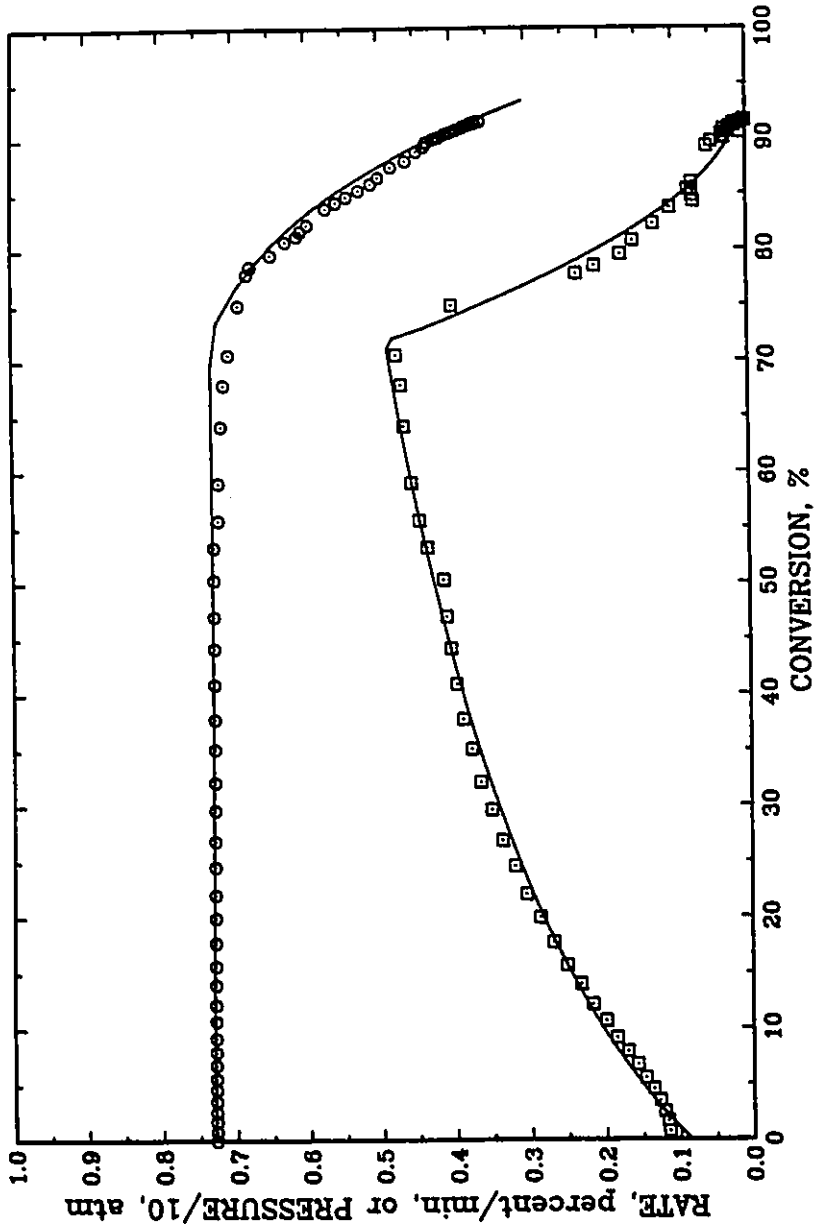

Figure 4.32. Conversion dependence of polymerization rate and reactor pressure for VCM suspension polymerization at 50 °C.
Initiator: Perkadox 16-W40, [I]=0.175-wt%.
o: pressure; □: reaction rate; ——: model prediction.

4.6 SUMMARY

In this chapter, the mechanisms of VCM polymerization were clearly described. On the basis of these mechanisms, a comprehensive kinetic model which seems to apply over the entire conversion range (to limiting conversion) and in a useful temperature range has been developed. The model predictions are in excellent agreement with independent experimental results with different reactor operational conditions and for different recipes.

The present model can describe the main features of two-phase polymerization quantitatively. Radical transfer between phases (monomer and polymer phases) is only important at very low conversions. Precipitation of radicals from the monomer phase can be expressed as a parameter K^* which depends on temperature. The modified desorption rate constant K'_{de} depends on both temperature and particle size. The partition coefficient of initiator is about 0.77 and is independent of temperature and the nature of initiator (for two initiator types studied). The concentration of radicals in the polymer phase is about 30 times higher than that in the monomer phase at 50°C. The acceleration behaviour of VCM polymerization rate continues until near X_f for the normal polymerization (initiator concentration has not fallen significantly). but the peak rate depends on the initiator half life and the concentration employed.

The bimolecular termination reaction in the polymer phase is diffusion-controlled over the entire conversion range. The propagation reaction becomes diffusion-controlled and the initiator efficiency falls dramatically after the monomer phase is consumed. The initiation mechanism at high conversions depends on the nature of initiator. The initiator efficiency for AIBN and the effective decomposition rate constant for the peroxide initiator decrease significantly at high conversions.

VCM polymerization above the glassy-state transition temperature of PVC involves a more complicated reaction mechanism. Pink PVC products were obtained for polymerization temperatures above 70°C. There appears to be a rate retardation which may be due to the effect of polyene double bonds formed by dehydrochlorination.

4.7 REFERENCES

1. Rigo, A., Palma, G. and Talamini, G. Makromol. Chem., 1972, 152, 219.

2. Bezdaea, E. C., Buruiana, E. C., Istrate-Robila, G. and Caraculacu, A. A. Eur. Polym. J., 1973, 9, 445.

3. Bovey, F. A., Abbas, K. B., Schilling, F. C. and Starnes, Jr. W. H. Macromolecules, 1975, 8, 437.

4. Starnes, Jr. W. H., Schilling, F. C., Abbas, K. B., CAIS, R. E. and Bovey, F. A. Macromolecules, 1979, 12, 556.

5. Starnes, Jr. W. H., Schilling, F. C., Abbas, K. B., Cais, R. E. and Bovey, F. A. Polym. Prepr., 1979, 20, 653.

6. Starnes, Jr. W. H., Schilling, F. C., Plitz, I. M., Cais, R. E., Freed, D. J., Hartless, R. L. and Bovey, F. A. Macromolecules, 1983, 16, 790.

7. Hjertberg, T. and Sörvik, E. M. J. Macromol. Sci.-Chem., 1982, A17, 983.

8. Hjertberg, T. and Sörvik, E. M. Polymer, 1983, 24, 673.

9. Hjertberg, T. and Sörvik, E. M. Polymer, 1983, 24, 685.

10. Talamini, G. J. Polym. Sci., 1966, A-2, 4, 535.

11. Crosato-Arnaldi, A., Talamini, G. and Vidotto, G. Makromol. Chem., 1968, 111, 123.

12. Ugelstad, J., Lervik, H., Gardinovacki, B. and Sundo, E. Pure Appl. Chem., 1971, 26, 121.

13. Abdel-Alim, A. H. and Hamielec, A. E. J. Appl. Polym. Sci., 1972, 16,783.

14. Kuchanov, S. J. and Bort, D. N. Polym. Sci. U.S.S.R., 1973, 15, 2712.

15. Olaj, O. F. J. Macromol. Sci.-Chem., 1977, A11, 1307.

16. Suresh, A. K. and Chanda, M. Eur. Polym. J., 1982, 18, 607.

17. Kelsall, D. K. and Maitland, G. C. 'Polymer Reaction Engineering', Eds. Reichert, K. H. and Geiseler, W., Hanser Publishers, Munich-Vienna, New York, 1983, 131.

18. Lewis, J., Okieimen, F. E. and Park, G. S. J. Macromol. Sci.-Chem., 1982, A17, 1021.

19. Marinin, V. G., Bort, D. N., Zhil'tsov, V. V., Kuchanov, S. I., Ivereva, G. F. and Rybkin, E. P. Polym. Sci. U.S.S.R., 1980, 22, 261.

20. Sielfeld, G. and Reichert, K. H. Appl. Polym. Symp., 1975, 26, 21.

21. Nass, L. I. 'Encyclopedia of PVC', Ed. Nass, L. I., Vol.1, Marcel Dekker Inc., 1976, 271.

22. Enomoto, S. J. Polym. Sci., 1969, A-1, 7, 1255.

23. Bengough, W. I. and Norrish, F. R. S. R.G. W. Proc. Royal Soc., 1950, (London) A, 200, 301.

24. Cotman, Jr., J. D. Ann. N. Y. Acad. Sci., 1953, 57,417.

25. Burnett, G. M. and Wright, W. W. Proc. Royal Soc., 1954, (London) A, 221, 37.

26. Mickley, H. S., Michaels, A. S. and Moore, A. L. J. Polym. Sci., 1962, 60, 121.

27. Marzurek, V. V. J. Polym. Sci., 1966, 8, 1292.

28. Park, G. S. and Smith, D. G. Trans. Faraday Soc., 1969, 65, 1854.

29. Talamini, G. and Peggion, E. 'Vinyl Polymerization', Ed. Ham, G., Vol. 1, Marcel Dekker, New York, 1967, 331.

30. Caraculacu, A. and Buruiana, E. C. J. Polym. Sci. Polym. Chem. Ed., 1978, 16, 2741.

31. Caraculacu, a. and Buruiana, E. C. and Robila, G. J. Polym. Sci., Polym. Symp., 1978, 64, 189.

32. Park, G. S. J. Vinyl Technol., 1985, 7, 60.

33. Darricades-Ilauro, M. F., Michel, A. and Guyot,. A. J. Macromol. Sci.-Chem., 1986, A23, 221.

34. Starnes, Jr., W. H. Polym. Propr., 1977, 18, 493.

35. Bovey, F. A., Schilling, F. C., Starnes, Jr., W. H. Polym, Prepr., 1979, 20, 160.

36. Starnes, Jr., W. H. 'Dev. Polym. Degradation', Ed. Grassie, N., Vol.5, Appl. Sci. Publishers, London, 1981, 135.

37. Razuvayev, G. A., Petukhov, G. G. and Dodonov, V. A. Polym. Sci. U.S.S.R., 1963, 3, 1020.

38. Park, G. S. and Smith, D. G. Makromol. Chem., 1970, 131, 1.

39. Starnes Jr., W. H., Plitz, I. H., Schilling, F. C., Park, G. S. and Saremi, A. H., Macromol., 1984, 17, 25-7.

40. Starnes Jr., W. H. Pure Appl. Chem., 1985, 57, 1001.

41. Hjertberg, T., Sorvik, E. and Wendel, A. Makromol. Chem., Rapid Commun., 1983, 4, 175.

42. Caraculacu, A. A. Pure Appl. Chem., 1981, 53, 385.

43. Okieimen, E. F. Eur. Polym. J., 1981, 17, 641.

44. Okieimen, E. F. Eur. Polym. J., 1983, 19, 255.

45. Okieimen, E. F. J. Macromol. Sci.-Chem., 1983, 20, 711.

46. Xie, T. Y., Hamielec, A. E., Wood, P. E. and Woods, D. R. **"Suspension, Bulk and Emulsion Polymerization of Vinyl Chloride — Mechanisms, Kinetics and Reactor Modelling"**, Submitted to J. Vinyl Technol., June, 1990.

47. Cotman, J. D., Gonzalez, M. F. and Claver, G. C. J. Polym. Sci., 1967, A1, 5, 1137.

48. Bort, D. N., Rylov, Ye. Ye., Okladnov, N. A., Shtarkman, B. P. and Kargin, V. A. Polym. Sci. U.S.S.R., 1965, 7, 50.

49. Bort, D. N., Marinin, V. G., Kalinin, A. I. and Kargin, V. A., Polym Sci. U.S.S.R., 1967, 9, 334.

50. Bort, D. N., Marinin, V. G., Kalinin, A. I. and Kargin, V. A., Polym. Sci. U.S.S.R., 1968, 10, 2989.

51. Barrclay, L. M. Angew. Makromol. Chem., 1976, 52, 1.

52. Boissel, J. and Fischer, N. J. Macromol. Sci.-Chem., 1977, 11, 1249.

53. Zichy, E. L. J. Macromol. Sci.-Chem., 1977, A11, 1205.

54. Wilson, J. C. and Zichy, E. L. Polymer, 1979, 20,264.

55. Cooper, W. D., Speirs, R. M. Wilson, J. C. and Zichy, E. L. Polymer, 1979, 20, 265.

56. Rance, D. G. and Zichy, E. L. Polymer, 1979, 20, 267.

57. Davidson, J. A. and Witenhafer, D. E. J. Polym. Sci. Polym. Phys. Ed., 1980, 18, 51.

58. Rance, D. G. and Zichy, E. L. Pure & Appl. Chem., 1981, 53, 377.

59. Willmouth, F. M., Rance, D. G. and Henmean, K. M. Polymer, 1984, 25, 1185.

60. Törnell, B. E. and Uustalu, J. M. J. Vinyl Technol., 1982, 4, 53.

61. Törnell, B. E. and Uustalu, J. M. Polymer, 1986, 27, 250.

62. Törnell, B. E., Uustalu, J. M. and Jonsson, B. Colloid & Polym. Sci., 1986, 264, 439.

63. Nilsson, H., Silvegren, C. and Uustalu, J. Polym. Commun., 1983, 24, 268.

64. Ravey, M., Waterman, J. A., Shorr, L. M. and Kramer, M. J. Polym. Sci., Polym. Chem. Ed., 1974, 12, 2821.

65. Fisher, N. J. Vinyl Technol., 1984, 6, 35.

66. Feldman, D., Macoveanu, M. and Robila, G. J. Macromol. Sci. Chem., 1977, A11, 1333.

67. Soni, P. L., Geil, P. H. and Collins, E. A. J. Macromol. Sci. Phys., 1981, B20, 479.

68. Törnell, B. and Uustalu, J. J. Appl. Polym. Sci., 1988, 35, 63.

69. Palma, G., Talamini, G. and Tavan, M. J. Polym. Sci., Polym. Phys. Ed., 1977, 15, 1537.

70. Smallwood, P. V. Polymer, 1986, 27, 1609.

71. Smallwood, P. V. Makromol. Chem., Macromol. Symp., 1989, 29, 1.

72. Marasi, B. J. Vinyl Technol., 1986, 8, 20.

73. Ueda, T., Takeuchi, K. and Kato, M. J. Polym. Sci., Polym. Chem. Ed., 1972, 10, 2841.

74. Johnson, G. R. J. Vinyl Technol., 1980, 2, 138.

75. Nilsson, H., Silvegren, C., Törnell, B., Lundgvist, J. and Pettersson, S. J. Vinyl Technol., 1985, 7, 123.

76. Cheng, J. T. J. Macromol. Sci. Phys. Ed., 1981, B20, 365.

77. Cheng, J. T. and Langsam, M. J. Macromol. Sci.-Chem., 1984, A21, 395.

78. Allsopp, M. W. Pure & Appl. Chem., 1981, 53, 449.

79. Allsopp, M. W. 'Manufacture and Processing of PVC', Ed. Burgess, R. H., Appl. Sci. Publishers Ltd., London, 1982, 151.

80. Meeks, M. R. Polym. Eng. Sci., 1969, 9, 141.

81. Nilsson, H., Silvegren, C. and Törnell, B. Angew. Makromol. Chem., 1983, 112, 125.

82. Cebollada, A. F., Schmidt, M. J., Farber, J. N., Capiati, N. J. and Valles, E. M. J. Appl. Polym. Sci., 1989, 37, 145.

83. Crosato-Arnaldi, A., Gasparini, P. and Talamini, G. Makromol. Chem., 1968, 117, 140.

84. Abdel-Alim, A. H. and Hamielec, A. E. J. Appl. Polym. Sci., 1974, 18, 1603.

85. Ugelstad, J., Mork, P. C., Dahl, P. and Pangnes, P. J. Polym. Sci., 1969, part C, 27, 47.

86. Russo, S. and Stannett, V. Makromol. Chem., 1971, 143, 47.

87. Arlman, E. J. and Wagner, W. M. J. Polym. Sci., 1952, 9, 561.

88. Bankoff, S. G. and Shreve, R. N. Ind. Eng. Chem., 1953, 45, 270.

89. Talamini, G. and Vidotto, G. Makromol. Chem., 1961, 50, 129.

90. Talamini, G. and Vidotto, G. Makromol. Chem., 1962, 53, 21.

91. Ryska, M., Kolinsky, M. and Lim, D. J. Polym. Sci., 1967, C16, 621.

92. Farber, E. and Koral, M. Polym. Eng. Sci., 1968, 8, 11.

93. Tavan, M., Pulnia, G., Carenza, M. and Brugnaro, S. J. Polym. Sci., Polym. Chem. Ed., 1974, 12, 411.

94. Ugelstad, J., Flogstad, H., Hertzberc, T. and Sund, E. Makromol., Chem., 1973, 164, 171.

95. Ugelstad, J. J. Macromol. Sci. Chem., 1977, A11, 1281.

96. Xie, T. Y., Yu, Z. Z., Cai, Q. Z. and Pan, Z. R. Huangong Xuebao, 1984, 2, 93.

97. Vidotto, G., Brugnaro, S. and Talamini, G. Makromol. Chem., 1971, 140, 249.

98. Russo, S. and Stannett, V. Makromol. Chem., 1971, 143, 57.

99. Pezzin, G., Talamini, G. and Vidotto, G. Makromol. Chem., 1961, 43, 12.

100. Sörvik, E. M. J. Polym. Sci. Polym. Letters Ed., 1976, 14, 735.

101. Hamielec, A. E., Gomez-Vaillard, R. and Marten, F L. J. Macromol. Sci.-Chem., 1982, A17, 1005.

102. Hjertberg, T. and Sörvik, E. M. 'Degradation and Stabilisation of PVC', Ed. Owen, E. D., Elsevier Appl. Sci. Publishers, London and New York, 1984, 21.

103. Hjertberg, T. and Sörvik, E. M. J. Polym. Sci.: part A: Polym. Chem., 1986, 24, 1313.

104. Bueche, F. 'Physical Properties of Polymers', Wiley-Interscience, New York, 1962.

105. Flory, P. J. 'Principles of Polymer Chemistry', Cornell University Press, Ithaca, New York, 1953.

106. Weast, R. C. and Astle, M. J. CRC Handbook of Chemistry and Physics, 64th Ed., 1983-1984.

107. Fedors, R. F. J. Polym. Sci., Polym. Letters Ed., 1979, 17, 719.

108. Reding, F. P., Walter, E. R. and Welch, F. J. J. Polym. Sci., 1962, 56, 225.

109. Ceccorulli, G., Pizzcli, M. and Pezzin, G., J. Macromol. Sci.-Phys., 1977, B14, 499.

110. Friis, N. and Hamielec, A. E. 'Emulsion Polymerization', Eds. Piirma, I. and Gardon, J. L., ACS Symp. Ser. 24, 1976, 82.

111. Berens, A. R. Org. Coat. and Plast. Chem., 1978, 39, 236.

112. Ibragimov, I. Y. and Bort, D. N. Vysokomol. Soedin, Ser. B, 1974, 16, 376.

113. Bawn, C. E. H. and Mellish, S. F. Trans. Faraday Soc., 1951, 47, 1216.

114. Van Hook, J. P. and Tobolsky, A. V., J. Am. Chem. Soc., 1958, 80, 779.

115. Barrett, K. E. J., J. Appl. Polym. Sci., 1967, 11, 1617.

116. Talat-Erben, M. and Bywater, S. J. Am. Chem. Soc., 1955, 77, 3712.

117. Lewis, R. and Friedman, R. Modern Plastics, 1973, March, 88.

118. Pan, Z. R. and Yu, Z. Z. 'Free Radical Polymerization', Chem. Ind., Beijing, 1983, 84.

119. Westmijze, H. AKZO Chemie, Noury Initiators, Personal Communication, 1987.

120. Arnett, L. M. and Peterson, J. H. J. Am. Chem. Soc., 1952, 74, 2031.

121. Mazurek, V. V. Polym. Sci. U.S.S.R., 1966, 8, 1292.

122. Olaj, O. F., Breitenbach, J. W., Parth, K. J. and Philippovich, N. J. Macromol. Sci. Chem., 1977, A11, 1319.

123. Burnett, G. M. and Wright, W. W. Proc. Royal Soc. (London) Ser. A, 1954, 221, 28.

124. M. Nomura, 'Emulsion Polymerization', Ed. I. Piirma, Academic Press, New York, 1982.

125. Westmijze, H. AKZO Chemicals Experimental Data, Personal Communication, 1989.

CHAPTER 5

PVC MOLECULAR WEIGHT DEVELOPMENT

5.1 INTRODUCTION

Detailed mechanisms of VCM polymerization have been described and a comprehensive model for conversion and polymerization rate development has been derived in Chapter 4. In the present Chapter, PVC molecular weight development modelling will be illustrated on the basis of the mechanism and kinetic model described previously.

PVC molecular weight development has been extensively investigated experimentally for bulk, suspension, emulsion and solution polymerization processes over wide temperature ranges. The main findings were as follows:

The molecular weight of PVC does not strongly depend on process type, monomer conversion[1-7] and initiator concentration[3-5] for isothermal polymerization, but it increases significantly with decreasing polymerization temperature.[5,7-9] These phenomena are attributed to the dominance of the chain transfer to monomer reaction in controlling PVC molecular weight development (most of the polymer chains are formed by chain transfer to monomer).

At high conversions (under subsaturation pressure), the number-average molecular weight decreases with conversion significantly while the weight-average molecular weight decreases only slightly so that the molecular weight distribution (MWD) becomes broader and the polydispersity increases with decreasing reactor pressure.[4,11-14]

Molecular weight modelling has, however, not been studied extensively, and the few attempts have had limited success under subsaturation conditions because of a lack of molecular weight data measured over a wide range of polymerization conditions. Abdel-Alim et al[5] first developed a model for the accumulated molecular weight averages and distribution for PVC assuming homogeneous kinetics to be valid to both monomer and polymer phases. The model does not predict the fall in accumulated number-average molecular weight nor the increasing polydispersity at high conversions which has been shown experimentally.[4,11-14] Kelsall et al[15], more recently, proposed a model for the calculation of molecular weight averages for PVC. The model predicts that the accumulated number-average molecular weight increases with conversion significantly at high conversions. It is contradictory to the experimental results mentioned above.

As discussed in Chapter 4, vinyl chloride polymerization involves a larger number of elementary reactions than previously realized. The objective of this investigation is to develop a comprehensive model which can predict the instantaneous and accumulated molecular weight averages and distribution for PVC made by suspension polymerization. The

model should account for all of the relevant elementary reactions discussed in Chapter 4 and include the parameters estimated using comprehensive experimental data over wide ranges of synthesis conditions to ensure narrow confidence intervals for the kinetic parameters.

5.2 MODEL DEVELOPMENT

The basic assumptions made in the polymerization rate modelling in Chapter 4 are again employed for molecular weight development modelling.

During free radical polymerization, live and dead macromolecules have chain length distributions. For any distribution function it is possible to define a series of moments. The i^{th} moments for the dead and live polymer distributions Q_i and Y_i are defined as

$$Q_i = \sum_{r=1}^{\infty} r^i P_r \qquad \text{(dead polymer)} \qquad (5.1)$$

$$Y_i = \sum_{r=1}^{\infty} r^i R_r^{\cdot} \qquad \text{(live polymer)} \qquad (5.2)$$

where i is zero or a positive number.

When conversion is less than the critical conversion, X_f, at which the monomer phase is consumed, polymer is produced in both the monomer and polymer phases simultaneously. However, all the polymer

produced in the monomer phase is assumed to precipitate onto the polymer phase instantaneously due to the low solubility of PVC in monomer. Hence, the moment equations will be derived separately for both phases.

5.2.1 Molecular Weight Development in the Monomer Phase

In the monomer phase, chain transfer to polymer can be neglected because of the very low concentration of dead polymer. Bimolecular termination between the polymer and primary radicals should be insignificant because of the very low concentration of primary radicals compared to that for polymer radicals. Hence, this reaction is neglected. Therefore, the rate of polymer production in the monomer phase can be expressed as:

$$\frac{d(P_r)_1}{V_1 dt} = K_{td1}[R^\cdot]_1[R^\cdot_r]_1 + \frac{K_{tc1}}{2}\sum_{s=1}^{r-1}[R^\cdot_s]_1[R^\cdot_{r-s}]_1 + K_{fm1}[M]_1[R^\cdot_r]_1 \qquad (r \geq 2) \qquad (5.3)$$

$$\frac{d(P_1)_1}{V_1 dt} = K_{td1}[R^\cdot]_1[R^\cdot_1]_1 \qquad (r=1) \qquad (5.4)$$

where the subscript 1 on the concentrations (square brackets) stands for monomer phase. Chain lengths equal to or greater than r_c for both live and dead polymer molecules do not exist in the monomer phase. According to assumptions described in Chapter 4, all polymer produced in the monomer phase is assumed to precipitate instantaneously. Therefore,

Eqs.(5.3) and (5.4) should be understood as polymer production rate in the monomer phase and should not be interpreted as polymer concentration change in the monomer phase. Radical concentration in the monomer phase is governed by a population balance for radicals described in Chapter 4. This only accounts for the number of radical centers in the monomer phase. Polymer radicals could partially precipitates, i.e.: radical center is in the monomer phase and the tail is in the polymer phase. This can be true for radicals on the surface of primary particles. these kinds of radical centers are considered in the monomer phase. Furthermore, according to the values of K^* estimated in Chapter 4, the critical chain length of polymer radicals to precipitate from the monomer phase is very large. Hence, the effect of precipitation of polymer radicals on the molecular weight development in the monomer phase can be neglected. Therefore, the production rate of polymer in the monomer phase can be treated by the conventional method (see Appendix B for detailed explanations). Chain transfer to monomer involves more than one elementary reaction. This has been discussed in Chapter 4.

From the definition of the moments and a summation of Eq.(5.3) and Eq.(5.4) over all chain lengths, the following moment equations may be derived for the monomer phase:

$$\frac{dQ_{om}}{V_1 dt} = (K_{td1} + \frac{1}{2} K_{tc1})[R^\cdot]_1^2 + K_{fm1}[R^\cdot]_1[M]_1 \qquad (5.5)$$

$$\frac{dQ_{1m}}{V_1 dt} = K_{p1}[M]_1[R^\cdot]_1 \qquad (5.6)$$

$$\frac{dQ_{2m}}{V_1 dt} = \{(K_{td1}+K_{tc1})[R^\cdot]_1+K_{fm1}[M]_1\}Y_{2m}+K_{tc1}Y_{1m}^2 \qquad (5.7)$$

$$\frac{dQ_{3m}}{V_1 dt} = \{(K_{td1}+K_{tdc1})[R^\cdot]_1+K_{fm1}[M]_1\}Y_{3m}+3K_{tc1}Y_{1m}Y_{2m} \qquad (5.8)$$

where the subscript m on the moments stands for monomer phase.

The solution of Eqs.(5.7) and (5.8) requires a knowledge of the moments of the polymer radical distribution. The polymer radical balances can be written as:

$$\frac{d(R_r^\cdot)_1}{V_1 dt} = K_{p1}[M]_1[R_{r-1}^\cdot]_1-K_{p1}[M]_1[R_r^\cdot]_1-(K_{td1}+K_{tc1})[R^\cdot]_1[R_r^\cdot]_1$$
$$- K_{fm1}[M]_1[R_r^\cdot]_1+K_{de}[R_r^\cdot]_2V_2/V_1 \qquad (2 \le r < r_c) \qquad (5.9)$$

$$\frac{dR_1^\cdot}{V_1 dt} = R_{i1}+K_{fm1}[R^\cdot]_1[M]_1-K_{p1}[M]_1[R_1^\cdot]_1-(K_{td1}+K_{tc1})[R^\cdot]_1[R_1^\cdot]_1$$
$$+K_{de}[R_1^\cdot]_2V_2/V_1 \qquad (r = 1) \qquad (5.10)$$

The desorption constant strongly depends on diameter of the primary particles so that the desorption of radicals from the polymer phase is significant only at very low conversions. However, the reaction volume in the monomer phase is much larger than that in the polymer phase at very low conversions. Hence, the effect of desorption on the concentration of radicals with chain length r and 1 can be neglected.

Therefore, the associated moment equations are:

$$\frac{dY_{1m}}{V_1 dt} = K_{p1}[M]_1[R^\cdot]_1-(K_{td1}+K_{tc1})[R^\cdot]_1 Y_{1m} - K_{fm1}[M]_1 Y_{1m} + K_{fm1}[M]_1[R^\cdot]_1+R_{I1} \tag{5.11}$$

$$\frac{dY_{2m}}{V_1 dt} = K_{p1}[M]_1([R^\cdot]_1+2Y_1)-(K_{td1}+K_{tc1})[R^\cdot]_1 Y_{2m}-K_{fm1}[M]_1 Y_{2m} + K_{fm1}[R^\cdot]_1[M]_1+R_{I1} \tag{5.12}$$

$$\frac{dY_{3m}}{V_1 dt} = K_{p1}[M]_1([R^\cdot]_1+3Y_{1m}+3Y_{3m})-(K_{td1}+K_{tc1})[R^\cdot]_1 Y_{3m} -K_{fm1}[M]_1 Y_{3m}+K_{fm1}[M]_1[R^\cdot]_1+R_{I1} \tag{5.13}$$

Applying the steady-state hypothesis to Eqs.(5.11)-(5.13), one can express the first to third moments of the polymer radical distribution as:

$$Y_{1m} = \frac{K_{p1}[M]_1[R^\cdot]_1+K_{fm1}[R^\cdot]_1[M]_1+R_{I1}}{(K_{td1}+K_{tc1})[R^\cdot]_1+K_{fm1}[M]_1} \tag{5.14}$$

$$Y_{2m} = \frac{K_{p1}[M]_1([R^\cdot]_1+2Y_{1m})+K_{fm1}[R^\cdot]_1[M]_1+R_{I1}}{(K_{td1}+K_{tc1})[R^\cdot]_1+K_{fm1}[M]_1} \tag{5.15}$$

$$Y_{3m} = \frac{K_{p1}[M]_1([R^\cdot]_1+3Y_{1m}+3Y_{2m})+K_{fm1}[R^\cdot]_1[M]_1+R_{I1}}{(K_{td1}+K_{tc1})[R^\cdot]_1+K_{fm1}[M]_1} \qquad (5.16)$$

Substituting Eqs.(5.14)-(5.16) for polymer radical moments in Eqs.(5.7) and (5.8) one obtains:

$$\frac{dQ_{2m}}{V_1 dt} = R_{p1}\left\{\frac{(2+\tau_1+\beta_1)R_{cm}}{\tau_1+\beta_1} + \beta_1\left(\frac{R_{cm}}{\tau_1+\beta_1}\right)^2\right\} \qquad (5.17)$$

$$\frac{dQ_{3m}}{V_1 dt} = R_{p1}\left\{\frac{6\beta_1 R_{cm}^2}{(\tau_1+\beta_1)^3} + \frac{3R_{cm}(2+\beta_1 R_{cm})}{(\tau_1+\beta_1)^2} + \frac{6R_{cm}}{\tau_1+\beta_1} + R_{cm}\right\} \qquad (5.18)$$

where

$$R_{p1} = K_{p1}[M]_1[R^\cdot]_1, \qquad R_{cm} = 1+CM_1+R_{I1}/R_{P1}$$

$$\tau_1 = \frac{K_{td1}[R^\cdot]_1}{K_{p1}[M]_1} + CM_1, \qquad \beta_1 = \frac{K_{dc1}[R^\cdot]_1}{K_{p1}[M]_1}$$

$$CM_1 = K_{fm1}/K_{p1}$$

The overall rate constant for chain transfer to monomer, K_{fm1}, has been derived in Chapter 4 and is given by

$$K_{fm1} = \frac{K_1K_2K_5}{(K_2+K_3[M]_1)(K_4[M]_1+K_5)} \qquad (5.19)$$

With the moment equations (Eqs.(5.5), (5.6), (5.17) and (5.18)) above, one can derive relationships for the instantaneous number-, weight- and Z-average molecular weights of PVC based on the following definition:

$$M_j = M_m \frac{dQ_{i+1}}{dQ_i} \qquad (i=0,\ j=n;\ i=1,\ j=w;\ i=2,\ j=z) \tag{5.20}$$

Thus, $(M_n)_m$, $(M_w)_m$ and $(M_z)_m$ are given by

$$(M_n)_m = \frac{M_m}{\tau_1 + (\beta_1/2)} \tag{5.21}$$

$$(M_w)_m = M_m \left\{ \frac{2R_{cm}}{\tau_1+\beta_1} + \beta_1 \left(\frac{R_{cm}}{\tau_1+\beta_1}\right)^2 \right\} \tag{5.22}$$

$$(M_z)_m = M_m \frac{S_1^3+6(S_1^2+S_1+\beta_1 R_{cm})+3\beta_1 S_1 R_{cm}}{S_1(S_1^2+2S_1+\beta_1 R_{cm})} \tag{5.23}$$

where

$$S_1 = \tau_1 + \beta_1$$

Using an order of magnitude analysis (both CM and R_{ll}/R_{pl} are in the order of 10^{-3} in the temperature range of interest, hence, $R_{cm} \cong 1$), one can simplify Eqs.(5.17), (5.18), (5.22) and (5.23) as:

$$\frac{dQ_{2m}}{V_1 dt} = R_{pl} \left\{ \frac{2\tau_1+3\beta_1}{(\tau_1+\beta_1)^2} \right\} \tag{5.17a}$$

$$\frac{dQ_{3m}}{V_1 dt} = R_{p1}\left\{\frac{6(\tau_1+2\beta_1)}{(\tau_1+\beta_1)^3}\right\} \tag{5.18a}$$

$$(M_w)_m = M_m \frac{2\tau_1+3\beta_1}{(\tau_1+\beta_1)^2} \tag{5.22a}$$

$$(M_z)_m = \frac{6M_m(\tau_1+2\beta_1)}{(\tau_1+\beta_1)(2\tau_1+3\beta_1)} \tag{5.23a}$$

However, for molecular weight calculations using a computer, Eqs.(5.17), (5.18), (5.22) and (5.23) are recommended.

The instantaneous molecular weight distribution (MWD) is defined as:

$$W(r)_m = \frac{r}{R_{p1}}\left[\frac{d(P_r)_1}{V_1 dt}\right] \tag{5.24}$$

Hence, the instantaneous polymer production rate has to be calculated in order to find the instantaneous molecular weight distribution.

Applying the steady-state hypothesis to Eqs.(5.9) and (5.10), one can find the concentration of polymer radical with chain length r as:

$$[R_r^\cdot]_1 = \left(\frac{1}{1+\tau_1+\beta_1}\right)^r (R_{I1}/R_{p1}+CM_1)[R^\cdot]_1 \tag{5.25}$$

Substituting Eq.(5.25) into Eq.(5.3), one obtains:

$$\frac{d(P_r)_1}{V_1 dt} = R_{p1}\left\{\tau_1\left(\frac{R_{I1}}{R_{p1}} + CM_1\right) + \frac{\beta_1}{2}(r-1)\left(\frac{R_{I1}}{R_{p1}} + CM_1\right)^2\right\}\left(\frac{1}{1+\tau_1+\beta_1}\right)^r \qquad (5.26)$$

Substituting Eq.(5.26) into Eq.(5.24), one obtains the following result:

$$W(r)_m = r\left\{\tau_1\left(\frac{R_{I1}}{R_{p1}} + CM_1\right) + \frac{\beta_1}{2}(r-1)\left(\frac{R_{I1}}{R_{p1}} + CM_1\right)^2\right\}\left(\frac{1}{1+\tau_1+\beta_1}\right)^r$$

$$= r(\tau_1+\beta_1)\left[\tau_1 + \frac{\beta_1}{2}(r-1)(\tau_1+\beta_1)\right]\left(\frac{1}{1+\tau_1+\beta_1}\right)^r \qquad (5.27)$$

Eqs.(5.21)-(5.23) and (5.27) allow one to calculate the instantaneous molecular weight averages and chain length distribution of PVC produced in the monomer phase.

5.2.2 Molecular Weight Development in the Polymer Phase

In the polymer phase, the concentration of polymer is high, about 70-wt% even at very low conversions. Therefore, polymer and chlorine radicals may transfer to dead polymer at significant levels and affect the PVC molecular weight development. However, the effect of the primary radical termination and the reaction with internal double bonds on the molecular weight development may be negligible due to the very

low concentrations of these species. Hence these reactions are neglected. Terminal double bonds on the polymer chains are mainly formed by chain transfer to monomer (the formation of 1-chloro-2-alkene structure as a result of abstraction of $Cl^{\cdot}$ as shown in Figure 4.1). However, the number of 1-chloro-2-alkene ($\sim CH_2-CH=CH-CH_2Cl$) and 1,2-dichloroalkane ($\sim CH_2-CHCl-CH_2Cl$) structures for commercial PVC is almost the same.[16] This implies that the terminal double bond ($\sim CH_2-CH=CH-CH_2Cl$) is not active during VCM polymerization. If, however, a polymer radical did react with 1-chloro-2-alkene, the following PVC structure would result:

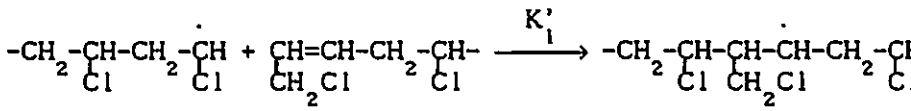

(I)

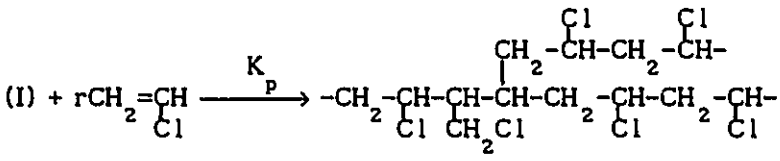

(5.28)

However, Hjertberg et al[17] examined PVC samples made under subsaturated VCM vapour pressure by ^{13}C NMR measurements and did not find any indications of the structure shown in Eq.(5.28). Hjertberg et al's results[17] proved that the reaction with this terminal double bond is unlikely during VCM polymerization. On the other hand, the reaction with the terminal double bonds should lead to an increase in the number-average molecular weight with conversion. However, the experimental results show that the number-average molecular weight hardly changes with conversion for $X < X_f$. All these considerations indicate that the terminal double bond in 1-chloro-2-alkene is not active during VCM polymerization.

Therefore, the reaction with this terminal double bond is neglected in the present modelling. Short chain branches formed by back biting reactions do not affect molecular weight development significantly according to the frequency of short chain branches in PVC chain.[16] Hence, back-biting reactions do not have to be accounted for in the molecular weight calculations. Hence, the production rate of dead polymer with chain length r in the polymer phase can be expressed as:

$$\frac{d(P_r)_2}{V_2 dt} = K_{td2}[R^\cdot]_2[R_r^\cdot]_2 + \frac{1}{2} K_{tc2} \sum_{s=1}^{r-1} [R_s^\cdot]_2 [R_{r-s}^\cdot]_2 + K_{fm2}[R_r^\cdot]_2[M]_2$$

$$+K_{fp}[R_r^\cdot]_2 Q_{1p}/V_2 - K'_{fp}[Cl^\cdot]_2 r[P_r]_2 - K_{fp}[R^\cdot]_2 r[P_r]_2$$

$$(r \geq 2) \qquad (5.29)$$

$$\frac{d(P_1)_2}{V_2 dt} = K_{td2}[R^\cdot]_2[R_1^\cdot]_2 + K_{fp}[R_1^\cdot]_2 Q_{1p}/V_2 + K'_{fp}[Cl^\cdot]_2[P_1]_2$$

$$-K_{fp}[R^\cdot]_2[P_1]_2$$

$$(r=1) \qquad (5.30)$$

From Eqs.(5.29) and (5.30) and the definition of moments as shown in Eq.(5.1), the moment equations for dead polymer chain length distribution may be derived as:

$$\frac{dQ_{op}}{V_2 dt} = R_{p1}\{\tau_2 + \frac{1}{2}\beta_2 - C'_p C M_2 Q_{1p}/(V_2[M]_2)\} \qquad (5.31)$$

$$\frac{dQ_{1p}}{V_2 dt} = K_{p2}[M]_2[R^\cdot]_2 \qquad (5.32)$$

$$\frac{dQ_{2p}}{V_2 dt} = \{(K_{td2}+K_{tc2})[R^{\cdot}]_2+K_{fm2}[M]_2+K_{fp}Q_{1p}/V_2\}Y_{2p}+K_{tc2}Y_{1p}^2$$
$$-(K'_{fp}[Cl^{\cdot}]_2+K_{fp}[R^{\cdot}]_2)Q_{3p}/V_2 \qquad (5.33)$$

$$\frac{dQ_{3P}}{V_2 dt} = \{(K_{td2}+K_{tc2})[R^{\cdot}]_2+K_{fm2}[M]_2+K_{fp}Q_{1p}/V_2\}Y_{3p}+3K_{tc2}Y_{1p}Y_{2p}$$
$$-(K'_{fp}[Cl^{\cdot}]_2+K_{fp}[R^{\cdot}]_2)Q_{4p}/V_2 \qquad (5.34)$$

where

$$\tau_2 = \frac{K_{td2}[R^{\cdot}]_2}{K_{p2}[M]_2} + CM_2, \qquad \beta_2 = \frac{K_{tc2}[R^{\cdot}]_2}{K_{p2}[M]_2}$$

$$CM_2 = K_{fm2}/K_{p2}, \qquad C'_p = K'_{fp}/K'_p$$

The rate constant for chain transfer to monomer can be expressed based on the mechanism discussed in Chapter 4 as:

$$K_{fm2} = \frac{K_1K_2K_5}{(K_2+K_3[M]_2)(K_4[M]_2+K_5)} \qquad (5.35)$$

where K_1, K_2, K_3, K_4, and K_5 are assumed to be the same in both phases for $X < X_f$.

Similarly, the polymer radical balance in the polymer phase can be written as:

$$\frac{d(R_r^{\cdot})_2}{V_2 dt} = K_{p2}[M]_2[R_{r-1}^{\cdot}]_2 + K'_{fp}[Cl^{\cdot}]_2 r[P_r]_2 + K_{fp}[R^{\cdot}]_2 r[P_r]_2$$
$$- K_{p2}[M]_2[R_r^{\cdot}]_2 - (K_{td2}+K_{tc2})[R^{\cdot}]_2[R_r^{\cdot}]_2 - K_{fm2}[R_r^{\cdot}]_2[M]_2$$
$$- K_{fp}[R_r^{\cdot}]_2 Q_{lp}/V_2 - K_{de}[R_r^{\cdot}]_2 \qquad (r \geq 2) \qquad (5.36)$$

$$\frac{d(R_1^{\cdot})_2}{V_2 dt} = R_{I2} + K_{fm2}[M]_2[R^{\cdot}]_2 + K'_{fp}[Cl^{\cdot}]_2[P_1]_2 + K_{fp}[R^{\cdot}]_2[P_1]_2$$
$$- K_{p2}[M]_2[R_1^{\cdot}]_2 - (K_{td2}+K_{tc2})[R^{\cdot}]_2[R_1^{\cdot}]_2$$
$$- K_{fp}[R_1^{\cdot}]_2 Q_{lp}/V_2 - K_{de}[R_1^{\cdot}]_2 \qquad (r = 1) \qquad (5.37)$$

where the effect of precipitation of polymer radicals from the monomer phase is neglected due to the very low precipitation constant estimated in Chapter 4. The total desorption rate of radicals from the polymer phase is also negligible at relatively high conversions as mentioned earlier. Therefore, the effect due to desorption on concentration of radical with chain length r can be neglected. However, the total radical concentration is calculated based on the population balance of radicals shown in Eqs.(4.61) and (4.62) in which radical desorption and absorption is considered. Thus, the moment equations for polymer radicals can be derived from Eqs.(5.36) and (5.37) as:

$$\frac{dY_{lp}}{V_2 dt} = R_{I2} + K_{p2}[M]_2[R^{\cdot}]_2 + K_{fm2}[M]_2[R^{\cdot}]_2 + (K'_{fp}[Cl^{\cdot}]_2 + K_{fp}[R^{\cdot}]_2)\frac{Q_{2p}}{V_2}$$
$$- \{(K_{td2}+K_{tc2})[R^{\cdot}]_2 + K_{fm2}[M]_2 + K_{fp}Q_{lp}/V_2\}Y_{lp} \qquad (5.38)$$

$$\frac{dY_{2p}}{V_2 dt} = R_{I2} + K_{p2}[M]_2([R^\cdot]_2 + 2Y_{1p}) + (K'_{fp}[Cl^\cdot]_2 + K_{fp}[R^\cdot]_2)Q_{3p}/V_2$$

$$+ K_{fm2}[M]_2[R^\cdot]_2 - \{(K_{td2} + K_{tc2})[R^\cdot]_2 + K_{fm2}[M]_2 + K_{fp}Q_{1p}/V_2\}Y_{2p} \qquad (5.39)$$

$$\frac{dY_{3p}}{V_2 dt} = R_{I2} + K_{p2}[M]_2\{[R^\cdot]_2 + 3(Y_{1p} + Y_{2p})\} + K_{fm2}[M]_2[R^\cdot]_2$$

$$+ (K'_{fp}[Cl^\cdot]_2 + K_{fp}[R^\cdot]_2)Q_{4P}/V_2$$

$$- \{(K_{td2} + K_{tc2})[R^\cdot]_2 + K_{fm2}[M]_2 + K_{fp}Q_{1p}/V_2\}Y_{3p} \qquad (5.40)$$

The concentration of chlorine radicals was given in Chapter 4 as:

$$[Cl^\cdot]_2 = K_{fm2}[R^\cdot]_2/K'_2$$

Applying the steady-state hypothesis to Eqs.(5.38)-(5.40), one can obtain the moments of polymer radical distribution in the polymer phase as follows:

$$Y_{1p} = \frac{R_{I2} + K_{p2}[M]_2[R^\cdot]_2 + K_{fm2}[M]_2[R^\cdot]_2 + K_{cp}Q_{2p}/V_2}{(K_{td2} + K_{tc2})[R^\cdot]_2 + K_{fm2}[M]_2 + K_{fp}Q_{1p}/V_2} \qquad (5.41)$$

$$Y_{2p} = \frac{R_{I2} + K_{p2}[M]_2([R^\cdot]_2 + 2Y_{1p}) + K_{fm2}[M]_2[R^\cdot]_2 + K_{cp}Q_{3p}/V_2}{(K_{td2} + K_{tc2})[R^\cdot]_2 + K_{fm2}[M]_2 + K_{fp}Q_{1p}/V_2} \qquad (5.42)$$

$$Y_{3p}=\frac{R_{I2}+K_{p2}[M]_2\{[R^\cdot]_2+3(Y_{1p}+Y_{2p})\}+K_{fm2}[M]_2[R^\cdot]_2+K_{cp}Q_{4p}/V_2}{(K_{td2}+K_{tc2})[R^\cdot]_2+K_{fm2}[M]_2+K_{fp}Q_{1p}/V_2} \quad (5.43)$$

where

$$K_{cp}=K'_{fp}[Cl^\cdot]_2+K_{fp}[R^\cdot]_2$$

Substituting Eqs.(5.41)-(5.43) into Eqs.(5.33) and (5.34), one can rewrite the moment equations for the second and third moments as:

$$\frac{dQ_{2p}}{V_2 dt}=R_{p2}\left\{R_{cp}+2\frac{R_{cp}+PQ_2}{S_2}+\beta_2\left(\frac{R_{cp}+PQ_2}{S_2}\right)^2\right\} \quad (5.44)$$

$$\frac{dQ_{3p}}{V_2 dt}=R_{p2}\left\{\frac{6\beta_2(R_{cp}+PQ_2)^2}{S_2^3}+\frac{(R_{cp}+PQ_2)[6+3\beta_2(R_{cp}+PQ_3)]}{S_2^2}\right.$$
$$\left.+\frac{3(2R_{cp}+PQ_2+PQ_3)}{S_2}+R_{cp}\right\} \quad (5.45)$$

where

$$R_{p2} = K_{p2}[M]_2[R^\cdot]_2$$
$$R_{cp} = 1+R_{I2}/R_{p2}+CM_2$$
$$PQ_2 = (C'_pCM_2+C_p)Q_{2p}/(V_2[M]_2)$$
$$PQ_3 = (C'_pCM_2+C_p)Q_{3p}/(V_2[M]_2)$$
$$S_2 = \tau_2+\beta_2+C_pQ_{1p}/(V_2[M]_2)$$
$$C_p = K_{fp}/K_{p2}$$

Using Eqs.(5.20), (5.31), (5.[illegible] (5.44) and (5.45), one can derive relationships for the instantaneous number-, weight- and Z-average molecular weights in the polymer phase as follows:

$$(M_n)_p = \frac{M_m}{\tau_2 + \frac{1}{2}\beta_2 - C_p' C M_2 Q_{1p}/(V_2[M]_2)} \tag{5.46}$$

$$(M_w)_p = M_m\left\{R_{cp} + 2\frac{R_{cp}+PQ_2}{S_2} + \beta_2\left(\frac{R_{cp}+PQ_2}{S_2}\right)^2\right\} \tag{5.47}$$

$$(M_z)_p = M_m \frac{\left\{\frac{6\beta_2 RQ_2^2}{S_2^3} + \frac{RQ_2(6+3\beta_2 RQ_3)}{S_2^2} + \frac{3(RQ_2+RQ_3)}{S_2} + R_{cp}\right\}}{\left\{R_{cp} + \frac{2RQ_2}{S_2} + \beta_2\left(\frac{RQ_2}{S_2}\right)^2\right\}} \tag{5.48}$$

where

$$RQ_2 = R_{cp} + PQ_2$$

$$RQ_3 = R_{cp} + PQ_3$$

The instantaneous molecular weight distribution in the polymer phase is similarly defined as:

$$W(r)_p = \frac{r}{R_{p2}}\left[\frac{d(P_r)_2}{V_2 dt}\right] \tag{5.49}$$

Applying the steady-state hypothesis to Eqs.(5.36) and (5.37), one can find:

$$[R_r^{\cdot}]_2=(\frac{1}{1+S_2})^r\left[\frac{R_{I2}}{K_{p2}[M]_2}+CM_2[R^{\cdot}]_2\right]+(C_p'CM_2+C_p)\frac{[R^{\cdot}]_2}{[M]_2}\sum_{i=1}^{r}\frac{i[P_i]_2}{(1+S_2)^{r+1-i}} \qquad (5.50)$$

Substituting Eq.(5.50) into Eq.(5.29), one obtains:

$$\frac{d(P_r)_2}{V_2 dt}=R_{p2}\left\{\left[(\tau_2+C_p\frac{Q_{1p}}{V_2[M]_2})(\frac{R_{I2}}{R_{p2}}+CM_2)+\frac{1}{2}\beta_2(r-1)(\frac{R_{I2}}{R_{p2}}+CM_2)^2\right](\frac{1}{1+S_2})^r\right.$$

$$\left.+(\tau_2+C_p\frac{Q_{1p}}{V_2[M]_2})C\sum_{i=1}^{r}\frac{i[P_i]_2}{(1+S_2)^{r+1-i}}-Cr[P_r]_2\right\} \qquad (5.51)$$

where

$$C = (C_p'CM_2+C_p)/[M]_2$$

Therefore, the instantaneous molecular weight distribution in the polymer phase can be expressed as:

$$W(r)_p=r\left\{\left[(\tau_2+C_p\frac{Q_{1p}}{V_2[M]_2})(\frac{R_{I2}}{R_{p2}}+CM_2)+\frac{1}{2}\beta_2(r-1)(\frac{R_{I2}}{R_{p2}}+CM_2)^2\right](\frac{1}{1+S_2})^r\right.$$

$$\left.+(\tau_2+C_p\frac{Q_{1p}}{V_2[M]_2})C\sum_{i=1}^{r}\frac{i[P_i]_2}{(1+S_2)^{r+1-i}}-Cr[P_r]_2\right\} \qquad (5.52)$$

Eqs.(5.32), (5.44)-(5.48), (5.51), and (5.52) allow one to solve for instantaneous molecular weight averages and chain length distribution in the polymer phase.

5.2.3 The Total Instantaneous Molecular Weight Averages and Distribution

The above equations permit one to calculate instantaneous molecular weight averages and MWD for each phase. Practically, one is not able to identify PVC produced in each phase. However, one can possibly determine the total instantaneous molecular weight averages under the special conditions (such as semi-batch process) and determine the accumulated molecular weight averages experimentally. Hence, it is necessary to know the total instantaneous molecular weight averages and distribution. The total instantaneous molecular weight averages and MWD depend on the quantity of polymer produced in the different phases. The instantaneous mass fraction of polymer can be calculated using instantaneous polymerization rate in both phases, such as

$$m_1 = \frac{R_{p1} V_1}{R_{P1} V_1 + R_{p2} V_2} \tag{5.53}$$

$$m_2 = 1.0 - m_1 \tag{5.54}$$

where R_{p1} and R_{p2} are the polymerization rates in the monomer and polymer phase, respectively. These can be calculated using the model described in Chapter 4. With mass fractions m_1 and m_2, therefore, the total instantaneous molecular weights and MWD can be expressed as a

function of the molecular weights and MWD in both phases according to the definitions of molecular weight averages.

The total instantaneous molecular weight distribution can be simply expressed as a function of MWD in each phase as:

$$W(r) = m_1 W(r)_m + m_2 W(r)_p \tag{5.55}$$

With Eq.(5.55), the total number of polymer molecules produced at conversion X can be expressed as:

$$\sum_{r=1}^{\infty} \frac{W(r)}{M_m r} = m_1 \sum_{r=1}^{\infty} \frac{W(r)_m}{M_m r} + m_2 \sum_{r=1}^{\infty} \frac{W(r)_p}{M_m r} \tag{5.56}$$

Hence, the total instantaneous number-average molecular weight is given by

$$M_n = \frac{\sum_{r=1}^{\infty} W(r)}{\sum_{r=1}^{\infty} \frac{W(r)}{M_m r}} = \frac{1}{m_1 \sum_{r=1}^{\infty} \frac{W(r)_m}{M_m r} + m_2 \sum_{r=1}^{\infty} \frac{W(r)_p}{M_m r}} \tag{5.57}$$

Applying the definition of number-average molecular weight to expression of each phase, one can obtain:

$$M_n = \frac{1}{m_1/(M_n)_m + m_2/(M_n)_p} \tag{5.58}$$

According to the definition, the total instantaneous weight-

average molecular weight is simply given by

$$M_w = m_1(M_w)_m + m_2(M_w)_p \tag{5.59}$$

The total instantaneous Z-average molecular weight is defined as:

$$M_z = \sum_{r=1}^{\infty} W(r)M_m^2\, r^2 / \sum_{r=1}^{\infty} W(r)M_m r$$

$$= \sum_{r=1}^{\infty} W(r)M_m^2\, r^2/M_w \tag{5.60}$$

Substituting Eq.(5.55) into Eq.(5.60) and using the definition of the Z-average molecular weight to the expression for each phase, one can obtain:

$$M_z = m_1 \frac{(M_w)_m}{M_w} (M_z)_m + m_2 \frac{(M_w)_p}{M_w} (M_z)_p \tag{5.61}$$

At high conversions ($X > X_f$), polymerization proceeds in the polymer phase only. Therefore, the total instantaneous molecular weight averages and MWD are the same as those in the polymer phase. Thus, Eqs.(5.55), (5.58), (5.59) and (5.61) are still valid for conversions X greater than X_f by setting $m_1=0$ and $m_2=1$. However, all the kinetic parameters for diffusion-controlled reactions change with conversion and are different from those used for $X < X_f$.

5.2.4 Accumulated Molecular Weight Averages and Distribution

With the total instantaneous MWD and molecular weight averages given in Eqs.(5.55), (5.58), (5.59) and (5.61), one can find the accumulated molecular weight averages and MWD by either integration or differentiation. However, for a two-phase polymerization system, the differentiation method seems more convenient because it avoids integration in two phases. It should be mentioned that the accumulated properties cannot be calculated from instantaneous properties when chain transfer to polymer is important. Moment equations can only be used for the system that chain transfer to polymer is important. However, this is not the case for VCM polymerization. Based on the definitions of molecular weight averages, the relationships between accumulated and instantaneous molecular weight averages and the distribution are governed by the following differential equations:

$$\frac{d(X/\overline{M}_n)}{dt} = R_p/M_n \tag{5.62}$$

$$\frac{d(X\,\overline{M}_w)}{dt} = R_p M_w \tag{5.63}$$

$$\frac{d(X\,\overline{\Psi})}{dt} = R_p M_w M_z \tag{5.64}$$

$$\overline{M}_z = \overline{\Psi} \,/\, \overline{M}_w \tag{5.65}$$

where

$$\bar{\Psi} = M_m^2 \int_0^\infty r^2 \, \overline{W}(r)dr, \text{ (based on the definition of } \overline{M}_z).$$

$$\frac{d(X \, \overline{W}(r))}{dt} = R_p W(r) \tag{5.66}$$

where

$$R_p = dX/dt.$$

The accumulated number-, weight- and Z-average molecular weights and chain length distribution can be obtained by solving Eqs.(5.62)-(5.66) using appropriate reactor operational conditions. These equations are valid over the entire conversion range.

5.3 EXPERIMENTAL

PVC was made by suspension polymerization. The detailed procedures for these polymerizations are given in Chapters 3 and 4. In this section, only details of the molecular weight measurements will be described.

Molecular weight measurements of PVC have been studied extensively by various methods.[18-52] Gel permeation chromatography (GPC) is the most powerful analytical method providing the full molecular weight distribution as well as molecular weight averages. However, it is not an absolute method and must be calibrated. Universal calibration after Grubisic et al[53] is used by most authors.[5,6,29,31,40,41,47-51] Many Mark-Houwink constants for PVC in the GPC solvent tetrahydrofuran (THF) and

other solvents have been published.[20,21,24,26,31,32,40,42-46,52] Unfortunately, the values for the Mark-Houwink constants vary widely. For PVC in THF, Freeman et al[20] and Bohdanecky et al's[26] values have been widely used in the literature. Although the PVC samples were carefully fractionated in these studies[20,26] there was appreciable polydispersity especially for the higher molecular weight fractions used. Because of these uncertainties, it was decided to calibrate the GPC using PVC accumulated weight-average molecular weights measured by low angle laser light scattering (LALLS).

5.3.1 LALLS Measurements

A Chromatix KMX-6 low-angle laser light scattering photometer (LALLS), with a cell length of 15 mm and a field stop of 0.2 corresponding to an average scattering angle of 4.8 degree, was used for $\overline{M}_w$ measurements. THF was used as a solvent. The concentration of PVC in the solution was in range of $(0.5\text{-}5.0)10^{-3}$ g/mL. The refractive index increment of PVC-THF solutions was determined using a Chromatix KMX-16 laser differential refractometer at 25°C and a wavelength of 632.8 nm. The dn/dc was found to be 0.106 mL/g for a PVC sample synthesized at 50°C. This value is in agreement with data in the literature[18,41,54] and was used for all PVC samples as dn/dc is independent of molecular weight for high molecular weight polymer.[55] (see Appendix C for detailed procedures calculating $\overline{M}_w$ from LALLS measurements).

5.3.2 GPC Measurements

A Waters 150-C GPC with a differential refractometer detector was used at 40°C with THF of HPLC grade as mobile phase. Five columns (TSK) with the following specifications were used: G1000H8, G2500HXL, G3000HXL, G4000H8 and G7000HXL of exclusion limits 10^3, $2x10^4$, $6x10^4$, $4x10^5$ and $4x10^8$, respectively. The flow rate was 1 mL/min. About 0.1 mL of PVC-THF solutions containing about 0.1-wt% PVC were injected.

5.3.3 GPC Calibration

Calibration is an important issue for application of GPC.[56,57] A computer search method for two parameters which are combinations of the Mark-Houwink constants of polystyrene standards and the polymer under study was suggested.[58-60] Mori[58] and Chiantore et al[59] used two broad MWD samples and Schroder et al,[60] more recently, used more than two samples to calibrate GPC. In the present work, the arithmetic method was modified to estimate the calibration parameters with twenty (20) samples measured by LALLS.

Using universal calibration,[53] one may write the molecular weight relationship between PVC and polystyrene standards (PS) as:

$$(M_{PVC})_i = \alpha(M_{PS})_i^{\xi} \qquad (5.67)$$

where

$$\alpha = \left(\frac{K_{PS}}{K_{PVC}}\right)^{1/(1+a_{PVC})}$$

$$\xi = \frac{1+a_{PS}}{1+a_{PVC}}$$

Hence, weight-average molecular weight of PVC sample i can be expressed as:

$$\overline{M}_{w,i} = \alpha \int_0^\infty F_i(t) M_{PS}(t)^{\xi} dt \tag{5.68}$$

where $F_i(t)$ is the normalized GPC response at retention time t, $M_{PS}(t)$ is the molecular weight of PS at retention time t, which can be expressed as a third degree polynomial with regard to retention time.

If n weight-average molecular weights of PVC are given, then the parameter α and ξ can be found using a nonlinear regression method based on the following equations:

$$\sum_{i=1}^{n-1} \left\{ \frac{\overline{M}_{w,i+1}}{\overline{M}_{w,i}} - \frac{\int_0^\infty F_{i+1}(t) M_{PS}(t)^{\xi} dt}{\int_0^\infty F_i(t) M_{PS}(t)^{\xi} dt} \right\}^2 = \min \tag{5.69}$$

$$\sum_{i=1}^{n} \left[\overline{M}_{w,i} - \alpha \int_0^\infty F_i(t) M_{PS}(t)^{\xi} dt \right]^2 = \min \tag{5.70}$$

where $\overline{M}_{w,i}$ are measured by LALLS and $F_i(t)$ and $M_{PS}(t)$ are measured by

GPC.

Given α and ξ, the molecular weight averages and MWD can be calculated by routine procedures using GPC detector responses. This method does not require prior knowledge of the specific Mark-Houwink constants for both polystyrene standards and PVC samples. In other words, errors in Mark-Houwink constants of polystyrene standards and PVC will not affect the molecular weight calculation as long as α and ξ satisfy the Eqs.(5.69) and (5.70). In addition, if the universal calibration method is not entirely valid, this method can correct for this potential error.

5.4 RESULTS AND DISCUSSION

5.4.1 Comparison of Molecular Weights Measured by Different Methods

It is well known that PVC molecules can form aggregates in solution and this can cause large errors in molecular weight measurements even with good solvents.[19,20,22-28,35-42,46-49] These aggregates can be disintegrated into single molecules by either heat[19,27,38,47] or ultrasonic treatment.[19,35] However, for the wide range of molecular weights (23,000-165,000)[43-45,52] or commercial PVC,[30,37,50] there is no evidence of aggregate formation. In the present work, LALLS measurements of the highest molecular weight PVC synthesized at 40°C were unchanged after heating the solution at 95°C for one hour. No anomalous chromatograms

were observed for the PVC samples under study. Therefore, aggregation for PVC polymerized above 40°C was considered negligible. This is in agreement with Abdel-Alim et al's results for PVC made by the bulk process.[38]

Using molecular weight averages measured by LALLS and GPC data, the parameters α and ξ in Eqs.(5.69) and (5.70) were estimated to be 1.74 and 0.931 respectively.

Mark-Houwink correlation for polystyrene standards in THF is given by

$$[\eta]_{PS} = 1.47 \times 10^{-4} \, M_{PS}^{0.702} \tag{5.71}$$

where $M_{PS} = \sqrt{\overline{M}_w \, \overline{M}_n}$

Eq.(5.71) was obtained from the data given by American Polymer Standards Corporation.[61] According to the definitions of α and ξ in Eq.(5.67) and parameters in Eq.(5.71), one can obtain the Mark-Houwink correlation for PVC-THF at 40°C as follows:

$$[\eta]_{PVC} = 5.30 \times 10^{-5} \, M_{PVC}^{0.828} \tag{5.72}$$

In the literature, intrinsic viscosity was correlated with either $\overline{M}_w$ or $\overline{M}_n$.[21,24,26] The values for K_{PVC} is in the range $(0.4\text{-}10)10^{-4}$ and a_{PVC} in the range 0.7-0.9 for the PVC-THF system at temperatures 20-30°C. Therefore, the present results shown as Eq.(5.72) seem reasonable. It should be mentioned that the accuracy of Eq.(5.72) depends on the

accuracy of the parameters in Eq.(5.71) and on the validity of universal calibration.

The weight-average molecular weights measured by GPC using the parameters shown above are in excellent agreement with those measured by LALLS as shown in Figure 5.1. If Bohdancky et al's Mark-Houwink constants[26] are used in the GPC calibration, the measured molecular weights

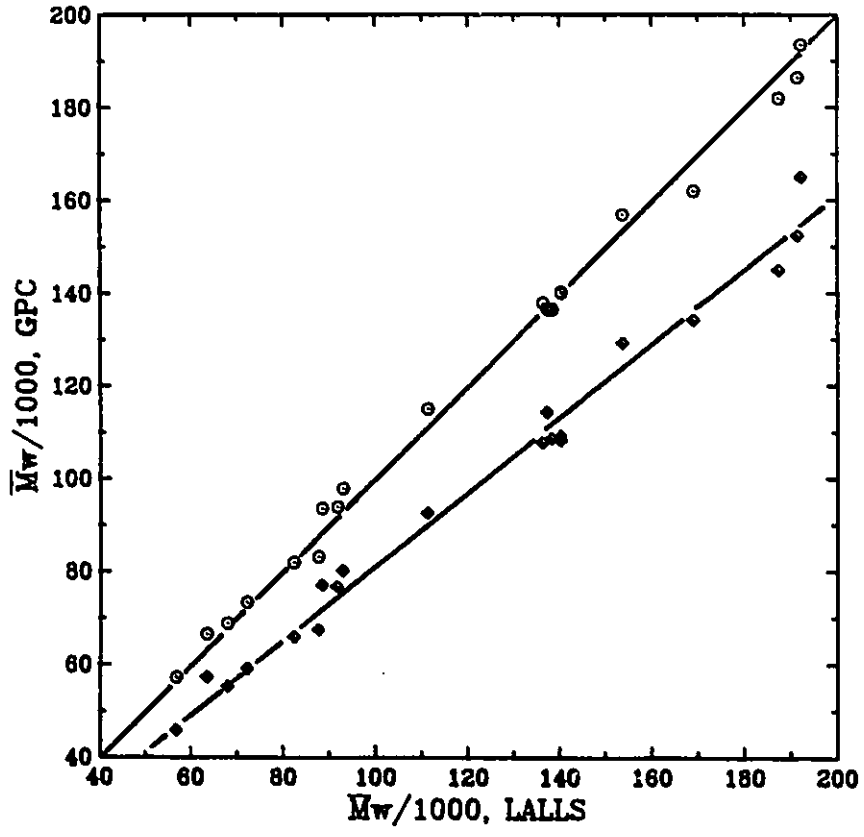

Figure 5.1. Comparison of weight-average molecular weights measured by different methods.
⊙: the present method
◇: $K_{PVC}=1.5\times10^{-4}$, $a_{PVC}=0.77$ (literature values[26])

are 20% lower than those measured by LALLS as shown in Figure 5.1. From Eq.(5.67), one may see that Mark-Houwink correlation with $\overline{M}_w$ or $\overline{M}_n$ may not be suitable for the universal calibration. Monodispersed molecular weight or root-mean-square average molecular weights should be used for the universal calibration. This was also demonstrated by Kolinsky et al.[29]

5.4.2 Estimation of Parameters in the Present Kinetic Model

All of the kinetic parameters estimated in our rate model in Chapter 4 should be valid in the present molecular weight model. The remaining parameters will be estimated using molecular weight information.

According to Eqs.(18) and (5.34), the parameters τ_i and β_i can be expressed as:

$$\tau_i = \frac{\lambda_i R_{pi}}{\left[\frac{K_p}{K_t^{1/2}}\right]_i^2 [M]_i^2} + CM_i \qquad (i = 1,2) \qquad (5.73)$$

$$\beta_i = \frac{(1-\lambda_i) R_{pi}}{\left[\frac{K_p}{K_t^{1/2}}\right]_i^2 [M]_i^2} \qquad (i = 1,2) \qquad (5.74)$$

where the fraction of bimolecular termination by disproportionation, λ_i, is given by

$$\lambda_i = \frac{K_{td1}}{K_{td1} + K_{tc1}} \qquad (i = 1,2)$$

which can be estimated with appropriate molecular weight information.

The overall rate constant for chain transfer to monomer given in Eqs.(5.19) and (5.35) involves five elementary rate constants. K_{fm} should remain constant in both phases, although each phase will have a different value due to the difference in monomer concentrations, at conversions less than X_f. At high conversions ($X > X_f$), however, K_{fm2} is not constant because of the decrease in monomer concentration and the effect of diffusion-controlled reactions. It is necessary to estimate all of the parameters in order to obtain K_{fm2}. In commercial PVC, the concentration of head-to-head structure is very low.[16] Hence, the propagation reaction by radical with head-to-head structure (as shown in Chapter 4, Figure 4.1) may be negligible so that Eq.(5.35) can be simplified to

$$K_{fm2} = \frac{K_1}{1 + \frac{K_4}{K_5}[M]_2} \qquad (5.75)$$

which was also suggested by Hjertberg et al.[13] Hence, one only has to estimate K_1 and K_4/K_5 to find K_{fm2}.

K_1 and K_4 are head-to-head and head-to-tail propagation rate constants respectively (see Figure 4.1). At high conversions, K_1 may become diffusion-controlled but its sensitivity to environmental effect may not as great as that for K_{p2}. However, the effect of diffusion

control on K_4 can be assumed to be the same as that on K_{p2}. The reaction involving the elimination of a chlorine atom radical should be chemically controlled over the entire conversion range so that K_5 may be considered constant for isothermal polymerization. Therefore, K_1 and K_4/K_5 can be expressed as a function of free volume fraction:

$$K_1 = K_{1xf} \exp\left[-CH^*\left(\frac{1}{V_{fp}} - \frac{1}{V_{fxf}}\right)\right] \qquad (X > X_f) \qquad (5.76)$$

$$K_4/K_5 = (K_4/K_5)_{xf} \exp\left[-B^*\left(\frac{1}{V_{fp}} - \frac{1}{V_{fxf}}\right)\right] \qquad (X > X_f) \qquad (5.77)$$

where B^* has been estimated in Chapter 4.

Therefore, the unknown parameters include λ, K_1, K_4/K_5, CH^*, C_p and C_p' for molecular weight calculations. These parameters were estimated by fitting the present model with weight- and number-average molecular weights simultaneously using a nonlinear regression technique. The interesting findings are as follows:

λ shown in Eqs.(5.73) and (5.74) could vary from zero to one. It was found that the present model cannot best fit the weight- and number-average molecular weights simultaneously if λ is greater than zero. The best fitting, however, can be achieved by setting $\lambda = 0$ as shown in Figures 5.2-5.6. This suggests that bimolecular termination of polymer radicals occurs exclusively by combination during VCM polymerization. Razuayev et al[62] studied the termination mechanism in bulk and suspension polymerization systems using ^{14}C-labelled initiator. They concluded

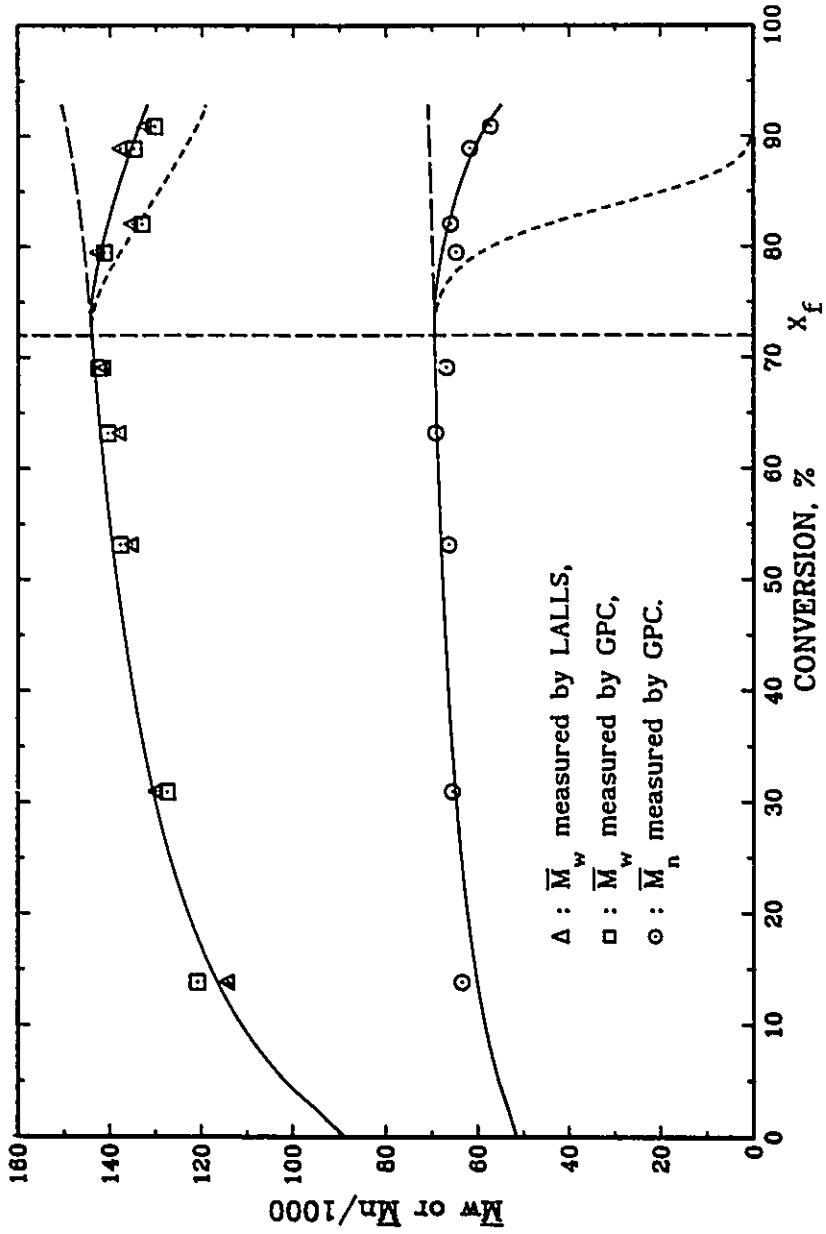

Figure 5.2. Effect of CM on the accumulated molecular weight averages of PVC at high conversions at 50°C. Perkadox 16-W40 as an initiator with [I]=0.15-wt%. — — — : model with CM as a constant. ------ : model with K_{fm} changing with $[M]_2$ only. ——— : model with K_{fm} changing with monomer concentration and free volume fraction.

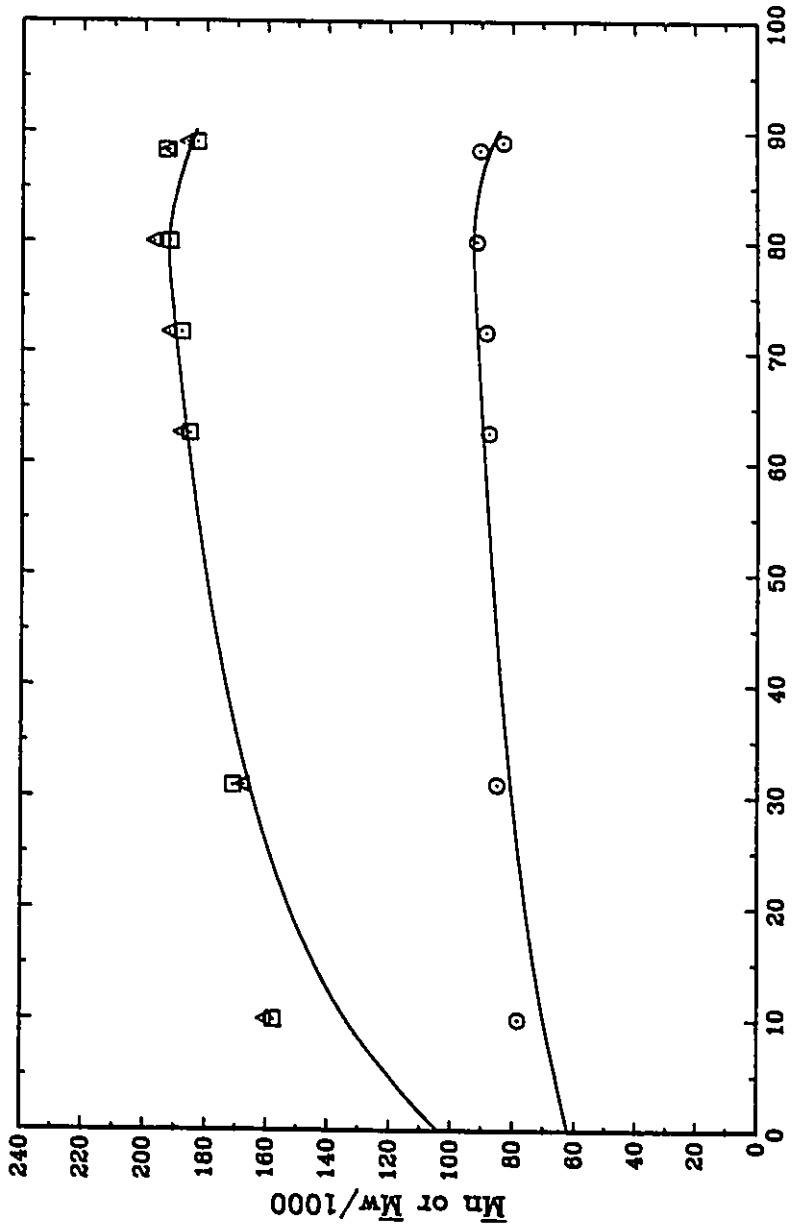

Figure 5.3. Conversion dependence of accumulated molecular weight averages at 40°C. Perkadox 16-W40 as an initiator with [I]=0.40-wt%. Δ: $\bar{M}_w$ measured by LALLS, □: $\bar{M}_w$ measured by GPC, ⊙: $\bar{M}_n$ measured by GPC, ——— : model.

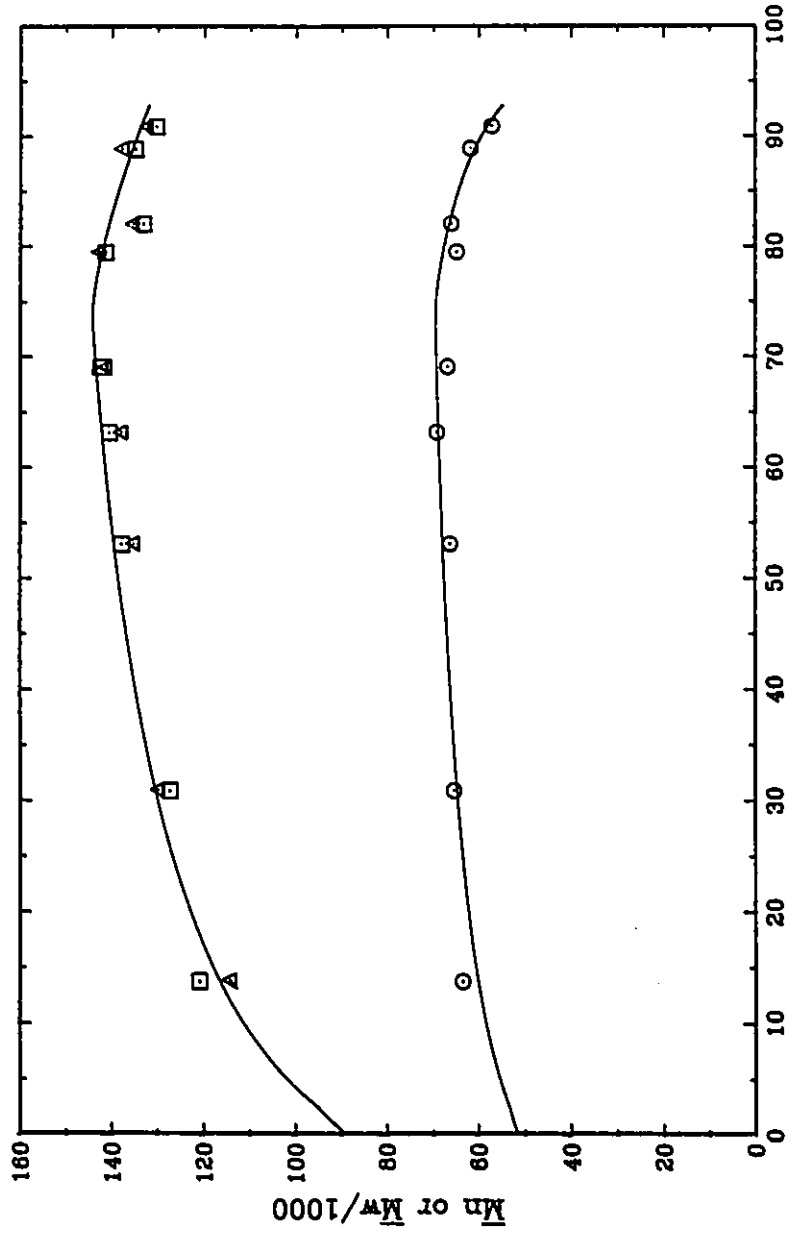

Figure 5.4. Conversion dependence of Accumulated molecular weight averages at 50°C. Perkadox 16-W40 as an initiator with [I]=0.15-wt%. Δ: $\overline{M}_w$ measured by LALLS, □: $\overline{M}_w$ measured by GPC, ○ :$\overline{M}_n$ measured by GPC, ——— : model.

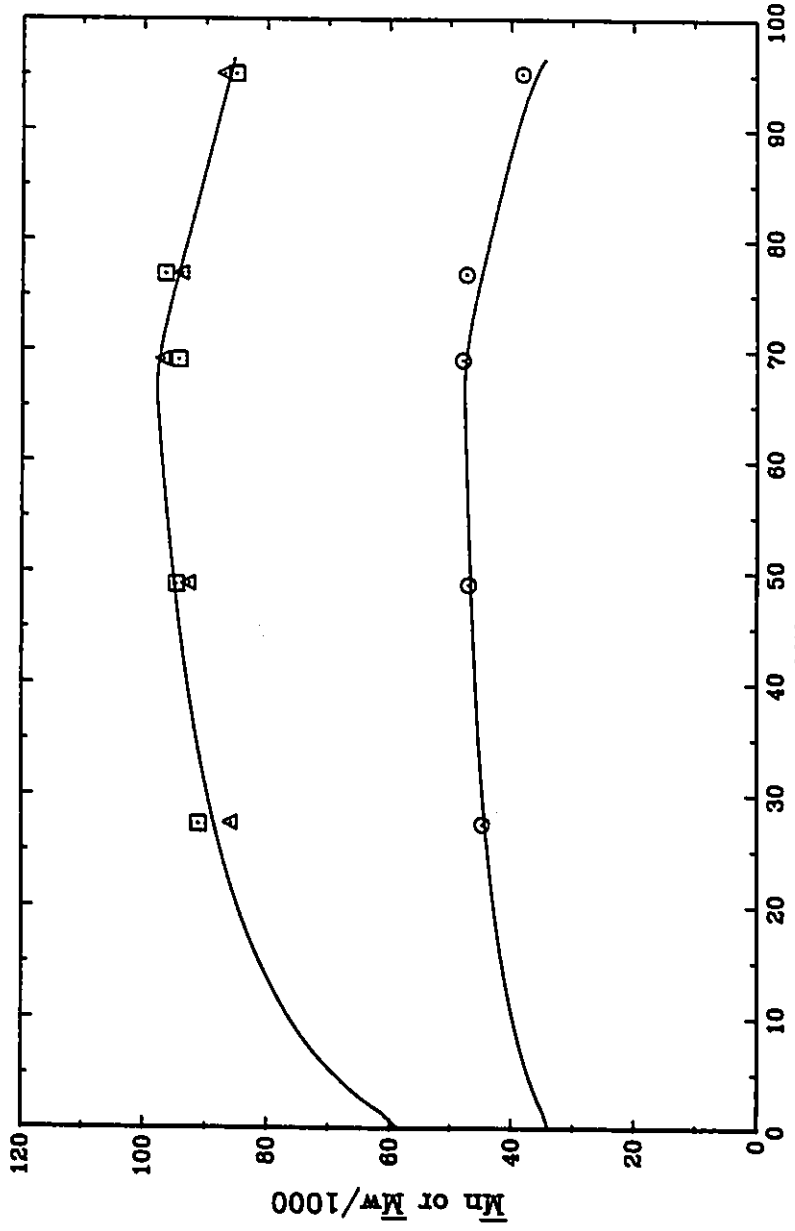

Figure 5.5. Conversion dependence of accumulated molecular weight averages at 60°C. Perkadox 16-W40 as an initiator with [I]=0.125-wt%. Δ: $\overline{M}_w$ measured by LALLS, □: $\overline{M}_w$ measured by GPC, ⊙: $\overline{M}_n$ measured by GPC, ——— : model.

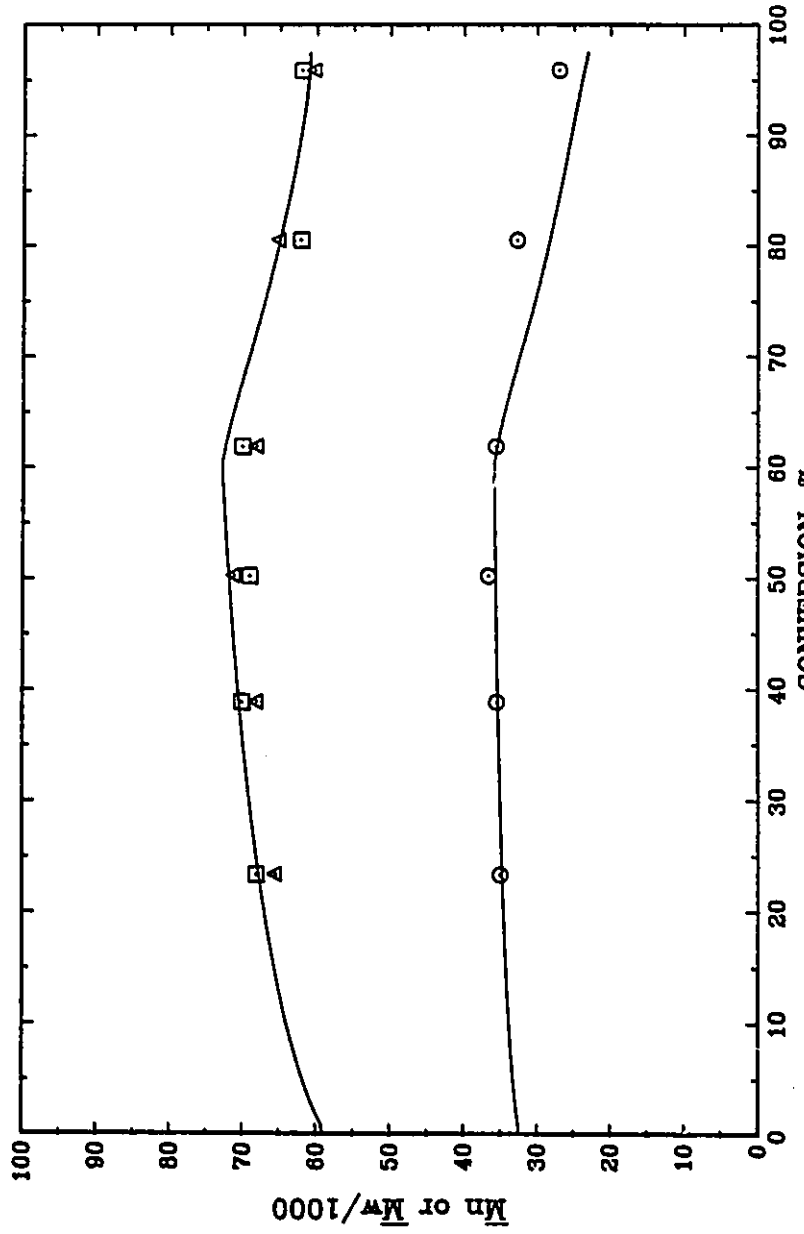

Figure 5.6. Conversion dependence of accumulated molecular weight averages at 70°C. AIBN as an initiator with [I]=0.15-wt%. Δ: $\bar{M}_w$ measured by LALLS, □: $\bar{M}_w$ measured by GPC, ⊙: $\bar{M}_n$ measured by GPC, ——— : model.

that the average number of end groups per polymer molecule is between 0.19–0.40, but they failed to distinguish between combination and disproportionation due to the significant chain transfer to monomer. Park et al[63] tried to reduce the importance of chain transfer to monomer using very high initiator (AIBN) levels in solution polymerization and concluded, based on very limited data, that 25% of mutual termination occurs by combination. At very high initiator levels, however, termination with primary radicals may be significant. Moreover, Starnes et al,[64,65] recently, examined the PVC structural segments derived from AIBN by NMR and found the copolymer structure of VCM and methacrylonitrile (which is from AIBN) in the PVC chains. Hence, Park et al's results based on ^{14}C labelled AIBN are open to question. In kinetic modelling, this uncertainty exists in the literature. Mickley et al[66] assumed that all of the termination was by combination. Abdel-Alim et al[5] and, more recently, Kelsall et al[15] assumed that all of the termination was by disproportionation. This study is the first to estimate λ using molecular weight information.

In the literature, the ratio of K_{fm}/K_p, CM, is reported to be a constant independent of conversion under certain polymerization temperatures. Figure 5.2 shows the effect of CM on weight- and number-average molecular weights over the entire conversion range. If CM is a constant over the entire conversion range, $\overline{M}_w$ should increase significantly and $\overline{M}_n$ increases slightly at high conversions as shown by the large dotted line (– – – –) in Figure 5.2. To fit the experimental data CM must increase with conversion for $X > X_f$. If K_1 and K_4/K_5 were constant and

K_{fm2} only affected by $[M]_2$, then CM would increase significantly and as a result, both $\overline{M}_w$ and $\overline{M}_n$ would decrease dramatically as shown by the small dotted line (.....) in Figure 5.2. Therefore, it appears that CM increases slightly at high conversions ($X > X_f$) while K_1 and K_4/K_5 should decrease with conversion. Using Eqs.(5.75)-(5.77) to calculate K_{fm2}, the results are shown as a solid line in Figure 5.2 which fits the experimental data well. These measurements further confirm the mechanism of chain transfer to monomer discussed in Chapter 4. A decrease in molecular weight at high conversions has been observed experimentally by many other workers.[4,11-14] The effect of monomer concentration on the rate constant of chain transfer to monomer has been discussed by Hjertberg et al.[13] However, this study is the first to estimate K_1 and K_4/K_5 values and measure the effect of conversion on these parameters.

The fits of the present model with the experimental molecular weight data over the entire conversion range studied for a wide range of temperatures are shown in Figures 5.3-5.6. One can see that the model fits the experimental data well over the entire range of monomer conversion and temperatures studied. Molecular weight increases slightly with conversion before X_f, then decreases gradually with conversion after X_f. The increase in number- and weight-average molecular weights with conversion at low conversions is due to the increase in the significance of the contribution of the polymer production rate in the polymer phase. At 60° and 70°C, the model values are slightly lower than experimental data at high conversions. Chain transfer to polymer may be more significant at higher temperatures than accounted for. The parameters estimated from

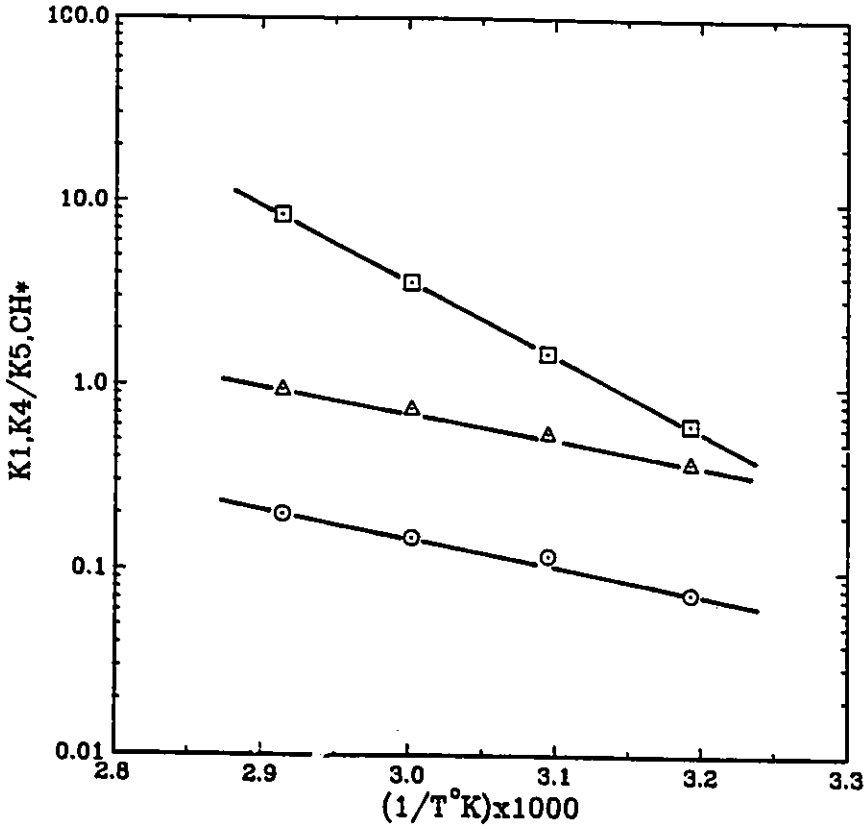

Figure 5.7. Temperature dependence of kinetic parameters
⊙: K_4/K_5, Δ: CH^*, □ : K_1.

the experimental data shown in Figures 5.3-5.6 are plotted in Figures 5.7 and 5.8. All the parameters are mild functions of temperature and can be correlated with the following Arrhenius type equations:

$$K_1 = 5.55 \times 10^{12} \exp(-9340/T) \qquad \text{(L/mole-sec)} \qquad (5.78)$$

$$K_4/K_5 = 4260 \exp(-3410/T) \qquad \text{(L/mole)} \qquad (5.79)$$

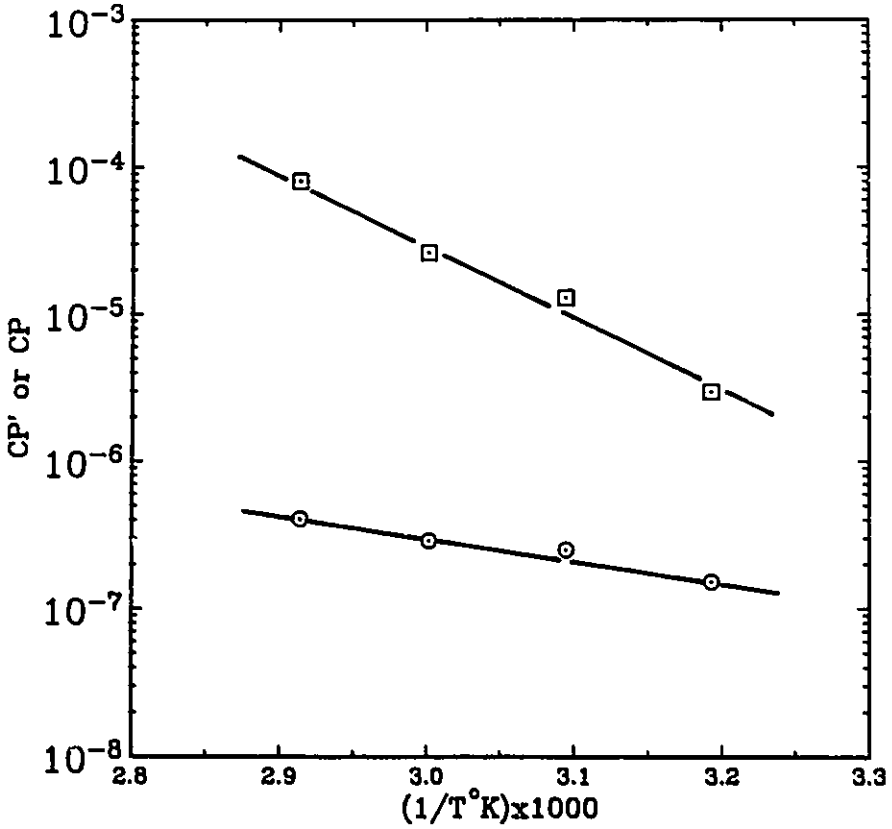

Figure 5.8. Temperature dependence of C_p and C_p' for VCM polymerization. ⊙: C_p', □: C_p

$$CH^* = 1.28X10^4 \exp(-3250/T) \tag{5.80}$$

$$C_p = 8.31x10^9 \exp(-11100/T) \tag{5.81}$$

$$C_p' = 6.48x10^{-3} \exp(-3320/T) \tag{5.82}$$

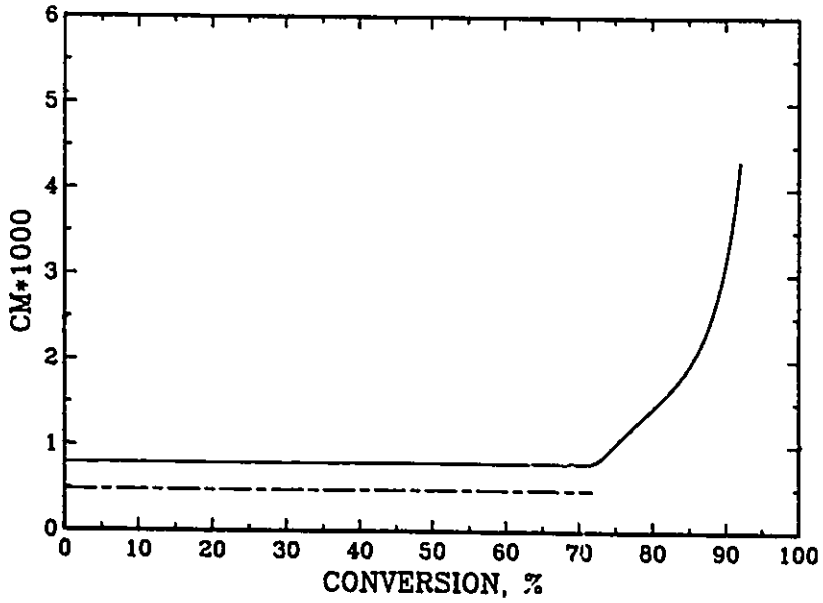

Figure 5.9. Conversion dependence of CM for VCM polymerization at 50°C.
——— : CM in the monomer phase,
——— : CM in the polymer phase.

With the parameters in Eqs.(5.78)-(5.82), one can estimate CM values at any conversion and temperature. Typical values at 50°C are shown in Figure 5.9. One can see that CM is a constant for $X < X_f$, and CM in the monomer phase is slightly smaller than that in the polymer phase due to the difference in monomer concentrations in these phases. Values of CM in the polymer phase increase significantly after X_f because of the decreasing monomer concentration and the increasing importance of diffusion-controlled reactions. Some typical values of CM for $X < X_f$ are shown in Table 5.1. The values of CM from the literature[3-5,12,13,66-72] are summarized in Table 5.2. All the data except Burnett's[72] in Table 5.2 are in reasonable agreement at a given temperature. The small

differences may be the result of using different models for data interpretation and using samples at different conversions. In fact, the present results are in excellent agreement with the literature data. The CM values shown in Figure 5.9, for instance, represents all the data at 50°C shown in Table 5.2. CM values in Table 5.2 estimated from solution polymerization are greater than those in the monomer phase but very close to those in the polymer phase as shown in Table 5.1. This is not surprising because the monomer concentrations in solution polymerization are always lower than those for the monomer phase. In solution polymerization, the molecular weight always increases with an increase in monomer concentration.[66,67,73] This cannot be explained by the classical mechanism of chain transfer to monomer during VCM polymerization. However, according to the present model, K_{fm} will decrease with increasing monomer concentration (although other kinetic parameters remain constant under homogeneous conditions). Consequently, the molecular weight of PVC increases. Strictly speaking, CM values for VCM polymerization must be specified by temperature, concentration of monomer, location of polymer-

Table 5.1. Some typical values of CM for $X < X_f$ from the current work.

Temp. °C	CMx10^3		Polymerization type
	monomer phase	polymer phase	
40	0.314	0.508	suspension
50	0.477	0.791	suspension
60	0.723	1.17	suspension
70	1.07	1.58	suspension

Table 5.2. CM values from the literature.

Temp. °C	CMx10^3	Polymerization type	References
6	0.171	bulk	[4]
20	0.32	bulk	[70]
25	0.385	bulk	[4]
30	0.63,0.625,0.51	bulk	[5],[69],[70]
40	0.710,0.71	bulk	[4],[70]
50	1.10,0.85,1.35,1.05,1.035	bulk	[5],[68]-[71]
60	1.23,1.48	bulk	[68],[70]
70	5.71,2.38,2.15	bulk	[5],[69],[70]
25	0.32,0.0657	solution	[67],[72]
40	5.0	solution	[66]
50	1.1,0.64,0.78	solution	[3],[68]
55	0.122	solution	[72]
60	1.08,1.28	solution	[68]
55	1.2±0.2,1.30	emulsion	[12],[13]

ization and conversion. The literature values prior to the present investigation are average values at certain conversion level. Therefore, one should use CM values with caution for modelling calculation.

Values of C_p and C_p' for VCM polymerization have never been reported in the literature. C_p is in the range 10^{-6}-10^{-5} and C_p' 10^{-7}-10^{-6} for the temperature range used in this study (see Figure 5.8). These values suggest that chain transfer to polymer is almost insignificant for commercial VCM polymerization. This is in agreement with the results for long chain branch measurements for commercial PVC.[16] It is also supported by weight- and number-average molecular weight results,[4,5,7,70,74] i.e. weight- and number-average molecular weights increase with conversion slightly at $X < X_f$. If C_p were greater, the weight-average molecular weight would increase significantly, particularly at high

conversions. The number-average molecular weight would also increase significantly if C_p' were large enough. Using PVC dimers and trimers as model PVC, Lim et al[75] estimated C_p to be of $5x10^{-4}$ at 50°C, which is one order of magnitude higher than the present value.

5.4.3 Model Evaluation

With the parameters estimated above, it is now possible to further evaluate the present model and explain other features of PVC molecular weight development. Figures 5.3-5.6 show that the present model is in excellent agreement with the experimental data over wide range of polymerization conditions. Figures 5.10 and 5.11 further show the relationships between instantaneous and accumulated molecular weight averages. The instantaneous molecular weight in the monomer phase is much lower than that in the polymer phase although CM in the polymer phase is higher. The reason is that the termination rate constant is much higher in the monomer phase. The total instantaneous molecular weight is close to that in the polymer phase with conversion gradually because the polymer phase dominates the polymerization rate gradually, as has been shown in Chapter 4. The instantaneous number- and weight- average molecular weights in each phase are almost constant at $X < X_f$ due to the low value of C_p and C_p' and other factors are constant. However, the total instantaneous number- and weight-average molecular weights increase gradually due to the significant increase in polymerization rate in the polymer phase. Therefore, the accumulated number- and weight-average molecular

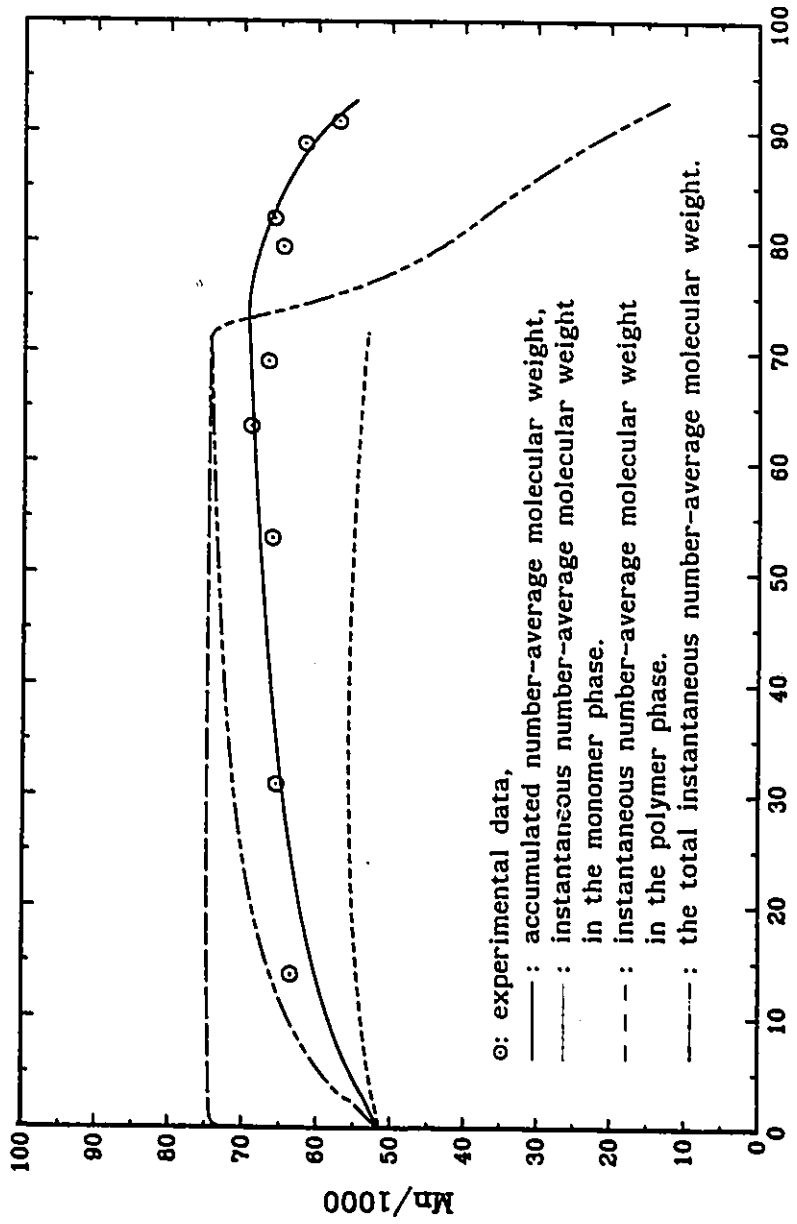

Figure 5.10. Conversion dependence of instantaneous and accumulated number-average molecular weights at 50°C. Perkadox 16-W40 as an initiator with [I]=0.15-wt%.

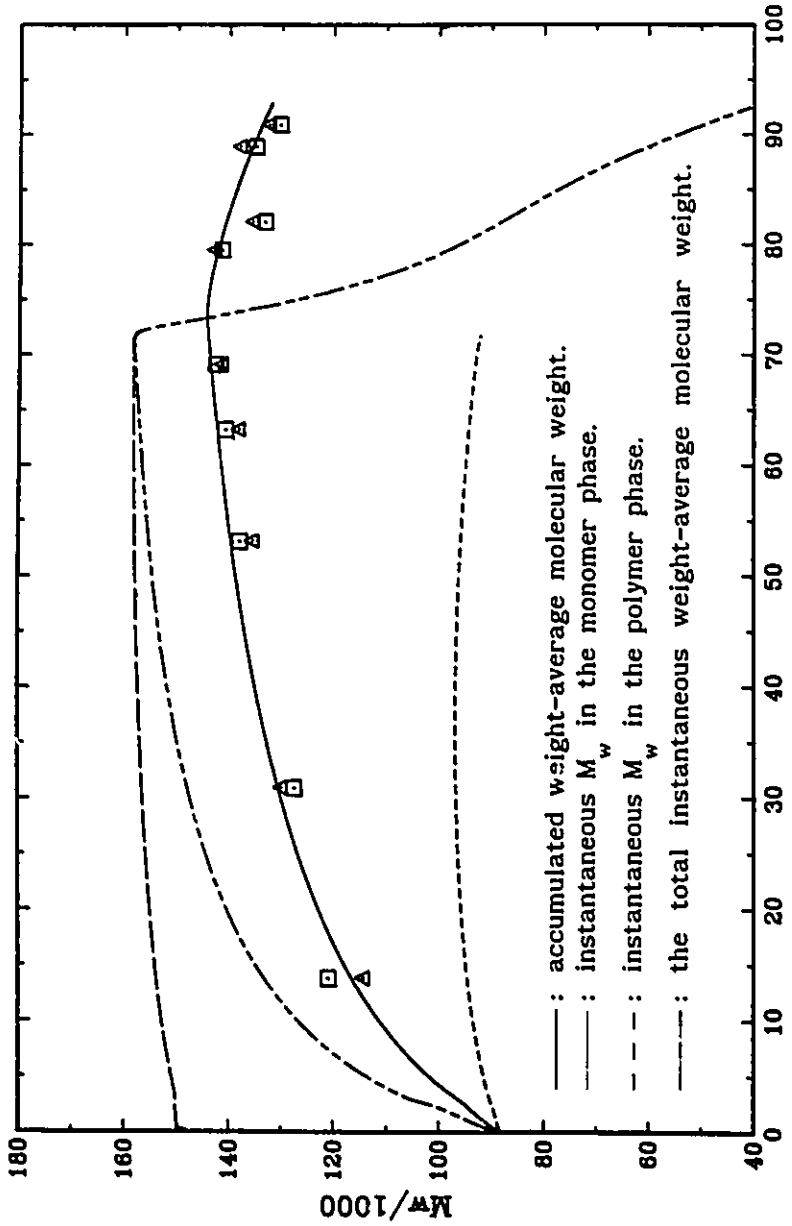

Figure 5.11. Conversion dependence of instantaneous and accumulated weight-average molecular weights at 50 °C. Perkadox 16-W40 as an initiator with [I]=0.15-wt%. Δ: measured by LALLS, □: measured by GPC.

weights are slightly lower than the total instantaneous number- and weight-average molecular weights for $X < X_f$. At higher conversions, the instantaneous number- and weight-average molecular weights decrease dramatically due to an increase in CM. However, the accumulated molecular weight averages decrease only slightly because of the small amount of polymer produced at this conversion level. These results are in agreement with Hamielec et al's[76] prediction considering effect of diffusion-controlled reactions on CM values and Hjertberg et al's[13] experimental results for VCM polymerization at reduced monomer levels (subsaturation pressure).

The effect of the initiator concentration on accumulated molecular weight averages is shown in Figure 5.12. One can see that the molecular weight decreases slightly with increasing initiator concentration. Again, this result confirms that chain transfer to monomer dominates molecular weight development. This is consistent with Abdel-Alim et al[5] and Danusso et al's[70] experimental results. The present model predictions are in excellent agreement with the experimental data.

Figure 5.13 shows the temperature dependence of $\overline{M}_n$, $\overline{M}_w$ and $\overline{M}_z$ at high conversions (~85%). The molecular weight is very sensitive to polymerization temperature as expected. This study provides for the first time experimental measurements and predictions of $\overline{M}_n$, $\overline{M}_w$, and $\overline{M}_z$ as a function of temperature and other reaction variables. The model predictions are in satisfactorily agreement with the experimental data over a wide range in temperature (see Figure 5.13).

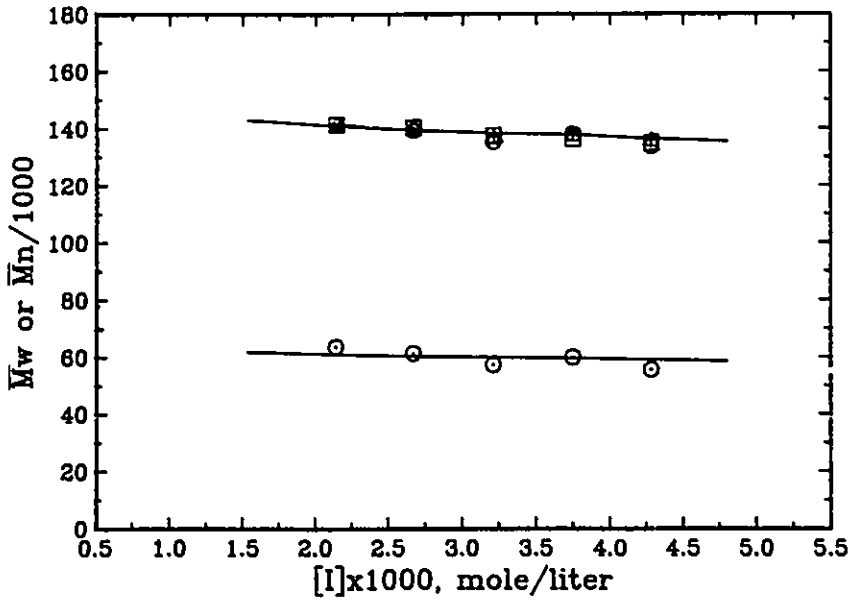

Figure 5.12. Effect of initiator concentration on accumulated number- and weight-average molecular weights at 50°C, Initiator: Perkadox 16-W40, conversion = 87%. Δ: $\overline{M}_w$ measured by LALLS, □: $\overline{M}_w$ measured by GPC, ⊙: $\overline{M}_n$ measured by GPC, ——— : model.

Given $\overline{M}_w$ and $\overline{M}_n$, one can calculate the polydispersity. Most often, the polydispersity of commercial PVC is between 2.0-2.5. Russo et al[4] noticed that the polydispersity of PVC increases with conversion at high conversions. However, this phenomenon has never been predicted quantitatively. Figure 5.14 shows a comparison between model prediction and experimental data at 50°C. One can see that the polydispersity increases with conversion and varies in the range, 1.75 to 2.5 over the entire conversion range at 50°C. The polydispersity increases slightly when $X < X_f$, which can be attributed to chain transfer to polymer in the polymer phase. Moreover, the molecular weight of PVC produced in the

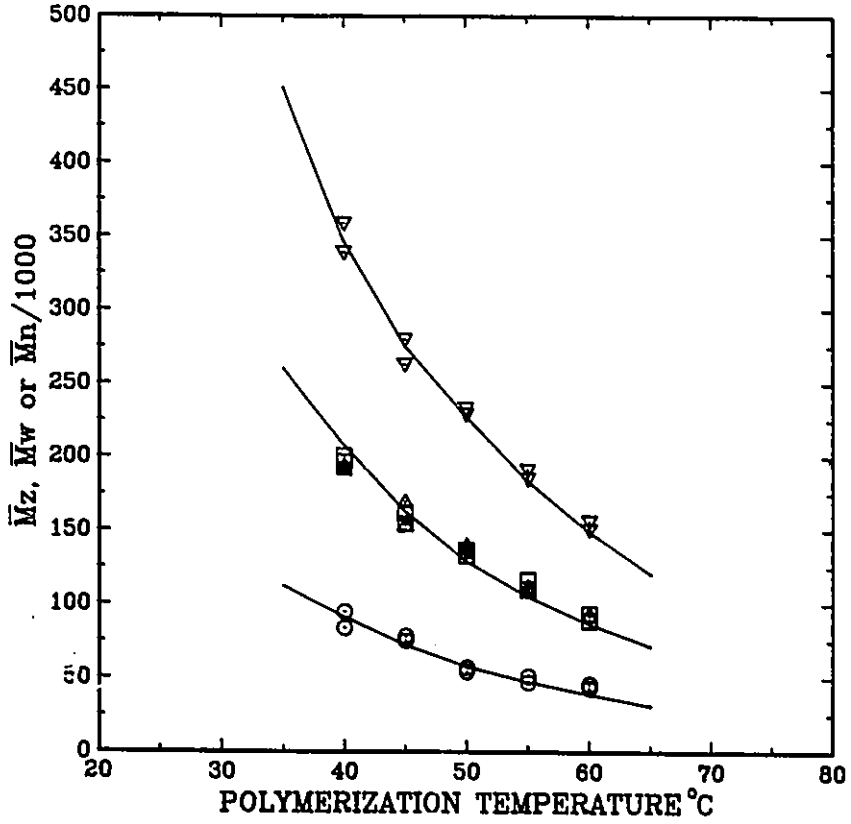

Figure 5.13. Temperature dependence of accumulated molecular weight averages, Perkadox 16-W40 as an initiator with [I]=0.175-wt%. ∇: $\bar{M}_z$ measured by GPC, Δ: $\bar{M}_w$ measured by LALLS, □: $\bar{M}_w$ measured by GPC, ⊙: $\bar{M}_n$ measured by GPC, ——— : model.

polymer phase is higher than that in the monomer phase due to the diffusion-controlled termination reaction in the polymer phase. The contribution of reactions in the polymer phase increases with conversion. This also leads to an increase in the accumulated polydispersity. At $X > X_f$, the polydispersity increases significantly, and this can be explained as

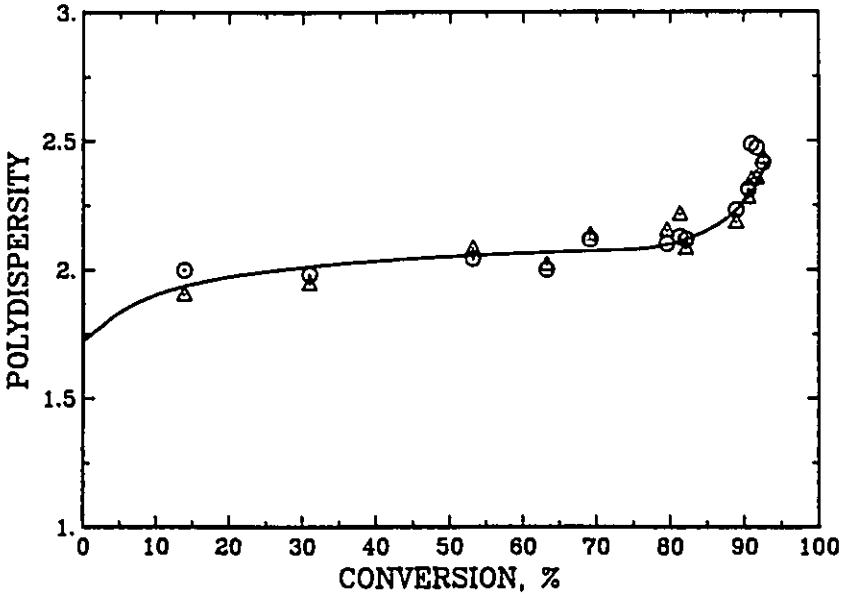

Figure 5.14. Conversion dependence of polydispersity of PVC synthesized at 50°C.
⊙: $\overline{M}_w$ measured by LALLS, Δ: $\overline{M}_w$ measured by GPC
———: model.

being caused by the chain transfer to monomer and polymer under diffusion controlled reaction conditions. The number-average molecular weight is independent of chain transfer to polymer but is very sensitive to the chain transfer to monomer and it decreases significantly with increasing CM. On the other hand, the effect of chain transfer to polymer on the weight-average molecular weight becomes more significant with increasing conversion even though the C_p is very low. Thus, the decrease in $\overline{M}_w$ with conversion is not as significant as for $\overline{M}_n$. Consequently, the polydispersity increases significantly at high conversions. The present model can satisfactorily describe this phenomenon.

With the parameters estimated above, one can solve Eqs.(5.27), (5.51), (5.52), (5.55) and (5.66) for instantaneous and accumulated molecular weight distributions of PVC at any conversion. However, it is not practical to solve Eq.(5.51) r times simultaneously at time t for the concentration of polymer with chain length r. The last two terms in Eq.(5.52) may be neglected because of the low values for C_p and C'_p. Thus, the solution of Eq.(5.51) is not required for calculation of MWD. Figures 5.15–5.18 show the MWD for conversion less than X_f at 40°, 50°, 60°and 70°C respectively. One can see that the present model predictions are in excellent agreement with the experimental data. All the distribution curves have a similar shape although the distribution shifts to lower molecular weight with increasing polymerization temperature. Figure 5.19 further illustrates the contribution of each phase to the accumulated MWD. The instantaneous molecular weight distribution in the monomer phase is narrower than that in the polymer phase. This can be attributed to no chain transfer to polymer and higher termination rate in the monomer phase. However the contribution of the monomer phase to the total MWD is very small because polymer is mainly produced in the polymer phase at conversions as high as 63.2%. In the model development, it is assumed that PVC is produced simultaneously in monomer and polymer phases. PVC production rate depends on the population of reaction species. Hence, the parameters estimated in the present study cannot precisely indicate the soluble chain length of PVC in the monomer phase. For example, it is possible for a polymer radical chain to partially precipitate, i.e. the radical center is still in the monomer phase while the tail of chain has been precipitated out. Such a radical center is

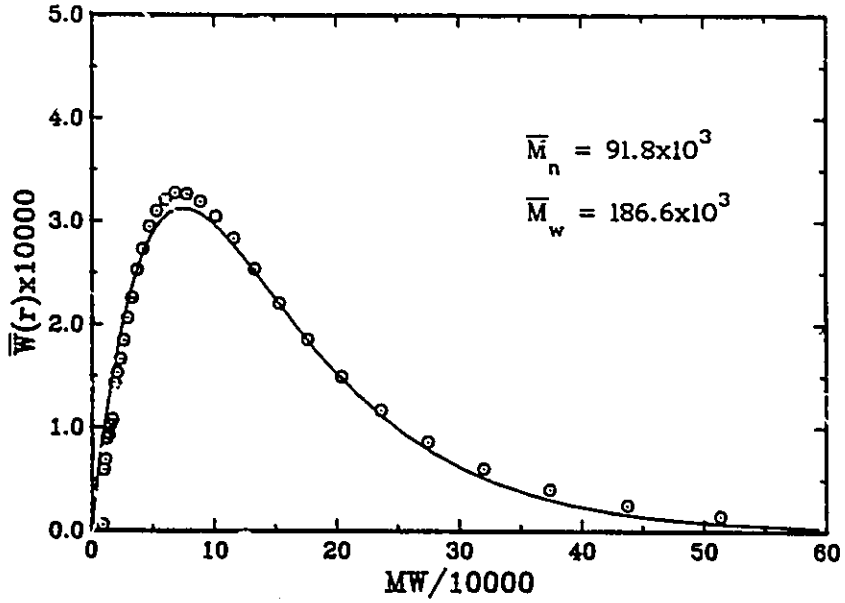

Figure 5.15, Accumulated molecular weight distribution at conversion 62.7% (MW=62.5r), temperature 40°C, Perkadox 16-W40 as an initiator with [I]=0.40-wt%, ⊙: experimental data, ———— : model.

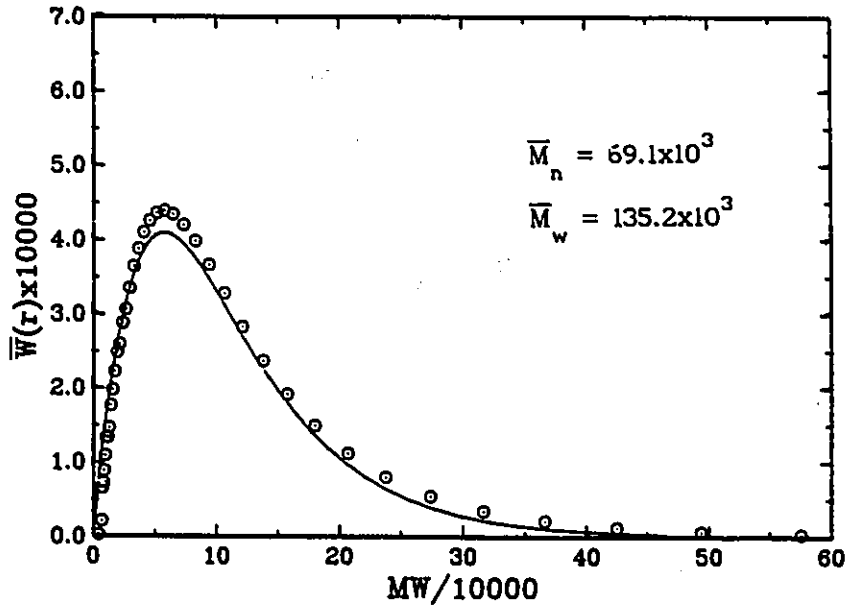

Figure 5.16. Accumulated molecular weight distribution at conversion 63.2% (MW=62.5r), temperature 50°C, Perkadox 16-W40 as an initiator with [I]=0.15-wt%, ⊙: experimental data, ———— : model.

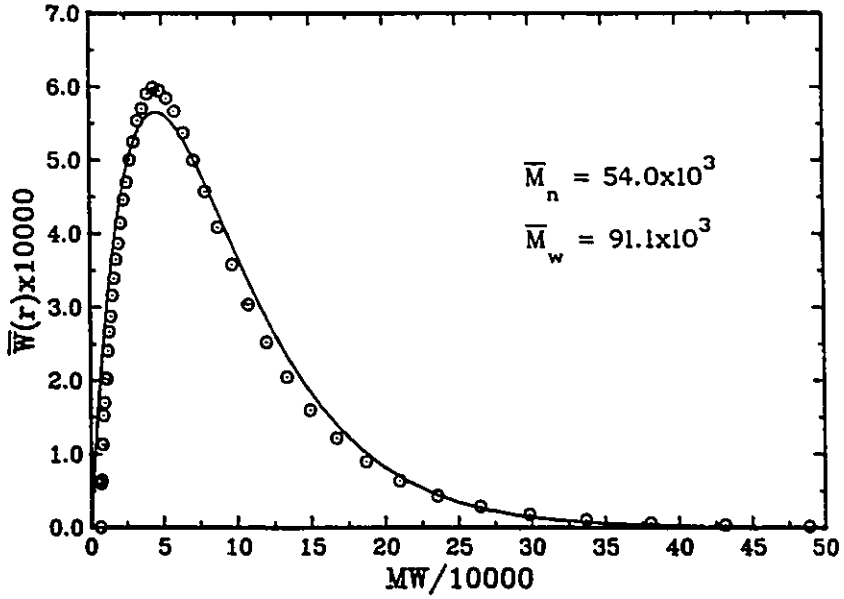

Figure 5.17. Accumulated molecular weight distribution at conversion 48.9% (MW=62.5r), temperature 60°C, Perkadox 16-W40 as an initiator with [I]=0.125-wt%, ⊙: experimental data, ———— : model.

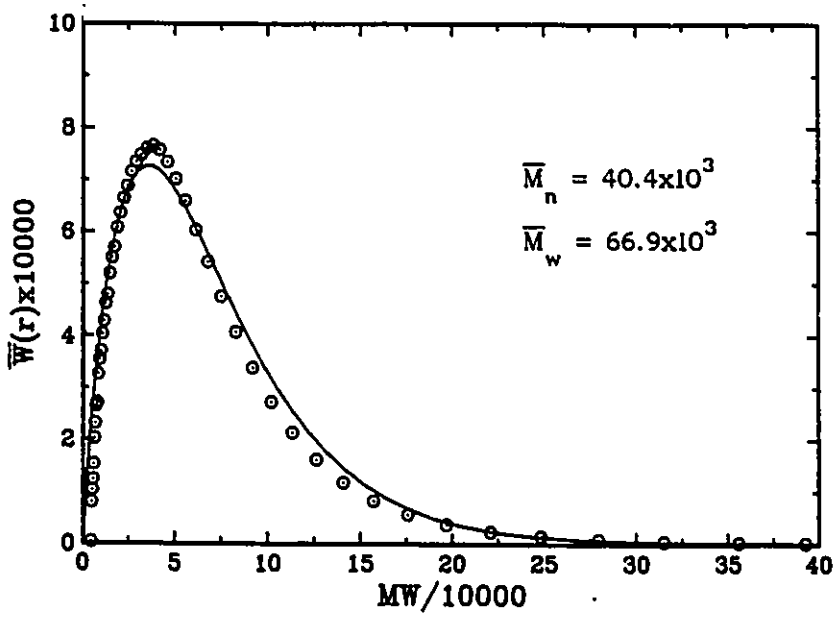

Figure 5.18. Accumulated molecular weight distribution at conversion 38.9% (MW=62.5r), temperature 70°C, AIBN as an initiator, [I]=0.15-wt%. ⊙: experimental data, ———— : model.

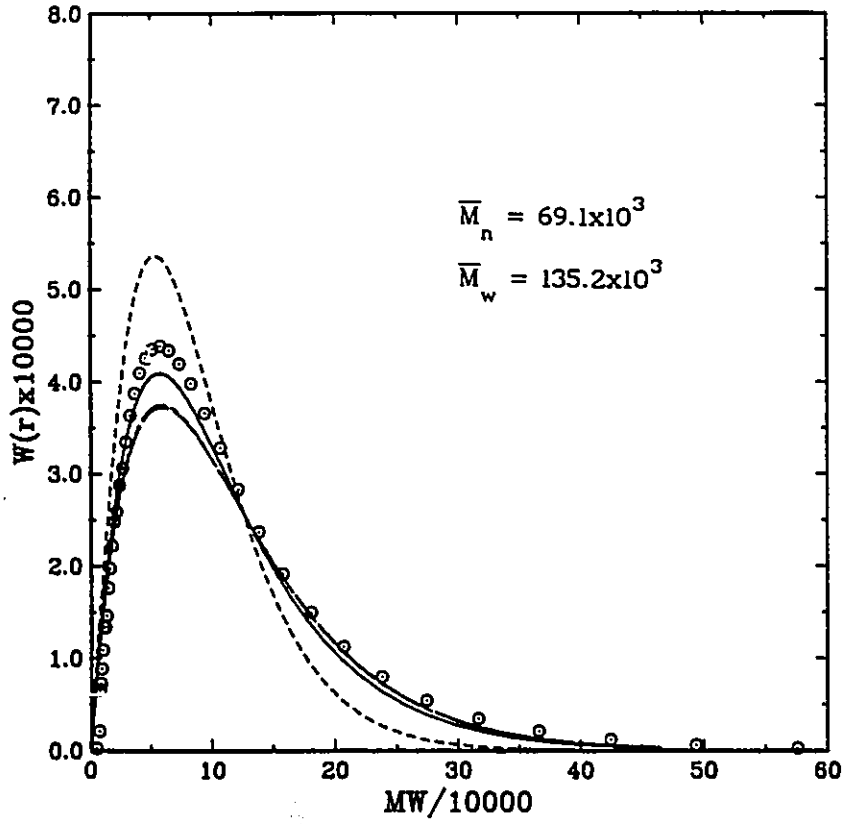

Figure 5.19. Instantaneous and accumulated molecular weight distributions at conversion 63.2% (MW=62.5r), temperature 50°C.
⊙: experimental data, ———— : accumulated MWD,
———— : instantaneous MWD in the monomer phase,
– – – – : instantaneous MWD in the polymer phase,
– – – – : the total instantaneous MWD.

still considered in the monomer phase. All the polymer produced in the monomer phase is assumed to precipitate exclusively. Therefore, the longer chain length produced in the monomer phase might be understood as extremely fast propagation rate, as a partial precipitation of the radicals and as PVC produced by combination termination (see Appendix B for detailed explanations). Because of the high contribution of the

polymer phase to production of PVC, in fact, the total instantaneous MWD is very close to the instantaneous MWD in the polymer phase.

However, the instantaneous MWD is quite different from the accumulated MWD for $X > X_f$ as shown in Figures 5.20-5.23. One can see that the instantaneous MWD shifts to lower molecular weights because of the increase in CM at high conversions. The amount of the polymer

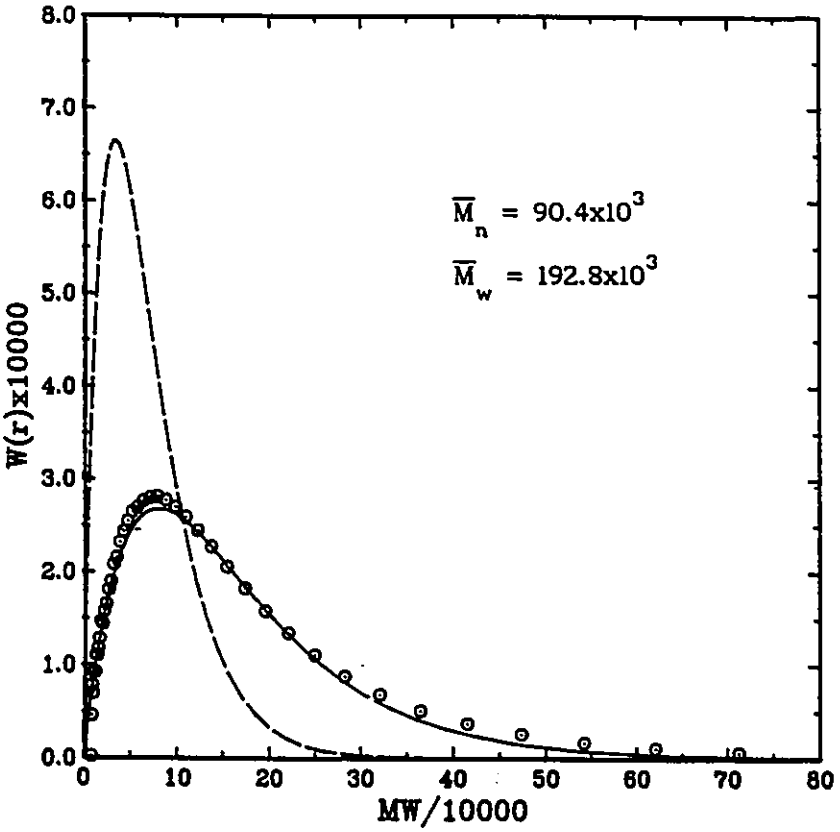

Figure 5.20. Instantaneous and accumulated molecular weight distributions at conversion 88.3% (MW=62.5r), temperature 40°C, Perkadox 16-W40 as an initiator with [I]=0.175-wt%.
⊙: experimental data, ———— : accumulated MWD,
– – – – : instantaneous MWD.

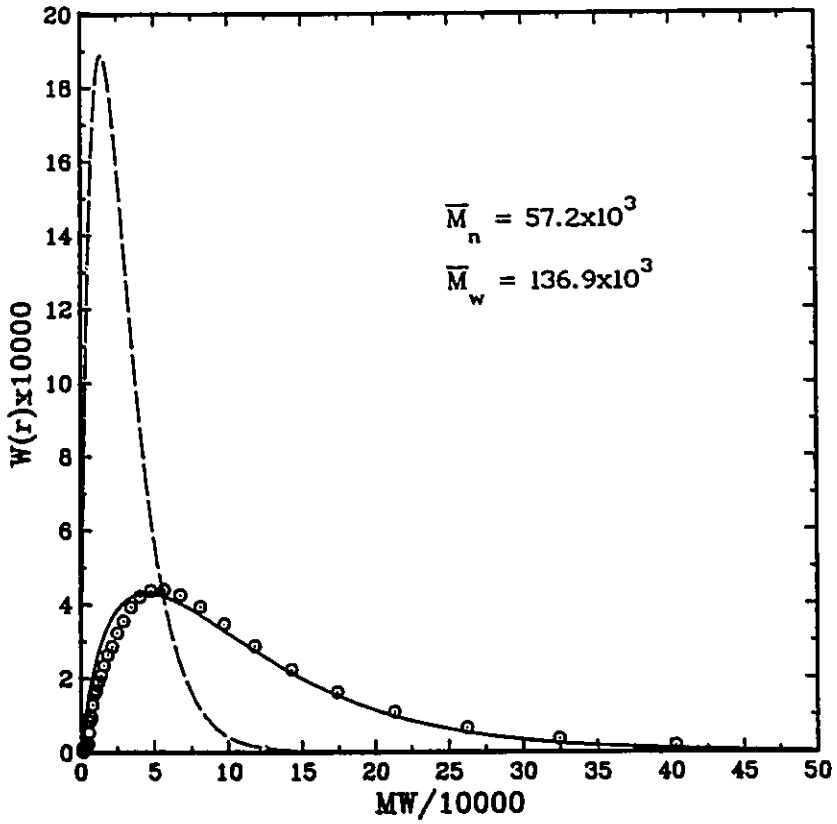

Figure 5.21. Instantaneous and accumulated molecular weight distributions at conversion 90.0% (MW=62.5r), temperature 50°C, Perkadox 16-W40 as an initiator with [I]= 0.15-wt%,
⊙: experimental data,
————: accumulated MWD,
– – – – –: instantaneous MWD.

produced at this stage is relatively small. However, this low molecular weight PVC may affect the quality of the final PVC product significantly. For example, the thermal stability of the low molecular weight polymer may be much lower. This subject will, however, be discussed in Chapter 7.

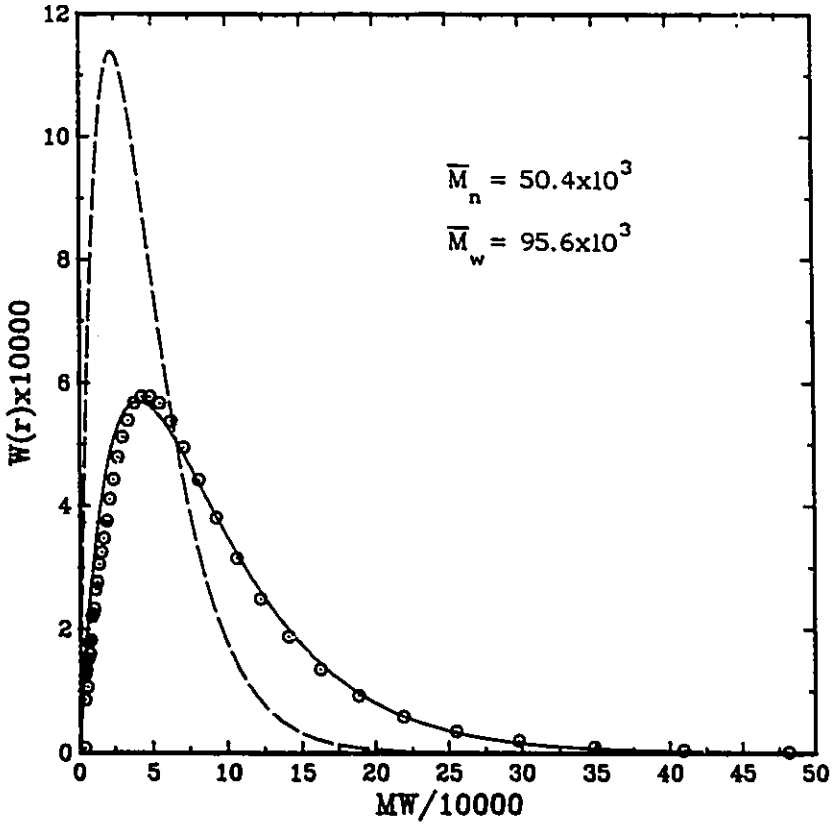

Figure 5.22. Instantaneous and accumulated molecular weight distributions at conversion 76.9% (MW=62.5r), temperature 60°C, Perkadox 16-W40 as an initiator with [I]=0.125-wt%,
⊙: experimental data,
————: accumulated MWD,
– – – – –: instantaneous MWD.

Little work has been done on MWD of PVC in the literature.[5,40] This study is the first to describe the MWD of PVC both theoretically and experimentally using a valid mechanism for chain transfer to monomer.

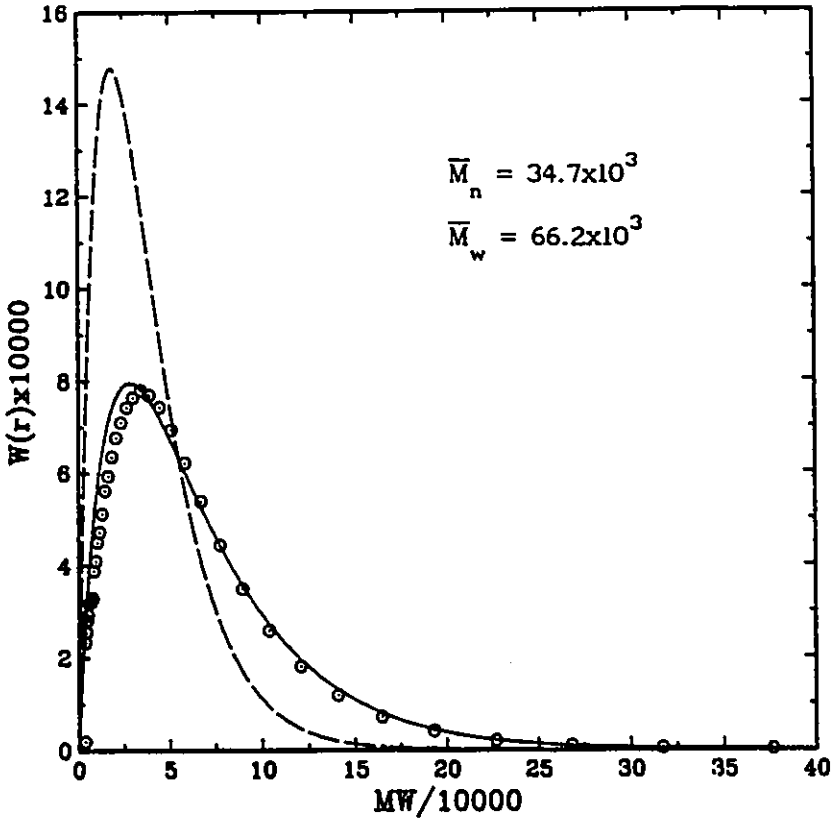

Figure 5.23. Instantaneous and Accumulated molecular weight distributions at conversion 80.5% (MW=62.5r), temperature 70 °C, AIBN as an initiator with [I]=0.15-wt%,
⊙: experimental data, ———— : accumulated MWD,
– – – – : instantaneous MWD.

From Figures 5.10-5.23, one can see that the parameters estimated above are reasonable. The present model can satisfactorily predict the molecular weight development of VCM polymerization over the entire conversion range.

5.5 SUMMARY

A comprehensive model for molecular weight development during VCM polymerization has been developed. The model was evaluated using a rather complete set of molecular weight averages and distribution measurements by LALLS and GPC.

The present model is in excellent agreement with experimental rate and molecular weight data over the conversion range of commercial interest for temperatures, 40-70°C. The model can satisfactorily describe the kinetic features of VCM polymerization quantitatively, which include molecular weight averages and distribution as a function of conversion, initiator concentration, polymerization temperature, and can account for the contribution of each phase to the molecular weight of the final polymer at the end of the reactor batch.

Chain transfer to monomer (which involves several elementary reactions) dominates molecular weight development. CM values differ for the two phases and increase significantly for conversions above X_f.

All the parameters estimated based on the present experimental data are given as a function of temperature and can be used for PVC reactor simulations.

5.6 REFERENCES

1. Bengough, W. I. and Norrish, R. D. W., F. R. S. Proc. Royal Soc. (London) A, 1950, 200, 301.

2. Pezzin, G., Talamini, G. and Vidotto, G. Makromol. Chem., 1961, 43, 12.

3. Vidotto, G., Crosato-Arnaldi, A. and Talamini, G. Makromol. Chem., 1968, 114, 217.

4. Russo, S. and Stannett, V. Makromol. Chem., 1971, 143, 57.

5. Abdel-Alim, A. H. and Hamielec, A. E. J. Appl. Polym. Sci., 1972, 16, 783.

6. Cebollada, A. F., Schmidt, M. J., Farber, J. N., Capiati, N. J. and Valles, E. M. J. Appl. Polym. Sci., 1989, 37, 145.

7. Pan, Z., Zhai, X., Weng, Z. and Huang, Z. 'Polymer Reaction Engineering', Ed. Reichert, K. H. and Geiseler, W., VCH Verlagsgesellschaft mbH, 1989, 302.

8. Talamini, G. and Vidotto, G. Makromol. Chem., 1961, 50, 129.

9. Talamini, G. and Vidotto, G. Makromol. Chem., 1962, 53, 21.

10. Sörvik, E. M. Polym. Lett. Ed., 1976, 14, 735.

11. Sörvik, E. M. and Hjertberg, T. J. Macromol. Sci.-Chem., A, 1977, 11, 1349.

12. Hjertberg, T. and Sörvik, E. M. J. Polym. Sci., Polym. Chem. Ed., 1978, 16, 645.

13. Hjertberg, T. and Sörvik, E. M. J. Polym. Sci., part A, Polym. Chem., 1986, 24, 1313.

14. Liegeois, J. M. J. Macromol. Sci.-Chem., 1977, A11, 1379.

15. Kelsall, D. G. and Maitland, G. C. 'Polymer Reaction Engineering', Ed. Reichert, K. H. and Geiseler, W., Hanser Publishers, Munich-Vienna, New York, 1983, 131.

16. Hjertberg, T. and Sörvik, E. M. 'Degradation and Stabisation of PVC', Ed. Owen, E. D., Elservier Appl. Sci. Publishers, London and New York, 1984, 21.

17. Hjertberg, T. and Sörvik, Polymer, 1983, 24, 673.

18. Laker, D. J. Polym. Sci., 1957, 25, 122.

19. Hengstenberg, J., Schuch, E. and Stuart, H. A. Makromol. Chem., 1964, 74, 55.

20. Freeman, M. and Manning, P. P. J. Polym. Sci., A, 1964, 2, 2017.

21. McKinney, P. V. J. Appl. Polym. Sci., 1965, 9, 583.

22. Vavra, J., Lapcik, J. and Sabados, J. J. Polym. Sci., A2, 1967, 5, 1305.

23. Pezzin, G. and Gligo, N. J. Appl. Polym. Sci., 1966, 10, 1.

24. Pezzin, G., Sanmartin, G. and Zilio-Grandi, F. J. Appl. Polym. Sci., 1967, 11, 1539.

25. Kolinsky, M., Ryska, M., Bohdanecky, M., Kratochvil, P., Solc, K. and Lim, D. J. Polym. Sci., part C, 1967, 16, 485.

26. Bohdanecky, M., Solc, K., Kratochvil, P., Kolnsky, M., Ryska, M. and Lim, D. J. Polym. Sci. part A-2, 1967, 5, 343.

27. Kratochvil, P., Bohdanecky, M., Solc, K., Kolinsky, M., Ryska, M. and Lim, D. J. Polym. Sci. part C, 1968, 23, 9.

28. Kratochvil, P., Petrus, V., Munk, P., Bhdanecky, M., Solc, K. J. Polym. Sci. part C, 1967, 16, 1257.

29. Kolinsky, M. and Janca, J. J. Polym. Sci. Polym. Chem. Ed., 1974, 12, 1181.

30. Crugnola, A. and Danusso, F. Polym. Lett., 1968, 6, 535.

31. Goedhart, D. and Opschoor, A. J. Polym. Sci., part A-2, 1970, 8, 1227.

32. Vries, A. J. De., Bonnebat, C. and Carrega, M. Pure Appl. Chem., 1971, 26, 209.

33. Bengough, W. I. and Grant, G. F. Eur. Polym. J., 1971, 7, 203.

34. Chan, R. K. S. Polym. Eng. Sci., 1971, 11, 152.

35. Rudin, A. and Benschop-Hendrychovra, I. J. Appl. Polym. Sci., 1971, 15, 2881.

36. Vidotto, G., Zannetti, R. and Cavalli, L. Makromol. Chem., 1971, 146, 159.

37. Baijal, M. D. and Kauppila, K. M. Polym. Eng. & Sci., 1971, 11, 182.

38. Abdel-Alim, A. H. and Hamielec, A. E. J. Appl. Polym. Sci., 1972, 16, 1093.

39. Abdel-Alim, A. H. and Hamielec, A. E. J. Appl. Polym. Sci., 1973, 17, 3033.

40. Lyngaae-Jorgensen, J. J. Polym. Sci. part C, 1971, 33, 39.

41. Lyngaae-Jorgensen, J. J. Chromatographic Sci., 1971, 9, 331.

42. Lyngaae-Jorgensen, J. H. Makromol. Chem., 1973, 167, 311.

43. Maron, S. H. and Lee, M. J. Macromol. Sci.-Phys., B, 1973, 7, 29.

44. Maron, S. H. and Lee, M. J. Macromol. Sci.-Phys., B, 1973, 7, 47.

45. Maron, S. H. and Lee, M. J. Macromol. Sci.-Phys., B, 1973, 7, 61.

46. Daniels, C. A. and Collins, E. A. J. Macromol. Sci.-Phys., B, 1974, 10, 287.

47. Andersson, K. B. and Sörvik, E. M. J. Polym. Sci., part C, 1971, 33, 247.

48. Andersson, K. B., Holmstrom, A. and Sorvik, E. M. Makromol. Chem., 1973, 166, 247.

49. Sörvik, E. M. J. Appl. Polym. Sci., 1977, 21, 2769.

50. Atkinson, C. M. L. and Dietz, R. Polymer, 1977, 18, 408.

51. Atkinson, C. M. L., Dietz, R. and Green, J. H. S. J. Macromol. Sci.-Phys., B, 1977, 14, 101.

52. Ahmad, N., Ali, S. and Nisar, N. M. J. Macromol. Sci.-Chem., 1986, A23, 329.

53. Grubisic, Z., Rempp, P. and Benoit, H. J. Polym. Sci., B, 1967, 5, 753.

54. Huglin, M. B. 'Light Scattering From Polymer Solutions', Ed. Huglin, M.B., Academic Press, London and New York, 1972, 280.

55. Margerison, D., Bain, D. R. and Kiely, B. Polymer, 1973, 14, 133.

56. Janca, J. Adv. Chromatogr., 1981, 19, 37.

57. Dawkins, J. V. Chromatographic Sci. Ser.25, 'Steric Exclusion Liquid Chromatography of Polymers', Ed. Janca, J., Marcel Dekker Inc. New York and Basel, 1984, 53.

58. Mori, S. Anal. Chem., 1981, 53, 1813.

59. Chiantore, O. and Hamielec, A. E. J. Liq. Chromatogr., 1984, 7, 1753.

60. Schroder, U. K. O. and Ebert, K. H. Makromol. Chem., 1987, 188, 1415.

61. American Polymer Standards Corporation, 'Catalog of Polymer Standards for Research and Development', 1987.

62. Razuvayev, G. A., Petukhov, G. G. and Dodnov, V. A. Polym. Sci. U. S. S. R., 1963, 3, 1020.

63. Park, G. S. and Smith, D. G. Makromol. Chem., 1970, 131, 1.

64. Starnes Jr., W. H., Plitz, I. H., Schilling, F. C., Park, G. S. and Saremi, A. H., Macromolecules, 1984, 17, 2507.

65. Starnes Jr., W. H. Pure Appl. Chem., 1985, 57, 1001.

66. Mickley, H. S., Michaels, A. S. and Moore, A. L. J. Polym. Sci., 1962, 60, 121.

67. Ryska, M., Kolinsky, M. and Lim, D. J. Polym. Sci., part C, 1967, 16, 621.

68. Uno, T., Yoshida, K. Kobunshi Kagaku, 1958, 15, 819.

69. Breitenbach, J. W. Makromol. Chem., 1952, 8, 147.

70. Danusso, F. and Sianesi, D. Chim. Ind. (Milan), 1955, 37, 695.

71. Danusso, F., Pajar, G. and Sianesi, D. Chim. Ind. (Milan), 1959, 41, 1170.

72. Burnett, G. M. and Wright, W. W. Proc. Roy. Soc. (London), Ser. A, 1954, 221, 41.

73. Crosato-Arnaldi, A., Talamini, G. and Vidotto, G. Makromol. Chem., 1968, 111, 123.

74. Hlousek, M. and Lanikova, J. J. Polym. Sci., part C, 1967, 16, 935.

75. Lim, D. and Kolinsky, M. J. Polym. Sci., 1961, 53, 173.

76. Hamielec, A. E., Gomez-Valillard, R. and Marten, F. L. J. Macromol. Sci.-Chem., 1982, A17, 1005.

CHAPTER 6

SEMI-BATCH REACTOR MODELLING

6.1 INTRODUCTION

In Chapters 4 and 5, the kinetic behaviour of vinyl chloride polymerization in a batch reactor was described quantitatively over the entire conversion range. During the two-phase polymerization period, the kinetic properties of the system are essentially constant because the composition of each phase is almost unchanged with conversion for $X < X_f$, at which point the liquid monomer phase is consumed and the reactor pressure begins to fall. The total reaction rate and the accumulated molecular weight averages and distribution change with conversion during this period because the relative contribution of each phase changes with conversion. At high conversions ($X > X_f$), the kinetic behaviour of VCM polymerization changes with conversion dramatically. This includes changes in reactor pressure, monomer concentration, polymerization rate, instantaneous and accumulated molecular weight averages. Kinetic parameters, such as the termination and propagation rate constants, the initiator efficiency and the decomposition rate constant fall while the radical concentration, the CM values and the polydispersity increase with conversion. Consequently, properties of PVC, such as the thermal stability, deteriorate with increasing conversion. All the kinetic features which change at high conversions can be attributed to the decrease in

monomer concentration. Therefore, these changes should be minimized if a constant monomer concentration were maintained at high conversions. Constant monomer concentration can be maintained by a semi-batch operation at high conversions, which is done by feeding fresh liquid monomer to the reactor at a certain rate.

A semi-batch process is applied commercially in emulsion polymerization of VCM[1], but has not been used commercially in bulk and suspension polymerizations. However, semi-batch or equivalent processes have been carried out, experimentally, in bulk[2,3] suspension[4-6] and emulsion[7-11] polymerizations under subsaturation pressure in order to study the kinetics, the PVC microstructure and the thermal stability of PVC produced at low monomer concentrations. In the literature[2-11] the presynthetic PVC powder or latex were often used as seed and monomer was fed as vapour by controlling the temperature of the monomer reservoir. Hence, the properties of the PVC product were relative to the seed used, i.e. the conversion history of the PVC seed affects the properties of the final product. In the present investigation, suspension polymerization was carried out in a batch process up to a certain conversion level, then the process was switched to semi-batch with liquid VCM fed to the reactor. A comprehensive model for such a system has not been published to date. Therefore, the objectives of the present work were to develop a comprehensive semi-batch reactor model which can be used with different pressure levels and to study the reactor dynamics of a semi-batch process and the PVC properties made under different pressure levels.

6.2 MODEL DEVELOPMENT

In general, semi-batch operation for VCM polymerization at high conversions involves feeding fresh monomer to the reactor over time to maintain a desired monomer concentration/time profile. Therefore, it is essential to know the feed rate of monomer required for the desired semi-batch operation.

A possible constraint condition for the semi-batch polymerization is that the concentration of monomer in the polymer phase is maintained constant, that is

$$\frac{d[M]_p}{dt} = 0 \tag{6.1}$$

However, both the number of moles of monomer and the volume of the polymer phase for a semi-batch process are a function of reaction time, hence, Eq.(6.1) becomes:

$$\frac{dN_{mp}}{dt} = [M]_p \frac{dV_p}{dt} \tag{6.2}$$

Equation (6.2) shows the relationship between the number of moles of monomer and the volume of the polymer phase as a function of polymerization time.

The monomer charging rate to the reactor is governed by the mass balance in the polymer phase as follows:

$$\frac{dN_{mp}}{dt} = - R_p V_p + F_{in} - \frac{dN_{mv}}{dt} \qquad (6.3)$$

where dN_{mv}/dt is the rate of change of moles of monomer in the vapour phase. This change is due to the net change of the volume in the vapour phase as a result of the monomer feed and the reaction volume shrinkage in the polymer phase. If the volume of monomer fed is greater than that of the reaction volume shrinkage, dN_{mv}/dt is negative.

The volume change in the polymer phase can be expressed as:

$$\frac{dV_p}{dt} = \frac{M_m}{D_m} \left(F_{in} + \frac{D_m R_p V_p}{D_p} - R_p V_p - \frac{dN_{mv}}{dt}\right) \qquad (6.4)$$

The volume of the vapour phase also varies with time due to the semi-batch feeding of monomer and due to shrinkage of reaction volume as the monomer is converted to polymer. Hence, the rate of volume change in the vapour phase can be expressed as:

$$\frac{dV_g}{dt} = R_p V_p M_m \left(\frac{1}{D_m} - \frac{1}{D_p}\right) + \frac{M_m}{D_m} \left(\frac{dN_{mv}}{dt} - F_{in}\right) \qquad (6.5)$$

The relationship between the monomer mole number and the volume change in the vapour phase can be expressed as:

$$\frac{dN_{mv}}{dt} = \frac{P_m}{RT} \left(\frac{dV_g}{dt}\right) \qquad (6.6)$$

when the ideal gas law is assumed to be valid.

Substituting Eq.(6.5) into Eq.(6.6), one obtains:

$$\frac{dN_{mv}}{dt} = \frac{D_g R_p V_p (1/D_m - 1/D_p) - D_g F_{in}/D_m}{1.0 - D_g/D_m} \qquad (6.7)$$

where $D_g = P_m M_m / RT$.

Eqs.(6.2)-(6.4) and (6.7) allow one to solve for the semi-batch monomer feed rate as:

$$F_{in} = \frac{R_p V_p [(1/D_m - 1/D_p)([M]_p M_m - D_g) + D_g/D_m - 1.0]}{[M]_p M_m / D_m - 1.0} \qquad (6.8)$$

Eq.(6.8) is a general equation for monomer feed rate for the semi-batch process at high conversions. In other words, Eq.(6.8) is valid for the conversion range $X \geq X_f$. However, R_p, V_p and $[M]_p$ are different for the semi-batch process operated at different pressure levels. These can be classified into two cases.

Case 1: The batch process proceeds up to conversion X_f, where the reactor pressure is still at VCM saturation vapour pressure and then the process is switched to semi-batch operation to keep the concentration of monomer in the polymer phase the same as that at conversion X_f. Therefore, D_g, V_p, $[M]_p$ and R_p in Eq.(6.8) can be expressed as follows:

$$D_g = D_{go} = \frac{P_{mo} M_m}{RT} \tag{6.9}$$

The concentration of monomer in this case is the same as that at conversion X_f, that is

$$[M]_p = [M]_{pxf} = \frac{M_o(1-X_f) - M_{gxf} - M_{wxf}}{M_m\left[M_o\left(\frac{X_f}{D_p} - \frac{1-X_f}{D_m}\right) - \left(\frac{M_{gxf}+M_{wxf}}{D_m}\right)\right]} \tag{6.10}$$

where

$$M_{gxf} = D_{go}\left[(1.0-W_l)V_r + \frac{X_f M_o (1/D_m - 1/D_p) D_m}{D_m - D_{go}}\right]$$

$$M_{wxf} = KW_w$$

Although the total volume of the polymer phase varies with conversion, the ratio of monomer to polymer in the polymer phase is constant at any conversion level as long as the vapour pressure of VCM is maintained and is the same as that at conversion X_f. This means

$$A = \frac{M_o(1-X_f) - M_{gxf} - M_{wxf}}{M_o X_f} = \text{constant} \tag{6.11}$$

hence,

$$V_p = M_o X\left[\frac{1}{D_p} + \frac{M_o(1-X_f) - M_{gxf} - M_{wxf}}{D_m M_o X_f}\right] \tag{6.12}$$

where conversion X is defined based on the initial monomer charged.

The polymerization rate under semi-batch condition (at VCM saturation vapour pressure) can be written as:

$$R_p = K_{p2}[M]_p\left\{\frac{2fK_dI_{xf}\exp[-K_d(t-t_{xf})]}{V_pK_{t2}}\right\}^{1/2} \qquad (6.13)$$

where I_{xf}, K_{p2}, K_{t2}, f and K_d are the same as those at conversion X_f. In other words, the kinetic parameters under semi-batch conditions are not a function of conversion. Eq.(6.13) can be rewritten in term of the monomer conversion per unit time as:

$$\frac{dX}{dt} = \frac{M_mK_{p2}}{M_o}[M]_p\left(\frac{2fK_dI_{xf}}{K_{tp}}\right)^{1/2}V_p^{1/2}\exp[-K_d(t-t_{xf})/2] \qquad (6.14)$$

Substituting Eq.(6.12) into Eq.(6.14), one obtains:

$$\frac{dX}{dt} = \Gamma_1X^{1/2}\exp[-K_d(t-t_{xf})/2] \qquad (6.15)$$

where

$$\Gamma_1=K_{p2}[M]_pM_m\left\{\frac{2fK_dI_{xf}}{M_oK_{t2}}\left[\frac{1}{D_p}+\frac{M_o(1-X_f)-M_{gxf}-M_{wxf}}{D_mM_oX_f}\right]\right\}^{1/2}$$

a constant during semi-batch polymerization. Therefore, Eq.(6.15) can be integrated from interval X_f to X corresponding to t_{xf} to t and becomes:

$$X = \left\{ \frac{\Gamma_1}{K_d}[1.0-\exp(-K_d(t-t_{xf})/2)]+X_f^{1/2} \right\}^2 \qquad (t \geq t_{xf}) \qquad (6.16)$$

Eq.(6.16) is the conversion history for the semi-batch process operating at vapour pressure of VCM.

Substituting Eqs.(6.12), (6.13) and (6.16) into Eq.(6.8), one can rewrite the monomer feed rate as:

$$F_{in} = \frac{dN_F}{dt} = \gamma_1 X^{1/2} \exp[-K_d(t-t_{xf})/2] \qquad (6.17)$$

where

$$\gamma_1 = \frac{\Gamma_1 M_o}{M_m} \left[\frac{(1/D_m - 1/D_p)([M]_p M_m - D_{go}) + D_{go}/D_m - 1.0}{[M]_p M_m / D_m - 1.0} \right]$$

where Γ_1 is shown in Eq.(6.15). Hence, the accumulated moles of monomer fed to the reactor can be found by integrating Eq.(6.17) from t_{xf} to t, that is

$$N_F = \gamma_1 \left[\frac{\Gamma_1}{K_d} + 2X_f^{1/2} \right] \{1-\exp[-K_d(t-t_{xf})/2]\}/K_d \qquad (6.18)$$

Eqs.(6.8), (6.14), (6.16) and (6.18) allow one to solve for the monomer feed and polymerization rates, the conversion history and the accumulated monomer consumption as a function of time in a semi-batch process operating at a pressure equal to the vapour pressure of VCM.

Case 2, The batch process proceeds to a conversion X_p ($X_p > X_f$), at which time the reactor pressure is lower than the saturation pressure of monomer, the process is then switched to semi-batch VCM feed to maintain the monomer concentration constant at that pressure. $[M]_p$, V_p, R_p, X and N_F, analogous to case 1, can be expressed as:

$$[M]_p = \frac{M_o(1-X_p) - M_{gxp} - M_{wxp}}{M_m\left\{M_o\left[\frac{X_p}{D_p} + \frac{1-X_p}{D_m}\right] - \frac{M_{gxp}+M_{wxp}}{D_m}\right\}} \tag{6.19}$$

$$V_p = M_o X\left[\frac{1}{D_p} + \frac{M_o(1-X_p) - M_{gxp} - M_{wxp}}{D_m M_o X_p}\right] \tag{6.20}$$

where

$$M_{gxp} = D_g\left\{(1-W_l)V_r + M_o(1/D_m - 1/D_p)\left[X_p + X_f\frac{D_{go}}{D_m - D_{go}}\right]\right\}$$

$$M_{wxp} = KM_w P_m / P_{mo}$$

$$R_p = K_{p2}[M]_p\left(\frac{2fK_d I_{xp}}{V_p K_{t2}}\right)^{1/2}\exp[-K_d(t-t_{xp})/2] \tag{6.21}$$

where K_{p2}, K_{t2}, f and K_d are calculated at the partial pressure of VCM, P_m, based on the equations described in Chapter 4.

$$X = \left\{\frac{\Gamma_2}{K_d}[1-\exp(-K_d(t-t_{xp})/2)] + X_p^{1/2}\right\}^2 \tag{6.22}$$

where

$$\Gamma_2 = K_{p2}[M]_p M_m \left\{ \frac{2fK_d I_{xp}}{M_o K_{t2}} \left[\frac{1}{D_p} + \frac{M_o(1-X_p) - M_{gxp} - M_{wxp}}{D_m M_o X_p} \right] \right\}^{1/2}$$

$$N_F = \gamma_2 \left[\frac{\Gamma_2}{K_d} + 2X_p^{1/2} \right] \{1-\exp[-K_d(t-t_{xp})/2]\}/K_d \qquad (6.23)$$

where

$$\gamma_2 = \frac{\Gamma_2 M_o}{M_m} \left[\frac{(1/D_m - 1/D_p)([M]_p M_m - D_g) + D_g/D_m - 1.0}{[M]_p M_m / D_m - 1.0} \right]$$

Equations (6.8), (6.21)-(6.23) allow one to solve for the monomer feed and the polymerization rates, the conversion history and the accumulated monomer consumption during semi-batch operation with subsaturation pressure P_m.

Using the same strategy shown above, one can derive an equation for the initiator feed rate for a semi-batch process. For example, if the semi-batch process operated at saturated vapour pressure of VCM, the initiator feed rate is given by

$$F_I = [I]_p V_p R_p \left\{ K_d + M_o \left[\frac{1}{D_p} + \frac{M_o(1-X_f) - M_{gxf} - M_{wxf}}{D_m M_o X_f} \right] \right\} M_m / M_o \qquad (6.24)$$

where

$$R_p = K_{p2}[M]_p \left[\frac{2fK_d[I]_p}{K_{t2}} \right]^{1/2}$$

$$[I]_p = [I]_{pxf} = \frac{I_o \exp(-K_d t_{xf})}{M_o\left(\frac{X_f}{D_p} + \frac{1-X_f}{D_m}\right) - \frac{M_{gxf}+M_{wxf}}{D_m}}$$

It should be mentioned that the polymerization and monomer feed rates have to be modified corresponding to the initiator concentration.

The molecular weight development of PVC for the semi-batch process can be obtained by appropriately modifying the batch reactor model which has been shown in Chapter 5.

6.3 EXPERIMENTAL

To evaluate the present model, a series of experiments for suspension polymerization of VCM using batch and semi-batch operation was carried out.

The equipment used for the experiments, reactor operational procedures and the basic polymerization recipe and conditions have been given in Chapter 4. Perkadox 16-W40 with 0.175-wt% (based on initial monomer charged) was used as an initiator. When the polymerization in the batch process proceeds up to the pressure drop or beyond to a certain pressure level, fresh monomer from a calibrated monomer cell was fed into the reactor by means of nitrogen pressure. The monomer flow rate was controlled by a manually operated valve. The accumulated amount of monomer fed to the reactor was weighed on-line. Conversion was measured by the on-line tracer method described in detail in Chapter 3.

The accumulated molecular weight averages and distribution were measured using a low-angle laser light scatting photometer and gel permeation chromatograph as described in Chapter 5. The rate of dehydrochlorination was measured by the conductimetric method. The details for the latter are given in Chapter 7.

6.4 RESULTS AND DISCUSSION

The present model can be solved either numerically or analytically. However, both methods require initial conditions for the semi-batch operation. According to the polymerization course described above, the initial conditions for the semi-batch process are the terminal conditions for the batch process. Therefore, a solution of the semi-batch model equations follows the solution of the batch reactor model equations in Chapters 4 and 5 with kinetic parameters and monomer concentration appropriately adjusted based on the semi-batch operation conditions.

6.4.1 Monomer Feed Rate

Figures 6.1 and 6.2 show accumulated moles of fresh monomer fed to the reactor. One can see that the model predictions are in good agreement with the experimental data. The accumulated moles of monomer increases with time almost linearly (not a linear function). This is not surprising because the kinetic parameters and the monomer concentration are constant; only the initiator concentration decreases with time due

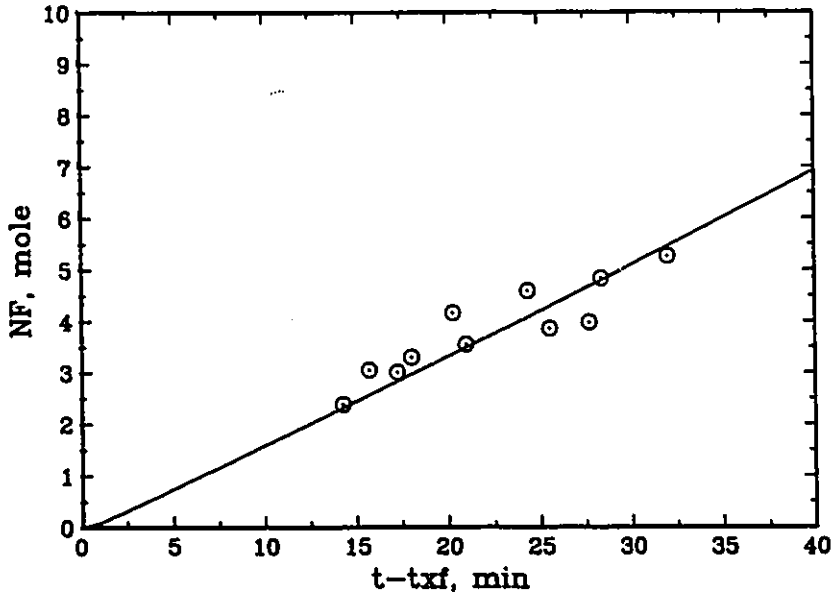

Figure 6.1. Monomer consumption for semi-batch polymerization with vapour pressure at 50 °C.
⊙: experimental data, —— : model.

to its decomposition and the increase of reaction mixture volume. Hence, the polymerization rate under these conditions is almost linear. A portion of the monomer fed is consumed by polymerization and the remainder swells the new PVC produced. It is obvious that the monomer consumption rate should decrease with decreasing pressure level. For seed polymerizations, the monomer consumption increases with time more significantly at the beginning of the process,[6,7] because the extra monomer is required to swell the PVC seed. The present model predictions agree with Sörvik and Hjertberg's experimental results.[6,7]

The model prediction of the monomer feed rate is shown in Figure 6.3. It is difficult to obtain instantaneous feed rate experimentally.

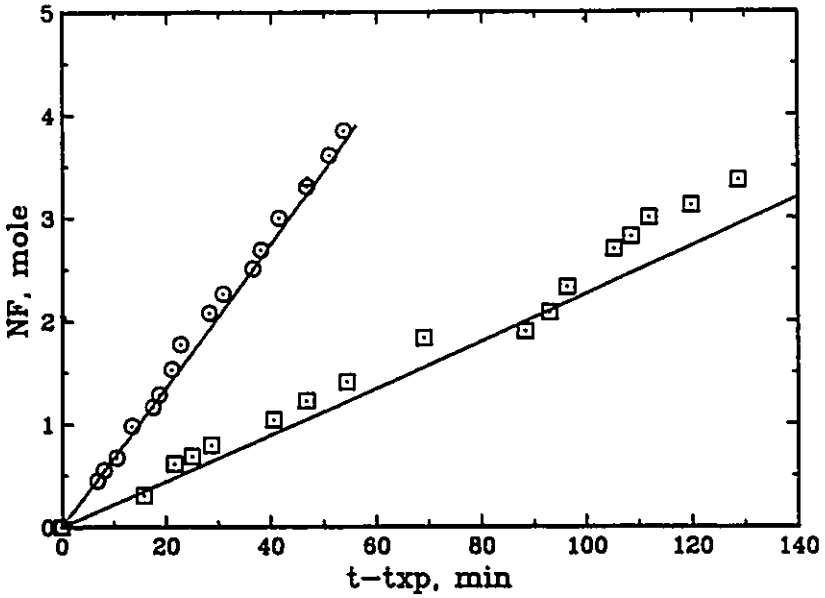

Figure 6.2. Monomer consumption for semi-batch polymerization with subsaturation pressure at 50°C.
⊙: at 90% P_{mo}, □: at 78% P_{mo}, —— : model.

As expected, the model predictions show that the required monomer feed rate decreases with decreasing pressure level. However, the feed rate increases with reaction time at a certain pressure level. This can be attributed to increasing the reaction consumption and swelling produced PVC due to increasing reaction volume. The monomer feed rate is a key variable for semi-batch operation. Hence, the present model should be useful for the design and control of commercial semi-batch reactor.

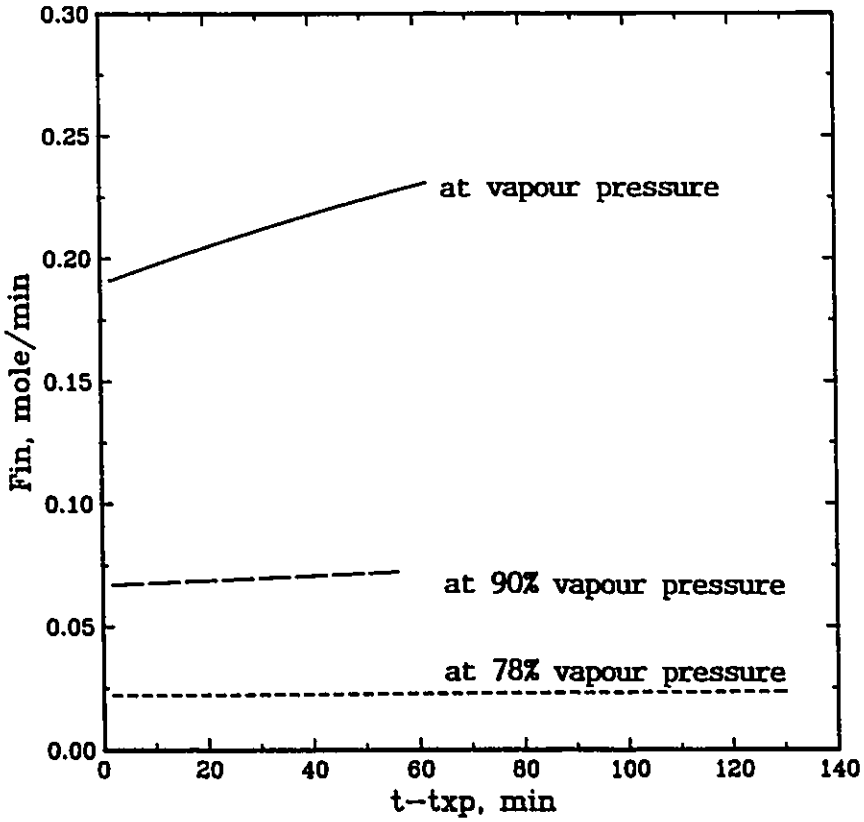

Figure 6.3. Instantaneous feed rate of VCM during semi-batch polymerization at different pressures at 50°C.

6.4.2 Reactor Dynamics

Conversion histories for seed or semi-batch polymerization which depend on initiator concentration[3,10] and pressure level[4,8,10] are experimentally demonstrated in the literature. However, a quantitative description of the conversion histories has not been reported. Both experimental data and model predictions of conversion histories for semi-batch process at different pressure levels are shown in Figures 6.4-6.6. One can see that the present model predictions are in excellent

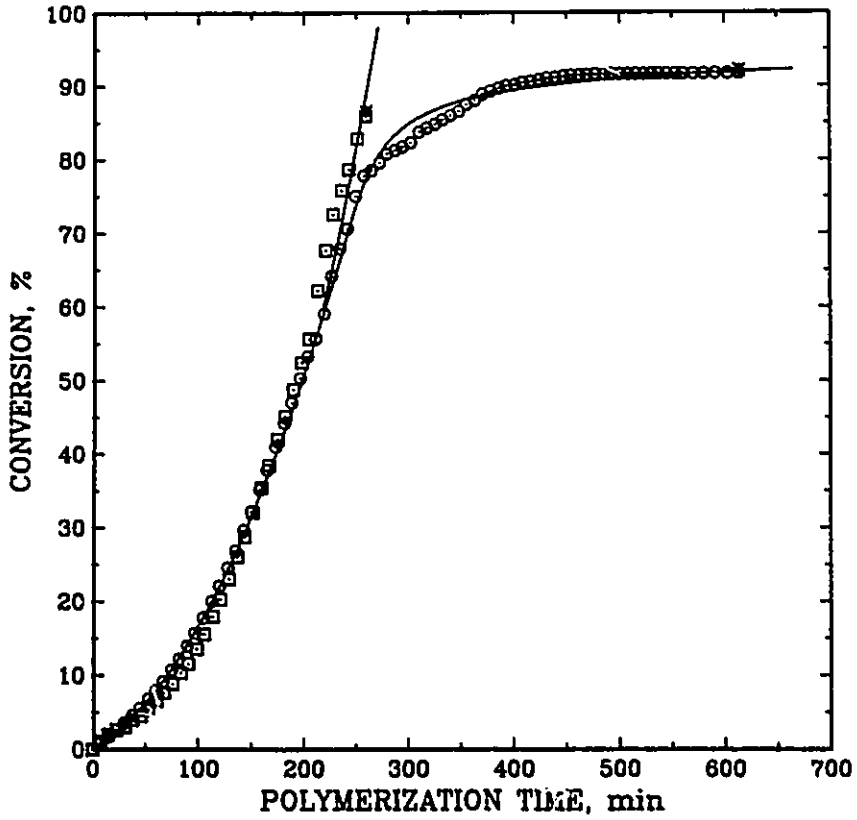

Figure 6.4. Comparison of conversion histories between batch and semi-batch processes at 50°C. ⊙: batch, □: semi-batch at P_{mo}, —— : model, *: gravimetry.

agreement with the experimental data at the different pressure levels. Polymerization rates with condition used are almost linear as expected. If the semi-batch process is operated at the vapour pressure of VCM, the polymerization rate is maximum. The increase in productivity is very significant if the semi-batch process is operated at above 90% vapour pressure levels as shown in Table 6.1. The semi-batch process requires only 52% of the batch polymerization time to obtain 91% conversion

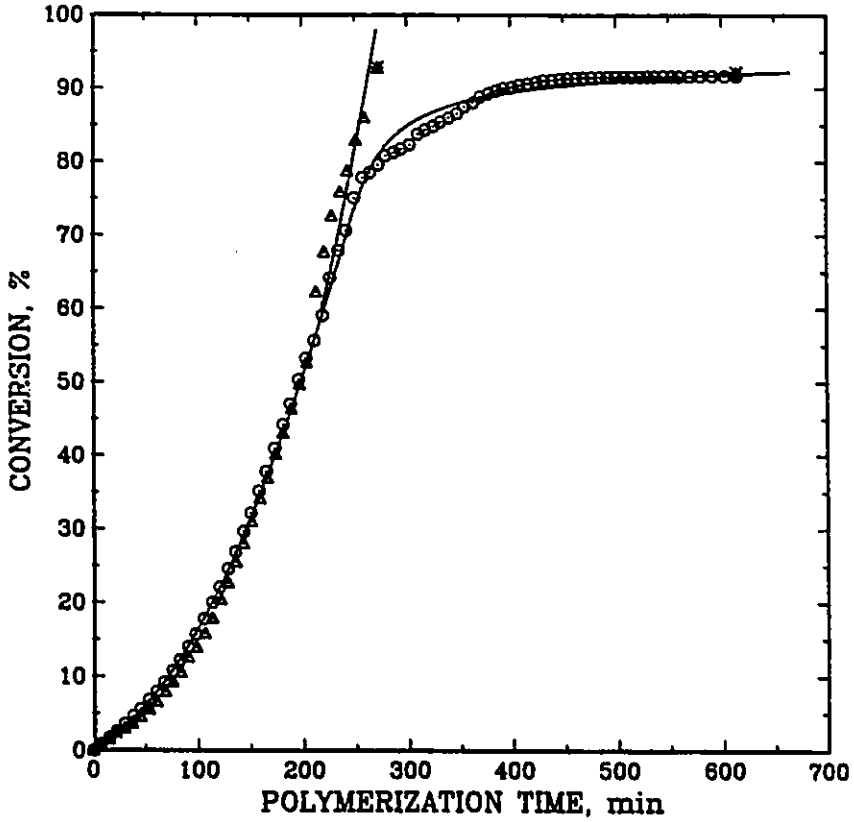

Figure 6.5. Comparison of conversion histories between batch and semi-batch processes at 50°C. ⊙: batch, Δ: semi-batch at P_{mo}, —— : model, *: gravimetry.

(based on the initial monomer charged) at 50°C with the present polymerization recipe. The reason is that the polymerization rate in the batch process falls significantly after 85% conversion whereas in semi-batch polymerization, the rate is maintained. Figures 6.4-6.6 also show the significant effect of monomer concentration (or conversion) on polymerization rate.

Reactor pressures corresponding to Figures 6.4-6.6 are shown in

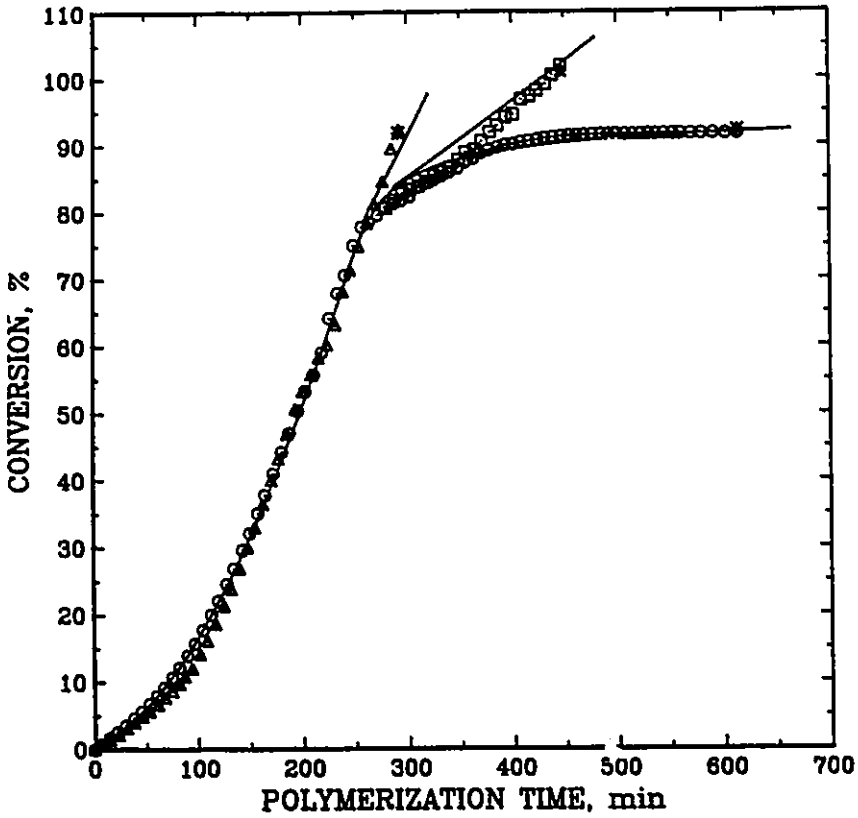

Figure 6.6. Comparison of conversion histories between batch and semi-batch processes with subsaturation pressure at 50°C. ⊙: batch, Δ: semi-batch at 90%P_{mo}, □: semi-batch at 78%P_{mo}, —— : model, *:gravimetry.

Table 6.1. Comparison of productivity between batch and semi-batch processes.

Process type	terminal conversion	terminal time, min	pressure level	time fraction
batch	91%	500	52%P_{mo}	1
semi-batch	91%	262	P_{mo}	0.52
semi-batch	91%	300	90%P_{mo}	0.60
semi-batch	91%	350	78%P_{mo}	0.70

Figure 6.7. The model for pressure and conversion relationship is given in Chapter 2. Figure 6.7 clearly shows pressure histories for semi-batch operations. It should be mentioned that the reactor pressure drops slowly before the critical conversion X_f. Therefore, the semi-batch operation at vapour pressure of VCM commences before X_f as shown in in Figure 6.7.

6.4.3 Molecular Properties

Instantaneous and accumulated molecular weight averages of PVC made in a batch process decrease with conversion after X_f due to the significant increase in CM (the ratio of chain transfer to monomer rate constant to propagation rate constant). This increase in CM is due both to the decrease in monomer concentration as well as to diffusion control of reaction rates. However, for the semi-batch process, CM should remain constant because of the constant monomer concentration and even diffusion-controlled kinetic parameters will be constant. The model predictions for CM values corresponding to semi-batch operations discussed above are shown in Figure 6.8. One can see that CM increases with decreasing pressure level but remains constant at a given pressure. Hence, the instantaneous molecular weight averages should be almost constant for the semi-batch process. A small effect of reduction in initiator concentration and transfer to polymer may be felt. If the semi-batch process is operated at the vapour pressure of VCM, the molecular weight averages should be almost the same as those produced in the polymer phase at conversion X_f. Figure 6.9 shows a comparison of accumulated

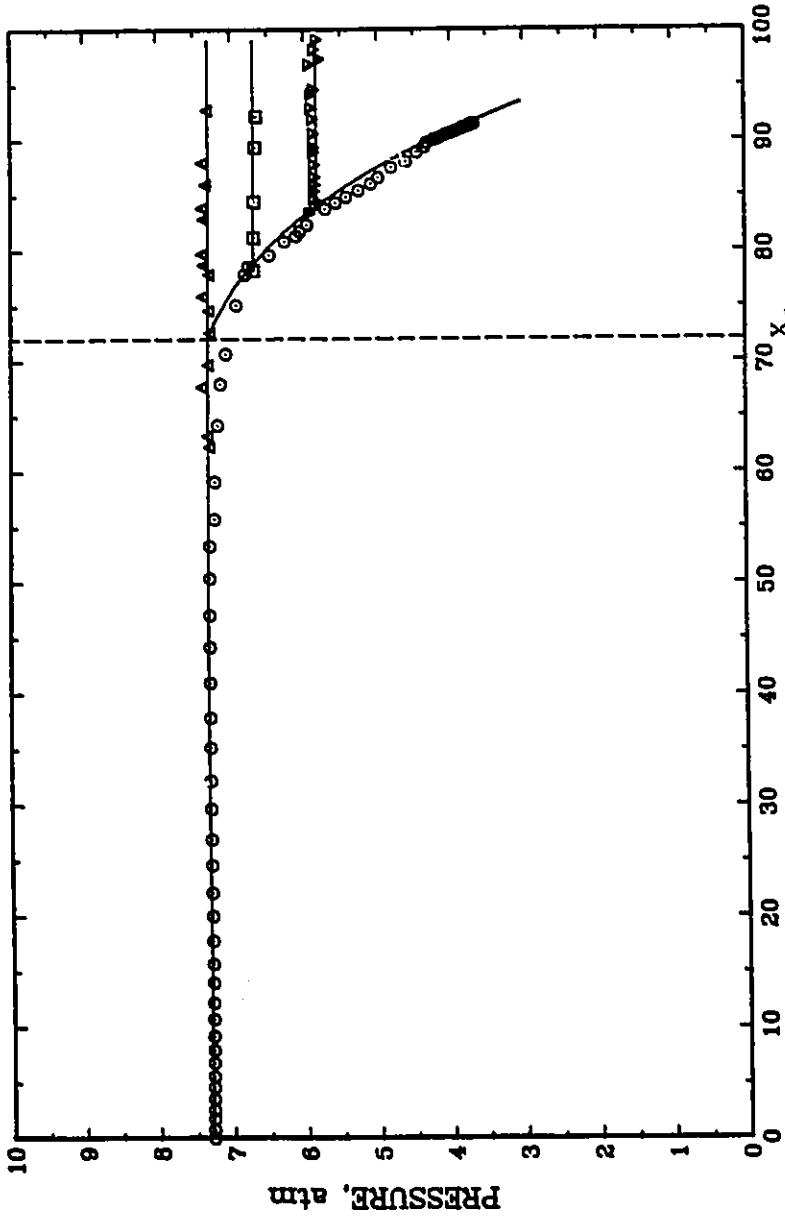

Figure 6.7. Conversion dependence of reactor pressure for batch and semi-batch polymerizations at 50 °C.
⊙: batch, Δ: semi-batch at P_{mo}, □: semi-batch at 90%P_{mo},
▽: semi-batch at 78%P_{mo}, ——— : model.

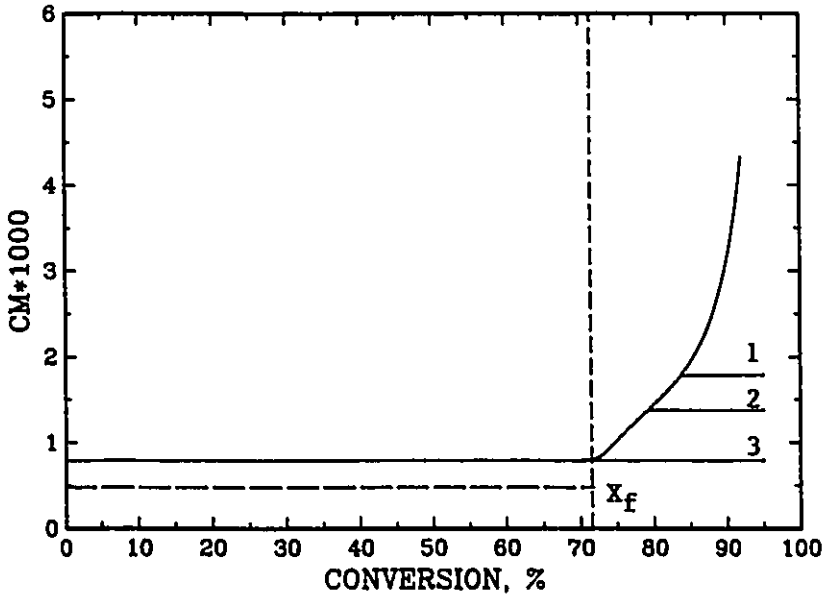

Figure 6.8. Conversion dependence of CM for batch and semi-batch polymerizations at 50 °C.
1: at 78%P_{mo}, 2: at 90%P_{mo}, 3: at P_{mo}

molecular averages for batch and semi-batch polymerizations. The model predictions for $\overline{M}_w$ and $\overline{M}_n$ increase slightly with conversion for semi-batch operated at VCM vapour pressure (see dash line). The experimental data are slightly lower than the model predictions. However, $\overline{M}_w$ and $\overline{M}_n$ of PVC made by the semi-batch process at vapour pressure seem higher than those by a batch process at the same conversion levels.

The accumulated molecular weight distributions (MWD) shown in Figure 6.10 also indicate a difference between batch and semi-batch processes at the same conversion. The accumulated MWD for the batch process shifts to lower molecular weights compared with the MWD for the semi-batch process at vapour pressure. Figures 6.11 and 6.12 show the accumu-

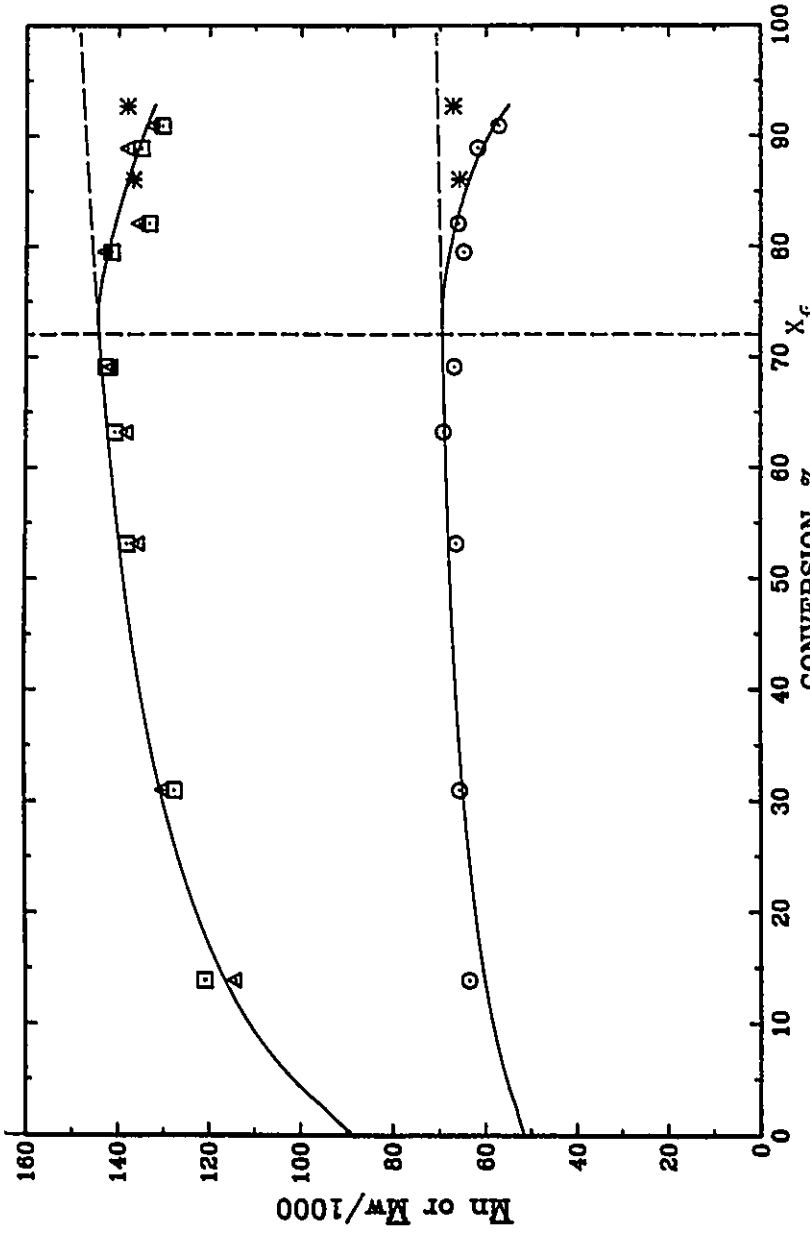

Figure 6.9. Conversion dependence of accumulated molecular weight averages for batch and semi-batch processes at 50°C.
Δ, □: $\bar{M}_w$, batch, ⊙: $\bar{M}_n$, batch, *: semi-batch,
——— : batch model, – – – – : semi-batch model.

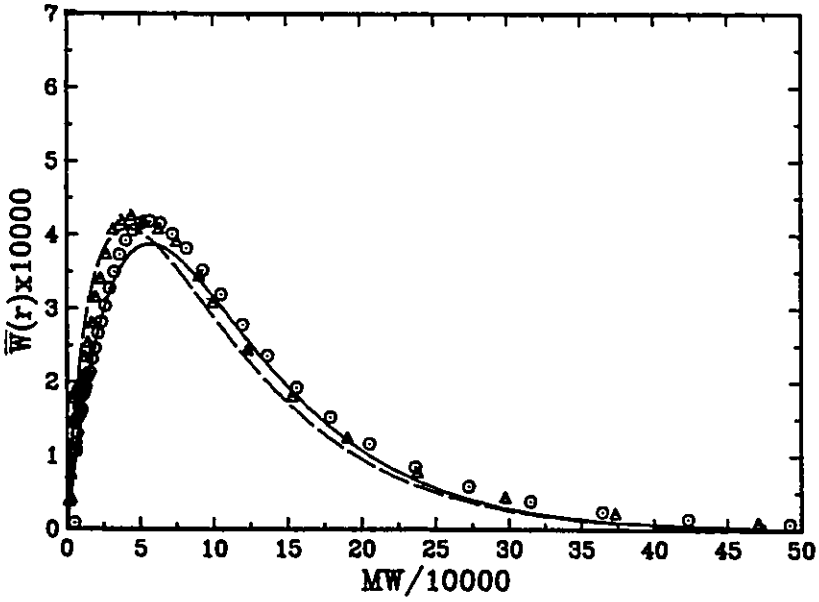

Figure 6.10. Comparison of accumulated MWD between batch and semi-batch polymerizations at 50°C (MW=62.5r). Δ: batch with X= 92.2%, ⊙: semi-batch with X=92.7%,– – – – : batch model, ——— : semi-batch model.

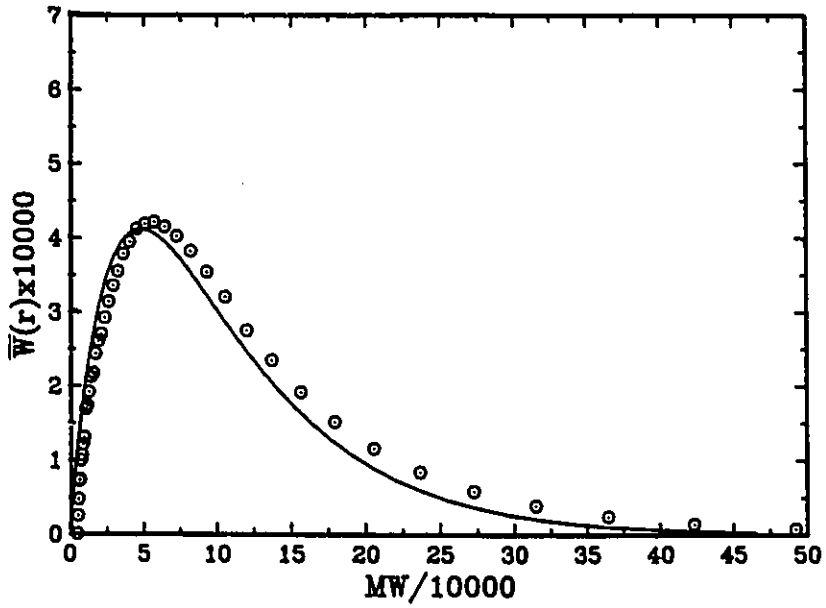

Figure 6.11. Accumulated MWD of PVC for semi-batch polymerization at 90%P_{mo}, at 50°C (MW=62.5r). ⊙: experimental data, ——— :model.

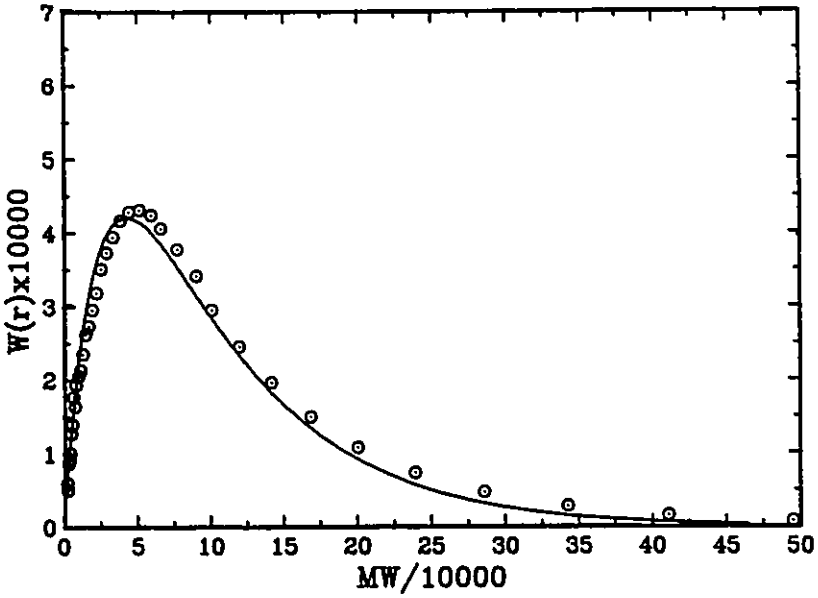

Figure 6.12. Accumulated MWD of PVC for semi-batch polymerization at 78%P_{mo}, at 50°C (MW=62.5r). ⊙: experimental data, ——— : model.

lated MWD for the semi-batch operation at pressure levels 90% and 78% P_{mo} (Case 2) respectively. These results demonstrate that the model in Chapter 5 is in excellent agreement with the experimental data for the semi-batch process when the monomer concentration and kinetic parameters are adjusted accordingly. The effect of the pressure level on the accumulated MWD is shown in Figure 6.13. One can see that the accumulated MWD shifts towards lower molecular weights with decreasing reactor pressure. These results are in agreement with Hjertberg et al's experimental data using seed polymerizations.[7] Although $\overline{M}_w$ and $\overline{M}_n$ and accumulated MWD vary with pressure level, these changes are not significant because the amount of PVC produced in the semi-batch process in the present

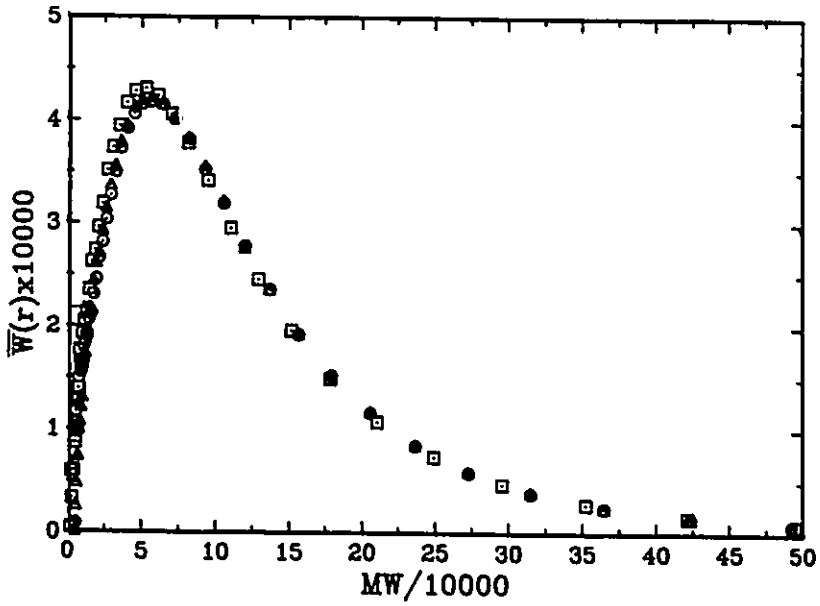

Figure 6.13. Effect of pressure level on accumulated MWD of PVC produced by semi-batch processes at 50°C (MW=62.5r). ⊙: at P_{mo}, X=92.7%, Δ: at 90%P_{mo}, X=91.8%, □: at 78%P_{mo}, X=101%.

experiments is relatively small compared with the total amount of PVC produced. However, the instantaneous MWD corresponding to Figures 6.10 and 6.13 varies with polymerization pressure dramatically as shown in Figure 6.14. The instantaneous MWD of PVC made by semi-batch at VCM vapour pressure, even at high conversions, is similar to the accumulated MWD at conversion X_f. Figures 6.15 and 6.16 further show that the instantaneous number- and weight-average molecular weights change significantly with pressure level. If the semi-batch process is operated at the VCM vapour pressure, the instantaneous M_n and M_w are similar to those at conversion X_f with M_w increasing slightly due to chain transfer to polymer. A decrease in the pressure level always leads to a decrease

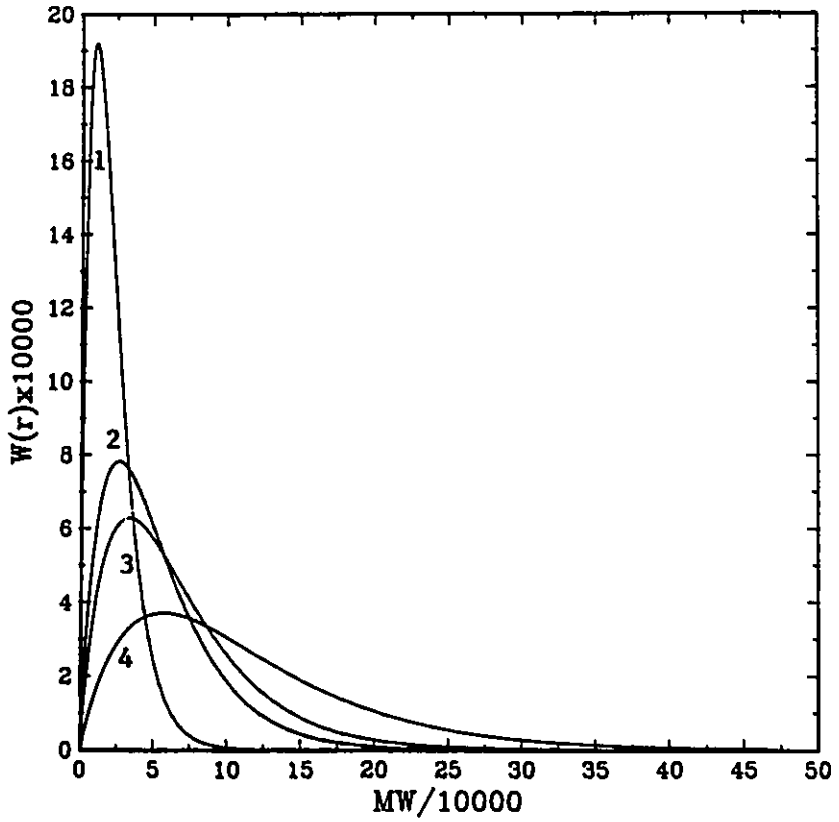

Figure 6.14. Effect of pressure level on instantaneous MWD for batch and semi-batch polymerizations at 50°C (MW=62.5r).
1: batch with terminal pressure 45%P_{mo},
2: semi-batch at 78%P_{mo}, 3: semi-batch at 90%P_{mo},
4: semi-batch at P_{mo}.

in molecular weight. Figure 6.17 shows how the instantaneous MWD shifts toward lower molecular weight as the pressure decreases at the same conversion level based on model predictions. Obviously, a lower polydispersity for PVC should result for the semi-batch process operated at VCM vapour pressure compared to those obtained at lower pressures.

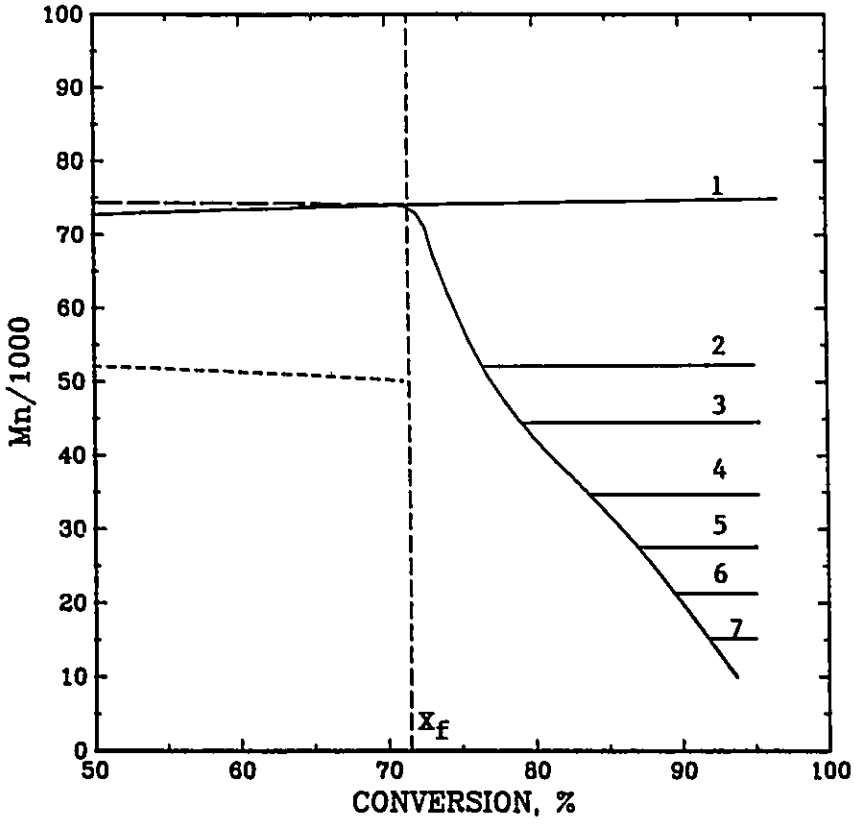

Figure 6.15. Effect of pressure level on instantaneous number-average molecular weight for batch and semi-batch polymerizations at 50°C. 1: at P_{mo}, 2: 95%, 3: 90%, 4: 80%, 5: 70%, 6: 60%, 7: 50%P_{mo}, respectively.
– – –: M_n in the polymer phase,
– – –: M_n in the monomer phase,
———: the total instantaneous M_n.

Based on the experimental data and model predictions above, one can conclude that the instantaneous molecular weight averages and MWD can be controlled by pressure in the semi-batch process. In other words, the instantaneous terminal groups and possibly other defect structures of PVC can be controlled by the pressure level or the monomer concentra-

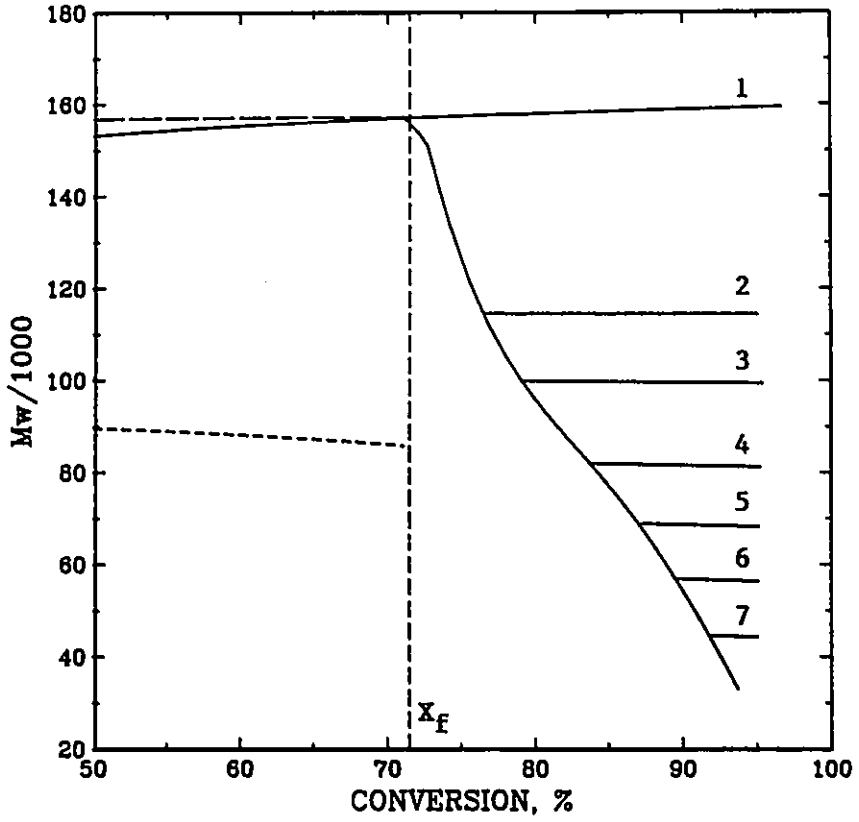

Figure 6.16. Effect of pressure level on instantaneous weight-average molecular weight for batch and semi-batch polymerizations at 50°C. 1: at P_{mo}, 2: 95%, 3: 90%, 4: 80%, 5: 70%, 6: 60%, 7: 50%P_{mo}, respectively.
– – –: M_w in the polymer phase,
– – –: M_w in the monomer phase,
———: the total instantaneous M_w.

tion. Therefore, dehydrochlorination measurements of PVC should reflect the effect of pressure level on the thermal stability of PVC. The results of dehydrochlorination rates (dHCl/dt) are shown in Table 6.2. For the batch process, thermal stability of PVC decreases significantly with conversion after the pressure drop. However, for the semi-batch process

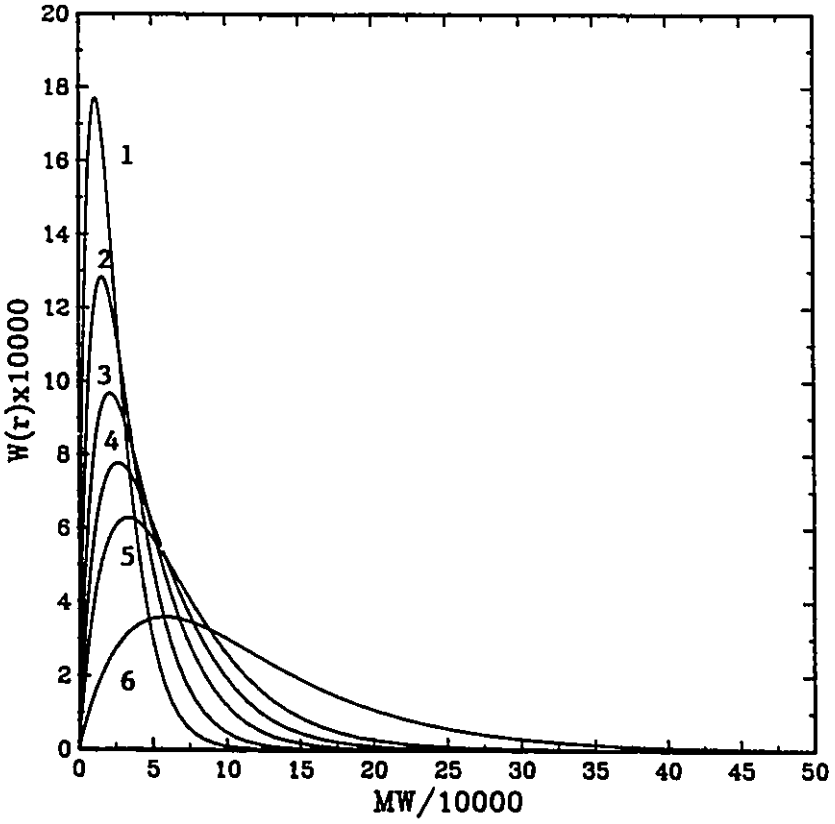

Figure 6.17. Pressure dependence of instantaneous MWD for semi-batch polymerization at 50°C, conversion 95% (MW=62.5r). 1: at 50%P_{mo}, 2: 60%P_{mo}, 3: 70%P_{mo}, 4: 80%P_{mo}, 5: 90%P_{mo} and 6: at P_{mo}.

at VCM vapour pressure, the dehydrochlorination rate is the same as that for the batch process before pressure drop (see Table 6.2). For the same conversion level, the dehydrochlorination rate for the semi-batch process at vapour pressure is much lower than that for the batch process. The dehydrochlorination rate increases with decreasing pressure level for the semi-batch process. These results agree with Sörvik and Hjertberg's experimental results using seed polymerizations.[5-8] The

Table 6.2. Effect of semi-batch process on the dehydrochlorination rate of PVC.

process type	terminal conversion	pressure level	$(dHCl/dt)10^3$ %/min
batch	$< X_f$	P_{mo}	16.5
batch	92.2%	$45\%P_{mo}$	19.5
semi-batch	86.1%	P_{mo}	16.5
semi-batch	92.7%	P_{mo}	16.5
semi-batch	91.8%	$90\%P_{mo}$	16.6
semi-batch	101%	$78\%P_{mo}$	23.8

dehydrochlorination rate measurements in the present work are based on the accumulated PVC samples. One can predict from these results that the dehydrochlorination rate of instantaneous PVC produced at subsaturation pressure must increase dramatically with decreasing pressure level. These results indicate that the defect structures, which are responsible for the decrease in thermal stability of PVC, increase dramatically with decreasing monomer concentration. At subsaturation pressure, the terminal structure of 1-chloro-2-alkene (which results in the chain transfer to monomer reactions) increases as a result of the decrease in monomer concentration and diffusion-controlled reactions. Meanwhile, the concentration of long chain branches, 2,4-dichloro-n-butyl branches and 2-chloroethyl branches also ought to increase with decreasing monomer concentration. All these branches contain tertiary chlorine atom.[12] Hjertberg et al's[13-15] and Van den Heuvel et al's[16] experimental results show that the terminal structure of 1-chloro-2-alkene is not signifi-

cantly involved in the degradation of PVC. Therefore, tertiary chlorine atoms seem to be responsible for the decrease in thermal stability of PVC with decreasing monomer concentration. Detailed microstructure measurements for these PVC samples are required to confirm that increasing levels of tertiary chlorine atoms are the cause of decrease in thermal stability of PVC with conversion (or reduced pressure). However, the present experimental results show that the semi-batch operation at the VCM vapour pressure can provide an effective way to limit the defect structures and to obtain high productivity and a PVC with higher thermal stability at a given polymerization temperature. The effect of the polymerization conditions on thermal stability of PVC will be further discussed in Chapter 7.

To confirm that semi-batch operation is commercially viable, one must examine the PVC produced via semi-batch operation for reduction in porosity and changes in bulk density, particle size and gelation times. The effect of the semi-batch operation on these properties of PVC is under study. Table 6.3 compares some physical properties of PVC made by batch and semi-batch processes at the same polymerization temperature. The degree of gelation is one of the important processing properties for rigid PVC applications. Table 6.3 snows that the degree of gelation of PVC made by the semi-batch process is essentially the same as that of PVC made by the batch process at the same conversion levels. The degree of absorption of di-2-ethylhexyl phthalate (DOP) (a common commercial plastisizer), is a measure of the relative porosity of a PVC powder. Relative porosity is an important factor for flexible PVC processing.

Table 6.3. Comparison of processing properties of PVC made by batch and semi-batch processes at 50°C.

Process type	Conversion %	Pressure level	Degree of[a] gelation at 201°C %	Relative[b] porosity DOP%	Particle[c] size (mean) μm
batch	81.2	78%P_{mo}	82	37.5	114
batch	89.3	60%P_{mo}	83	36.4	131
batch	93.0	43%P_{mo}	81	37.7	118
semi-batch	86.1	P_{m0}	86	32.9	116
semi-batch	92.7	P_{mo}	82	32.1	120
semi-batch	91.8	90%P_{mo}	83	39.5	127
semi-batch	101	78%P_{mo}	82	37.5	130

a: Degree of gelation was measured by T. Aalto (MIPPT).
b: Relative porosity was measured by NESTE Chemicals (Finland).
c: Particle size was measured with Coulter Counter method by NESTE Chemicals (Finland).

The results in Table 6.3 suggest that the semi-batch process (operated under the present conditions) does not change the porosity of PVC. The volume-average particle size is not affected by the semi-batch process (in the present experiments) as shown in Table 6.3. All of the results indicate that the semi-batch process operated under the present experimental conditions does not significantly affect the PVC physical properties which are important for PVC processing. Hence, a semi-batch process operating at the VCM vapour pressure provides the benefits of a PVC with higher thermal stability and a significantly increased productivity without changing particle size, porosity and gelation time. However, the

mechanisms which are responsible for the effect of polymerization conditions on the physical properties of PVC needs to be further studied. It should also be mentioned that further addition of VCM via semi-batch operation to give yet higher conversions based on the initial charge of monomer will eventually lead to significant decrease in porosity. This limiting factor has not been established in this investigation.

6.5 SUMMARY

In this Chapter, a comprehensive model for semi-batch operation of VCM suspension polymerization at high conversions ($X > X_f$) has been developed. The present model, combined with the batch reactor model developed in the previous chapters, can be used to predict the monomer feed rate, the total monomer consumption, conversion history, polymerization rate and the PVC molecular weight development of VCM polymerization in a semi-batch process operated at different pressure levels. The model predictions are in excellent agreement with present experimental data.

The advantages of the semi-batch process operated at vapour pressure of VCM include increase in productivity and improvement of the molecular properties, such as narrowing the MWD and enhancing the thermal stability of PVC without deteriorating such physical properties as the gelation time, the porosity of PVC powder and the final particle size. However, the PVC molecular properties will deteriorate if the

semi-batch process is operated at subsaturation pressures substantially below VCM vapour pressure. The lower the pressure, the lower the thermal stability of PVC at a given polymerization temperature.

The present model together with the batch reactor model developed herein should be useful for commercial semi-batch reactor design, operation and optimization.

6.6 REFERENCES

1. Min, K. W. and Gostin, H. I. Ind. Eng. Chem. Prod. Res. Dev., 1979, 18, 272.

2. Kahle, G. R. and Moberly, C. W. J. Appl. Polym. Sci., 1971, 15, 545.

3. Sielfeld, G. and Reichert, K. H. Appl. Polym. Symp. 1975, 26, 21.

4. Allsopp, M. W. J. Macromol. Sci.-Chem. 1977, A11, 1223.

5. Sörvik, E. M. Polym. Lett. Ed. 1976, 14, 735.

6. Sörvik, E. M. and Hjertberg, T. J. Macromol. Sci.-Chem. 1977, A11, 1349.

7. Hjertberg, T. and Sörvik, E. M. J. Polym. Sci. Polym. Chem. Ed. 1978, 16, 645.

8. Hjertberg, T. and Sörvik, E. M. J. Polym. Sci.: part A: Polym. Chem., 1986, 24, 1313.

9. Hjertberg, T. J. Appl. Polym. Sci., 1988, 36, 129.

10. Ugelstad, J., Mork, P. C., Dahl, P. and Rangnes, P. J. Polym. Sci., part C, 1969, 27, 49.

11. Ugelstad, J., Flogstad, H., Hansen, F. K. and Ellingsen, T. J. Polym. Sci. Symp., 1973, 42, 473.

12. Starnes, W. H. Jr., Schilling, F. C., Plitz, I. M., Cais, R. E., Freed, D. J., Hartless, R. L. and Bovey, F. A. Macromol., 1983, 16, 790.

13. Hjertberg, T. and Sörvik, E. M. J. Macromol. Sci.-Chem., 1982, A17, 983.

14. Hjertberg, T. and Sörvik, E. M. Polymer, 1983, 24, 673.

15. Hjertberg, T. and Sörvik, E. M. Polymer, 1983, 24, 685.

16. Van den Heuvel, C. Jurriaan M. and Weber, Anton J. M. Makromol. Chem., 1983, 184, 2261.

CHAPTER 7

EFFECT OF POLYMERIZATION CONDITIONS ON POLYMER PROPERTIES

7.1 INTRODUCTION

In the previous chapters, the kinetic behaviour of VCM polymerization in both batch and semi-batch processes has been described quantitatively. In the present chapter, the effect of the polymerization conditions on the PVC product properties will be further discussed.

As mentioned in Chapter 4, the propagation reaction of VCM polymerization is considered to be mainly a head-to-tail addition of the monomer double bond to the polymer radical center. Therefore, the theoretical structure of PVC has the head-to-tail sequence[1], that is

$$-CH_2-\underset{Cl}{CH}-CH_2-\underset{Cl}{CH}-CH_2-\underset{Cl}{CH}-CH_2-\underset{Cl}{CH}-CH_2-\underset{Cl}{CH}-$$

However, thermal dehydrochlorination of commercial PVC starts at a temperature as low as 100°C while the equivalent degradation temperature of low molecular weight compounds taken as models for the "ideal" PVC structure is above 200°C.[2,3] Therefore, the thermal stability of commercial PVC is much lower than expected based on this ideal structure. This low thermal stability of PVC is attributed to structural defects produced during VCM polymerization. A fundamental understanding of the

mechanisms by which defect structures form and the effect of polymerization conditions on the abundance of these structures is essential if PVC with improved thermal stability is to be produced.

During the last fifteen years considerable progress has been made in understanding the defect structures and their relation to the thermal stability of PVC. These advances are because of the improvement in NMR and other characterization techniques. The important achievements are summarized in recent comprehensive reviews and monographs.[4-15] The main microstructural features of PVC have been well identified and the mechanisms forming the defect structures have been deduced.[16-43] Nevertheless, there is still controversy in the literature[43] with regard to the relative importance, as labile moieties, of the various irregular structures that PVC contains. Based on PVC and model-compound thermal stability studies, the defect structures, which are considered responsible for low thermal stability of PVC, include allylic and tertiary chlorine atoms,[21,29,31,33,43,45-47] carbonyl structure[3,48-55] and other oxygenated structures.[43,56,57] The allylic and tertiary structures are formed by secondary reactions during VCM polymerization. Therefore, these structures are kinetically controlled. On the other hand, the oxygenated structures formed by unexpected oxygen impurity can only be eliminated by improving the quality of reactants and reactor operation techniques. Although it is well recognized that the low thermal stability of PVC is strongly related to the amount of structural defects, little work[31,42,43,58] has been done on the effect of polymerization conditions on the concentration of defect structures and on the thermal

stability of PVC.

In the previous chapters, the main kinetic characteristics of vinyl chloride polymerization have been illustrated quantitatively over the entire conversion range based on the principal reactions. The kinetic behaviour of VCM polymerization in batch reactors changes dramatically at high conversions due to the decrease in monomer concentration. In the present investigation, the effect of polymerization conditions on the molecular properties, especially thermal stability, of PVC is emphasized. How the polymerization conditions affect the secondary reactions will be further discussed.

7.2 EXPERIMENTAL

To investigate the effect of polymerization conditions on polymer properties, a series of experiments using suspension polymerization of VCM with various reactor operational conditions was carried out. The equipment used for the experiments, the reactor operational procedures and the methods for molecular weight measurements have been given earlier. Temperature progamming, increasing reactor temperature to a desired temperature level when reactor pressure begins to fall, was used for some PVC syntheses. The conversion histories were measured by an on-line tracer method and by gravimetry as described in Chapter 3.

The dehydrochlorination rate measurements were done in Professor Oscar Chiantore's laboratory (University of Torino, Via Bidore, Torino,

Italy). The dehydrochlorination rates of PVC were measured at 190°C by the conductimetric method. The PVC samples, in powder form (ca. 150-180 mg), were put into quartz crucibles and inserted in a pyrex degradation apparatus which can be held at a constant temperature. Preheated high purity nitrogen as a carrier gas (60 cm^3/min) was introduced into the reaction cell, so that the HCl evolved during the degradation of PVC was removed by the carrier gas and dissolved in deionzed water in the cell of a digital conductivity meter (Amel Mod. 134, Italy) which gave a continuous record of conductivity values as a function of time. The observed rates were transformed, through calibration of the electrode response, into evolved HCl in percent of the theoretical amount per minute. All the measurements were carried out to 0.4% maximum conversion of HCl in the PVC samples. The standard deviation of the measurements, as determined by replicated experiments, was 1% of the mean rate values.

7.3 RESULTS AND DISCUSSION

The effect of conversion, monomer concentration, temperature, initiator type and other additives on the molecular structure and thermal stability of PVC is now discussed.

7.3.1 Conversion Effect

The kinetic behaviour of VCM polymerization strongly depends on the monomer concentration at high conversions. When the conversion is greater than the critical conversion X_f, the polymerization rate and

instantaneous molecular weight averages decrease with conversion dramatically due to the decrease in monomer concentration and to the resulting diffusion-controlled reactions. It is believed that the molecular structure of PVC produced instantaneously must change significantly with conversion at subsaturation pressure for a batch process. If the concentration of the defect structures which are responsible for the decrease in thermal stability of PVC increase with conversion, the dehydrochlorination rate of PVC should also increase with conversion. Figure 7.1 shows, as expected, that the dehydrochlorination rate increases significantly with conversion beyond X_f at a given polymerization temperature. When the conversion is less than X_f, the dehydrochlorination rate appears to be independent of conversion. In the literature, PVC samples used for thermal stability studies often have unknown conversion histories. Hence, the effect of conversion history on thermal stability has not been emphasized. Hjertberg et al[59] found that the dehydrochlorination rate of PVC samples made by seed polymerization at subsaturation pressure increases significantly with conversion. They deduced that the dehydrochlorination rate of ordinary PVC would be a mild function of conversion. The present experimental results are consistent with Hjertberg et al's results.[59]

From the results shown in Figure 7.1, one might conclude that the defect structures produced instantaneously which are responsible for low thermal stability of PVC must increase dramatically with conversion. Unfortunately, it is impossible to separate the instantaneously produced molecules from the whole PVC sample. Recently, Darricades-Llauro et al[42]

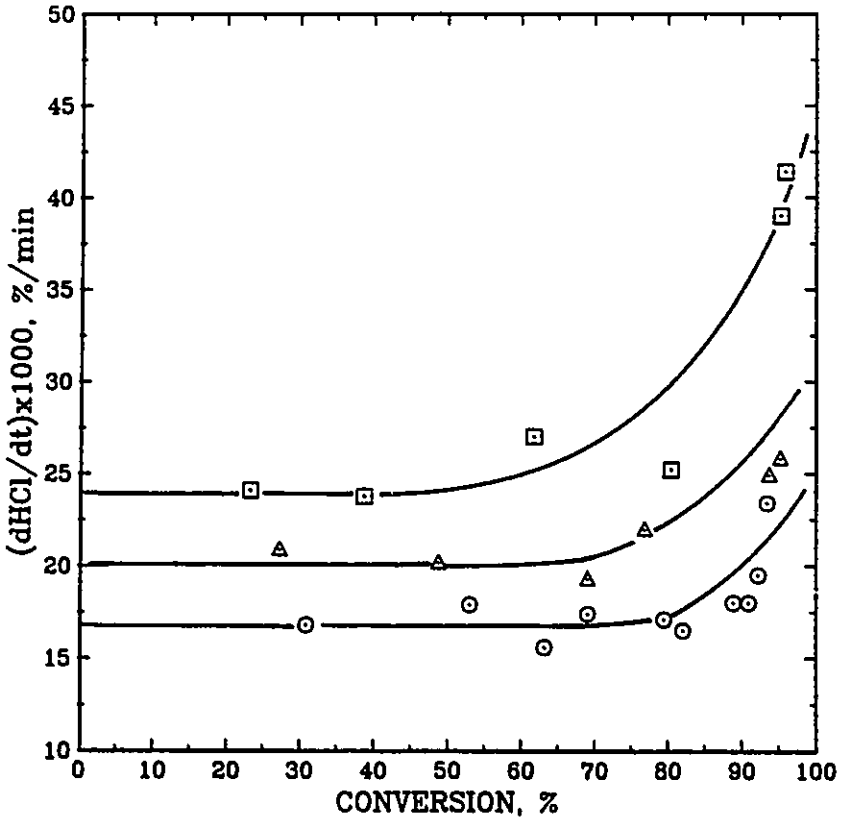

Figure 7.1. Effect of conversion on the dehydrochlorination rate of PVC at different polymerization temperatures.
⊙: 50°C, Δ: 65°C, □: 70°C.

determined the defect structures of PVC with different conversion histories made in both suspension and solution polymerizations. Their results show that the concentrations of most of the defect structures are higher when the polymerization is carried out in solution, and that internal double bonds, saturated and unsaturated end groups and branches increase with conversion. These observations, together with the present results, can be explained using diffusion-controlled free radical polymerization theory.

Based on the VCM polymerization mechanisms discussed earlier (in Chapters 4 and 5), the effective transfer to monomer reaction rate constant is a function of monomer concentration and temperature. At high conversions ($X > X_f$), the monomer concentration decreases with increased conversion. Reactions involving macromolecules become diffusion controlled, so that the ratio of the transfer to monomer rate constant to the propagation rate constant increases with conversion significantly. As a result, the instantaneous number- and weight-average molecular weights decrease dramatically. Therefore, the number of groups on the chain ends increases significantly with conversion. The main unsaturated end group is 1-chloro-2-alkene ($-CH_2-CH=CH-CH_2Cl$) (see Figure 4.1).

Long chain branches are formed by tertiary hydrogen abstraction from the polymer chains by polymer radicals (and perhaps by $Cl^{\cdot}$) and by the subsequent head-to-tail propagation as shown in Eqs.(7.1) and (7.2).

$$-CH_2-CHCl-CH_2-\dot{C}HCl + -CH_2-CHCl-CH_2- \xrightarrow{K_{fp}}$$

$$-CH_2-CHCl-CH_2-CH_2Cl + -CH_2-\dot{C}Cl-CH_2- \qquad (7.1)$$

$$-CH_2-\dot{C}Cl-CH_2- + rCH_2=CHCl \xrightarrow{K_p} -CH_2-\underset{\displaystyle CH_2-CHCl-}{\overset{|}{C}}Cl-CH_2- \qquad (7.2)$$

The 2-chloroethyl and 2,4-dichloro-n-butyl branches are formed by mechanisms involving the intramolecular abstraction of hydrogen from a backbone CHCl moiety (back-biting reaction) and the subsequent head-

to-tail propagation[14,21] as follows:

$$-CH_2-\dot{C}HCl-CH_2-CHCl \xrightarrow{K_b} \begin{cases} -CH_2-\dot{C}Cl-CH_2-CH_2Cl \quad (I) \\ -CH_2-\dot{C}Cl-CH_2-CHCl-CH_2-CH_2Cl \ (II) \end{cases} \tag{7.3}$$

$$\begin{cases} (I) \\ \quad + rCH_2=CHCl \\ (II) \end{cases} \xrightarrow{K_p} \begin{cases} \quad\quad\quad\quad\quad\quad CH_2-CH_2Cl \\ -CHCl-CH_2-CCl-CH_2-CHCl- \\ \\ \quad\quad\quad\quad\quad\quad CH_2-CHCl-CH_2-CH_2Cl \\ -CHCl-CH_2-CCl-CH_2-CHCl- \end{cases} \tag{7.4}$$

Reactions (7.1) and (7.3) are competing with propagation reactions during polymerization. At low conversions ($X < X_f$), the monomer concentrations in both monomer and polymer phases are constant and all these reactions are chemically controlled. Therefore, the number of branches per PVC chain should be independent of conversion. This may also be the reason why the dehydrochlorination rate is independent of conversion for $X < X_f$. However, at high conversions ($X > X_f$), the monomer concentration decreases with conversion, the number of chain entanglement points increases rapidly and the bimolecular termination rate constant for polymer radicals falls dramatically. Consequently, the total radical concentration increases significantly with conversion as shown in Chapter 4 (Figure 4.19). Although the ratio of K_{fp} to K_p should increase, assuming it is to be constant, the long chain branches still

increase with conversion due to the increase in the radical and polymer concentrations. The reaction in Eq.(7.3), which is unimolecular, will likely not be diffusion-controlled. At high conversions, the reaction in Eq.(7.3) is favoured due to the significant increase in radical concentration. Therefore, short chain branches should increase significantly with conversion.

The internal unsaturated structures can be formed by mechanisms involving the abstraction of hydrogen from a backbone $-CH_2-$ moiety by polymer radicals[6,60] or chlorine radicals[11,28,29] and the subsequent abstraction of chlorine radicals as follows:

$$-CH_2-CHCl-CH_2-\dot{C}HCl + -CH_2-CHCl-CH_2-CHCl- \xrightarrow{K_{fp}}$$

$$-CH_2-CH_2Cl + -CH_2-CHCl-\dot{C}H-CHCl-CH_2- \qquad (7.5)$$

$$Cl^{\cdot} + -CH_2-CHCl-CH_2-CHCl- \xrightarrow{K'_{fp}} -CH_2-CHCl-\dot{C}H-CHCl- + HCl \qquad (7.6)$$

$$-CH_2-CHCl-\dot{C}H-CHCl- \xrightarrow{K_{ab}} -CH_2-CHCl-CH=CH-CH_2-CHCl- + Cl^{\cdot} \qquad (7.7)$$

The reaction in Eq.(7.5) is equivalent to reaction in Eq.(7.1) and should be diffusion-controlled at high conversions. The reactions in Eqs.(7.6) and (7.7) should be chemically controlled over the entire conversion range. All these reactions in Eqs.(7.5)-(7.7) are favoured at high conversions due to the increase in radical and polymer concentra-

tions. Therefore, the number of internal unsaturated structures should increase with conversion.

Based on the qualitative discussion above, it is likely that the internal and terminal unsaturated groups, the allylic and tertiary chlorine atoms should increase with a decrease in monomer concentration. From Darricades-Llauro et al's results,[42] one can deduce that the instantaneous number of these structures must increase dramatically with conversion. This also explains why the defect structures are concentrated in the low molecular weight fractions.[61] The phenomenon in which the number of the defects is higher in solution polymerization also can be explained by the same argument. The initial monomer concentration of 2 mole per litre is equivalent to monomer concentrations at 85-90% conversion for suspension and bulk polymerizations. The reactions in Eqs.(7.1), (7.3) and (7.5)-(7.7) are competing with propagation reaction during polymerization. Although all the reactions in solution polymerization are chemically controlled, the reactions in Eqs.(7.1), (7.3) and (7.5)-(7.7) are favoured at very low monomer concentration. In fact, the number of defects in solution polymerization can be understood as an instantaneous number of defects. Therefore, it is not surprising that the number of the defects is much higher when the polymerization is carried out in solution where the monomer concentration is low.

Comparing the end groups before and after degradation at 180°C in helium, Van den Heuvel et al[38] experimentally demonstrated that the end groups formed from chain transfer to monomer reactions are not

significantly involved in the degradation of PVC. Therefore, the increase in dehydrochlorination rate of PVC with conversion, shown in Figure 7.1, cannot be attributed to an increase in terminal unsaturated and other end groups. This suggests that the internal defect structures, tertiary and allylic chlorine atoms, should be responsible for the deterioration in thermal stability of PVC at high conversions. This is in agreement with Hjertberg et al's[28,29] and Li et al's[47] experimental results. More recently, Starnes[62] found that, in model-compound experiments, a high HCl concentration makes internal allylic chlorine atoms less stable than tertiary chlorine atoms, but that the stability order reverses when the HCl concentration is low. Hence, it depends on the environment of degradation whether tertiary or allylic chlorine is the most important type of labile moiety in the PVC chains.

It is now clear that the dehydrochlorination rate increase with conversion is due to the increase in the number of tertiary and allylic chlorine atoms as a result of decrease in monomer concentration. Therefore, these defects can be minimized if a constant monomer concentration is maintained at high conversions by semi-batch operation as described in Chapter 6. As expected, the thermal stability of PVC made by the semi-batch process operated at the vapour pressure of VCM is improved significantly as shown in Figure 7.2. One can see, from Figure 7.2, that the dehydrochlorination rate is independent of conversion for semi-batch process operated at the saturation pressure of monomer. These results further confirm the mechanisms discussed above. The experimental results shown in Figures 7.1 and 7.2 cannot be explained by the defects having

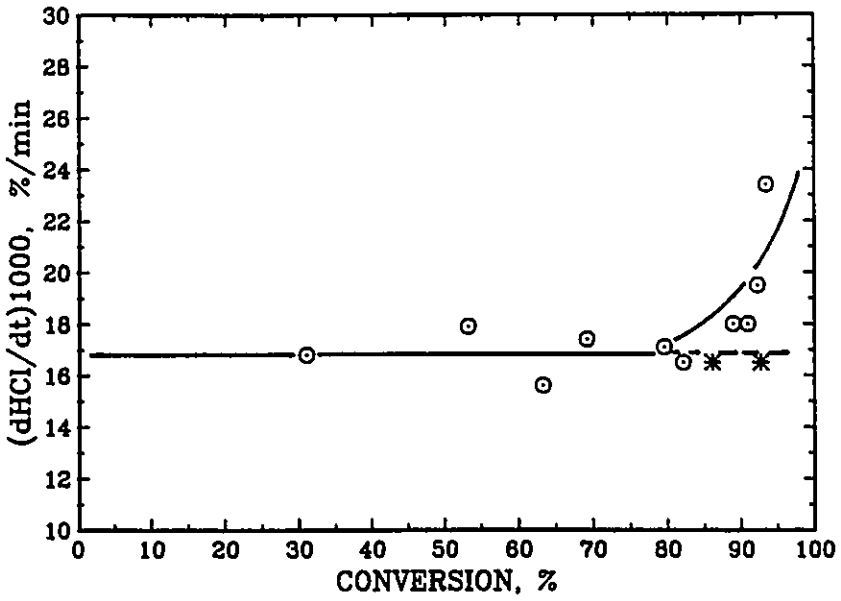

Figure 7.2. Effect of polymerization processes on the dehydrochlorination rate of PVC at high conversions.
⊙: batch polymerization at 50°C
*: semi-batch polymerization at 50°C

carbonyl structure emphasized by Minsker et al.[3,48-50]

Cuthbertson et al.[51] recently, studied the thermal stability of PVC prepared at very low conversions (0.1-2.0%) and found that the dehydrochlorination rate decreases significantly with increase in conversion. Compared with high conversion PVC, the low conversion PVC is more syndiotactic and less thermally stable. These observations are opposite from the behaviour of PVC found in the present investigation at high conversions. For the very low conversion PVC, the effect of impurities, oxygen inhibitors and initiator residue on thermal stability may be more significant.

7.3.2 Temperature Effect

The effect of polymerization temperature on thermal stability has not been extensively studied. From Figure 7.1, one may notice that the dehydrochlorination rate is a function of both conversion and polymerization temperature. Therefore, the conversion and polymerization temperature should be specified to compare the dehydrochlorination rates of PVC. Figure 7.3 shows the dehydrochlorination rate as a function of polymerization temperature at conversions (89-97% corresponding to 40-80°C) close to the corresponding limiting conversion. The dehydrochlorination rate increases with temperature linearly. Hjertberg et al[33] found that, in seed polymerization under subsaturation pressure, there is a minimum dehydrochlorination rate at 55°C. However, the present experimental results do not show such a minimum. The dehydrochlorination rate increases with temperature implies that the reactions forming the defects are most sensitive to the polymerization temperature. In general, the reaction rate constants, such as those in reactions in Eqs.(7.1), (7.3) and (7.5), are 3-5 orders of magnitude smaller than the propagation rate constants. Hence, the activation energies for the reactions forming defects are much higher than those for the propagation reactions. Hence, these reactions forming defects are favoured by increasing temperature.

A batch reactor can be operated under nonisothermal conditions, for instance, increasing polymerization temperature to a desired level at a certain conversion. Hamielec et al[63] suggested that the procedure of raising the temperature at the end of the batch would maximize

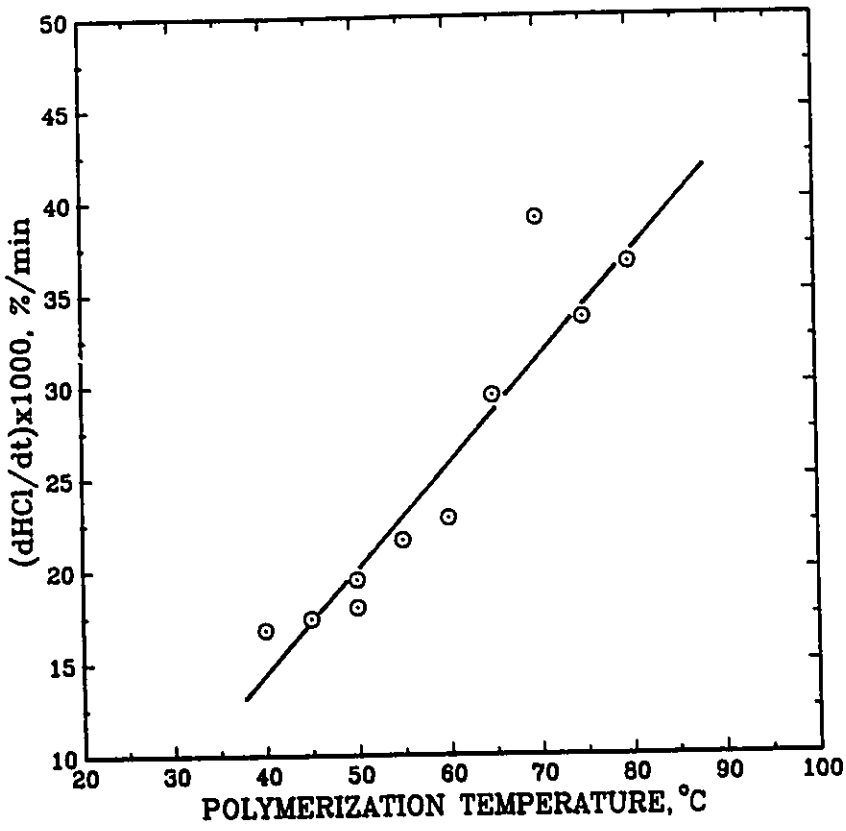

Figure 7.3. Effect of polymerization temperature on the dehydrochlorination rate of PVC at high conversions.

productivity and limit the effect of diffusion-controlled reactions on PVC thermal stability. The present investigation further pursues the effect of temperature programming on the reactor performance and the polymer properties. Figure 7.4 shows conversion histories of VCM polymerization operated with rising temperature at the point when the reactor pressure begins to fall. It took less than 5 minutes to raise the temperature from 40°C to 50°and 60°C under the present experimental conditions. One can see, from Figure 7.4, that the conversion increases

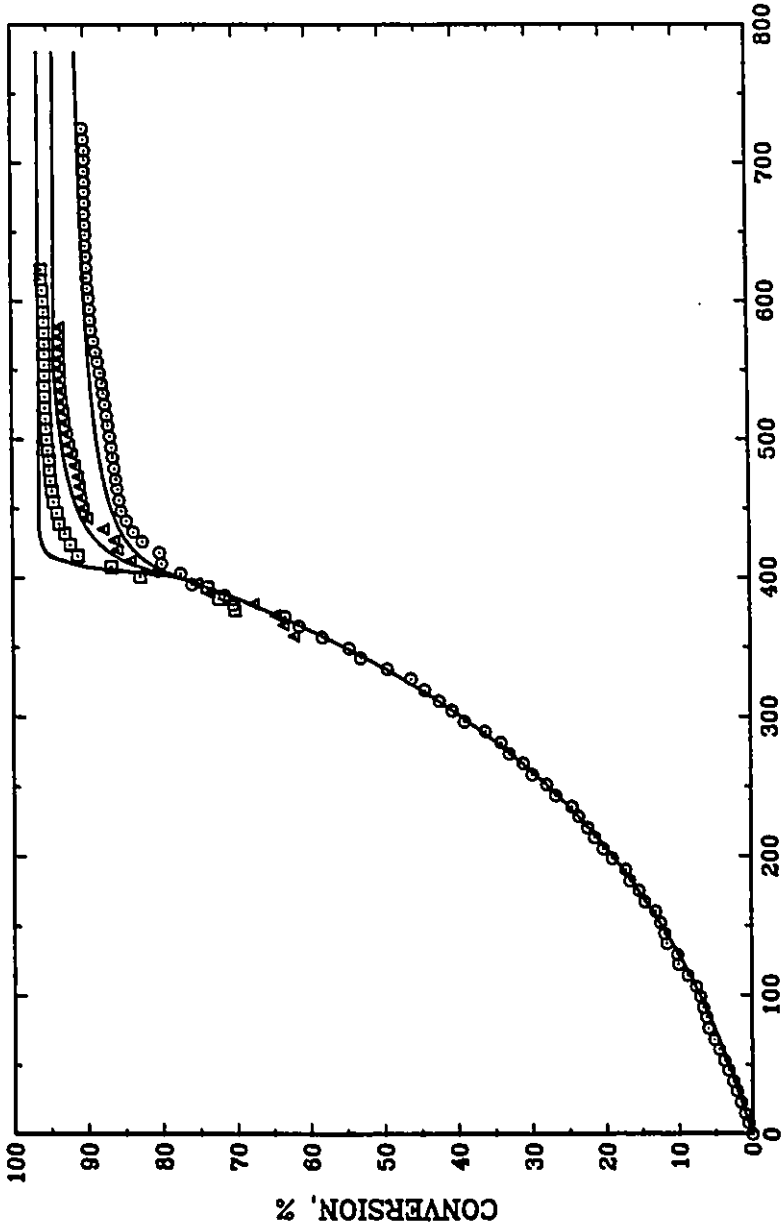

Figure 7.4. Effect of temperature programming on the conversion histories of VCM polymerization at high conversions.
o: at 40°C, Δ: at 50°C, □: at 60°C, ——: model.

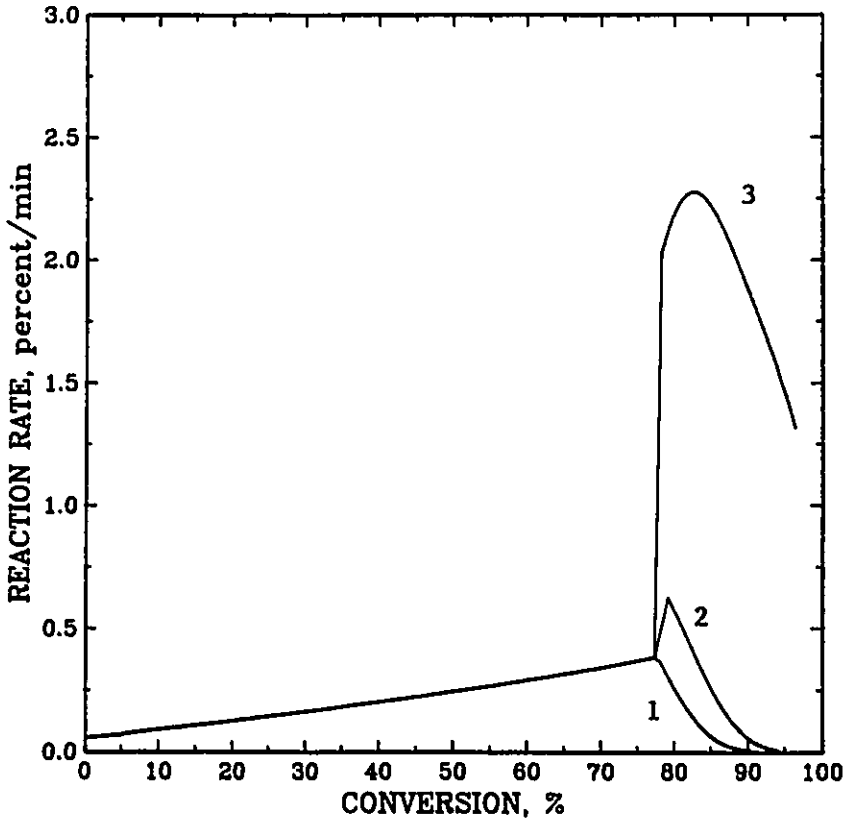

Figure 7.5. Effect of temperature programming on the polymerization rate. 1: at 40°C, 2: at 50°C, 3: at 60°C.

significantly within a short time. Figure 7.5 shows the model predictions of polymerization rates corresponding to the conversion histories shown in Figure 7.4. The polymerization rates increase dramatically with increase in temperature. The reactor pressure increases sharply at the point when the temperature is raised then decreases gradually with conversion as shown in Figure 7.6. However, the maximum pressure is always less than the vapour pressure of VCM at the same temperature because the liquid monomer phase has been consumed at that conversion (X_f decreases

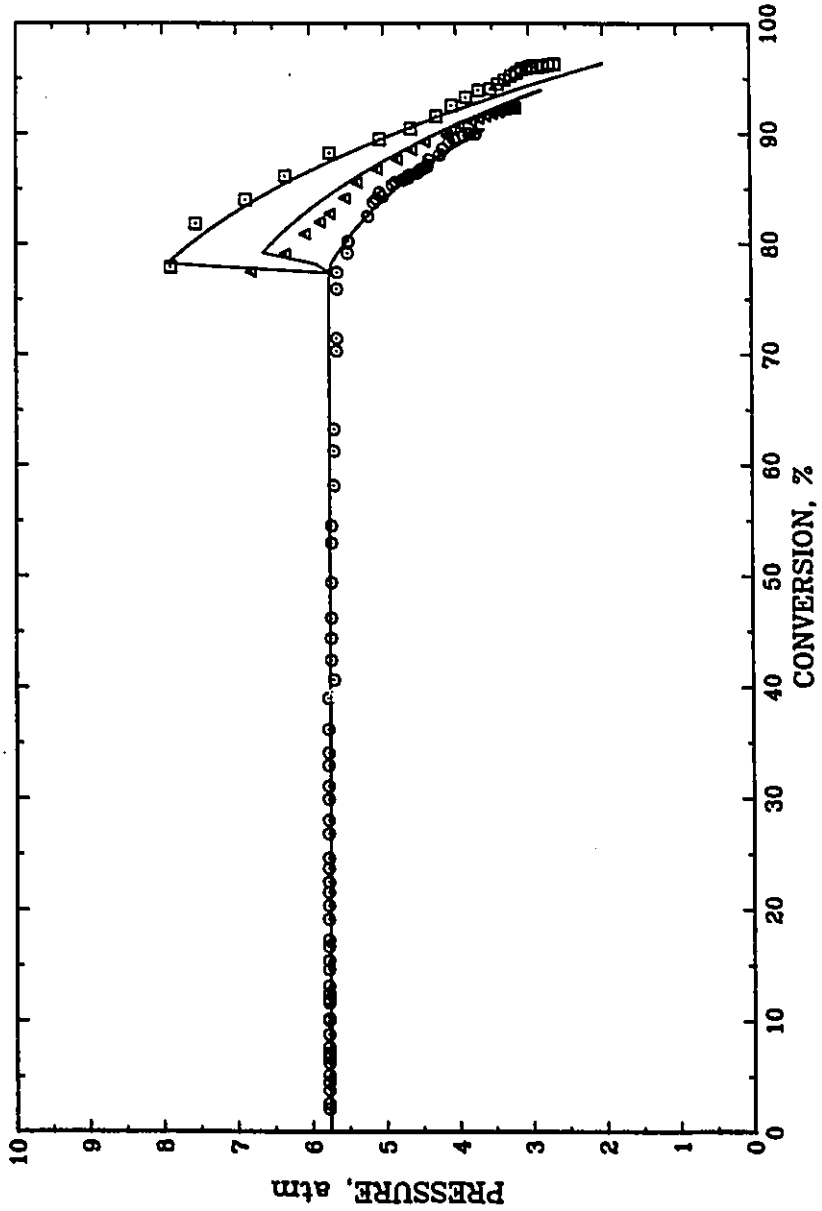

Figure 7.6. Effect of temperature programming on the reactor pressure.
⊙: 40°C, Δ: 50°C, □: 60°C, ——: model.

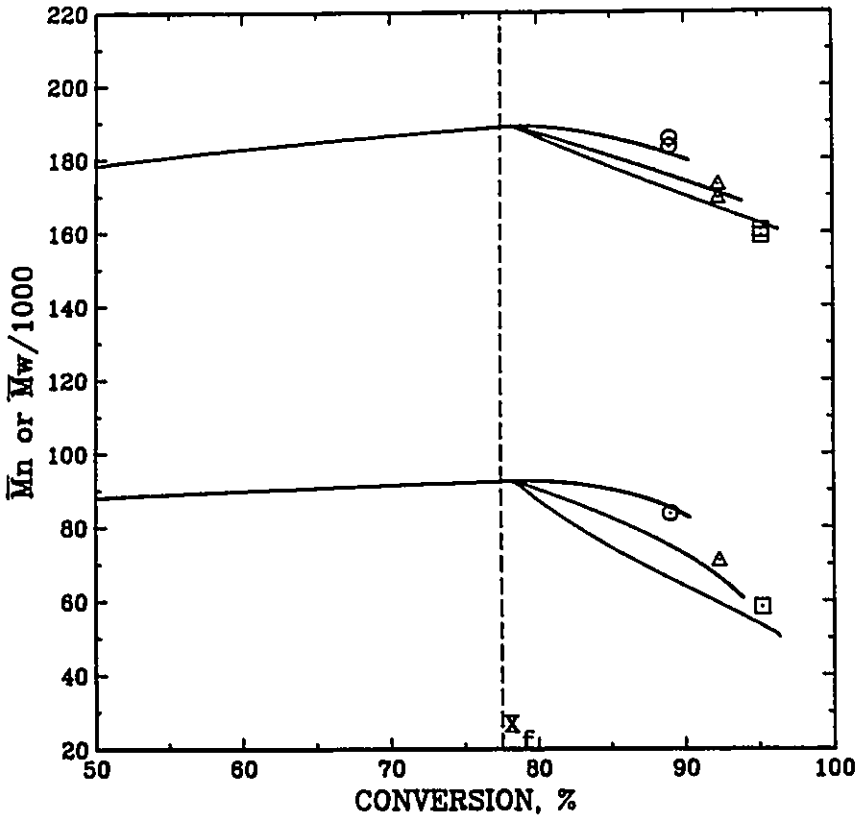

Figure 7.7. Effect of temperature programming on the accumulated number- and weight-average molecular weights at high conversions.
⊙: 40°C, Δ: 50°C, □: 60°C, ———: model.

with increase in temperature). It is obvious, therefore, that higher productivity can be achieved using temperature programming at high conversions. This operational procedure is clearly safe due to the low levels of monomer present. In the meantime, all the chemical reaction rates are affected by raising the temperature. The relative sensitivity of the reactions to temperature depends on their activation energies and the level of diffusion-controlled of individual reaction. Figure 7.7

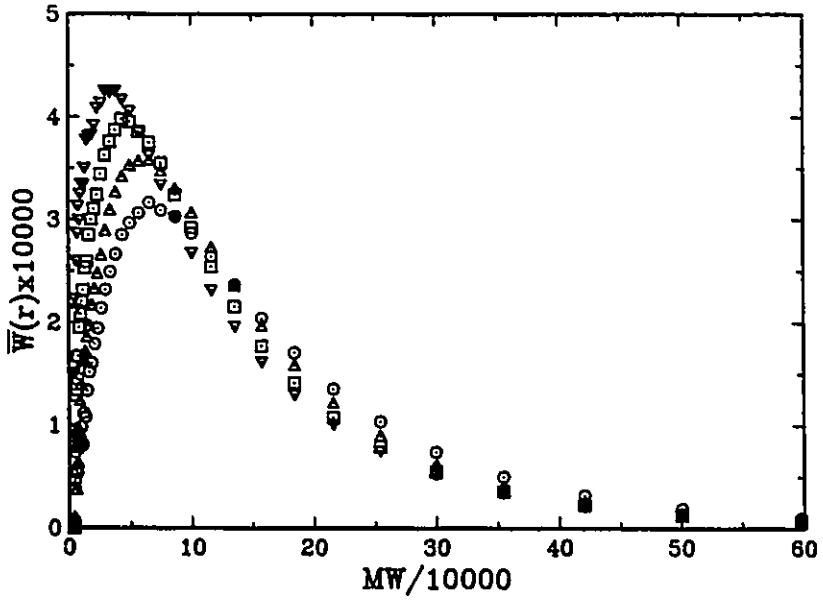

Figure 7.8. Effect of temperature programming on the accumulated molecular weight distribution at high conversions. ⊙: 40°C ,X = 89%, Δ: 50°C, X = 92%, □: 60°C, X = 95%, ∇: 70°C, X = 97%.

shows the accumulated molecular weight averages changing with conversion and temperature. It is not surprising that the accumulated molecular weight averages decrease with increase in temperature due to the increase in CM (the ratio of K_{fm} to K_p) which dominates PVC molecular weight. However, the decrease in accumulated molecular weight averages is not very significant because the amount of polymer produced at the higher temperatures is relatively small compared with the accumulated polymer. The effect of temperature on the accumulated molecular weight distribution (MWD) is shown in Figure 7.8. The MWD shifts toward lower molecular weights as the weight fraction of low molecular weight polymer increases with an increase in temperature.

Table 7.1. Effect of temperature programming on the dehydrochlorination rate of PVC.

Temperature programming	Terminal conversion	$(dHCl/dt)10^3$ %/min
40°C	89%	18.6
40 ⟶ 50°C	92%	20.4
40 ⟶ 60°C	95%	21.3
40 ⟶ 70°C	97%	29.1
40 ⟶ 50 ⟶ 60 ⟶ 70°C	97%	31.5

The effect of temperature programming on the dehydrochlorination rate is shown in Table 7.1. One can see that the dehydrochlorination rate increases with increasing programming temperature. This suggests that the reactions forming defect structures are more sensitive to temperature. However, the terminal conversions also increase with temperature. These terminal conversions are very close to the limiting conversions at the corresponding temperatures. Therefore, the results shown in Table 7.1 in fact include the effect of temperature, conversion and time. If the temperature increase is less than 10 degrees over the original temperature, the thermal stability decreases slightly. The last sample shown in Table 7.1 was made by increasing temperature at the limiting conversions respectively. One can see that the dehydrochlorination rate increases significantly. Therefore, polymerization close to the limiting conversions should be avoided if thermal stability is to be maintained. For commercial reactor operation, polymerization is not normally taken to limiting conversion (with maximum conversion about 93%). It should be possible to obtain higher productivity without losing

the thermal stability significantly by using appropriate temperature programming technique. To do this properly, one should vaporize the unreacted monomer to stop the polymerization at precisely the required terminal conversion.

The effect of conversion and temperature on the thermal stability of PVC involves very complicated phenomena. In the present investigation, it was noticed that the PVC made at higher than 70°C is pink when the conversion is higher than X_f. This implies that the dehydrochlorination has occurred significantly during polymerization at high conversions and temperatures. Gelation measurements also show that the PVC made at high temperature degrades seriously at the processing temperature. This suggests that this kind of PVC is difficult to process because its degradation temperature is close to or even lower than the processing temperature.

The effect of temperature programming on the other physical properties of PVC, which are important for PVC product processing, is shown in Table 7.2. The degree of gelation seems not very sensitive to temperature programming based on these limited data shown in Table 7.2. This suggests that temperature programming at high conversions may not affect the important processing properties significantly for rigid PVC applications. However, the relative porosity of PVC decreases with an increase in the programming temperature while the bulk density of PVC powder increases. These results suggest that the primary particles and agglomerates further fuse together and form fused agglomerates of low porosity.

Table 7.2. Effect of temperature programming on the physical properties of PVC.

Temperature programming °C	Degree of[a] gelation at 201°C %	Relative[b] porosity DOP %	Bulk[b] density K_g/m^3	Particle[b] size (mean) μm
40	74	41.2	370	124
40⟶50	68	39.6	399	127
40⟶60	68	37.8	411	125
40⟶70	76	34.5	429	128
40⟶50⟶60⟶70	59	39.4	-	116

a: Degree of gelation was measured by T. Aalto (MIPPT).
b: Relative porosity, bulk density and particle size were measured by NESTE Chemicals (Finland).

This is in agreement with the particle formation mechanism described in Chapter 4. Hence, the temperature programming will affect important processing properties for flexible PVC applications. However, an increase in bulk density is always desirable for PVC processing whether for rigid or flexible grades. The volume-average particle size is not affected by temperature programming as one might expect, because the external structure of the PVC particle has been fixed during temperature programming. With the data shown above, one can conclude that the temperature programming technique can be used profitably by achieving higher productivity for rigid PVC grades production.

7.3.3 Effect of Initiator and Other Additives

Two initiators, Azobis(isobutyronitrile) (AIBN) and Bis(4-tert-butylcyclohexyl) peroxydicarbonate (Perkadox 16-W40), have been used to

Table 7.3. Effect of initiator type on the dehydrochlorination rate of PVC.

Initiator	$[I]_o$ wt%	Temp. °C	Conversion %	$\overline{M}_w \times 10^{-3}$	$\overline{M}_n \times 10^{-3}$	$(dHCl/dt)10^3$ %/min
AIBN	0.50	45	88	156	77	20.4
Perkadox 16-W40	0.175	45	90	161	77	17.4

synthesize the PVC samples in the present investigation. Typical results are shown in Table 7.3. At the same polymerization temperature, the molecular weight averages are the same at similar conversion levels. However, the dehydrochlorination rates are quite different. These limited data suggest that the PVC synthesized with AIBN as an initiator has lower thermal stability. This is in agreement with Titova et al's experimental data.[64] Starnes et al[65] found that the PVC structural segments derived from AIBN contain copolymer structure of VCM with methacrylonitrile. The effect of this structure on the thermal stability of PVC remains unknown. AIBN, an initiator with a longer half life should produce higher radical concentrations for $X > X_f$. Hence, the concentration of defect structures may be higher in the PVC chains produced using AIBN than that using the fast peroxide initiators at high conversions.

As discussed above, the PVC thermal stability decreases with conversion due to the effects of diffusion-controlled reactions as a

result of decrease in monomer concentration. Hence, the effect of diffusion-controlled reactions may be limited if the free volume of the polymer phase can be maintained by feeding in an inert chemical at high conversions. The PVC samples shown in Table 7.4 were synthesized by feeding in n-butane to the reactor at the pressure drop. No significant kinetic behaviour change can be determined. One can see, from Table 7.4, that there is no effect of n-butane on the thermal stability of PVC. These results imply that n-butane cannot sufficiently swell PVC to limit the effect of diffusion-controlled reactions. These results also suggest that the reactions competing with the propagation reactions are the most important ones in affecting the PVC thermal stability. Therefore, increasing the monomer concentration seems to be the most effective way to minimize the defect structures during polymerization at high conversions.

Table 7.4. Effect of n-butane on the dehydrochlorination rate of PVC.

polymerization temperature °C	n-butane wt%	conversion %	$(dHCl/dt)10^3$ %/min
50	-	92	19.5
50	5.0	92	19.5
60	-	95	22.8
60	10.0	94	24.0
70	-	95	41.4
70	20.0	96	39.0

7.4 SUMMARY

The thermal stability of PVC strongly depends on polymerization conditions, in terms of conversion histories, reaction temperature and initiator types. When the conversion is less than X_f, the dehydrochlorination rate of PVC is independent of conversion. At high conversions ($X > X_f$), however, the thermal stability of PVC decreases significantly with an increase in conversion. The reactions forming defect structures are favoured at high conversions due to an increase in the radical and polymer concentrations as a result of decrease in monomer concentration during batch polymerization.

Dehydrochlorination rates always increase with an increase in the polymerization temperature because the secondary reactions are more sensitive to temperature compared with the propagation reaction. However, the proper use of temperature programming techniques at high conversion can give benefits of higher productivity without a significant lose in thermal stability. Temperature programming will not affect other physical properties significantly.

Based on kinetic studies and diffusion-controlled theory, tertiary and allylic chlorine should be responsible for the low thermal stability of PVC. These defect structures can be minimized using a semi-batch process operating at the vapour pressure of monomer. However, further microstructure measurements are required to confirm this conclusion.

7.5 REFERENCES

1. Nass, L. I. 'Encyclopedia of PVC',Ed. Nass, L. I., VOL.I, Marcel Dekker Inc., 1976, 271.

2. Suzuki, T., Nakamuea, M., Yasuda, M. and Tstsumi, J., J. Polym. Sci., 1971, C33, 281.

3. Minsker, K. S., Lisitsky, V. V and Zaikov, G. E. J. Vinyl Technol., 1980, 2, 77.

4. Mukherjee, A. K. and Gupta, A. J. Macromol. Sci.-Revs. Macromol. Chem., 1981, C20, 309.

5. Starnes, W. H. Jr., 'Developments in Polymer Degradation-3', Ed. Grassie, N., Appl. Sci. Publishers, London, 1981, p135.

6. Caraculacu, A. A. Pure Appl. Chem., 1981, 53, 385.

7. Braun, D. Pure Appl. Chem., 1981, 53, 549.

8. Braun, D. 'Developments in Polymer Degradation-3' Ed. Grassie, N., Appl. Sci. Publishers, London, 1981, p101.

9. Minsker, K. S., Lisitsky, V. V., Kolesov, S. V. and Zaikov, G. E. J. Macromol. Sci.-Rev. Macromol. Chem., 1981, C20, 243.

10. Minsker, K. S., Abdullin, M. I., Kolesov, S. V. and Zaikov, G. E. 'Developments in Polymer Stabilisation-6', Ed. Scott, G., Appl. Sci. Publishers, London and New York, 1983, p173.

11. Hjertberg, T. and Sörvik, E. M. 'Degradation and Stabilisation of PVC', Ed. Owen, E. D., Elsevier Appl. Sci. Publishers, London and New York, 1984, p21.

12. Wypych, J. 'Polyvinylchloride Degradation', Elsevier Sci. Publishers B. V., 1985.

13. Nagvi, M. K. J. Macromol. Sci.-Rev. Macromol. Chem. Phys., 1985, C25, 119.

14. Starnes, W. H. Jr. Pure Appl. Chem., 1985, 57, 1001.

15. Minsker, K. S., Kolesov, S. V. and Zaikov, G. E. 'Degradation and Stabilization of Vinyl Chloride-based Polymers', Pergamon press, 1st Ed., 1988.

16. Bovey, F. A., Abbas, K. B., Schilling, F. C. and Starnes, W. H. Jr. Macromol., 1975, 8, 437.

17. Bovey, F. A., Schilling, F. C. and Starnes, W. H. Jr. Polym. Prepr., 1979, 20, 160.

18. Starnes, W. H. Jr., Schilling, F. C., Abbas, K. B., Cais, R. E. and Bovey, F. A. Polym. Prepr., 1979, 20, 653.

19. Starnes, W. H. Jr., Schilling, F. C., Abbas, K. B., Cais, R. E. and Bovey, F. A. Macromol., 1979, 12, 556.

20. Starnes, W. H. Jr., Schilling, F. C., Plitz, I. M., Cais, R. E. and Bovey, F. A. Polym. Bulletin, 1981, 4, 555.

21. Starnes, W. H. Jr., Schilling, F. C., Plitz, I. M., Cais, R. E., Freed, D. J., Hartless, R. L. and Bovey, F. A. Macromol., 1983, 16, 790.

22. Caraculacu, A. and Bezdedea, E. J. Polym. Sci. Polym. Chem. Ed., 1977, 15, 611.

23. Caraculacu, A., Buruiana, E. and Robila, G. J. Polym. Sci., Polym. Symp 1978, 64, 189.

24. Petiaud, R. and Pham, Q. Makromol. Chem., 1977, 178, 741.

25. Abbas, K. B. J. Macromol. Sci.-Phys., 1977, B14, 159.

26. Abbas, K. B. Pure Appl. Chem., 1981, 53, 411.

27. Hjertberg, T. and Sörvik, E. M. J. Macromol. Sci.-Chem., 1982, A17, 983.

28. Hjertberg, T. and Sörvik, E. M. Polymer, 1983, 24, 673.

29. Hjertberg, T. and Sörvik, E. M. Polymer, 1983, 24, 685.

30. Hjertberg, T., Sörvik, E. M. and Wendel, A. Makromol. Chem. Rapid. Commum., 1983, 4, 175.

31. Hjertberg, T. and Sörvik, E. Polym. Prepr., 1984, 25, 69.

32. Hjertberg, T. and Sörvik, E. J. Vinyl Technol., 1985, 7, 53.

33. Hjertberg, T. and Sörvik, E. M. 'Polymer Stabilization and Degradation', Ed. Klemchuk, P. P., American Chem. Soc., Washington, D. C., 1985, p259.

34. Lukas, R., Pradova, O., Michalcova, J. and Paleckova, V. J. Polym. Sci.: Polym. Lett. Ed., 1985, 23, 85.

35. Lukas, R., Pradova, O. Makromol. Chem., 1986, 187, 2111.

36. Park, G. S. J. Vinyl Technol., 1985, 7, 60.

37. Maddams, W. F. J. Vinyl Technol., 1985, 7, 65.

38. Van den Heuvel, C. J. M. and Weber, A. J. M. Makromol. Chem., 1983, 184, 2261.

39. Guyot, A. Pure Appl. Chem., 1985, 57, 833.

40. Guyot, A. J. Vinyl Technol., 1985, 7, 92.

41. Darricades-Llauro, M. F., Michel, A. and Guyot, A. J. Macromol. Sci.-Chem., 1986, A23, 221.

42. Darricades-Llauro, M., Bensemra, N., Guyot, A. and Petiaud, R. Makromol. Chem. Macromol. Symp., 1989, 29, 171.

43. Bensemra, N., Tran Van Hoang and Guyot, A. Polym. Degrad. Stab., 1990, 28, 173.

44. Adeniyi, J. B. and Scott, G. Polym. Degrad. Stab., 1987, 17, 117.

45. Berens, A. R. Polym Eng. Sci., 1974, 14, 318.

46. Haynie, S. L., Villacorta, G. M., Plitz, I. M. and Starnes, W. H. Jr. Polym. Prepr., 1983, 24, 3.

47. Li, D., Zhou, D. and Zhao, D. Polym. Degrad. Stab., 1988, 22, 31.

48. Minsker, K. S., Berlin, A. A., Lisitskii, V. V. and Kolesov, S. V. Polym. Sci. U.S.S.R., 1977, A19, 35.

49. Minsker, K. S., Lisitskii, V. V. and Zaikov, G. Ye. Polym. Sci. U.S.S.R., 1981, 23, 535.

50. Minsker, K. S. Makromol. Chem. Macromol. Symp., 1989, 29, 41.

51. Svetly, J., Lukas, R. and Kolinsky, M. Makromol. Chem., 1979, 180, 1363.

52. Svetly, J., Lukas, R. Michalcova, J. and Kolinsky, M. Makromol. Chem. Rapid. Commum., 1980, 1, 247.

53. Svetly, J., Lukas, R., Pokorny, S. and Kolinsky, M. Makromol. Chem. Rapid. Commum., 1981, 2, 149.

54. Svetly, J., Lukas, R., Michalcova, J. and Kolinsky, M. Makromol. Chem., 1984, 185, 2183.

55. Panek, M. G., Villscorts, G. M. and Starnes, W. H. Jr. Polym. Prepr., 1985, 26, 120.

56. Braun, D. and Sonderhof, D. Eur. Polym. J., 1982, 18, 141.

57. Zegelman, V. I., Titova, V. A., Pomerantseva, E. G., Taikova, T. A. and Zilberman, E. N. Makromol. Chem. Macromol. Symp., 1989, 29, 277.

58. Cuthbertson, M. J., Bowley, H. J., Gerrard, D. L., Maddams, W. F. and Shapiro, J. S. Makromol. Chem., 1987, 188, 2801.

59. Hjertberg, T. and Sörvik, E. M. J. Polym. Sci., part A,: Polym. Chem., 1986, 24, 1313.

60. Caraculacu, A., Buruiana, E. C. and Robila, G. J. Polym. Sci. Polym. Chem. Ed., 1978, 16, 2741.

61. Guyot, A., Bert, M., Burille, P., Marie-France Llauro and Michel, A. Pure Appl. Chem., 1981, 53, 401.

62. Starnes,. W. H. Jr. Polym. Mater. Sci. Eng., 1988, 58, 220.

63. Hamielec, A. E., Gomez-Vaillard, R. and Marten, F. L. J. Macromol. Sci. Chem., 1982, A17, 1005.

64. Titova, V. A., Zegel'man, V. I., Pessina, A. YA., Popov, V. A. and Bort, D. N. Polym. Sci. U.S.S.R., 1982, 24, 1360.

65. Starnes, W. H. Jr., Plitz, I. M., Schilling, F. C., Villacorta, G. M., Park, G. S. and Saremi, A. H. Macromol., 1984, 17, 2507.

CHAPTER 8

CONCLUSIONS AND RECOMMENDATIONS

8.1 CONCLUSIONS

The main contributions of the present investigation can be stated as the development of a novel online GC tracer method for the measurement of experimental kinetic data, the measurement of comprehensive experimental data, the estimation of thermodynamic and kinetic parameters and finally the modelling of the kinetics of the heterogeneous free radical suspension polymerization of vinyl chloride.

A novel conversion measurement method for VCM heterogeneous polymerization was developed in the present study. This method can provide detailed conversion/time and polymerization rate/time profiles efficiently. The principles described in the present investigation can be extended to other polymerization systems, such as bulk, emulsion and microsuspension polymerizations of vinyl chloride. However, recalibration may be necessary for the different systems because the species distributions may be affected by process conditions. This method provides a effective tool not only for kinetic studies but also for developing polymerization recipes for the synthesis of new polymer products.

The comprehensive measured data include the solubility of VCM in

water and PVC, the solubility of n-butane in VCM, monomer conversion histories, polymerization rates, reactor pressure, accumulated molecular weight averages and distributions over wide ranges of polymerization temperatures and conversions of commercial interest. A series of thermodynamic and kinetic parameters which are necessary for kinetic calculations was estimated and confirmed through independent studies.

In the present investigation, the detailed mechanisms for VCM polymerization were refined and clarified including elementary chemical reactions, physical phenomena and reactant species distributions in the course of heterogeneous free radical polymerization of VCM. The process of radical migration between phases during two-phase polymerization period was made clear. A comprehensive reactor model for VCM heterogeneous polymerization was developed based on these mechanisms, including the reactor pressure development, the conversion history, the polymerization rate profile, the critical conversion for the end of two-phase polymerization and the limiting conversion for the polymerization temperature lower than PVC glassy-state transition temperature, and the instantaneous and accumulated molecular weight averages and distributions. The present model predictions are in excellent agreement with the experimental data obtained from the present work and with the data measured in other independent laboratories. The present model has also been successfully generalized to include semi-batch polymerization and batch polymerization with temperature programming at high conversions.

The present model gives great insight into the VCM heterogeneous

free radical polymerization and provides a quantitative description of the main dynamic features of VCM heterogeneous polymerization over the entire conversion range, which include reactor pressure, the monomer conversion and polymerization rate development with time, the monomer, initiator and radical distributions among the phases during polymerization, the instantaneous molecular weight averages and distributions in the different phases, the total instantaneous molecular weight averages and distribution, and the accumulated molecular weight averages and distribution. The contribution of each phase to the total kinetic behaviour was described quantitatively. The monomer phase plays an important role only at low conversion stage (5-10% conversion), and thereafter polymer phase dominates the polymerization.

In the present investigation it was observed that the polymerization rate, instantaneous and accumulated molecular weight averages decrease and the thermal stability of PVC deteriorates at high conversions due to the effects of diffusion-controlled reactions as a result of decrease in monomer concentration. The sensitivity of the elementary the reactions to reaction environment depends on the nature of the individual chemical reaction. Therefore, these property changes at high conversions can be controlled. The present investigation demonstrated that the deterioration of the thermal stability of PVC can be avoided by using a semi-batch process operated at or near the vapour pressure of VCM. A dynamic model for the semi-batch process at high conversions has been developed and it can be used to predict the instantaneous and accumulated monomer consumption and other kinetic features under semi-batch

operation conditions.

8.2 RECOMMENDATIONS

The present investigation was focused on elementary reactions and reactor modelling. The following topics can be further investigated based on the present study.

1. **Modelling PVC microstructure.** Secondary reactions may not significantly affect VCM polymerization rate and accumulated molecular weight averages and distribution. However, these reactions may affect the PVC chain microstructure as well as thermal stability significantly. Therefore, the modelling of the microstructure of PVC chains is important to understand the mechanism of low thermal stability of PVC and improve the quality of PVC product. The kinetic parameters for these secondary reactions need to be estimated using data on PVC microstructure measured by ^{13}C-NMR method.

2. **Physical properties of PVC.** Relationship between PVC physical properties and kinetic behaviour need to be further studied. These include such properties as the degree of gelation, the bulk density and the porosity of PVC. If correlations between these physical properties and kinetic parameters are established, the process properties of PVC could be improved dramatically.

3. **PVC morphology.** Modelling PVC morphology requires a knowledge

of the kinetics of VCM polymerization. Based on the present investigation, it is possible to further model the internal structure of PVC, which includes the rate of formation of primary particle of PVC and the porosity of PVC particles.

4. **Applications of the model and techniques developed in the present investigation.** The present reactor model can be further applied to different scale reactor systems to predict the reactor dynamics under different polymerization conditions. These include the reactor safety estimation, the kinetic behaviour of bi-initiator systems and the effect of other different recipes and reactor operation conditions on the dynamics of VCM polymerization. The semi-batch policy can be applied to larger scale reactor systems so as to further investigate the effect of monomer concentration on chemical and physical properties of PVC. The conversion measurement method developed in the present investigation can be further extended to other polymerization systems such as bulk, emulsion polymerizations and copolymerizations.

5. **Fundamental studies.** The mechanism of polymer and polymer radical precipitation, the critical chain length to precipitate, the radical concentrations in the different phases and radical concentration at high conversions need to be further investigated by other independent experimental methods in order to further fundamental understanding of heterogeneous free radical polymerization and to estimate the individual reaction parameters precisely.

APPENDIX A

MODELLING DIFFUSION-CONTROLLED REACTIONS USING FREE VOLUME THEORY

A.1 INTRODUCTION

The bimolecular termination reaction of two macroradicals in free radical polymerization involves three consecutive processes, namely, (1) translational diffusion; (2) segmental diffusion; and (3) chemical reaction.[1,2] These steps can be expressed as:

$$R_r^{\cdot} + R_s^{\cdot} \xrightarrow[\text{translational diffusion}]{K_T} R_r^{\cdot} \cdots R_s^{\cdot} \xrightarrow[\text{segmental diffusion}]{K_S} R_r^{\cdot}R_s^{\cdot} \xrightarrow[\text{chemical reaction}]{K_C} P \qquad (A.1)$$

where K_T, K_S and K_C refer, respectively, to the net rate constants for the translational and segmental diffusion processes and for the chemical reaction step.

The overall rate for bimolecular termination of radicals is defined as:

$$R_t = \sum_{r=1}^{\infty} \sum_{s=1}^{\infty} K_t(r,s)[R_r^{\cdot}][R_s^{\cdot}]$$

$$= \bar{K}_{tn}[R^{\cdot}]^2 \qquad (A.2)$$

where $K_t(r,s)$ is the rate constant for termination of radicals with chain length r and s and $\overline{K}_{tn}$ is the number-average termination rate constant. If $K_t(r,s)$ is chain length independent, then, Eq.(A.2) can be rewritten as:

$$R_t = K_t[R^{\cdot}]^2 \qquad (A.3)$$

with $K_t = \overline{K}_{tn} = \overline{K}_{tw} = - - -$

Equation (A.3) is the conventional definition for the overall rate constant for bimolecular termination. The conventional termination rate constant K_t used in the literature should be understood as usually equal to $\overline{K}_{tn}$ when bimolecular termination of macroradicals is diffusion-controlled. In fact, K_t is not only a function of temperature but also depends on the chain lengths of the macroradical reactants, the concentration and molecular weight distribution of the accumulated polymer.

Translational diffusion of a polymer molecule in solution occurs when the centre of mass of the polymer molecule changes. The polymer molecule does not move as a single unit; instead, a small segment of the chain will jump from one position to another. Whenever a segment of the polymer moves, the centre of mass of the molecule must change also. Therefore, the rate of diffusion of polymer molecule is intimately related to the jump frequency of a segment of the polymer chain. During polymerization polymer molecules become increasingly entangled with each other, the number of pathways along which a polymer molecule can diffuse

is restricted and eventually multiple physical entanglement points result in significant polymer/polymer friction. Therefore, the translational diffusion rate of polymer molecules falls dramatically reflecting how it strongly depends on the environment including polymer concentration, MWD of accumulated polymer and polymer chain length and flexibility. At low concentrations of polymer or at low monomer conversions, the polymer chains are not entangled. Therefore, translational diffusion is not rate controlling. However, the controlling step involves the motion of macroradical centres to within a reaction volume. In this case, rate of termination is controlled by segmental diffusion. It is generally agreed that the bimolecular termination reaction is segmental diffusion-controlled even at zero conversion for high molecular weight radicals in a good solvent.[1-3] This implies that segmental diffusion is the slow step at low polymer concentrations. With increase in polymer concentration the polymer coil size contracts increasing the rate of termination and with further increase in conversion, polymer chains become entangled and the termination rate falls dramatically with the bimolecular termination rate being controlled by translational diffusion of macroradical chains. The termination rate constant decreases significantly with an increase in monomer conversion and kinetic behaviour changes dramatically, with an acceleration increase in polymerization rate, large increase in polymer molecular weight (for termination domination system) and radical concentration. These phenomena are called as "gel effect". The diffusion controlled reactions considered in the present kinetic modelling are the result of translational diffusion control with segmental diffusion considered not rate controlling. It is very

important to properly model translational diffusion-controlled reactions (bimolecular termination and propagation) because these are important over wide ranges of conversion for most polymerization systems. At very high conversions, for instance, close to a glassy-state transition, the system is so rigid that translational diffusion rates are effectively zero, however the termination rate is still not equal to zero. The radical centre can move spatially by adding monomer and hence the diffusion rate of the radical centre is not zero. In this case, the bimolecular termination reaction is called reaction-diffusion-controlled and the termination rate constant is proportional to $K_p[M]$. At this high conversion level, the propagation reaction itself is also diffusion-controlled.

A.2 MODELLING DIFFUSION-CONTROLLED REACTIONS

Much work has been conducted to find the relationship between translational diffusion rate and the physical properties of reacting system. Most of the work was carried out in a polymerization system where the polymer is soluble in its own monomer, such as methyl methacrylate, styrene polymerization systems.[4-22] Bevington[23-25] outlined the main findings for diffusion-controlled reaction modelling. Hamielec,[26,27] Mita et al[28] and O'Driscoll,[29] recently, gave more comprehensive reviews about diffusion-controlled free radical polymerization. The important approaches include the chain length dependence of K_t;[10-12] the free volume dependence of K_t[5,8] and the combination of the entanglement and the free volume concepts.[16-20] Although these models cannot fully describe

the complex behaviour of the termination process in free radical polymerization, they give reasonable fits to rate data when the gel effect is significant in different monomer systems over wide ranges of conversion. For VCM polymerization, the average chain length does not change with conversion significantly (as described in Chapter 5). Therefore, the free volume approach for modelling diffusion-controlled bimolecular termination should be adequate for the reactor modelling purpose. The relationship between rate constant of a diffusion-controlled reaction and free volume is further illustrated below.

Historically, the free volume concept was developed to explain the non-Arrhenius dependence of the viscosity of liquids or polymer solution with temperature;[30-35] the melt behaviour and glassy-state transition temperature of polymers;[30-39] and the diffusion of small molecule in amorphous polymers.[33,35,40-45] Bueche[40] also derived a relationship for the diffusion coefficient of polymer molecules as follows:

$$D_p = (\phi_o \delta^2/6N^*) \exp(-\beta^* \nu^*/v_f) \qquad (A.3)$$

where ϕ_o is jump frequency of a chain segment, δ is jump distance of segment, N^* is the number of segments in an entangled polymer molecule, ν^* is a critical free volume fraction for a segment to jump, v_f is the free volume fraction for a segment and β^* is defined as:

$$\beta^* = \ln(\nu^*/v_f) - 1$$

Assuming the total free volume consisting of n packets, one for each segment and each packet having the same size, then, one can write the total free volume fraction of polymer system as:[40]

$$V_f = n\, v_f \tag{A.4}$$

Substituting Eq.(A.4) into Eq.(A.3), one obtains:

$$D_p = (\phi_o \delta^2 / 6N^*) \exp(-n\beta^* \nu^* / V_f) \tag{A.5}$$

Equation (A.5) is the starting point for diffusion-controlled reaction rate constant modelling. Marten and Hamielec[5,8] first related Eq.(A.5) to the diffusion-controlled reaction rate constant by assuming that the reaction rate constant after the start of the diffusion control is proportional to the diffusion coefficient of polymer chain. That is:

$$K = C_k(\phi_o \delta^2 / 6N^*)\exp(-n\beta^* \nu^* / V_f) \tag{A.6}$$

where C_k is a proportionality constant.

The variables ϕ_o, δ, N^*, β^*, ν^* and n in Eq.(A.6) refer to a segment of polymer, which remain unknown for a polymer system at the present time. For reactor modelling purposes, however, Eq.(A.6) can be further simplified as:[8,26]

$$K = C_k'[\phi_o \delta^2 / (\overline{M}_w)^m] \exp(-A^* / V_f) \tag{A.7}$$

where A^* is an adjustable parameter defined by

$$A^* = n\beta^* \nu^*$$

At the onset of diffusion-control, the critical reaction rate constant can be written as:

$$K_{crl} = C_k'[\phi_o \delta^2/(\overline{M}_w)^m]_{crl} \exp(-A^*/V_{fcrl}) \qquad (A.8)$$

where C_k', ϕ_o, δ and A^* are assumed to be same before and after diffusion control. For VCM polymerization, the effect of the molecular weight also can be neglected because the accumulated weight-average molecular weight is almost independent of conversion. Therefore, dividing Eq.(A.7) by Eq.(A.8) leads to:

$$K = K_{crl} \exp\left[-A^*\left(\frac{1}{V_f} - \frac{1}{V_{fcrl}}\right)\right] \qquad (A.9)$$

Equation (A.9) is a general formula used to calculate the diffusion controlled reaction rate constants described in Chapters 4 and 5.

From the description above, one can see that Eq.(A.9) is a simplified function which approximates the complicated translational diffusion process. All the effects of physical property changes on the diffusion controlled reaction rate constant are included in the change in free volume fraction. Therefore, the calculation of V_f is very crucial for the evaluation of the diffusion-controlled reaction rate constant.

A.3 CALCULATION OF V_f

Although the free volume concept has been used to describe the properties of liquids or solution for long time, the free volume had not been clearly defined[46] until the work of Vrentas et al.[42,43] According to Vrentas and Duda's theory,[42,43] the volume of the material is divided into the occupied volume, the interstitial free volume and the hole-free volume. The specific occupied volume of a pure liquid is defined to be the specific volume of the equilibrium liquid at 0°K which, for the polymer, is denoted by V_p°. The specific interstitial free volume of the effectively pure polymer, V_{FI}, is the unoccupied volume which is distributed uniformly among the molecules of a given species. The specific hole-free volume of the polymer, V_F, is the volume associated with the discontinuous distribution of holes in the liquid, and it is assumed that this free volume can be redistributed with no increase in energy. The hole-free volume is the quantity which is available for molecular transport. Therefore, the free volume mentioned in the previous section should refer to the hole-free volume as defined by Vrentas and Duda's theory.

Based on the definition of free volume above, one can write the hole-free volume as:

$$V_F = V_p - V_{FI} - V_p^\circ \qquad \text{(A.10)}$$

where V_p is the specific volume of the polymer at temperature T.

For the pure polymer, the thermal expansion coefficient for the sum of the occupied volume and the interstitial free volume is defined by the equation:

$$\alpha_c = \frac{1}{V_{FI} + V_p^\circ}\left[\frac{\partial(V_{FI} + V_p^\circ)}{\partial T}\right]_p \tag{A.11}$$

and this equation upon integration yields the following result:

$$V_{FI} + V_p^\circ = [V_{FI}(T_{gp}) + V_p^\circ]\exp\left(\int_{T_{gp}}^{T} \alpha_c dT\right) \tag{A.12}$$

The thermal expansion coefficient for the polymer liquid, α_l, can be defined as:

$$\alpha_l = \frac{1}{V_p}\left(\frac{\partial V_p}{\partial T}\right)_p \tag{A.13}$$

For the temperature interval of interest, α_c and α_l can be simplified by

$$\exp[\alpha(T-T_{gp})] = 1 + \alpha(T-T_{gp}) \tag{A.14}$$

With Eqs.(A.10)-(A.14), one can find the hole-free volume in term of fraction as:

$$V_f = V_{fg} + [\alpha_l - (1-V_{fg})\alpha_c](T - T_{gp}) \tag{A.15}$$

where the free volume fraction is defined by

$$V_f = V_F/V_p$$

Equation (A.15) is very interesting because it is of the same form as a semiempirical relation proposed by Williams, Landel and Ferry[38] which is

$$V_f = 0.025 + \alpha(T-T_{gp}) \qquad (A.16)$$

where $\alpha = \alpha_l - \alpha_g$; α_l is thermal expansion coefficient for the liquid state, α_g is the thermal expansion coefficient for the glass state. However, Eq(A.15) gives a clear fundamental meaning of hole-free volume. It is obvious that Eq.(A.15) or (A.16) is valid for temperatures above the glassy-state transition temperature.

To calculate glassy-state transition temperature of polymer-solvent system, Kelley and Bueche[39,40] extended equation (A.16) to polymer-diluent system with the assumption that the free volume of each constituent is additive, that is

$$V_f = [0.025+\alpha_p(T-T_{gp})]\Phi_p + [0.025+\alpha_m(T-T_{gm})](1-\Phi_p) \qquad (A.17)$$

This is the relation used to calculate the free volume fraction of the polymer-monomer mixture in the present work as shown in Chapter 4, Eq.(4.89).

It should be mentioned that a temperature less than T_{gp} is used in Eq.(A.17) because the glassy-state transition temperature of polymer-diluent system is always less than T_{gp}. For the diffusion-controlled reaction modelling described in the present work, the polymerization temperature is also less than the glassy-state transition temperature of pure polymer. According to definition of free volume in Eq.(A.10), the free volume fraction is zero at 0°K. Therefore, at any polymerization temperature, the contribution of the polymer to total free volume of mixture should be:

$$[0.025+\alpha_p(T-T_{gp})] > 0 \qquad (A.18)$$

When the polymerization temperature T is lower than T_{gp}, $\alpha_p(T-T_{gp})$ is negative. This means that the contribution of the polymer to the free volume fraction at T ($T < T_{gp}$) is less than 0.025 (which is the free volume fraction of polymer at T_{gp}). Fujita et al[34] found that the free volume of material decreases with decreasing temperature, and that the thermal expansion coefficient at below T_g is much smaller than that above T_g. Therefore, caution must be taken that the α_p in Eq.(A.17) is different from that in Eq.(A.16). To account for the glassy-state transition effect, Vrentas et al[44] modified the equation for free volume fraction to be:

$$V_f = 0.025 + \zeta\alpha(T-T_{gp}) \qquad (T < T_{gp}) \qquad (A.19)$$

where ζ is a parameter ($0 < \zeta < 1.0$).

Soh et al[18] used a similar formula as Eq.(A.19) to calculate V_f, however, they used a reference temperature below T_{gp}. Marten et al[8] and Stickler et al[9] used the universal parameter $\alpha_p=0.48\times10^{-3}$ $(^\circ C)^{-1}$ for their kinetic model calculations. However, in the present model calculations, α_p and α_m were found by fitting Eq.(A.17) with the experimental data below T_{gp} as shown in Chapter 4, Figure 4.9. Therefore, α_p found by the present method is equivalent to $\zeta\alpha$ shown in Eq.(A.19). These parameters should be valid within the present polymerization temperature range. However, for lower temperatures, α_p should be reestimated from the corresponding experimental data. For model calculations with wide range of temperature, a temperature dependence of α_p should be used.

A.4 REFERENCES

1. North, A. M. and Reed, G. A. Trans. Faraday Soc., 1961, 57, 859.

2. Hughes, J. and North, A. M. Trans. Faraday Soc., 1964, 60, 960.

3. Matthews, C. Y. and Rosen, S. L. J. Polym. Sci.: Polym. Phys. Ed., 1984, 22, 139.

4. Friis, N. and Hamielec, A. E. 'Emulsion Polymerization', ACS Symp. Ser., 24, ACS., Washington D. C., 1976, p82.

5. Marten, F. L. and Hamielec, A. E. 'Polymerization Reactor and Processes', ACS Symp. Ser., 104, ACS. Washington, D.C., 1979, p43.

6. Harris, B., Hamielec, A. E. and Marten, F. L. 'Emulsion Polymers and Emulsion Polymerization', ACS. Symp. Ser., 165, ACS. Washington D. C., 1981, P315.

7. Ross, R. T. and Laurence, R. L. A. I. Ch. E. Symp. Ser., 1976,160, 74.

8. Marten, F. L. and Hamielec, A. E. J. Appl. Polym. Sci., 1982, 27, 489.

9. Stickler, M., Panke, D. and Hamielec, A. E. J. Polym. Sci.: Polym. Chem. Ed., 1984, 22, 2243.

10. Cardenas, J. N. and O'Driscoll, K. F. J. Polym. Sci.: Polym. Chem. Ed., 1976, 14, 883.

11. Cardenas, J. N. and O'Driscoll, K. F. J. Polym. Sci.: Polym. Chem. Ed., 1977, 15, 1883.

12. Cardenas, J. N. and O'Driscoll, K. F. J. Polym. Sci.: Polym. Chem. Ed., 1977, 15, 2097.

13. O'Driscoll, K. F., Dionisio, J. M. and Mahabadi, H. KH. 'Polymerization Reactors and Processes', ACS. Symp. Ser., 104, ACS. Washington D. C., 1979, p261.

14. Sundberg, D. C and James, D. R. J. Polym. Sci.: Polym Chem. Ed., 1978, 16, 523.

15. Sundberg, D. C., Hsieh, J. Y., Soh, S. K. and Baldus, R. F. 'Emulsion Polymers and Emulsion Polymerization', ACS. Symp. Ser., 165, ACS. Washington, D. C., 1981, p327.

16. Soh, S. K. and Sundberg, D. C. J. Polym. Sci.: Polym. Chem. Ed., 1982, 20, 1299.

17. Soh, S. K. and Sundberg, D. C. J. Polym. Sci.: Polym. Chem. Ed., 1982, 20, 1315.

18. Soh, S. K. and Sundberg, D. C. J. Polym. Sci.: Polym. Chem. Ed., 1982, 20, 1331.

19. Soh, S. K. and Sundberg, D. C. J. Polym. Sci.: Polym. Chem. Ed., 1982, 20, 1345.

20. Soh, S. K. and Sundberg, D. C. 'Computer Application in Applied Polymer Science', Provder, T. Ed., ACS. Symp. Ser., 197, ACS. Washington, D. C., 1982, p27.

21. Ito, K. J. Polym. Sci., A-1, 1969, 7, 827.

22. Budtov, V. P. and Podosenova, N. G. International Polymer Sci. Technol., 1986, 13, 89.

23. Bevington, J. C. Macromol. Chem., 1980, 1, 45.

24. Bevington, J. C. Macromol. Chem., 1982, 2, 24.

25. Bevington, J. C. Macromol. Chem., 1984, 3, 49.

26. Hamielec, A. E. Chem. Eng. Commun., 1983, 24, 1.

27. Hamielec, A. E. NATO ASI Ser., Ser. E. 67, Sci. Technol. Polym. Colloids, 1983, Vol.1, p140.

28. Mita, I. and Horie, K. J. Macromol. Sci.-Rev., Macromol. Chem. Phys., 1987, C27, 91.

29. O'Driscoll, K. F. 'Comprehensive Polymer Science', Vol.3, Eastmond, G. C., Ledwith, A., Russo, S. and Sigwalt, P. Eds., Pergamon Press, 1989, p161.

30. Doolittle, A. K. J. Appl. Phys., 1951, 22, 1031.

31. Doolittle, A. K. J. Appl. Phys., 1951, 22, 1471.

32. Doolittle, A. K. J. Appl. Phys., 1952, 23, 236.

33. Fujita, H. and Kishimoto, A. and Matsumoto, K. Trans. Faraday Soc., 1960, 56, 424.

34. Fujita, H., Kishimoto, A. J. Chem. Phys., 1961, 34, 393.

35. Kishimoto, A. J. Polym. Sci.: part A, 1964, 2, 1421.

36. Fox Jr., T. G. and Flory, P. J. J. Appl. Phys., 1950, 21, 581.

37. Fox, T. G. and Flory, P. J. J. Polym. Sci., 1954, 14, 315.

38. Williams, M. L., Landel, R. F. and Ferry, J. D., J. Am. Chem. Soc., 1955, 77, 3701.

39. Kelley, F. N. and Bueche, F. J. Polym. Sci., 1961, 50, 549.

40. Bueche, F. 'Physical Properties of Polymers', Interscience Publishers, New York, 1962.

41. Vrentas, J. S. and Duda, J. L. Macromolecules, 1976, 9, 785.

42. Vrentas, J. S. and Duda, J. L. J. Polym. Sci.: Polym. Phys. Ed., 1977, 15, 404, 417, 441.

43. Vrentas, J. S. and Duda, J. L. J. Appl. Polym. Sci., 1977, 21, 1715.

44. Vrentas, J. S. and Duda, J. L. J. Appl. Polym. Sci., 1978, 22, 2325.

45. Vrentas, J. S. , Liu, H. T. and Duda, J. L. J. Appl. Polym. Sci., 1980, 25, 1297.

46. Haward, R. N. J. Macromol. Sci.-Revs., Macromol. Chem., 1970, C4, 191.

APPENDIX B

PRECIPITATION OF POLYMER RADICALS FROM THE MONOMER PHASE

It is a well known fact that PVC has very low solubility in its monomer. However, what is the solubility of PVC in VCM and what is the critical chain length of PVC above which equilibrium precipitation occurs? Does the growing chain complete its normal growth in the monomer phase, form dead polymer and then precipitate? Perhaps the growth rate of the polymer chain is too great for equilibrium precipitation to occur? These questions have not been adequately addressed in the literature.

Using the solubility of a telomer of structure $CCl_3(CH_2CHCl)_xBr$ in vinyl chloride monomer, Cotman et al (see ref.47 in Chapter 4) estimated that a small amount of telomers with chain length 25-32 was insoluble in VCM. Based on this observation, they assumed that the macroradicals precipitate from the monomer phase at degree of polymerization of 25-32. If this value is the critical chain length to precipitate, one can estimate the maximum amount of PVC produced in the monomer phase, assuming that every polymer chain has 32 monomeric units formed in the monomer phase when conversion is less than X_f, as follows:

$$\begin{matrix}\text{maximum fraction of} \\ \text{PVC produced} \\ \text{in the monomer phase}\end{matrix} = \frac{32X_f}{\bar{r}} \qquad (B.1)$$

where $\bar{r}$ is the average chain length of PVC.

The average chain length of PVC is about 1100 at 50°C for $X < X_f$ according to the present investigation. Using Eq.(B.1), one can estimate that the maximum fraction of PVC produced in the monomer phase is about 2%. Hence, the contribution of the monomer phase to the total PVC produced is less than 2% based on Cotman et al's data. This is obviously in contradiction with the kinetic observations. In fact, polymer chains are also initiated in the polymer phase. Therefore, radical chain lengths attained before precipitation from the monomer phase occurs should be much greater than 32.

Based on a population balance for radicals, the critical chain length to precipitate was derived in Chapter 4 as:

$$K^* = \left[\frac{1-CM_1}{1+K_{t1}[R^\cdot]/K_{p1}[M]_1}\right]^{r_c-2} \qquad (B.2)$$

where K^* was estimated in Chapter 4 as shown in Eq.(4.110). At 50°C, the following parameters for monomer phase can be estimated based on the results shown in Chapters 4 and 5:

$$K^* = 4.6\times10^{-4}$$

$$CM_1 = 5\times10^{-4}$$

$[R^{\cdot}]_1 = 1.2X10^{-8}$, mole/L

$[M]_1 = 13.7$, mole/L

$K_{p1} = 1.3x10^{3}$, L/mole-sec

$K_{t1} = 1.9x10^{9}$, L/mole-sec

Substituting these values into Eq.(B.2), one can estimate the critical chain length to be about 4300 which is much larger than the average polymer chain length at 50°C. As mentioned in Chapter 4, precipitation of radicals does not affect radical concentration in the monomer phase, however, it does affect radical concentration in the polymer phase at very low conversions because the volume of the monomer phase is much larger than that of the polymer phase at these very low conversions.

The critical chain length estimated based on a population balance for radicals seems to be in contradiction to the fact of low solubility of PVC in VCM. In fact, they are based on different fundamental concepts. Polymer dissolution in a solvent or precipitation out of a solvent are physical processes which require a certain amount of time, perhaps seconds. According to the parameters shown above, one can estimate the monomer addition rate per radical at 50°C to be:

$$K_{p1}[M]_1 = 1.7x10^{4} \quad (1/sec) \qquad (B.3)$$

It only requires 0.06 second to produce a polymer radical chain with an chain length of 1100. Therefore, the chain propagation rate should be much faster than the physical processes associated with chain precipita-

tion and the molecular weight distribution of PVC produced in the monomer phase should be same whether chain precipitation occurs or not. Although PVC has a very low solubility in VCM, polymer radicals will terminate in the monomer phase before precipitation occurs. Dead polymer then goes through the precipitation process if its chain length is greater than about 25-32. Therefore, the VCM polymerization system is not in thermodynamic equilibrium with respect to polymer chain precipitation. The polymer phase is formed mainly by precipitation of dead polymer chains instead of polymer radicals. Particle nucleation is completed at very low conversions (2-5% conversion). Later, some of the polymer radical chains are captured by existing primary particles because of the large interfacial areas generated. The probability for polymer radical precipitation is very small due to the extremely fast chain growth rates in the monomer phase.

In conclusion, the molecular weight development of PVC in the monomer phase is governed by chain transfer to monomer, bimolecular termination and the concentration of monomer in the monomer phase and does not depend on the polymer precipitation phenomenon. Therefore, molecular weight development in the monomer phase can be treated by conventional methods. The assumption that all of the dead polymer precipitates instantaneously satisfies the physical phenomenon of low solubility of PVC in the monomer. Cotman et al's data for equilibrium solubility cannot be used to describe polymer radical precipitation from the monomer phase.

APPENDIX C

MANIPULATION OF LIGHT SCATTERING DATA

In Chapter 5, the accumulated weight-average molecular weight measured by LALLS has been described briefly. Detailed procedures for $\overline{M}_w$ calculation from LALLS measurements are illustrated here.

The low angle laser light scattering from a dilute polymer solution can be expressed in the following form[1]:

$$\frac{KC}{R_\theta} = \frac{1}{\overline{M}_w} + 2A_2C + 3A_3C^2 + \ldots \qquad (C.1)$$

where R_θ is the measured excess scattering intensity of solution over that of pure solvent; C is concentration of polymer solution; $\overline{M}_w$ is weight-average molecular weight of polymer; A_2 and A_3 are second and third virial coefficients; K is an optical constant for the particular scattering system given by:

$$K = \frac{2\pi^2 n_o^2}{\lambda_o^4 N_{av}} (dn/dc)^2(1 + \cos^2\theta) \qquad (C.2)$$

here λ_o is wavelength of light in vacuum (632.8×10^{-7}cm in the present experiment); N_{av} is Avogadro's number (6.023×10^{23}); θ is light scattering angle (4.8°); n_o is refractive index of solvent and dn/dc is

specific refractive index increment of the polymer solution.

Values for n_o and dn/dc have to be found in order to calculate K for PVC-THF solution.

The refractive index n_o is a complex function of wavelength λ_o. Normally, n_o decreases with an increase in λ_o. A value of n_o for THF at given λ_o (632.8×10^{-7}cm) is not available in the literature. For a certain range of wavelength, n_o can be described by simplified Couchy formula[2]:

$$n_o = a + b/\lambda_o^2 \qquad (C.3)$$

where a=1.393, b=0.00383 for THF which were estimated from literature data.[2,3] Hence, n_o for THF was estimated to be 1.403 at λ_o 632.8×10^{-7}cm.

The specific refractive index increment of PVC-THF was determined experimentally in the present work (equipment is described in Chapter 5). The results are shown in Figure C.1. The refractive index is a linear function of concentration of PVC in THF. The slope (dn/dc) of the plot was found by the least squares method to be 0.106 mL/g.

With parameters provided above, one can find K using Eq.(C.2) under the present experimental conditions as:

$$K = 8.913 \times 10^{-8} \qquad (C.4)$$

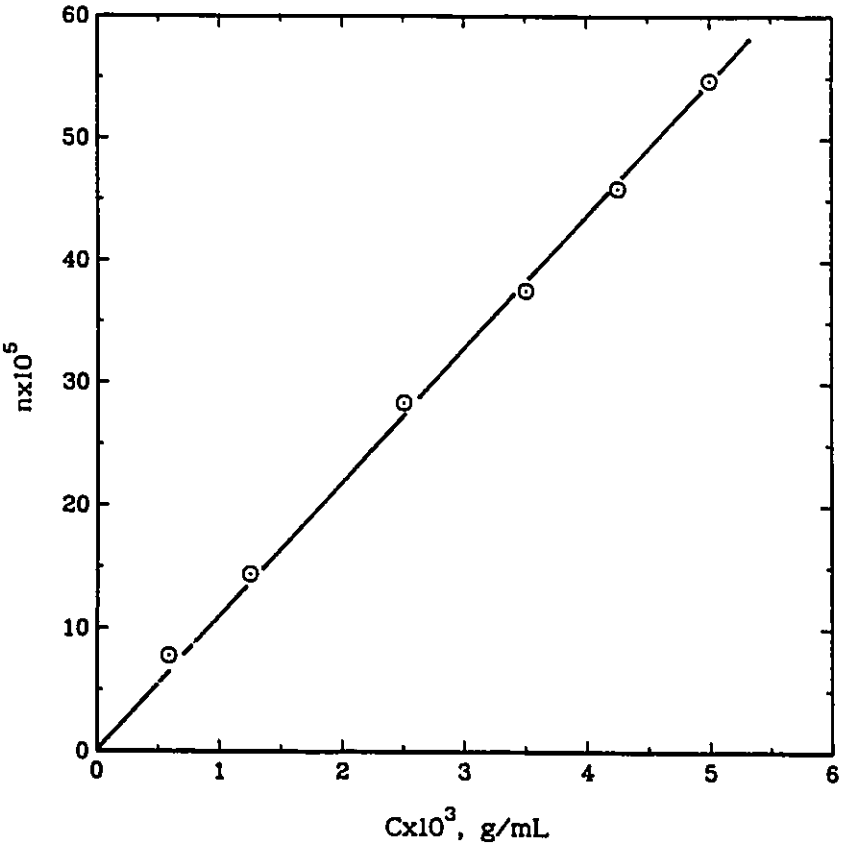

Figure C.1. Concentration dependence of refractive index of PVC-THF solution at 25°C.

Plotting KC/R_θ against C, one can find weight-average molecular weight from the intercept of the plot and From Eq.(C.1). A typical plot is shown in Figure C.2.

Figure C.2 shows the LALLS measurements for the highest molecular weight sample of PVC synthesized at 40°C in the present investigation. For the same PVC sample, one was prepared at ambient tempera-

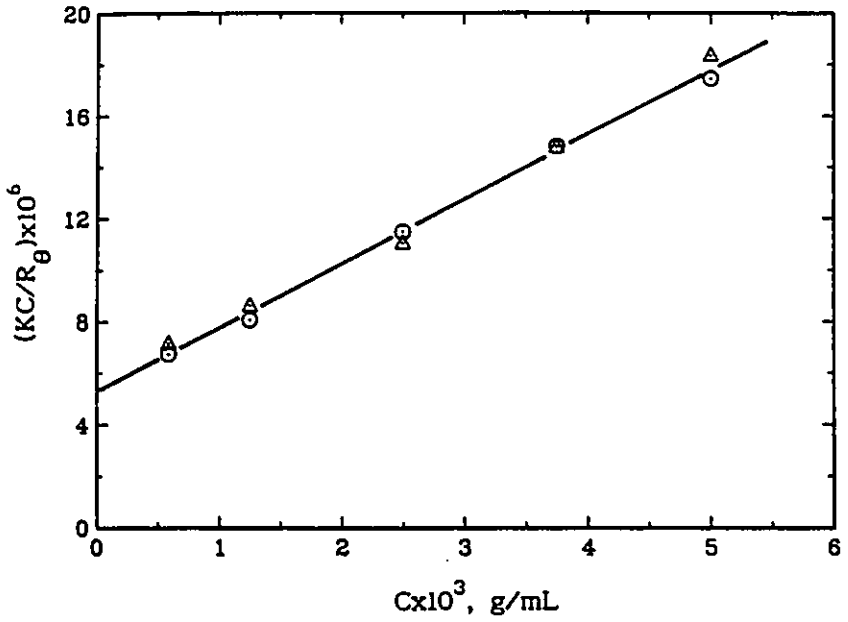

Figure C.2. Determination of $\overline{M}_w$ by LALLS measurements.
⊙: without heating solution,
Δ: heating solution at 95°C for one hour.

ture, another solution was heated at 95°C for one hour. One can see that the effect of heat on molecular weight measurements is within measurement error, and hence, is negligible. The molecular weights calculated from Figure C.2 are as follows:

$\overline{M}_w = 193x10^3$ (without heating solution)

$\overline{M}_w = 192x10^3$ (heating solution at 95°C for one hour)

Therefore, aggregation for PVC polymerized above 40°C was considered negligible.

REFERENCES

1. Huglin, M. B. 'Light Scattering From Polymer Solutions', Academic Press, London and New York, 1972.

2. Johnson, B. L. and Smith, J. 'Light Scattering From Polymer Solutions', Huglin, M. B. Ed., Academic Press, London and New York, 1972, p27.

3. Weast, R. C., Lide, D. R., Astle, M. J. and Beyer, W. H. 'CRC Handbook of Chemistry and Physics', 70th Ed., 1989-1990, pE382.

APPENDIX D

SENSITIVITY OF THE KINETIC PARAMETERS

Comprehensive kinetic parameters were estimated in the present investigation. The reliability of the parameters was confirmed by the independent experimental results obtained in different laboratories. The sensitivity of some important kinetic parameters is further tested herein.

With the present kinetic model, the reactor simulations were done on the basis of the following conditions: reactor volume 5-L; monomer 1116 grams; water 2232 grams; initiator Perkadox 16-W40, 0.175-wt% and polymerization temperature 50°C. Figure D.1 shows the effects of K_p and K_t changes on the conversion histories. The solid line is the simulation based on the parameters estimated in this study. The large dashed line was obtained by increasing K_p by 10% with other parameters unchanged. One can see that the conversion histories shift toward the left side of the solid line, i.e. the polymerization rate increases significantly because the reaction rate is proportional to K_p. The dash-dotted line was obtained by increasing K_{t1} and K_{t2} by 10%. One can see that the conversion histories shift toward the right side of the solid line, i.e. the polymerization rate decreases significantly. Increase in termination rate constant will lead to a decrease in the

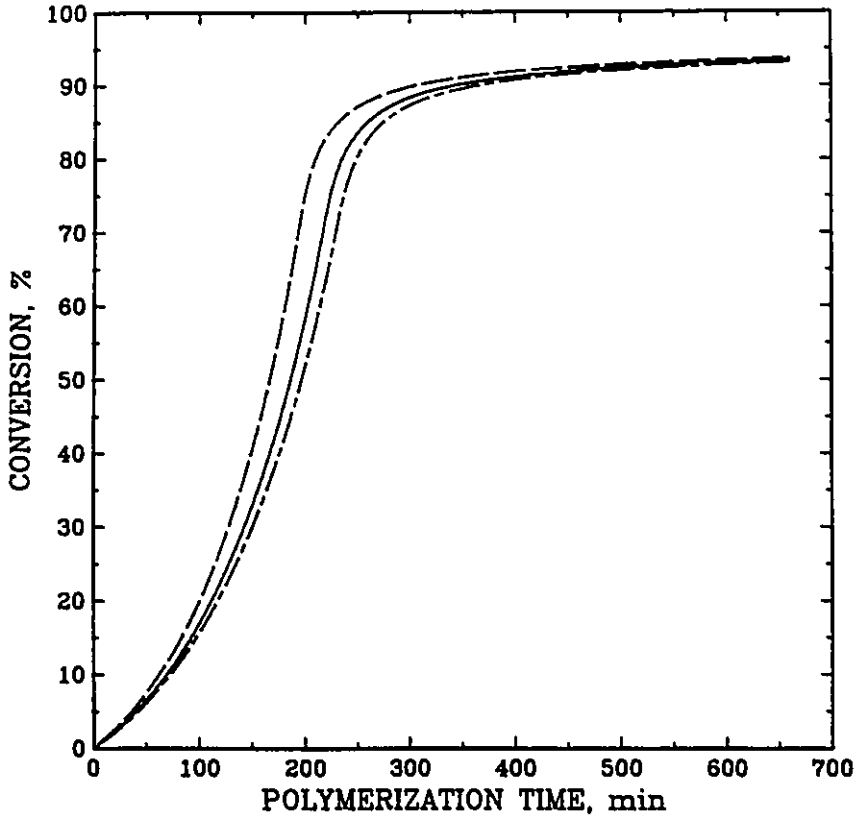

Figure D.1. The effect of kinetic parameters on the conversion histories of VCM polymerization.
———: model prediction with present parameters;
– – –: increasing K_p by 10%;
———: increasing K_t by 10%.

radical concentrations in both phases so that the polymerization rate decreases. However, the conversion history changes due to K_t are not as sensitive as those due to K_p because the polymerization rate is inversely proportional to the square root of K_t. The effects of A^* and K_I on the conversion histories are shown in Figure D.2. The dash-dotted line in Figure D.2 was calculated by increasing A^* by 10%. The

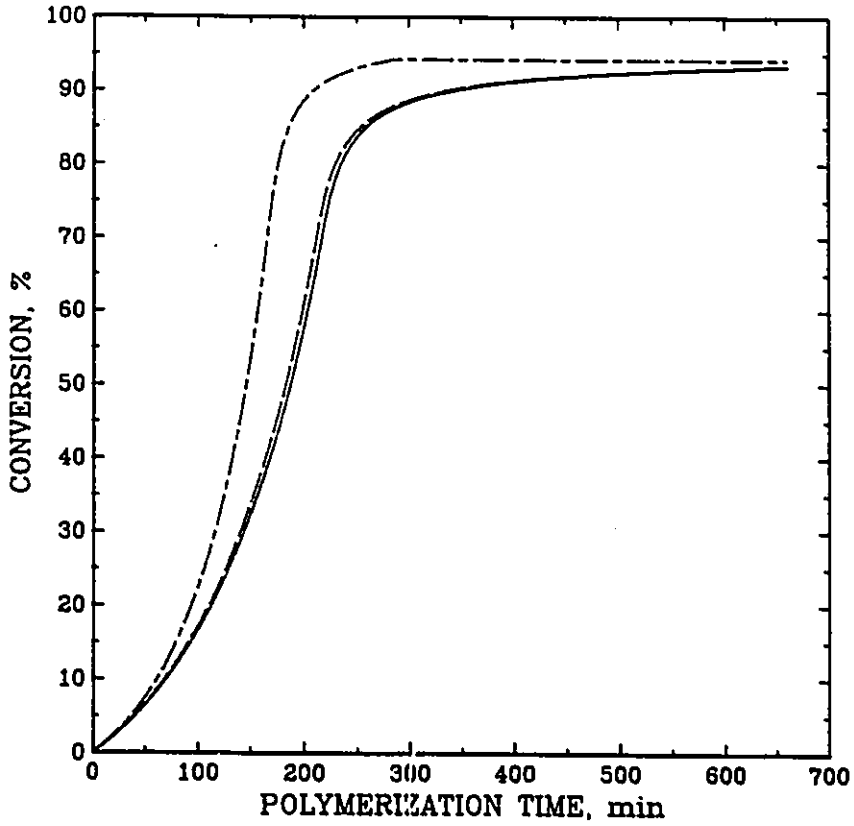

Figure D.2. The effect of kinetic parameters on the conversion histories of VCM polymerization.
———: model prediction with present parameters;
– – –: increasing K_I by 10%;
———: increasing A^* by 10%.

termination rate constant in the polymer phase is an exponential function of A^* [see equation (4.92)]. Therefore, increase in A^* will lead to a dramatic decrease in K_{t2}. Consequently, the polymerization rate increases dramatically because of a significant increase in radical concentration in the polymer phase as shown in Figure D.2. The dashed line in Figure D.2 was obtained by increasing K_I by 10%. One can see

that the effect of K_I on the conversion histories is not very significant because the initiator concentration in the polymer phase does not increase by 10% although K_I does. On the other hand, the initiator concentration in the monomer phase decreases as K_I increases [see equations (4.75) and (4.76)]. Furthermore, the polymerization rate is proportional to square root of the initiator concentration.

In summary, the conversion histories are very sensitive to the parameters K_p, K_t and A^*. Therefore, the ratio of $K_p/K_t^{1/2}$ and A^* estimated in the present study should have narrow confidence limits. However, the conversion history is not sensitive to initiator partition coefficient K_I. This is why the data for K_I estimated in the present study are somewhat scattered (see Figure 4.15). Therefore, K_I estimated using conversion/time data has a large confidence interval. An accurate K_I would be obtained by direct analysis of initiator concentrations in the monomer and polymer phases under polymerization conditions. However, this was not done because of experimental difficulties. For reactor modelling purposes, K_I estimated in the present study should be adequate.

APPENDIX E

PUBLICATIONS BASED ON THE PRESENT RESEARCH

In Refereed Journals:

1. T. Y. Xie, A. E. Hamielec, P. E. Wood and D. R. Woods, "**Experimental Investigation of Vinyl Chloride Polymerization at High Conversion —— Temperature/Pressure/Conversion and Monomer Phase Distribution Relationships**", J. Appl. Polym. Sci., 34, 1749(1987).

2. T. Y. Xie, A. E. Hamielec, P. E. Wood, D. R. Woods and H. Westmijze, "**Experimental Investigation of Vinyl Chloride Polymerization at High Conversion —— Conversion and Tracer Response Relationships**", J. Appl. Polym. Sci., 41, 2327(1990).

3. T. Y. Xie, A. E. Hamielec, P. E. Wood and D. R. Woods, "**Experimental Investigation of Vinyl Chloride Polymerization at High Conversion —— Mechanism, Kinetics and Modelling**", Polymer, (accepted for publication on January 19, 1990).

4. T. Y. Xie, A. E. Hamielec, P. E. Wood and D. R. Woods, "**Experimental Investigation of Vinyl Chloride Polymerization at High Conversion —— Molecular Weight Development**", Polymer, (accepted for publication on April 29, 1990).

5. T. Y. Xie, A. E. Hamielec, P. E. Wood and D. R. Woods, "**Experimental Investigation of Vinyl Chloride Polymerization at High Conversion —— Semi-batch Reactor Modelling**", Polymer, (accepted for publication on June 30, 1990).

6. T. Y. Xie, A. E. Hamielec, P. E. Wood, D. R. Woods and O. Chiantore, "**Experimental Investigation of Vinyl Chloride Polymerization at High Conversion —— Effect of Polymerization Conditions on Polymer Properties**", Polymer, (accepted for publication on June 19, 1990).

7. T. Y. Xie, A. E. Hamielec, P. E. Wood and D. R. Woods, "**Suspension, Bulk and Emulsion Polymerization of Vinyl Chloride —— Mechanism, Kinetics and Reactor Modelling**", J. Vinyl Technology, (accepted for publication on August 30, 1990).

8. T. Y. Xie, A. E. Hamielec, P. E. Wood and D. R. Woods, "**Experimental Investigation of Vinyl Chloride Polymerization at High Conversion —— Reactor Dynamics**", J. Appl. Polym. Sci., (submitted for publication on November 14, 1990).

In Conference Proceedings:

9. T. Y. Xie, A. E. Hamielec, P. E. Wood and D. R. Woods, "**Suspension Polymerization of Vinyl Chloride at High Conversion, Modelling Conversion and Tracer Response by Gas Chromatography**", Polym. Mater. Sci. Eng., 58, 766(1988). (Presented in the third Chemical Congress of North American, Toronto, Ontario, Canada, June 1988).

10. T. Y. Xie, A. E. Hamielec, P. E. Wood and D. R. Woods, "**Suspension, Bulk and Emulsion Polymerization of Vinyl Chloride —— Mechanism, Kinetics and Reactor Modelling**", PVC Symposium 1988 (The Netherlands).

11. T. Y. Xie, A. E. Hamielec, P. E. Wood and D. R. Woods, "**An Investigation of the Kinetics of The Polymerization of Vinyl Chloride in Suspension at Conversions Beyond the Pressure Drop**", PVC Symposium 1988 (The Netherlands).

12. T. Y. Xie, A. E. Hamielec, P. E. Wood and D. R. Woods, "**Suspension, Bulk and Emulsion Polymerization of Vinyl Chloride —— Dynamic Modelling of Polymer Properties and Reactor Performance**", PVC Symposium 1990 (Singapore).